Editorial Journal of Facade Design & Engineering

Knaack, U.; Klein, T.

DOI
10.7480/jfde.2020.2

Publication date
2020

Document Version
Final published version

Published in
Journal of Facade Design and Engineering

JOURNAL OF FACADE DESIGN & ENGINEERING

VOLUME 8 / NUMBER 2 / 2020

EDITORS IN CHIEF ULRICH KNAACK AND TILLMANN KLEIN

SUPPORTED BY THE EUROPEAN FACADE NETWORK

JOURNAL OF FACADE DESIGN & ENGINEERING

VOLUME 8 / NUMBER 2 / 2020

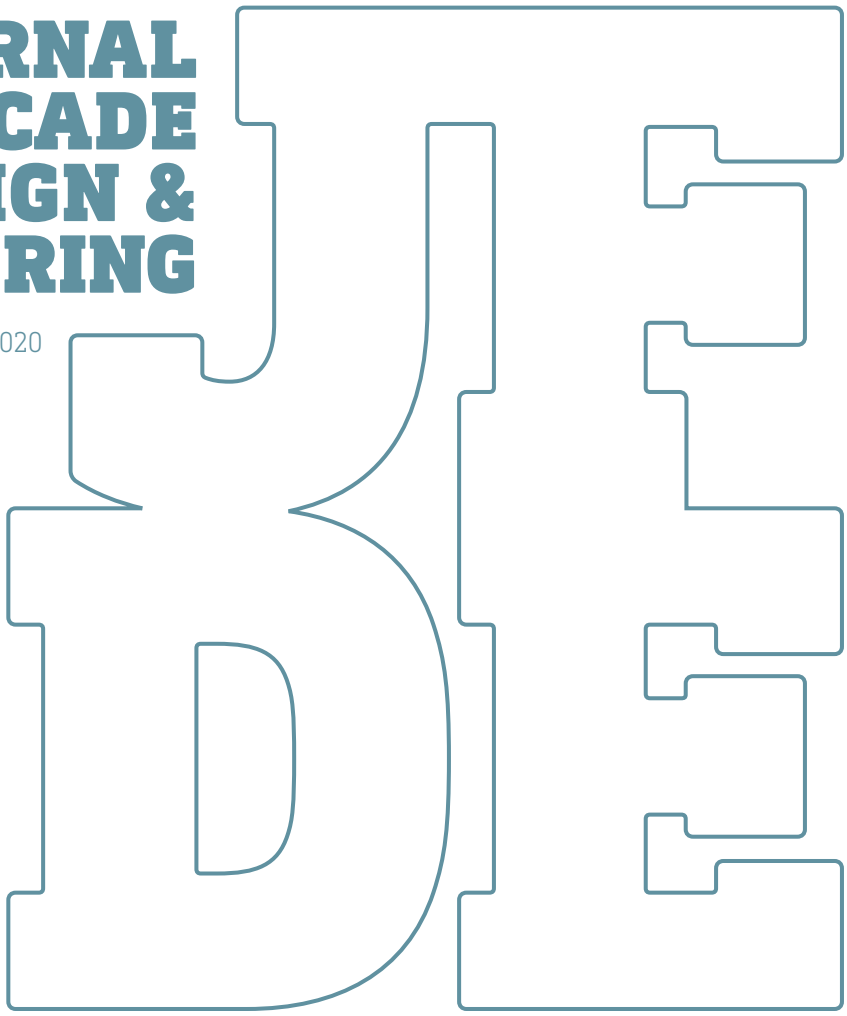

JFDE Journal of Facade Design and Engineering

JFDE presents new research results and new proven practice of the field of facade design and engineering. The goal is to improve building technologies, as well as process management and architectural design. JFDE is a valuable resource for professionals and academics involved in the design and engineering of building envelopes, including the following disciplines:

– Architecture
– Building Engineering
– Structural design
– Climate design
– Building Services Engineering
– Building Physics
– Design Management
– Facility Management

JFDE will – initially - be directed at the scientific community, but it will also feature papers that focus on the dissemination of science into practice and industrial innovations. In this way, readers explore the interaction between scientific developments, technical considerations and management issues.

Publisher
TU Delft Open
TU Delft / Faculty of Architecture and the Built Environment
Julianalaan 134, 2628 BL Delft, The Netherlands

Contact
Alejandro Prieto
JFDE-BK@tudelft.nl
http://jfde.tudelft.nl/

Design & layout
Design – Sirene Ontwerpers, Rotterdam
Layout – Nienke Blaauw, TU Delft

ISSN 2213-302X (Print)
ISSN 2213-3038 (Online)
ISBN 978-94-6366-359-5

Submissions
All manuscripts and any supplementary material should be submitted to the Editorial Office (JFDE-BK@TUDelft.nl), through the Open Journal System (OJS) at the following link: http://jfde.tudelft.nl/

Author Guidelines
Detailed guidelines concerning the preparation and submission of manuscripts can be found at the following link:
https://journals.open.tudelft.nl/index.php/jfde/about/submissions

Contents

Editorial

Welcome to our final JFDE issue of 2020, a year defined by the global covid-19 outbreak, which has had a drastic impact on all our lives, ranging from global politics to our daily routines. Conversely, most academic activities had to switch from a physical setting to a virtual environment (a situation that is still very much the case in Europe). We have had to learn how to interact via digital tools and especially seize and promote the value of not just written information, but also the potential behind virtual conferences, workshops, and events to keep in touch with our colleagues, friends, and fellow researchers.

Well, what else can we say... it has worked surprisingly well. Although most of us are certainly looking forward to regaining the closeness that regular, daily interaction brings to our academic lives -may this be in education or research-, we are also truly aware of, and amazed by, the benefits that have come from this widespread digital conversion to virtual settings. We currently have the possibility to easily engage with researchers and students from all over the world, increasing the dissemination of relevant knowledge, and sparking the formation of new exchange networks, regardless of our physical distance. A special mention in this regard goes to the potential CO_2 emissions that may be saved by decreasing our work-related travels. Does it really make sense to fly around the globe for just one talk at a conference? - maybe not. And yes, we can even have social interaction via digital tools, which of course works, but this is one aspect in which it can be shown that things are not the same. Personal contact cannot be replaced. Organised matches at scientific events, spontaneous meetings over coffee, and, of course, the direct contact among students are all essential activities that we will be happy to resume once this crisis is over, while hopefully we will continue to reap the unintended benefits and lessons that came with it. So, expect hybrid to be the new normal!

Now, about the articles showcased in this issue: Prefab, Bricks, and Water seem to be the core topics addressed by the researchers. It is interesting to see so many different approaches when it comes to prefabrication as a general strategy for the development of a design concept. The same goes for the articles that explore the use of water, either as a thermal energy carrier, or its impact on the hygrothermal performance of buildings. Finally, it is always fascinating to see clear links between theoretical scientific developments and the design and production of components for application in real buildings. So, once again we have quite a wide range of themes throughout this issue, but as it often is with the built environment, all of these different aspects add to the general knowledge about façades, finding their way into real building envelopes that perform and function under a holistic approach.

The Editors in Chief,

Ulrich Knaack
Tillmann Klein

Environmental and Economic Benefits of Japanese *Koshi*-Inspired Mini-Louvres in Residential Buildings in Jakarta, Indonesia

Alexander Rani Suryandono[1,2*], Agus Hariyadi[1], Hiroatsu Fukuda[2]

* Corresponding author
1 Department of Architecture and Planning, Universitas Gadjah Mada, Yogyakarta, Indonesia, alexanderrs@ugm.ac.id
2 Faculty of Environmental Engineering, The University of Kitakyushu, Kitakyushu, Japan

Abstract

The increase in energy consumption for cooling is a global problem, especially in hot regions, including Indonesia. It happens because of wealth, population growth, climate, building designs, and electronic appliances. Focusing on Jakarta, Indonesia's capital city, louvres in 18 different dimensions and overhangs in 2 different dimensions are simulated using Rhinoceros and Grasshopper with EnergyPlus to show their performance in reducing cooling energy. The design of the louvres is inspired by Japanese koshi. L-shaped aluminium profiles are used as mini-louvres. These mini-louvres can be placed on the outside surface of a glass window or can be attached to the window frame. The cost saving in electricity is obtained from the resulting reduction in cooling energy consumption, which utilises air-conditioning units that follow government regulations. The construction cost includes the price of aluminium profiles and attachment elements. The results show that the horizontal koshi mini-louvres are environmentally beneficial as they reduce the annual cooling energy by around 7-18% on average for all orientations. Moreover, all the proposed horizontal koshi types attached to the window frame are economically beneficial since they can achieve a simple payback period of less than a year when used in a westerly orientation.

Keywords

Cooling energy, simulation, shading, louvres, Japanese koshi

DOI 10.7480/jfde.2020.2.4100

1 INTRODUCTION

1.1 COOLING ENERGY CONSUMPTION

Energy used for cooling comprised only a small part of global energy consumption in the past. The International Energy Agency (2017c) noted that there are five factors that drive the growth of cooling energy. Wealth is the first factor. People want to achieve comfort by using air conditioning and can afford to do so. Population growth is the second factor. The population increases in countries with warmer temperatures, and people tend to migrate from colder to warmer areas. The third factor is climate. Global temperatures continue to rise, leading to higher average temperatures. The frequency of extremely high temperatures is increasing due to the urban heat island phenomenon and climate change. The fourth factor is building designs. Fewer new buildings utilise heavy materials such as brick, and there is a shift towards lighter materials with lower thermal mass. According to the International Energy Agency (IEA), the last factor leading to higher cooling energy consumption is electronic appliances. There has been an increase in the use of electronic tools, devices, and office machinery inside buildings, which produce heat as a by-product. The IEA (2018) noted that overall energy use worldwide, between 2000 and 2017, in buildings and appliances has increased by 21%, reaching 120 EJ. The IEA (2018) specifically noted that space cooling accounts for a large portion of energy demand, and residential buildings utilised three times more energy than is consumed by end-uses in non-residential buildings, in 2017. The expansion of usage of air-conditioning units increased the energy used for space cooling, causing it to almost double since 2000. According to the IEA (2018), cooling energy consumption is the fastest growing energy end-use in buildings; it increased from 3.6 EJ in 2000 to 7 EJ in 2017 globally. Global increase in energy use in buildings has been largely driven by six countries with major emerging economies: Brazil, China, India, Indonesia, Mexico, and South Africa, which account for one-third of global primary energy demand, equivalent to the energy demand of all Europe and the USA (the IEA, 2018). In Southeast Asia, energy use has increased by 60% in the past 15 years (the IEA, 2017b). The IEA (2019) reported that fewer than 10% of households in Indonesia used air conditioning, in comparison with around 80% of households in wealthier countries with less challenging climatic conditions. However, the IEA (2019) also noted that the use of air conditioning become higher because of the rise of income and urbanisation. Higher incomes make air conditioning units more affordable. Since temperatures tend to be higher in urban areas, the demand for cooling is intensified by urbanisation.

Indonesia is the country with the largest economy in Southeast Asia, and the tenth largest in the world in terms of purchasing power parity (the World Bank, 2019). Indonesia has shown an average economic growth rate consistently above 5% since the year 2010, accompanied by an increase gross national income increase per capita from USD $823 in the year 2000 to USD $3932 according to the World Bank (2019). An IEA special report on Indonesia`s energy efficiency (2017a) showed that Indonesia was accountable for 36% of the primary energy used in Southeast Asia, the largest energy consumption of any country in that region. Indonesia's GDP growth doubled from 2000 to 2015 and electricity consumption increased by 150% (the IEA, 2017a). According to the World Bank (2020), Indonesia has a population of 267 million, of whom 55% live in cities, whereas 48% of the population lived in cities ten years previously. However, based the IEA data (2020), people in Indonesia consume only 900 kWh electricity per capita per year, just a quarter of the world average annual electricity consumption (3200 kWh) in 2017. Electricity consumption in the residential sector grew around 159% from 2010 to 2017 (the IEA, 2020). The residential sector accounted for the largest portion of total final consumption of energy in 2017, with a 41% share (Fig. 1).

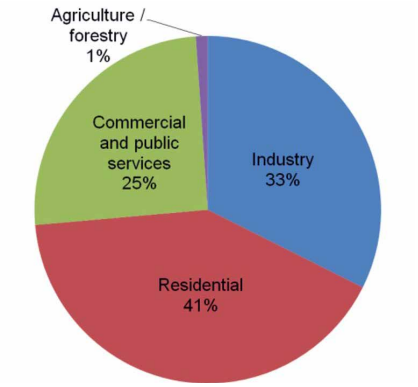

FIG. 1 Total final energy consumption in Indonesia by sector in 2017. Data from the International Energy Agency [2020]

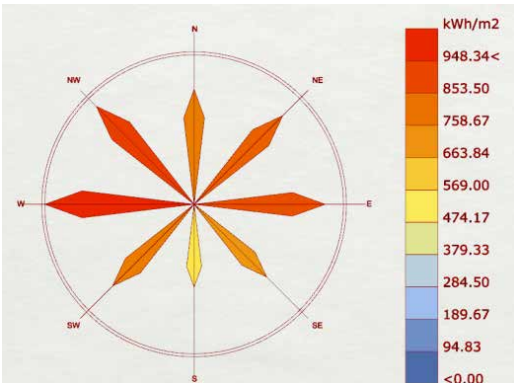

FIG. 2 Total solar radiation in a year in Jakarta. Data were extracted from the weather file for simulation, and the visualisation was created using Lady Bug. Image by Author

The IEA (2018) highlighted that indoor cooling represents a big portion of building energy demand and requires policy consideration to make energy consumption more efficient. The IEA (2018) noted that in hot climates, low-cost technologies, such as reflective roofs and walls, exterior shades and low-e window coatings and film can cut cooling energy consumption. The IEA (2018) suggested that national and local governments should establish and enforce energy codes for new buildings using affordable technological solutions. The codes should be adapted to local situations and market barriers. The IEA (2018) stated that energy-inefficient building materials, such as single, clear, glazed windows should be avoided, and existing materials should be replaced or upgraded with window attachments. Exterior shading is one of the possible window attachments that can be used in both new construction and older building retrofits. The IEA (2018) noted that available products, costs, climate, and energy prices at the local level have to be examined to meet the balance between envelopes and the equipment needed to apply the designs. They also highlighted that exterior shading is cost effective and is therefore becoming more prominent.

This research is done to provide one possible solution to reduce cooling energy consumption. Existing solutions are widely offered in other sectors, such as the office and commercial sectors, using advanced technology. This paper shows one alternative solution that is suitable for, but not limited to, end-users in the residential sector. The solution is a sun shading device utilising low technology that can be applied without requiring specific skills during the constructional and operational phase. The simulated computer model, followed by calculation based on the survey, is chosen for its ability to predict the effect of the application in a real situation. The objective of this paper is to determine the performance of Japanese *koshi*-inspired mini-louvres in terms of environmental and economic benefits. The results of this research can be used by end-users in the residential sector to contribute to cooling energy reduction, for design applications to other building sectors, and for expansion of further research on mini-louvres sun shading.

1.2 PREVIOUS RESEARCH

There has already been some previous research undertaken to find solutions to reduce the cooling energy using shading devices, especially louvres, while considering the economic feasibility. Ghosh and Neogi (2018) simulated south-oriented windows in Kolkata, India with horizontal overhangs, vertical fins, horizontal overhangs with triangular fins, four-sided fins, and a new shading design which consists of four partially overlapping fins below an overhang deflected downward at 65.77°.

A window with no shading devices was used for base case comparison. They concluded that the proposed new shading design performed best, by reducing annual cooling energy by around 4% in comparison with the base case, even though the size is smaller than horizontal overhang which cuts only around 2% of the annual cooling energy. Samaan, Farag, and Khalil (2018) simulated the cooling load of three drawing halls of the Faculty of Engineering, Mansoura University, using DesignBuilder with EnergyPlus. Using the same 0.5 metre overhang, side fin, and louvres, they found that the louvres performed best, reducing annual cooling energy by 10% in comparison with base case. The overhang cut around 7%, while the side fin reduced the annual cooling energy by around 2%. Darwish and Gomaa (2017) measured four retrofitting strategies of three existing buildings in Egypt by applying external wall insulation, changing windows glazing type, increasing airtightness, and adding 0.5 metre metal louvres, using computer simulation in Design Builder, incorporating EnergyPlus. The results of the study showed that the use of metal louvres was the most efficient of the strategies, reducing the energy consumption of the three buildings by up to 23%, on average.

Several studies explore the economical aspect of sun shading strategies. Huang, Niu, and Chung (2012) analysed a retrofitting strategy for existing school buildings in Hong Kong using overhangs to reduce cooling energy demand. The overhang consisted of a 38 mm fibreglass grating platform with aluminium cladding and supporting structure. They showed that the annual electricity saving was 55,700 kWh or 52,400 HKD. However, the lowest bidding price for the retrofitting project was 29,784,000 HKD, thus showing that the overhang system required a long payback period and the investment cost could not be recovered within the project life cycle. Cho, Yoo, and Kim (2014) conducted simulations of 48 exterior shading types using DOE-2.1 E to measure the cooling energy savings. Horizontal and vertical panels can reduce cooling energy demand by 19.7% and 17.3% respectively. The economic feasibility study showed a simple payback period of around 3.4 years for the horizontal overhang and 8.7 years for the vertical overhang. The authors noted that sun shading is expected to replace the use of expensive high-performance glass.

Research focusing on louvres has been undertaken to provide solutions for cooling energy reduction. Hariyadi, Fukuda, and Ma (2017) tested *"sudare"*, a traditional Japanese external blind, using Rhinoceros and Grasshopper as the modelling software and EnergyPlus as the simulation engine. They found that *sudare* with a diameter of 10.01 mm and 5 mm spacers reduced Overall Thermal Transfer Value (OTTV) by 5% and thermal energy use for cooling by 6% in comparison with the base line. Hernández, Cejudo López, Peña Suárez, González Muriano, and Rueda (2017) proposed horizontal and angled vertical louvres as an environmentally friendly solution to reduce cooling energy use for the south and east façades of buildings with a high window to wall ratio. They simulated the buildings in Málaga, Spain using TRNSYS for calculating cooling energy. They showed that the horizontal louvres reduce around 60% of cooling energy for south façades of buildings, while 60° facing north and south angled vertical louvres cut 68% and 64% respectively. Ralegaonkar and Gupta (2010) studied the criteria for passive solar strategies to develop recommendations for climate-responsive architecture. They found that one of the most significant design parameters to alter the building cooling and heating energy for passive-solar architecture is sun shading. They suggested small-scale modelling as one of the easiest and best methods to examine the effectiveness of specific systems. Simulations using computer software are the most suitable choice to predict real conditions. They mentioned that external static sun shading is the most efficient of all types of sun shading reviewed in their study. The efficiency of sun shading needs to be examined according to the location, following the sun paths in the particular geographic location.

1.3 CLIMATE CONDITION IN JAKARTA, INDONESIA

The problem of cooling energy consumption becomes greater in hot climate areas, especially in countries with increasing economic growth, high populations, and urbanisation, such as Indonesia. Jakarta, Indonesia's capital city, is chosen for this study. According to downloaded weather data used for the simulation in this study, the monthly average temperature ranges from a minimum of 26.87°C in January to a maximum of 29.1°C in October (OneBuilding, 2020a). The annual average temperature is 28.23°C.

Total diffuse and direct solar radiation for one year can be seen in Fig. 2, utilising the same weather data for simulation. The average annual total solar radiation per hour in 8 orientations is 762.14 kWh/m^2. The west direction suffers the highest annual total solar radiation of 948.34 kWh/m^2. The south direction gets the lowest annual total solar radiation of 525.02 kWh/m^2. The sun shading performance of reducing excessive solar gain is simulated to calculate the total annual cooling energy.

1.4 JAPANESE *KOSHI* LATTICEWORK

Koshi (**格子**)is traditional Japanese latticework which is commonly used for fences, doors, or parts of windows. The use of *koshi* as a window attachment was established after the Onin civil war in Kyoto (Tsushi-nikai, 2020). Traditional Japanese houses in Kyo-Machiya, which are protected by law as one of the most culturally significant and valuable types of architecture in Kyoto, usually have *koshi*. In another area in Uchiko, Ehime, all of the preserved houses and buildings in the village have *koshi*. One of *koshi's* functions is to allow sunlight into the buildings while also reducing the excessive heat from the sun. *Koshi* can be placed close to the outdoor surface of window (Fig. 3), or on the window frame. Traditional *koshi* are made of wood. However, some modern *koshi* use newer materials such as aluminium or PVC. The pattern is also varied, by placing the *koshi* members not only vertically but also horizontally (Fig. 4).

FIG. 3 *Koshi* placement close to the exterior window surface in a house, in Uchiko, Ehime

FIG. 4 Horizontal *koshi* in a commercial building in Kitakyushu, Fukuoka

Based on the weather data in Kyoto (OneBuilding, 2020b) and Matsuyama – a city close to Uchiko (OneBuilding, 2020c), the average solar radiation per hour in Kyoto and Uchiko from May to August is 234.08 Wh/m^2 and 257.82 Wh/m^2 respectively. There is the possibility to use Japanese *koshi* as a shading device in Jakarta, which has a slightly higher average solar radiation per hour value. The inspiration for the proposed design in this paper comes from *koshi* that utilises a small profile of sun shading device, which is attached close to the window's exterior surface. The proposed designs use aluminium with small L-shaped profiles, which can be placed close to the window, mimicking the idea of Japanese *koshi.*

1.5 L-SHAPED ALUMINIUM PROFILES

An L-shaped aluminium profile is a building material with a wide variety of uses. It can be used for structural or decoration purposes, such as bracing, framing, moulding, and edge protection. However, this research explores another opportunity to use it as a shading device. There are multiple reasons for proposing the use of these components as mini-louvres for shading devices. First, the L-shaped aluminium profile is widely available. It can be found in nearby building material stores. The second reason is its price, which is relatively low in Jakarta. A grey coloured L-shaped aluminium profile with dimension of 12 mm × 12 mm and a thickness of 0.08 mm costs USD $0.29 per metre. Third, many sizes are available, from as small as 8 mm to 30 mm. L-shaped aluminium profiles with different leg lengths are also available. The first three reasons are based on a market survey carried out in early 2019 in Jakarta, Indonesia. In general, the proposed raw materials for horizontal *koshi* can be easily found in any city in Indonesia. The fourth reason for its use is its high level of durability. Aluminium can be placed outdoors, last for years, and requires little maintenance. Stacey and Bayliss (2015) carried out a case study of 12 buildings using non-destructive tests to review the durability of aluminum used for windows. They noted that aluminium has a high durability and suggested a revision of standard life span of aluminium windows from 40 to 80 years. This was based on their finding that after 26 years, PVDF-coated aluminium looked very similar to its condition when first installed in 1988. Aluminium with polyester powder coating was still in use after 41 years. The fifth reason is the weight of the aluminium. Skejic, Boko, and Neno (2015) stated that aluminium is a low self-weight material that reduces the building load, reduces physical labour needs, and saves energy during construction. They noted that aluminium has a high corrosion resistance that lessens the maintenance costs and shows good performance in high corrosion environments. Sixth, aluminium is recyclable, making it environmentally friendly (Wondermetals, 2019). It can be recycled without losing its physical properties.

2 RESEARCH METHODOLOGY

2.1 RESEARCH WORKFLOW

Cooling energy is the main problem in this study. Based on the recent cooling energy consumption, and previous research, sun shading is chosen as one of the possible solutions. Suitable materials for the proposed types are determined based on a survey performed in the selected locations. Computer software is used to simulate the annual cooling energy according to the selected setting to resemble real world conditions, such as the building function, materials, and location-based weather data. The proposed designs are built parametrically in the Rhinoceros 3D with Grasshopper plug-in

and simulated using Ladybug and Honeybee with the EnergyPlus engine (Ladybug tools, 2019). The results are used to calculate the economic benefits of the energy savings, based on the electricity price in Jakarta, Indonesia. The air-conditioning unit used in this research follows the regulations from the Ministry of Energy and Mineral Resources number 57/ 2017 (JDIH Kementrian ESDM, 2017). The price of materials and sun shading construction are used to determine the cost. A comparison between electrical savings and construction costs is calculated to show the simple payback period. The whole process of study in this paper is presented in Fig. 5.

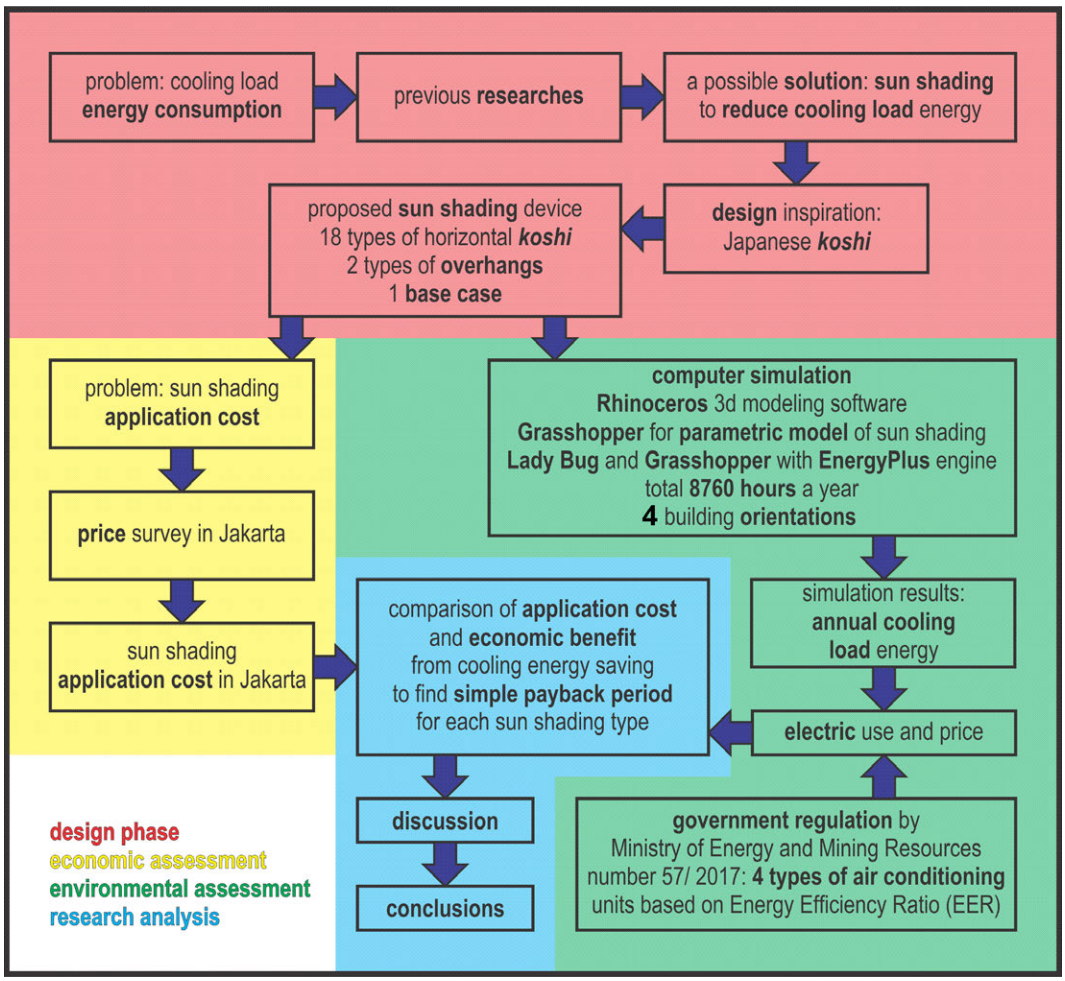

FIG. 5 Research workflow

2.2 SIMULATION SETTINGS

The simulations are all done in the Rhinoceros 3D software. Grasshopper is the main plugin for hosting LadyBug and HoneyBee. EnergyPlus is the simulation engine behind HoneyBee. First, a 3000 mm × 3000 mm box is created to represent a simple room, completed with a 2000 mm × 2000 mm window in the middle of one side of the wall. The roof construction consists of 100 mm thick lightweight concrete, ceiling air void, and acoustic tiles. Brick walls, with a total thickness of 150 mm, are constructed from 120 mm bricks with a 15 mm stucco finish to both the

interior and exterior surfaces of the bricks. The floor construction consists of 50 mm insulation board and 200 mm heavyweight concrete. The detailed properties of the construction materials for the roof, walls, and floor are shown in Table 1. The window is made from a single pane of clear 3 mm glass. The glass properties are shown in Table 2. These are common building materials in Indonesia. The EnergyPlus shading object property for both diffuse solar and visible reflectance of the unglazed part of shading surface is 0.2.

TABLE 1 Properties of the opaque materials

MATERIAL TYPE	ROUGHNESS	THICKNESS (MM)	CONDUCTIVITY (W/m-K)	DENSITY (kg/m^3)	SPECIFIC HEAT (J/kg-K)	THERMAL absorptance	SOLAR absorptance
Lightweight concrete	Medium rough	101,6	0,53	1.280,00	840	0,9	0,5
Acoustic tile	Medium smooth	19,1	0,06	368	590	0,9	0,3
Stucco	Smooth	15	0,69	1.858,00	836,99	0,9	0,92
Brick	Medium rough	120	0,89	1.920,00	790	0,9	0,7
Insulation board	Medium rough	50,8	0,03	43	1.210,00	0,9	0,7
Heavyweight concrete	Medium rough	203,2	1,95	2.240,00	900	0,9	0,7

TABLE 2 Window properties of single clear 3mm glass panel

OPTICAL DATA TYPE	SPECTRAAL AVERAGE
Thickness	2.9 mm
Solar transmittance at normal incidence	0,837
Front side solar reflectance at normal incidence	0,075
Visible transmittance at normal incidence	0,898
Front side visible reflectance at normal incidence	0,081
Front side infrared hemispherical emissivity	0,84
Back side infrared hemispherical emissivity	0,84
Conductivity	0.9 W/m-K
Dirt correction factor for solar and visible transmittance	1

The base case for the comparison study in this paper is a simple box-shaped building with no shading device attached to the single glass pane window (Fig. 6). Eighteen models of horizontal *koshi* are made parametrically utilising the same script. The differences among horizontal *koshi* types are the size of the L-shaped aluminium mini-louvres, the gap between louvres, and their placement on the windows. Three sizes of L-shaped aluminium profiles: 12 mm × 12 mm, 15 mm × 15 mm, and 30 mm × 30 mm, are chosen to represent the different sizes of available materials. There are two possible options for attaching the horizontal *koshi* to the window. The first possibility is to directly attach the horizontal *koshi* to the exterior window surface using outdoor double-sided tape. A second possibility is to use screws to attach the horizontal *koshi* to the window frame. Both the outdoor double-sided tape and screws for attaching horizontal *koshi* are widely available. The performances of different shading types in reducing annual cooling energy are analysed in this study.

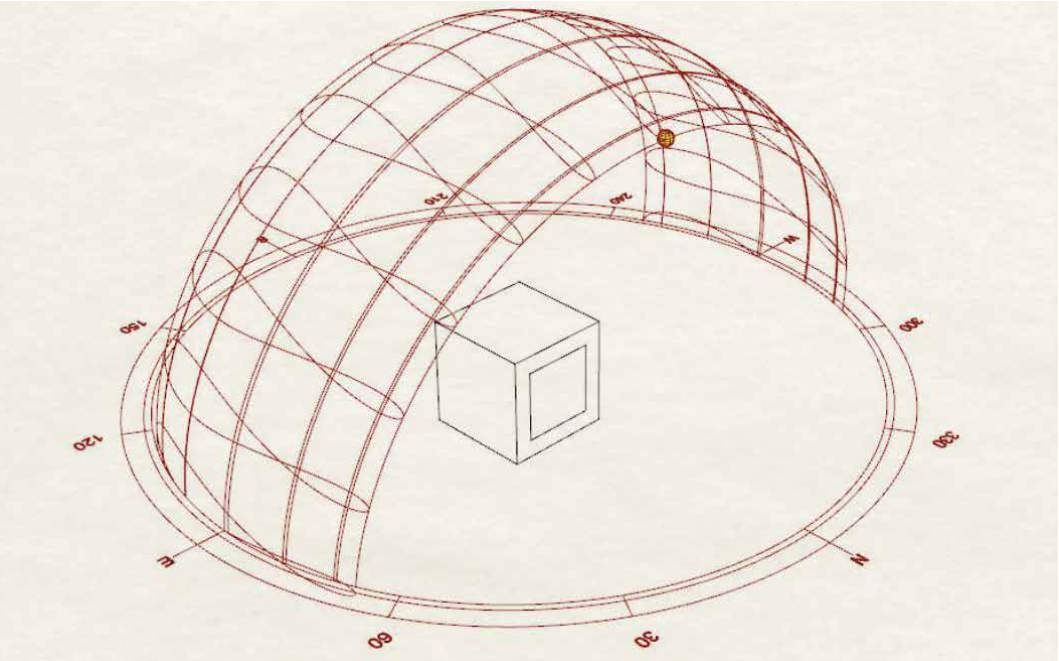

FIG. 6 Simulation setting. The picture shows the base case model without a shading device

Simulation model types A 1 to 9 are designed to mimic the condition of direct attachment by leaving only a millimetre gap between the horizontal *koshi* and the window's outer surface. Simulation model types B 1 to 9 are proposed to imitate the attachment of the horizontal *koshi* to the window frame with a 50 mm gap between the horizontal *koshi* and the window's exterior surface. Visualisation of horizontal *koshi* types A and B 1 to 9 can be seen in Fig. 7. There are three basic ratios between L-shaped mini-louvres and the gaps between them. The first is 1:1, meaning that the gaps are the same size as the L-shaped mini-louvres that form the horizontal *koshi.* The second ratio is 1:2, which means the gap size is twice the size of the L-shaped mini-louvres. The last ratio is 1:3, which gives a gap size three times larger than the size of the L-shaped mini louvres. An additional two horizontal overhang types, which are more common shading devices in the selected research location, are simulated for comparison with the performance of the horizontal *koshi*. These overhang models are types C1 and C2. Fig. 8 shows a schematic perspective view of the overhang type. Details of 21 buildings with detailed shading sizes and types for simulation are shown in Table 3.

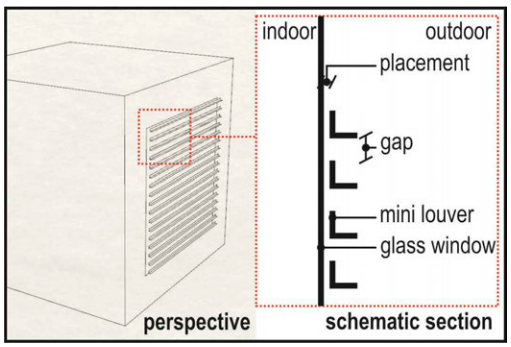

FIG. 7 Schematic of horizontal *koshi* mini-louvres design

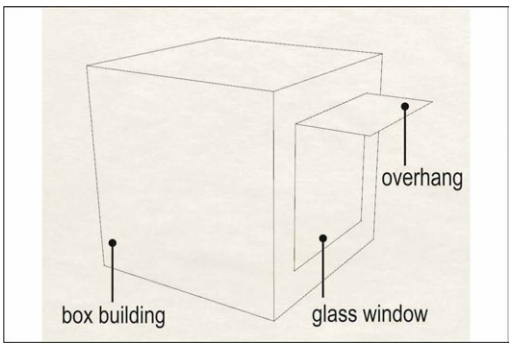

FIG. 8 Overhang type

TABLE 3 Simulated model types size parameters

MODEL NAME	SHADING TYPE	SIZE (MM)	GAP (MM)	PLACEMENT OUTSIDE WINDOW SURFACE (MM)
Base case	No shading	-	-	-
Type A1	Horizontal koshi mini-louvres	12	12	1
Type A2			24	
Type A3			36	
Type A4		15	15	
Type A5			30	
Type A6			45	
Type A7		30	30	
Type A8			60	
Type A9			90	
Type B1		12	12	50
Type B2			24	
Type B3			36	
Type B4		15	15	
Type B5			30	
Type B6			45	
Type B7		30	30	
Type B8			60	
Type B9			90	
Type C1	Overhang	750	-	1
Type C2		1000	-	

TABLE 4 EnergyPlus settings for apartment zone program

APARTMENT	
Equipment load per area	3.875028 W/m^2
Infiltration load per area	0.000227 m^3/s-m^2 at 4Pa
Lighting density per area	11.840357 W/m^2
Number of people per area	0.028309 People/m^2
Ventilation per area	0
Ventilation per person	0
Honeybee zone schedule	default midrise apartment schedule
Ideal air load system	1
Heating set point	21.1°C
Cooling set point	23.9°C

The weather data for Jakarta, Indonesia are Typical Meteorological Year 3 (TMY3), downloaded directly using Ladybug from the OneBuilding website (2019). OneBuilding is a reputable website providing global weather data that are commonly used for simulation studies. The simulation scripts are made and executed in Grasshopper using Ladybug and Honeybee. There are various building programs in EnergyPlus, one of which is a midrise apartment with three schedules of rooms: apartment, office, and corridor. The target building type for the simulation is residential, so the building schedule for the apartment zone program is chosen to mimic a general residential room. The settings used for the midrise apartment zone programs are shown in Table 4. The equipment and infiltration load, lighting density, and the number of the people per area value are changed

hourly according to the apartment program schedule in the simulation. The heating and cooling set point are constant through the year. However, this research focuses on cooling energy consumption since the temperature in Jakarta is high all year round.

3 RESULTS AND DISCUSSION

3.1 ANNUAL COOLING ENERGY SIMULATION RESULTS: ENVIRONMENTAL BENEFIT

All 21 buildings are tested in an hour-based simulation to obtain the cooling energy results for one year. There are 8760 hours of simulation per building in a year. Residential houses in Jakarta face a multitude of directions; however, in this research only 4 main orientations of the building are simulated. The results of simulations are defined as total cooling annual energy in Joules per hour, which then are converted to kilo British Thermal Units per hour. The unit conversion is necessary since the government of Indonesia uses the Energy Efficiency Ratio (EER) as standard for air-conditioning rating systems. The EER is used for showing the electricity consumption of selected air conditioning systems. The regulation on mandatory application of the star rating to air-conditioning systems was established in 2017 and also affects all air-conditioning devices in Indonesia, including those already in operation (JDIH Kementrian ESDM, 2017). These results are presented in Fig. 9.

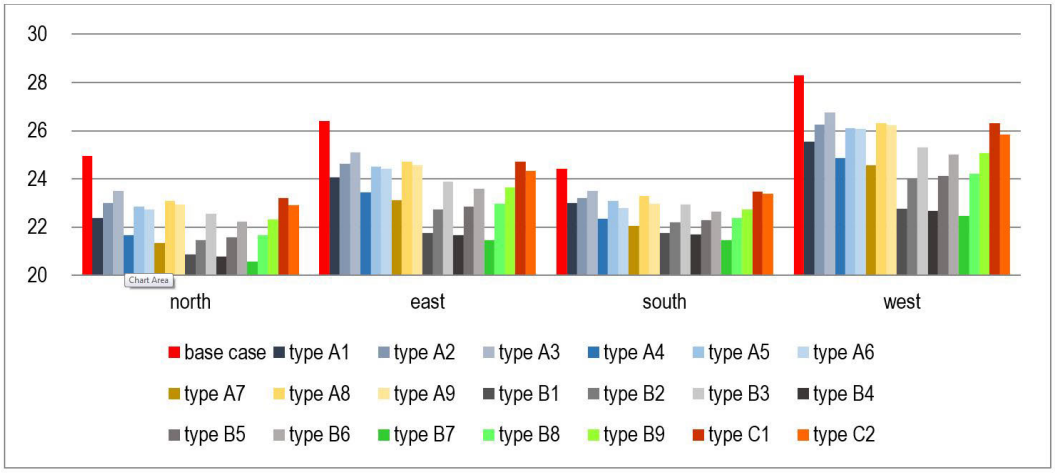

FIG. 9 Results of simulation of annual cooling energy (megaBtu/ h)

The base case shows the effect of the window on annual cooling energy for every orientation. The windows without sun shading on the west façade have an annual cooling energy of 28.29 mBtu/h, the highest among the orientations. In contrast, openings in the south require the minimum cooling energy of 24.43 mBtu/h, which amounts to 86% of the highest energy value. The difference between highest and lowest annual cooling energy is 3.86 mBtu/h.

The mini-louvres reduce the annual cooling energy, despite their small size. Denser mini-louvres give the lowest cooling energy in comparison to larger gaps between louvres, except for types A5 and A6, and types A8 and A9, which have louvre gap ratios of 1:2 to 1:3. On average, for all orientations, type A1 cuts the annual cooling energy by 2 percentage points compared to type A2. Type A2 cuts the annual cooling energy by 2 percentage points when compared to type A3. Type A4 cuts the annual cooling energy by 4 percentage points compared to type A5, while type A7 cuts it by 6 percentage points compared to type A8. However, changing mini-louvres' size to gap ratios to type A6 from type A5 and to type A9 from type A8 does not have a negative effect on the annual cooling energy. Rather than only considering direct sunlight, EnergyPlus also simulates reflective light and diffuse radiation (EnergyPlus Shading Calculations, 2019). A combination of a larger louvre size and a distance of only 1 mm from the window surface leads to a higher annual cooling energy, even though types A5 and A8 provide more shading than types A6 and A9, respectively. Significantly different results for annual cooling energy reduction occur even though types A1 to A9 have the same horizontal *koshi* design as types B1 to B9. On average, for all orientations, type A7, which is the best among the A types, consumes 88% of annual cooling energy compared to the base case, leaving a 5 percentage point difference in comparison with the amount consumed by type B7, 83%. Notably in the west façade, which requires the highest annual cooling energy, type A7 reduces consumption by around 13 percentage points in comparison to the base case but is inferior to type B7 which reduces it by around 21 percentage points. On average, for all orientations, types A1 to A9 reduce annual cooling energy by around 8 percentage points while types B1 to B9 reduce the annual cooling energy by 13 percentage points. There are two reasons for the higher annual cooling energy as a result of the sun shading being closer to the window's surface. First, closer sun shading makes the cooling energy higher because instead of only providing shading, the shading surface also reflects the direct sunlight onto the window's surface. The heat generated by the solar reflection has a negative impact on the cooling energy. The second reason is the heat radiation generated by the *koshi* mini-louvres themselves (EnergyPlus documentation, 2019). The small 1 mm distance between the horizontal *koshi* and the window allows the diffuse radiation to reach the window surface. . Placing the horizontal *koshi* mini-louvres further away from the surface, on the window frame, allowing a 50 mm distance from the window surface, reduces the annual cooling energy.

Increasing the gaps between mini-louvres in type B also increases the annual cooling energy. On average, for all orientations, increasing the louvre gap ratio from 1:1 to 1:2, from type B1 to B2, from type B4 to B5, and from type B7 to B8, increases the annual cooling energy by 3, 4, and 5 percentage points, respectively. On average, for all orientations, increasing the louvre gap ratio from 1:2 to 1:3, from type B2 to B3, from type B5 to B6, and from type B8 to B9, increases the annual cooling energy by 4, 3, and 2 percentage points, respectively. Type B7 shows the best performance among other sun shading devices by reducing the annual cooling energy by around 21 percentage points in the west, 19 in the east, 18 in the north, and 12 percentage points in the south orientation.

Common overhangs which are represented by types C1 and C2 show worse results than the proposed horizontal *koshi,* except for types A2 and A3, on average, for all orientation. Type C1 reduces the annual cooling energy by around 6 percentage points, while type C2 reduces it by around 7 percentage points. Type C1 reduces the annual cooling energy more than type A2 by around 1 percentage point and type A4, which is the worst sun shading device model in this study, by around 5 percentage points . Types C1 and A4 have a difference of 1.35 mBtu/ h. Types A2 and C2 cut the annual cooling energy by around 7 percentage points, but type C2 performs slightly better, by 0.15 mBtu/h. However, type C2 performs significantly worse than type B7, which can provide a reduction of around 17 percentage points , which is higher than the 7 percentage point reduction provided by type C2. This 10 percentage points, gap between types B7 and C2 equates to2.63 mBtu/h.

In summary, type B7 performs best among other sun shading types in this study of the annual cooling energy consumption. Type A4 is the best among all type A models, while type C2 is better than type C1. The results for each direction and average annual cooling energy saving of these models are presented in table 5.

TABLE 5 Annual cooling energy consumption of the best models (megaBtu/ h)

MODEL NAME	NORTH	EAST	SOUTH	WEST	AVERAGE
type A7	21,35	23,13	22,04	24,57	22,77
type B7	20,57	21,47	21,47	22,47	21,5
type C2	22,92	24,34	23,39	25,86	24,12

Based on the simulation results of annual cooling energy, the differences between the base case and all 20 types of sun shading are calculated to show the annual cooling energy saving. Since west-facing buildings in Jakarta have the highest annual cooling energy compared to other orientations, the energy savings are also highest for this façade. The annual cooling energy savings are used to calculate electricity consumption.

3.2 ELECTRICITY CONSUMPTION

There is a rating system for specific air-conditioning units based on the government regulation issued by the Ministry of Energy and Mineral Resources No. 57, 2017 (JDIH Kementrian ESDM, 2017) concerning the minimum energy performance standard. The air-conditioning unit is a single split wall mounted inverter and non-inverter type with a capacity of less than 27,000 Btu/ h. This type of air conditioning is commonly used for residential buildings and is suitable for following up the simulation results by calculating the electricity consumption for cooling in this study. One star, which is the lowest rating, is used for air-conditioning units which have an EER from 8.53 to less than 9.01. The highest rating, four stars, can only be obtained if the air-conditioning units have EER values equal to or more than 10.41. The simulation results from Fig. 9 are used for calculating the electricity consumption of four-star air-conditioning units. An EER 10.41 is used for the electricity consumption calculation to show that even using the best air-conditioning units, the proposed design of the mini-louvres has significant environmental and economic benefits. The electrical power consumption savings using the four-star air-conditioning unit are presented in Fig. 10.

For the west façade, which requires the highest electrical power to maintain the indoor conditions, type B7, which is the best model, can reduce the annual electricity consumption by 559.82 kWh. Type B8 reduces the annual electricity consumption by 391.28 kWh, while type B9 reduces it by 308.93 kWh, around 95% and 93% respectively in comparison with type B7. Type B7's horizontal *koshi* louvre size of 30 mm × 30 mm and gap ratio of 1:1 leads to greater savings than those given by type B4's 15 mm × 15 mm and B1's 12 mm ×12mm. Type B4 consumes 96% while type B1 consumes 95% of the annual electric in comparison with type B7's.The horizontal *koshi* louvre size and gap ratio of 1:2 of type B8 give the lowest saving of 367.62 kWh, while B5 saves 377.08 kWh and B2 saves 386.28 kWh of annual electricity consumption. Type B6's horizontal *koshi* louvre size and gap ratio of 1:3 shows the best reduction in annual electricity consumption, at 315.70 kWh, followed by type B9 with 308.93 kWh and type B3 with 285.99 kWh. This result shows that a mini-louvre size of 30 mm × 30 mm with a 1:1 gap works best in type B7, but adding larger gaps by changing the ratio

does not lead to better results. For the 1:2 ratio, the mini-louvres size of 12 mm × 12 mm is better than the other sizes, while for the 1:3 ratio, the size of 15 mm × 15 mm performs slightly better. For example, in the west orientation, types B6 and B9 have a difference of 6.76 kWh of the annual electricity consumption saving.

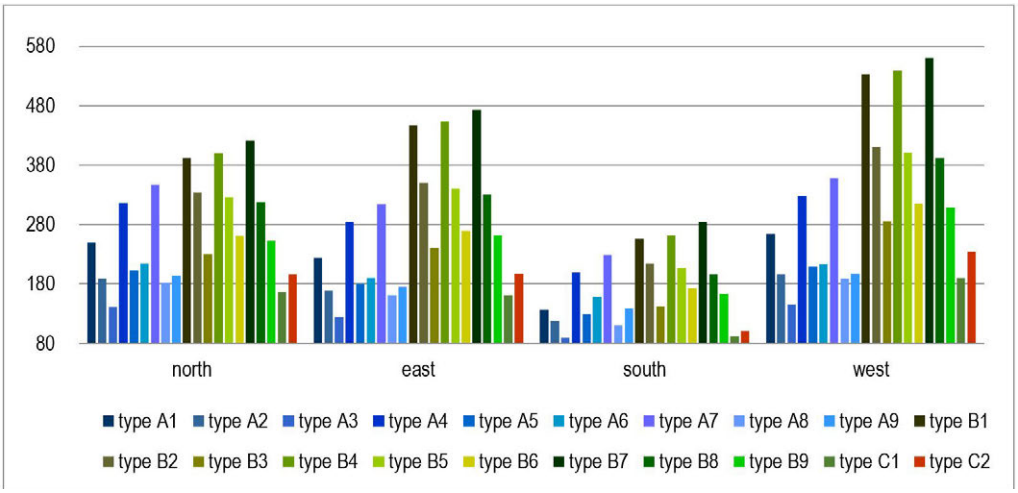

FIG. 10 Annual electricity consumption saving of four-stars air-conditioning unit (kWh)

3.3 COST OF PROPOSED HORIZONTAL *KOSHI* APPLICATION

The materials and construction price of the proposed sun shading are calculated to obtain the cost of the horizontal *koshi* application. A comparison between the energy savings and the application cost of the proposed sun shading can be shown to determine the economic benefits of each design by checking the simple payback period of each sun shading type. The L-shaped aluminium profiles are used for making horizontal *koshi*. The double-faced tape is used to directly attach the horizontal *koshi* to the outdoor glass window surface. A quarter of a metre of double-sided tape is used to attach each metre of L-shaped aluminium profile. Galvanized screws are used to attach the L-shaped aluminium profile forming the horizontal *koshi* to the window frame. Two screws are used per metre of L-shaped aluminium profile. For overhang sun shading, the material commonly used is reinforced concrete.

The price of the L-shaped aluminium profile with dimensions of 12 mm × 12mm, 15 mm × 15 mm, 30 mm × 30 mm are USD$ 0.29, $0.32, and $0.72 respectively. All three L-shaped aluminium profile sizes used in this study have the same thickness of 0.8 mm. The price of reinforced concrete for the overhang is USD$ 759.41/m^3. Outdoor double-sided tape costs USD$ 1.43/m while the galvanized screws cost USD$ 0.005 per piece. There is no special skill requirement to apply the proposed horizontal *koshi* so there is no labour cost for these types of sun shading. In this study, the price of the structural support for types C1 and C2 is excluded. The calculations of the total application costs of the proposed design types are presented in Fig. 11. The application cost of type C2 is USD$ 121.51, which is the most expensive type of sun shading of all the types proposed in this study. Type B6 is the cheapest, costing only USD$ 21.45. Even without considering the price of the structural support, the cost of applying the reinforced concrete overhang is higher than the cost of applying the horizontal *koshi*, except for type A1.

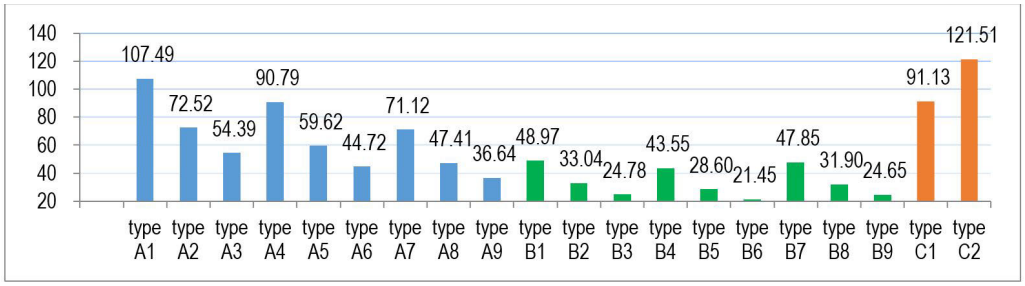

FIG. 11 Aun shading application cost (USD)

3.4 COMPARISON BETWEEN ELECTRICAL PRICE AND APPLICATION COST: ECONOMIC BENEFIT

The electricity price in Indonesia is Rp. 1,428.67/ kWh, or around $0.1 USD/ kWh, based on the March 2017 price, which is still in use as of the beginning of 2020 (Perusahaan Listrik Negara, 2020). The annual electricity price is calculated by multiplying the annual electricity consumption by the electricity price per kilowatt hour for all types of sun shadings, in all eight façades, using four-star air-conditioning units. The annual economic benefits from the energy saving are shown in Table 6 for every orientation of all sun shading types.

TABLE 6 Annual electricity payment saving (USD)

MODEL NAME	NORTH	EAST	SOUTH	WEST
type A1	24,93	22,4	13,69	26,42
type A2	18,93	16,86	11,77	19,65
type A3	14,13	12,47	8,93	14,59
type A4	31,66	28,48	19,95	32,79
type A5	20,26	18,03	13	20,88
type A6	21,4	19	15,8	21,37
type A7	34,69	31,38	22,97	35,79
type A8	18,11	16,14	11	18,86
type A9	19,42	17,49	13,96	19,77
type B1	39,2	44,66	25,56	53,22
type B2	33,47	35,03	21,5	41,1
type B3	23,03	24,06	14,26	28,6
type B4	40,04	45,31	26,2	53,93
type B5	32,59	34,1	20,71	40,14
type B6	26,12	26,95	17,29	31,57
type B7	42,18	47,3	28,44	55,98
type B8	31,69	33,01	19,65	39,13
type B9	25,26	26,24	16,35	30,89
type C1	16,69	16,11	9,29	19
type C2	19,62	19,75	10,08	23,42

The annual economic benefits from the total application cost (Fig. 11) and annual electricity payment saving (Table 5) of the proposed shading types are calculated to determine the payback period of each sun shading type. A faster payback period is better since the sun shading can still be used on the building. The simple payback periods of all sun shading types in all orientations are shown in Fig. 12.

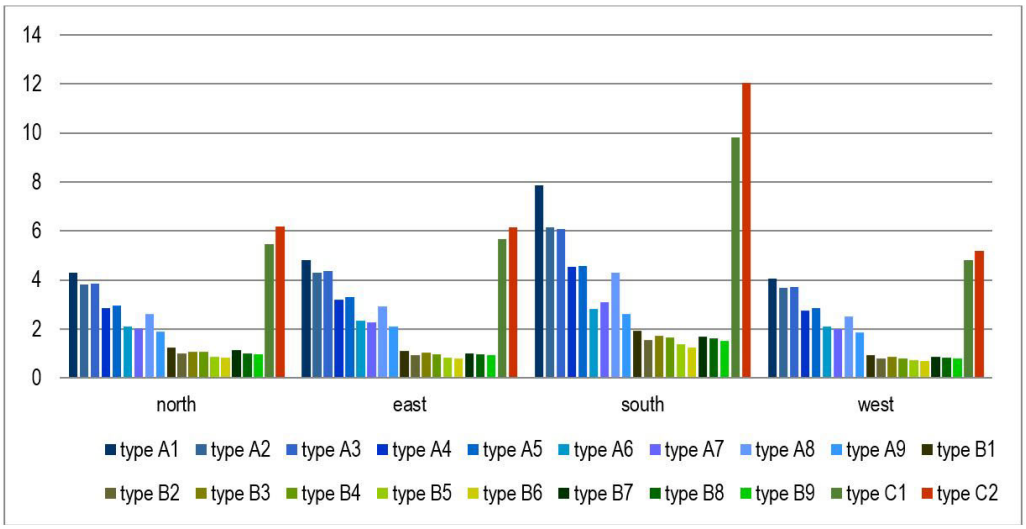

FIG. 12 Simple payback period of sun shading devices using four-star rated air-conditioning units (year)

The west orientation, which has the highest annual cooling energy has the fastest payback period of the sun shading applications. Type B6 shows the best performance, achieving a simple payback period of 0.68 years (around 8 months and 4 days), followed by type B5 with 0.71 years, and then types B2 and B9 with 0.8 years. All type B horizontal *koshi* can achieve simple payback periods of less than one year, and even the worst one, type B1, achieves a simple payback period of 0.92 years (around 11 months). Type A9 is the best of the type A sun shadings, having a simple payback period of 1.85 years (around 1 year, 10 months and 5 days). However, type A1, the worst of the A types has a payback period of 4.07 years (around 4 years and 21 days) although this is still faster than the type C1 overhang's payback period of 4.8 years (around 4 years 9 months and 16 days).

An opening in the south orientation has the lowest annual cooling energy consumption. This gives it the longest payback period among all of the orientations. Overhang type C2, which is the worst, has a payback period of 12.06 years (around 12 years 16 days). However, all type B applications have payback periods of less than two years. Type B6 is the best, with a payback period of 1.24 years (around 1 year 2 months and 26 days).

The results for other orientations fall between the results for west and south. Overall, the proposed horizontal *koshi* performs better than overhangs. Even though the same designs are used, the simple payback period of A types is longer than that of B types. The performance of A types in terms of annual cooling energy reduction is not as high as that of B types. Moreover, the application cost of A types is higher than B types.

4 CONCLUSION

Horizontal *koshi* mini-louvres have the effect of reducing the annual cooling energy in Jakarta, Indonesia, despite their small size. On average, in four orientations, horizontal *koshi* placed at the exterior surface of the window cut the annual cooling energy by around 5-12 percentage points in comparison with the base case. The cooling energy saved by the horizontal *koshi* on the window's exterior surface is similar to that saved by traditional overhangs, which can cut annual cooling energy consumption by around 6-7 percentage points in comparison with the base case. Placing horizontal *koshi* at the window frame improves the performance in terms of reducing the annual cooling energy. *Koshi* performs significantly better than overhangs, since around 10-17 percentage points reduction in the annual cooling energy can be achieved, depending on the type of horizontal *koshi*. All sun shading types in this study show their best performance in the west direction. Type B7, which is the best sun shading in this study, reduces around 21 percentage points of annual cooling energy in the west façade in comparison with the base case. On average, all of the proposed sun shading types cut the annual cooling energy in the west orientation by 12 percentage points in comparison with the base case. They perform worst for the south orientation, reducing the annual cooling energy by only around 7 percentage points of the average. Type B7 is the best sun shading among other tested models in this research, reducing annual cooling energy by 17 percentage points on average for all orientations. However, the construction cost is a consideration when applying the design to real buildings.

The double-sided tape price for attaching horizontal *koshi* is more expensive than the L-shaped aluminium profile in Jakarta. This makes the application cost of types A1 to 9 more expensive than those of types B1 to 9, even though they use the same designs. However, attaching horizontal *koshi* directly to the window's exterior surface gives a faster payback period than overhangs. Type A1, which is the worst among the A types has a payback period of 5.16 years, faster than that of type C1 which is 6.29 years. Type A9 is the best among other type A mini-louvres, with a simple payback period of 2.12 years. On the other hand, rather than just being environmentally friendly, placing horizontal *koshi* on the window frame is economically beneficial. Types B1 to 9 horizontal *koshi* can achieve a simple payback period of less than a year, even when using the highest rated, most effective four-star air-conditioning units in the west façade. Type B6 performs best, achieving a payback period of 0.68 years, when using the four-star air-conditioning unit. This means that horizontal *koshi* is economically beneficial during the building's operational period since it requires no maintenance. Horizontal *koshi* uses low technology. Its application does not require specific skills. The materials required to make horizontal *koshi* are widely available and relatively cheap. Horizontal *koshi* can be applied to new constructions as well as to old buildings as retrofits. The L-shaped aluminium profile does not occupy a lot of space in comparison to traditional overhangs due to its small size. It can be applied in space-limited area. It can also be applied to high rise buildings

Many further researches are possible following this study. The consideration of daylighting as well as privacy issues following the application of horizontal *koshi* mini-louvres can be researched. User acceptance of the proposed design can be studied to predict the probability that the application horizontal *koshi* will be successful. Location-based research is another possibility. As mentioned in the introduction to this paper, many tropical countries will demand a significantly higher cooling energy, such as India and Brazil. The results of this study show the possibility of applying such designs in other locations with conditions similar to those of Jakarta, Indonesia. Since the proposed design is simple, everyone can participate in reducing the need for cooling energy while saving money on electricity costs.

Acknowledgement

The first author's study and research at the University of Kitakyushu is supported by LPDP scholarship (Indonesia Endowment Fund for Education) from the Ministry of Finance, the Republic of Indonesia. This research was done at Fukuda Laboratory, the University of Kitakyushu, Japan.

References

Cho, J., Yoo, C., & Kim, Y. (2014). Viability of exterior shading devices for high-rise residential buildings: Case study for cooling energy saving and economic feasibility analysis. *Energy and Buildings*, *82*, 771–785. https://doi.org/10.1016/j.enbuild.2014.07.092

EnergyPlus (n.d.). Climate, Sky, and Solar Shading Calculations. Retrieved October 11, 2019 from https://www.energyplus.net/sites/default/files/docs/site_v8.3.0/EngineeringReference/05-Climate/index.html

EnergyPlus Documentation. (n.d.). Tips and Tricks Using EnergyPlus. Retrieved October 11, 2019 from https://energyplus.net/sites/default/files/pdfs_v8.3.0/Tips_and_Tricks_Using_EnergyPlus.pdf

El-Darwish, I., & Gomaa, M. (2017). Retrofitting strategy for building envelopes to achieve energy efficiency. *Alexandria Engineering Journal*, *56*(4), 579–589. https://doi.org/10.1016/j.aej.2017.05.011

Food for Rhino (n.d.). Ladybug tools for Rhinoceros 3d. Retrieved October 11, 2019 from https://www.food4rhino.com/app/ladybug-tools

Ghosh, A., & Neogi, S. (2018). Effect of fenestration geometrical factors on building energy consumption and performance evaluation of a new external solar shading device in warm and humid climatic condition. *Solar Energy*, *169*, 94–104. https://doi.org/10.1016/j.solener.2018.04.025

Hariyadi, A., Fukuda, H., & Ma, Q. (2017). The effectiveness of the parametric design 'Sudare' blind as external shading for energy efficiency and visibility quality in Jakarta. *Architectural Engineering and Design Management*, *13*(5), 384–403. https://doi.org/10.1080/17452007.2017.1296811

Hernández, F. F., Cejudo López, J. M., Peña Suárez, J. M., González Muriano, M. C., & Rueda, S. C. (2017). Effects of louvers shading devices on visual comfort and energy demand of an office building. A case of study. *Energy Procedia*, *140*, 207–216. https://doi.org/10.1016/j.egypro.2017.11.136

Huang, Y., Niu, J., & Chung, T. (2012). Energy and carbon emission payback analysis for energy-efficient retrofitting in buildings—Overhang shading option. *Energy and Buildings*, *44*, 94–103. https://doi.org/10.1016/j.enbuild.2011.10.027

JDIH Kementrian ESDM. (2017). Peraturan Menteri ESDM 57 tahun 2017. Retrieved November 21, 2019, from https://jdih.esdm.go.id/index.php/web/result/1725/detail

Perusahaan Listrik Negara. (2020). Tariff Adjustment. Retrieved February 6, 2020, from https://www.pln.co.id/statics/uploads/2020/01/Januari-Maret-2020.jpg

Ralegaonkar, R. V., & Gupta, R. (2010). Review of intelligent building construction: A passive solar architecture approach. *Renewable and Sustainable Energy Reviews*, *14*(8), 2238–2242. https://doi.org/10.1016/j.rser.2010.04.016

Samaan, M. M., Farag, O., & Khalil, M. (2018). Using simulation tools for optimizing cooling loads and daylighting levels in Egyptian campus buildings. *HBRC Journal*, *14*(1), 79–92. https://doi.org/10.1016/j.hbrcj.2016.01.001

Skejic, D., Boko, I., & Neno, T. (2015). Aluminum as a material for modern structures. *Gradevinar*, *67*(11), 1075–1085. https://doi.org/10.14256/JCE.1395.2015

Stacey, M., & Bayliss, C. (2015). Aluminium and durability: Reviewed by inspection and testing. *Materials Today: Proceedings*, *2*(10), 5088–5095. https://doi.org/10.1016/j.matpr.2015.10.100

The International Energy Agency. (n.d.). Statistics. Retrieved November 21, 2019, from https://www.iea.org/statistics/

The International Energy Agency. (2017a). Energy Efficiency 2017: Laporan Khusus Efisiensi Energi di Indonesia. Retrieved November 21, 2019 from https://www.iea.org/publications/freepublications/publication/EnergyEfficicency2017IndonesiaFocusBahasaIndonesia.pdf

The International Energy Agency. (2017b). *Southeast Asia Energy Outlook 2017*. https://doi.org/10.1787/9789264285576-en

The International Energy Agency. (2017c). Space Cooling Energy Insight Brief. Retrieved from https://www.iea.org/publications/freepublications/publication/SpaceCoolingEnergyEfficiencyInsightsBrief.pdf

The International Energy Agency. (2018). *Energy Efficiency 2018: Analysis and Outlooks to 2040*. Retrieved from https://doi.org/10.1787/9789264024304-en

The International Energy Agency. (2019). Southeast Asia Energy Outlook 2019. Retrieved from https://webstore.iea.org/download/direct/2887?fileName=Southeast_Asia_Energy_Outlook_2019.pdf

The Onebuilding. (n.d.). Jakarta Indonesia TMY3. Retrieved October 3, 2019, from http://climate.onebuilding.org/WMO_Region_5_Southwest_Pacific/IDN_Indonesia/JW_Jawa/IDN_JW_Jakarta.Obs.967450_TMYx.zip

The World Bank (n.d.). Urban population (% of total population) Indonesia | data. Retrieved February 6, 2020, from https://data.worldbank.org/indicator/SP.URB.TOTL.IN.ZS?locations=ID&view=chart

The World Bank (2019, December 11). Overview [Text/HTML]. Retrieved February 6, 2020, from World Bank website: https://www.worldbank.org/en/country/indonesia/overview

The Wondermetals. (2019, July 30.). The many benefits of aluminum louvers. Retrieved February 6, 2020, from http://wondermetals.com/benefits-of-aluminum-louvers/

Tsushi-nikai. (n.d.). Retrieved November 21, 2019, from http://www.hachise.com/kyomachiya/features/exteriorKoshi.html

Hygrothermal Potential of Applying Green Screen Façades in Warm-dry Summer Mediterranean Climates

Claudio Vásquez*, Renato D'Alençon, Pedro Pablo de la Barra, Francisca Salza, Madeleine Fagalde

* Corresponding author
Pontificia Universidad Católica de Chile, Architecture and Facades research group, Chile, cvz@uc.cl

Abstract

Green screen façades (GSF) remain an unexplored field of study in warm-summer climates with Mediterranean conditions.

This research aims to establish whether or not these thermal comfort façade systems are worth developing in cities with dry summers and a high range of thermal oscillation.

A comparative study of four buildings´ green screen façades in Santiago de Chile was carried out, with different orientations and plant species, both in type and state of maturity.

Temperature and relative humidity outside and inside the cavity were measured during summer days. It was observed that, during the day, interior relative humidity was higher while the temperature was lower, reverting this behaviour during the afternoon and night. This result accounts for the existence of two different daily periods: passive cooling through evapotranspiration in the presence of solar radiation - reaching up to an 8°C temperature reduction and a 30% increase of the relative humidity - and passive heating in its absence.

The results show that the determining parameters in the behaviour of a green screen façade in a temperate-warm climate are, first, the orientation of the façade, and second, the density of foliage. Regarding orientation, it was also found that the sun exposure was directly proportional to the performance of a green screen façade.

Keywords

Green façade, green screen façade, thermal comfort

DOI 10.7480/jfde.2020.2.5109

1 INTRODUCTION

Global warming has a high impact in densely populated urban areas. In the coming years, temperatures are expected to increase in all major cities, including Santiago de Chile. Projections suggest an increase in temperatures of 2° to 4°C throughout the country, and a reduction of around 40% of the rainfall in the central area, where the city of Santiago is located (Cifuentes & Mesa, 2008). Among the strategies to mitigate the effects of climate change, the increase of urban green areas is widely accepted, since they promote the creation of microclimates capable of regulating the phenomenon of urban heat islands (Cheng, Cheung, & Chu, 2010; Hunter et al., 2014; Mohamed & Magdy, 2012), due to the evapotranspiration of plants. Evapotranspiration is defined as the loss of moisture from a surface, in this case the soil in which the plant is supported, by direct evaporation together with the loss of water by transpiration from vegetation. It is an organic process that can be used as a passive regulator of temperature and the relative humidity of the environment, depending on the application conditions of the plant material.

Increasing urban green areas by 10% allows a temperature reduction of 2.5°C locally, due to their contribution to shade and humidity (Cameron, Taylor, & Emmet, 2014), thus promoting the reduction of environmental pollution and preservation of biodiversity. In buildings, green façades and roofs allow greater urban vegetation, reducing heat loss in winter and avoiding overheating in summer (Schettini et al., 2016; Cameron et al., 2014; Pérez, Rincón, Vila, González, & Cabeza, 2011). By regulating the surface temperature of the walls, green façades hold the potential to improve the energy performance of buildings (Carpenter & Sikander, 2015).

Green walls, or vertical greening systems (VGS), can be subdivided into two main systems: living walls and green façades. Living walls allow plants to grow through the direct reception of moisture provided by a substrate adhered to the wall in a continuous or modular way, creating a regular growth along the surface; on the other hand, green façades consist of climbing plants which grow along the wall covering it, in a direct or indirect manner (Hunter et al., 2014; Manso & Castro-Gómez, 2016). Direct green façades are those in which the vegetation grows attached to the wall through self-clinging climbers or self-adhesive pads that adhere to the building's exterior walls. Indirect green façades are those in which the vegetation is arranged at a distance from walls and openings using support structures that assist the upward growth of a wider variety of climbing plants (Hunter et al., 2014), working as a solar screen that generates a camera or thermal buffer that blocks the incidental solar radiation, while at the same time reducing the effect of wind on the surface of the façade.

Solar screens are external shading devices, built with different materials configurated as plans arranged parallel to the windows or transparent surfaces of a façade, with the purpose of protecting them from solar gains and visual discomfort produced by glare. Indirect green façades are a special kind of solar screen that contributes to the thermal control of the building through the use of biomaterial, such as plants, and can therefore be considered as a green screen façade (GSF).

Unlike conventional sunscreens, GSF work passively and dynamically. Only a small proportion of the incidental sun radiation is destined to photosynthesis and the rest contributes to evapotranspiration that regulates temperature within the cavity. Research results have shown that, with the same incidental sun radiation, the use of GSF can reduce to a half the surface temperature on the walls, in comparison to that of conventional sun protection. Vegetation surface temperature never exceeds 35°C and sun protection can easily reach 55°C. The use of vegetation allows for the reduction of cooling demands of up to 20% in comparison to that of conventional sunscreens (Mohamed & Magdy, 2012).

For the design of GSF, the vegetation must consider the density of the foliage, its evapotranspiration potential and the planting substrate (Pérez et al., 2011). Different plant species have their own coverage capacity and leaf area index, and therefore their own light and solar transmission coefficients (Susorova, Angulo, Bahrami, & Stephens, 2013; Dahanayake, Chow, & Hou, 2017; Hoelscher, Nehls, Jänicke, & Wessolek, 2016; Susorova et al., 2013; Pan, Wei, Lai, & Chu, 2020). It is important to select species with a high moisture retention capacity and a high leaf density to optimise water use (Pérez et al., 2011). At the same time, the availability and local adaptation of plants must also be considered (Hoelscher et al., 2016) (Cameron, Taylor, & Emmet, 2014). In GSF, species that allow the growth of vertical foliage and the least irrigation substrate requirements are usually used. The support structure is decisive in their growth and in the density of their foliage, since plants tend to increase their biomass in the roots, so adequate vertical support becomes fundamental to their growth (Den Dubbelden & Oosterbeek, 1995).

In experimental studies of GSF, the most widely used indicators are: exterior and interior surface temperature of the walls; relationship between the leaf surface and the planting substrate; foliage density; orientation; plant density; incidental sun radiation; outdoor air temperature; cavity air temperature; and wind speed (Safikhani, Megat, Remaz, & Baharvand, 2014; Hunter et al., 2014). In hot and humid climates, studies have recorded that temperatures on green façades can decrease to 20.8°C on the exterior surface of the façade and 7.7 °C in the interior space, showing reductions of 3.1°C within the cavity (Chen, Li, & Lui, 2013). In Mediterranean climates, reductions between 3°C and 4.5°C during the day and increases between 2°C and 3°C during the night have been recorded (Schettini et al., 2016). This type of study requires laboratory infrastructure in order to control the various parameters on a regular and controlled basis.

Studies based on digital modelling face various difficulties due to the indeterminate geometry and density of vegetation and the difficulty of incorporating evapotranspiration in the model. The most common method used is to experimentally calibrate the models (Safikhani et al., 2014; Šuklje, Medved, & Arkar, 2016). This allows for the prediction of the optical properties of the vegetation and adjustment of the energy balance from the metabolism of the plants, which is associated with the reference climate of the experiment (Allan & Kim, 2016). Experimentally verified calculation modules in the TRNSYS software have shown that green façades have a greater impact in hot climates, since they reduce the cooling demands if provided with an efficient irrigation system (Djedjig, Bozonnet, & Belarbi, 2015). A model based on vegetation morphology has also been proposed and experimentally verified, determining that, in order of importance, the relevant climatic variables are: solar radiation; wind speed; relative humidity; and outdoor air temperature exposure (Susorova et al., 2013). This method also requires a laboratory infrastructure to control the calibration process accurately.

Measurements in buildings are more usual, as the results are variable and valid only to the specific climates and orientations of the case, since they determine the temperature, relative humidity, and solar radiation, which are, in these cases, the most usual variables to be tested. However, orientation is decisive in the performance of green façades since it determines the incidental solar radiation, its duration and intensity throughout the day (Djedjig, Bozonnet, & Belarbi, 2015; Pérez et al., 2017). In Berlin - marine coast climate, Cfb - measurements were conducted in buildings with different orientations, shading being determined as the main factor, followed by evapotranspiration (Hoelscher et al., 2016). In Shanghai - humid subtropical climate, Cfa - the performance before and after the installation of GSF for south and north orientations was compared, determining an average daily reduction of 0.4°C and 0.2°C, and a maximum of 5.5°C and 3.3°C, respectively (Yang, Yuan, Zhuang, & Yao, 2018). In Hong Kong -humid subtropical climate, Cwa - it was determined that on sunny, cloudy or rainy days, 1.30, 0.84, and 0.71 kW/h could be saved in air conditioning respectively,

reducing energy consumption during summer by 16% (Pan & Chu, 2016). Also in Hong Kong, research determined that on sunny and cloudy days the orientation had an important effect on the performance of the GSF, reaching a reduction of 6.1°C within the cavity and of 3.6°C in the interior space (Pan, Wei, & Chu, 2018).

In Chile, the integration of vegetation on façades has been carried out intuitively by some architects, with no studies that support its effectiveness. Currently, there are only studies related to the phenomenon of urban heat islands associated with environmental pollution, showing that vegetation improves the city temperatures (Romero, Irarrázaval, Opazo, Salgado, & Smith, 2010). This work aims at evaluating the potential of the hygrothermal performance of the GSF, to determine if and how evapotranspiration works in the climate of Santiago that, according to the Köppen climate classification, is located in a "warm-dry summer Mediterranean" climate zone (33°27′ S-70°41′ W), characterised by dry and warm summers (38.5% average daily relative humidity)(Peel, Finlayson, & McMahon, 2007), a wide thermal oscillation (15°C daily and 13°C in annual maximum ranges) and high levels of sun irradiation (above 1000 W/m^2 in summer).

Our goal is to establish a baseline that allows future experimental studies to be opened, depending on whether or not GSF have potential for application in dry and warm climates. The study was made through the measurement of four case studies with different orientations and different plant species, both in their type and in their state of maturity, applied in different architectural configurations of the façade.

2 EXPERIMENT

2.1 PRESENTATION OF CASE STUDIES

This study was conducted in the city of Santiago de Chile (33.46° lat. South, 70.65 ° long. West, 580 m.a.s.l.) in order to comparatively evaluate the performance of GSF in four case studies. Temperature and relative humidity outside and inside the cavity were measured at three different heights to assess the performance in each case.

2.1.1 Case 1

Case 1 is a three-storey office building, where the GSF has a north-west orientation that covers its entire height. The support consists of pillars and an expanded metal mesh spaced 70 cm from the building enclosure (Fig. 1). The plant species used is called *Parthenocissus quinquefolia*, commonly known as "Virginia creeper", and was planted directly into the ground. It is a climbing species native to North America and is often used for ornamental purposes. It is characterised for being a woody plant with climbing habits and deciduous leaves, of fast and intense growth, able to reach 20 meters of height in its mature state. It adheres firmly to the support structure due to the presence of tendrils with suction cups at the tip of their leaves, that facilitate their vertical growth. Its leaves range from 3 to 20 cm long and 10 cm wide, divided into five elongated leaflets with serrated edges. It changes colours that vary from a dark green in summer to an intense red colour in autumn, until they fall off the branches as the cold season progresses. It can be placed in semi-shaded areas or those exposed directly to sun, without distinction. Although it grows in any type of soil, the foliage will be denser if planted deep in a humid ground.

FIG. 1 Schematic section and north-west façade of Case 1

The pictures in Fig. 1 show that at the time of taking the measurements, the foliage of the plants was dense, and the leaves had regular sizes, constituting multiple layers that reached a thickness of at least 30 cm. Among those analysed, this is the case in which vegetation is most dense and the only one in which the plant grows from the natural soil.

2.1.2 Case 2

Case 2 is a four-storey building in a university campus, with a north-facing GSF. It grows in planters located on the second and fourth floors, along the entire façade. The support consists of vertical elements and horizontal wiring 82 cm apart from the glazing (Fig. 2). The plant species used is a climber called *Wisteria sinensis* or "Chinese wisteria". It is native to China and belongs to the legume family. It is characterised by high density deciduous foliage that is lost when autumn arrives. The leaves reach up to 25 cm long, divided into between 7 to 13 leaflets of 2 to 6 cm length each. Being a plant of powerful growth and thick trunks, it needs firm structures capable of supporting its weight, able to reach heights of up to 30 meters. It stands out for its fragrant flowering in early spring, before its leaves sprout, lasting for several months. It is considered shade tolerant, but it only blossoms when exposed to the sun. Presenting an important root system, it requires deep soils, ideally directly into the ground.

FIG. 2 Schematic section and north façade of Case 2

The photographs in Fig. 2 show that, in this case, the foliage of the vegetation varies in height without covering the entire façade because its planting has been recent, and the expected growth at the time of taking the measurements has not yet been achieved. However, in some areas, the leaves´ density is high, reaching a thickness of 15 to 20 cm. The measuring instruments were installed in this area of the second floor.

2.1.3 Case 3

Case 3 is a seventeen-storey office building, located in a financial district (Fig. 3). The GSF is oriented to the south-west and has been planted every three floors at the top of the façade. The support consists of horizontal and vertical profiles that follow the curved shape of the façade, at a distance of 120 cm from the face. The plant species used, as in Case 1, is the *Parthenocissus quinquefolia* or "Virginia creeper", with characteristics that have already been explained. Unlike the previous case, these are planted in large planters to provide them with sufficient substrate to their roots.

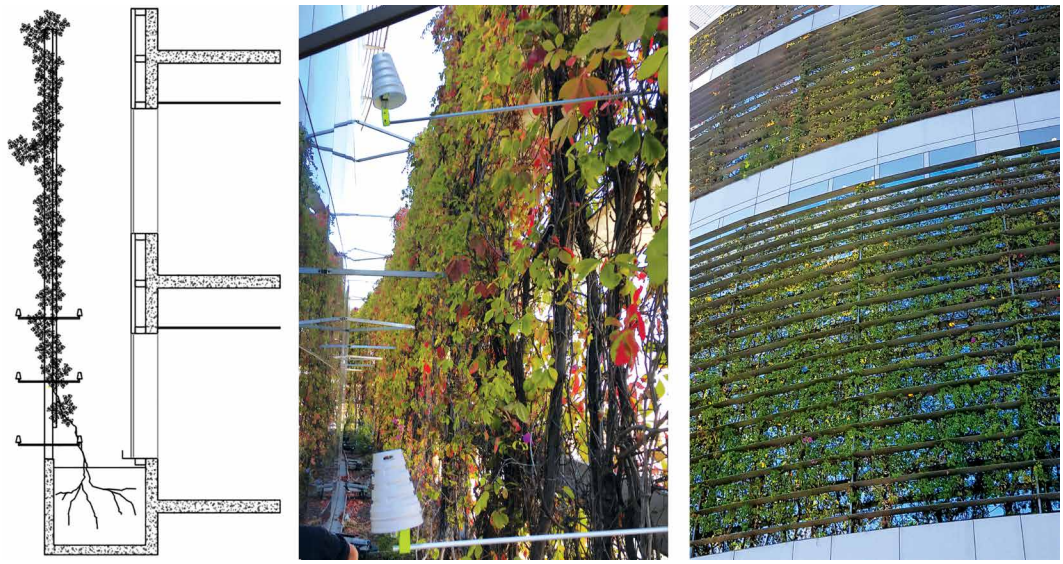

FIG. 3 Schematic section and south-west façade of Case 3

The photographs in Fig. 3 show that the foliage of the vegetation is variable. As it is a species in an adult state, the vegetation near the substrate presents a greater amount of woody branches which were predominant at the time of measurement, so its density can be considered average in relation to the set of cases.

2.1.4 Case 4

Case 4 is a twelve-storey high-rise university building. The GSF is located on the north-east façade and has been planted in planters on each floor. The support consists of vertical profiling and horizontal wiring separated 105 cm from the building's façade (Fig. 4). The species used was a perennial climber named *Jasminum grandiflorum*, known as "Spanish jasmine", native to the Himalayas and Southern Asia. It is characterised by irregular growth, with branches that wrap around each other, forming a wide set that are difficult to keep orderly. However, in the presence of a support, it can climb up to 6 or 7 m in height, forming a hanging semi-dense crown, depending on the support, since it does not reach it spontaneously. Its leaves are green and compound, divided into 5 to 7 leaflets of 2 cm in length. Its flowering is continuous, from the end of spring until the beginning of autumn, and may continue even in winter. This species is only adapted to warm-

temperate climates as it does not resist cold very well and it is recommended that it be planted in sunny soil and protected from the wind.

FIG. 4 Schematic section and north-east façade of Case 4

The photographs in Fig. 4 show that the density of the foliage is low, related to the set of case studies, practically comprising a layer of leaves as protection. In addition, the growth is not uniform on the façade since its maintenance is the responsibility of the building managers. The location of the instruments was defined at the point where the highest growth maturity and foliage uniformity were found.

Table 1 summarises the characteristics of the four cases studied, reflecting their diversity, an issue that will allow us to have a comparative analysis of different conditions and characteristics of application of GSF in Santiago de Chile.

TABLE 1 Characteristics of the case studies synthesis

	CASE 1	CASE 2	CASE 3	CASE 4
Species Sc. Name	Parthenocissus quinquefolia	Wisteria sinensis	Parthenocissus quinquefolia	Jasminum grandiflorum
Foliage type	Deciduous	Deciduous	Deciduous	Perennial
Foliage density	Very high	High	Medium	Low
Building use	Offices	Educational	Offices	Educational
Green façade orientation	North-West	North	South-West	North-East

2.2 MEASUREMENTS

The goal of the measurements was to establish the hygrothermal performance of the GSF of the case studies to detect the effect of evapotranspiration within the different conditions in which they are located. As for the measurement, Voltcraft DL-121TH Data Logger Thermohygrometers were used. Measurements were carried out over five days in March 2019. Temperature and humidity records were made in intervals of one minute. Fig. 5 schematically shows that the measuring instruments were installed at three different heights (0.5, 1.5, and 2.5m from the monitoring floor) to work within the average. Temperature and relative humidity, inside and outside the cavity, were measured to compare the differences. The sensors were protected from direct solar radiation.

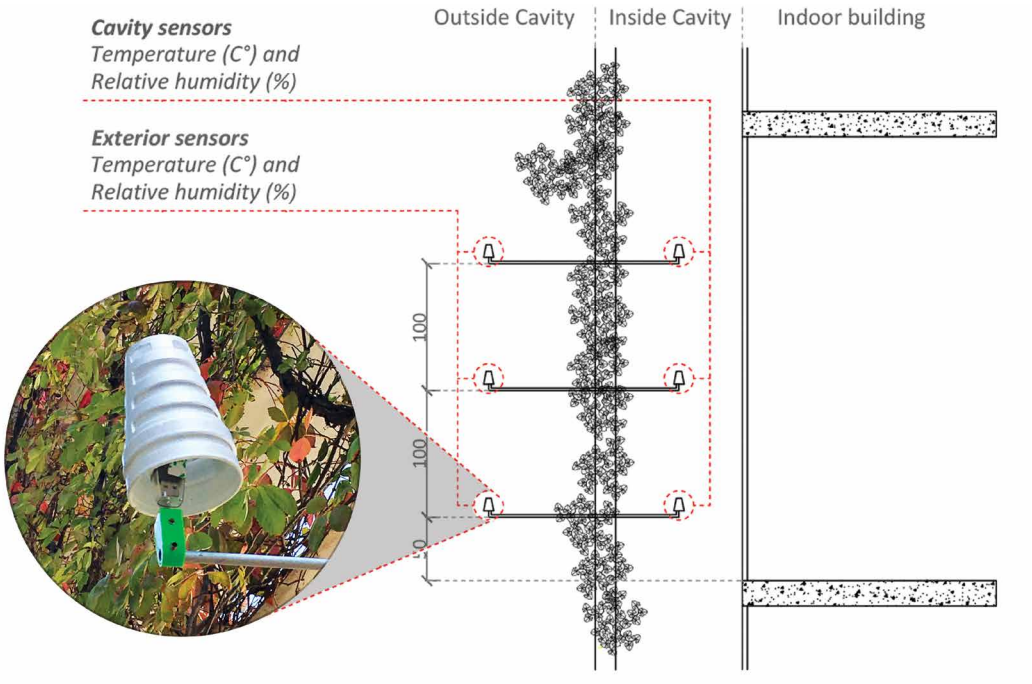

FIG. 5 Sensors location

Fig. 6 shows the climatic conditions during the days measured, with different cloud conditions, as shown by the icons above. Day 2 was completely sunny and day 4 was completely cloudy. The other days were partially clouded and sunny throughout the day. Temperatures ranged from 10° to 27° C, and the maximum daily relative humidity was close to 90% at noon and around 30 to 40% in the afternoon. Sun radiation measured in the horizontal plane was correlative to cloud cover, reaching between 800 and 900 W/m^2 as a daily maximum.

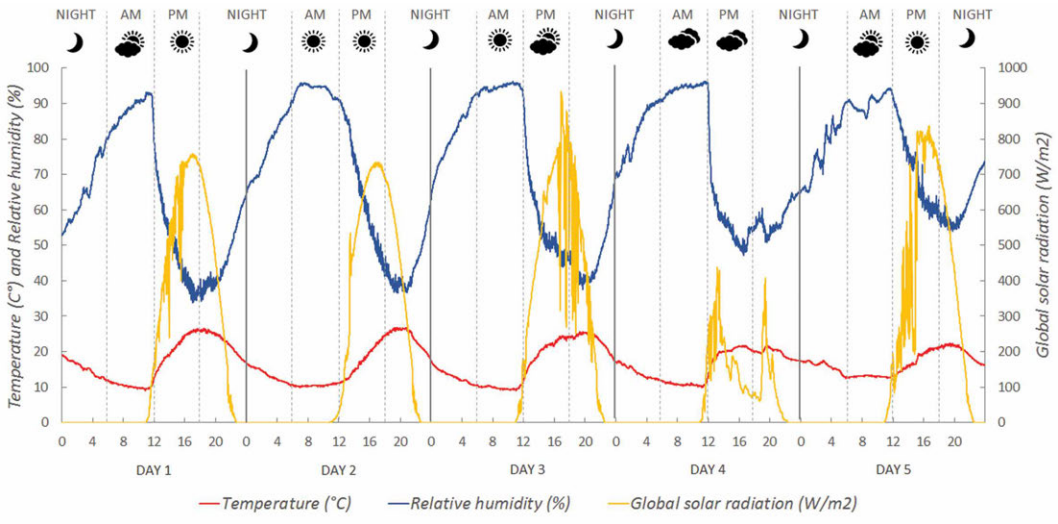

FIG. 6 Weather conditions March 27-31, 2019 in Santiago de Chile

3 RESULTS

In general, it was observed in all cases, that inside the cavities of the GSF, in the afternoon and at night, the relative humidity outside was higher and the temperature was lower. However, during the day this behaviour was reversed, with a temperature decrease and a relative humidity increase with respect to the outside. This performance accounts for the existence of two different daily periods: passive cooling by evapotranspiration in the presence of sun radiation and passive heating in its absence.

Table 2 summarises the global statistics of temperature and humidity differentials for each case in the periods of passive cooling due to evapotranspiration, which is the one of interest for the climate of Santiago. The differential is obtained by calculating the difference between the data recorded outside and inside the cavity, meaning when result is zero, inside and outside data are equivalent. Otherwise, the minimums differential normally corresponds to cloudy days and the maximums to sunny days.

TABLE 2 Global statistics of temperature and humidity differentials

	CASE 1		CASE 2		CASE 3		CASE 4	
	Temp. (°C)	R. Hum. (%)	Temp. (°C)	R. Hum. (%)	Temp. (°C)	R. Hum. (%)	Temp. (°C)	R. Hum. (%)
Maximum	8,0	30,4	4,2	14,4	2,5	6,4	4,3	6,9
Minimum	0,0	0,0	0,0	0,0	0,0	0,0	0,0	0,0
Average	2,8	8,8	1,4	4,6	0,6	1,5	0,9	1,6
Std. Dev.	2,2	6,5	1,1	3,0	0,6	1,2	0,8	1,4

The results of each case study are presented in the following.

3.1 CASE 1

Fig. 7 shows that the passive cooling effect due to evapotranspiration occurred between approximately 8:00 a.m. and 5:00 p.m., with an observed average temperature reduction of 2.8°C, a maximum of 8°C, and an increase in relative humidity average of 8.8%, with a maximum of 30.4%. The standard deviations of temperature and relative humidity were of 2.2° C and a 6.5%, respectively, which accounts for constant cooling, with moderate oscillating relative humidity. On cloudy days, the hydrothermal effect of the cavity decreased, and the relative humidity worked less intensively. On sunny days, the effect of evapotranspiration was regular from morning until the hours of greatest global radiation, due to its north-west orientation.

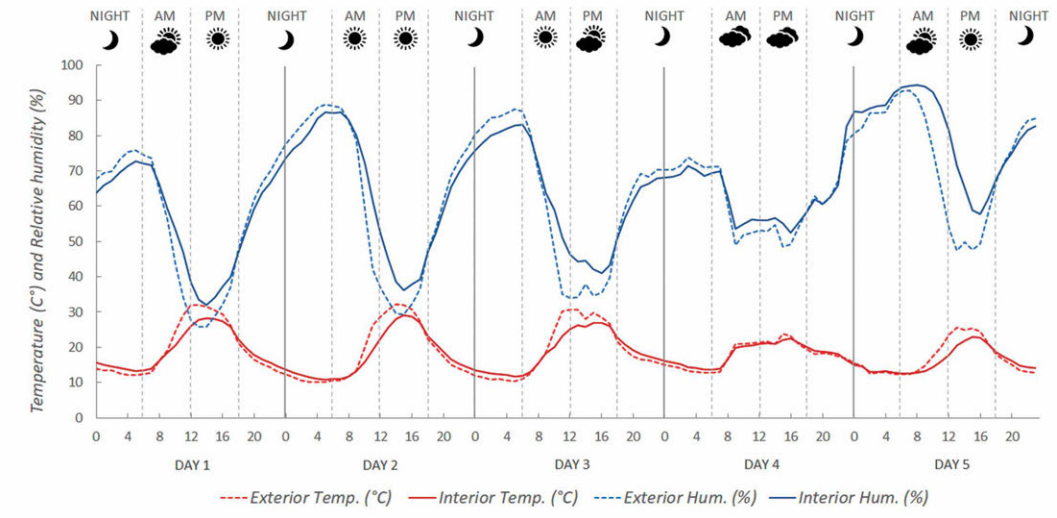

FIG. 7 Daily interior/exterior cavity temperature and relative humidity recorded for Case 1

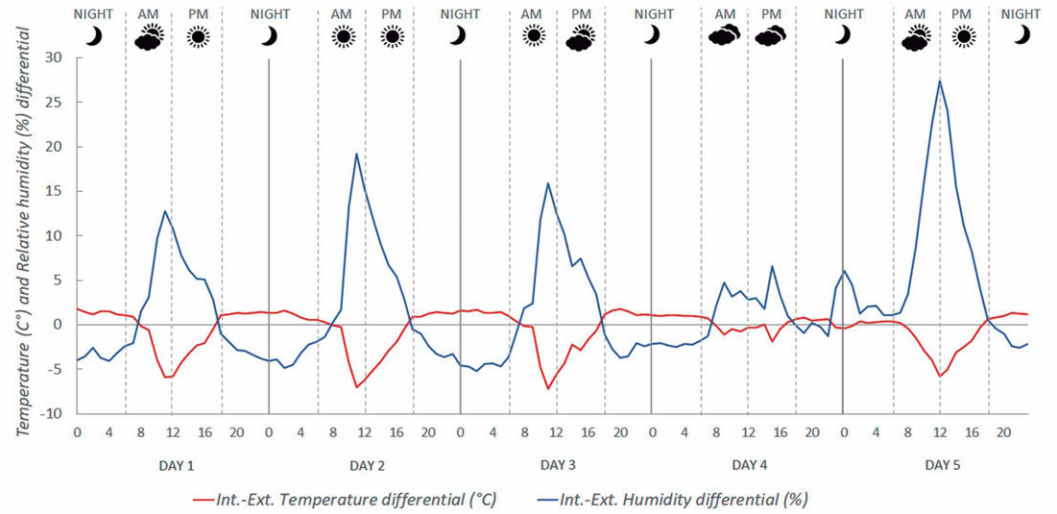

FIG. 8 Daily interior/exterior cavity temperature and relative humidity recorded for Case 1

Fig. 8 shows that, inside the cavity, there were temperature reductions every day during the passive cooling period (day) and temperature increases in the passive heating periods (afternoon-night). The hygrothermal inversion occurred at 8:00 and 17:00. The decrease in passive cooling was also observed on day 4, which was cloudy, compared to sunny or partial days, although the hygrothermal inversion schedule was persistent.

3.2 CASE 2

Fig. 9 shows that the passive cooling effect due to evapotranspiration worked between approximately 9:00 a.m. and 6:00 p.m., reaching an average reduction of 1.4°C and a maximum of 4.2°C, with an average increase in the relative humidity of 4.7% and a maximum of 14.4%. The standard deviations of temperature and relative humidity were of 1.1°C and a 3.0%, respectively, which accounts for persistent but moderate passive cooling. On the other hand, the difference between cloudy and sunny days is less relevant, especially in the temperature differences of the cavity with respect to the outside. Passive cooling was more relevant throughout the morning, decreasing the temperature at midday, even though the increase in relative humidity was more persistent. The regularity of the performance of this GSF can be associated with its north orientation, which ensures sun exposure for most of the day.

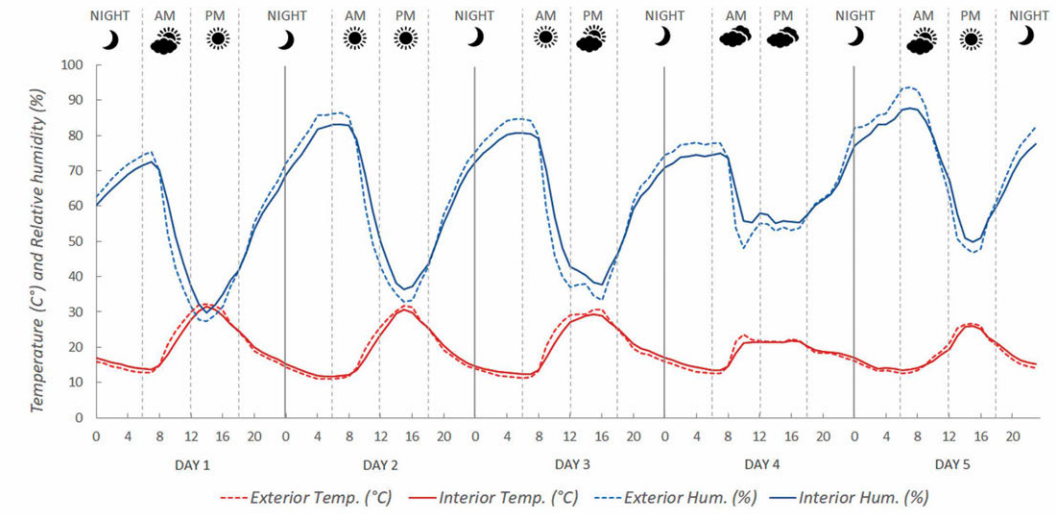

FIG. 9 Daily interior/exterior cavity temperature and relative humidity recorded for Case 2

Fig. 10 shows how, inside the cavity, the phenomenon of hygrothermal inversion was also observed at 9:00 and 18:00 and passive cooling was similar on both cloudy and sunny days, with more significant increases in relative humidity in the cooling periods, that is, when the foliage received solar radiation.

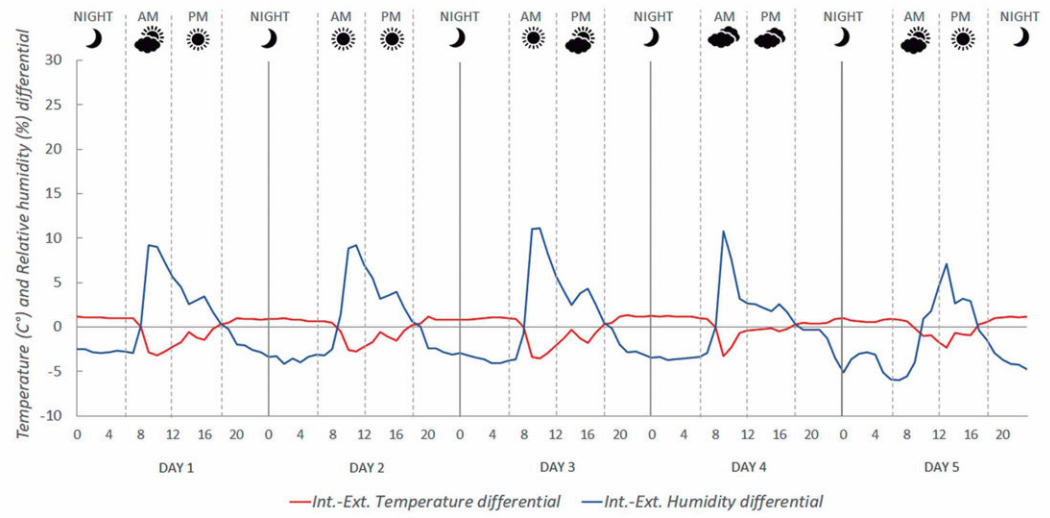

FIG. 10 Daily interior/exterior cavity temperature and relative humidity differential recorded in Case 2

3.3 CASE 3

Fig. 11 shows that the passive cooling effect due to evapotranspiration was active between approximately 9:00 a.m. and 7:00 p.m., reaching an average reduction of 0.6°C, a maximum of 2.5°C, and an average increase in relative humidity of 1.5%, with a maximum of 6.4%. The standard deviations of temperature and relative humidity were of 0.6°C and 1.5%, respectively, which shows persistent passive cooling, although of low overall intensity. The performance of this particular GSF is relatively low and almost irrelevant on cloudy days; however, on sunny days it is possible to appreciate that it reached its peak between approximately 15:00 and 18:00.

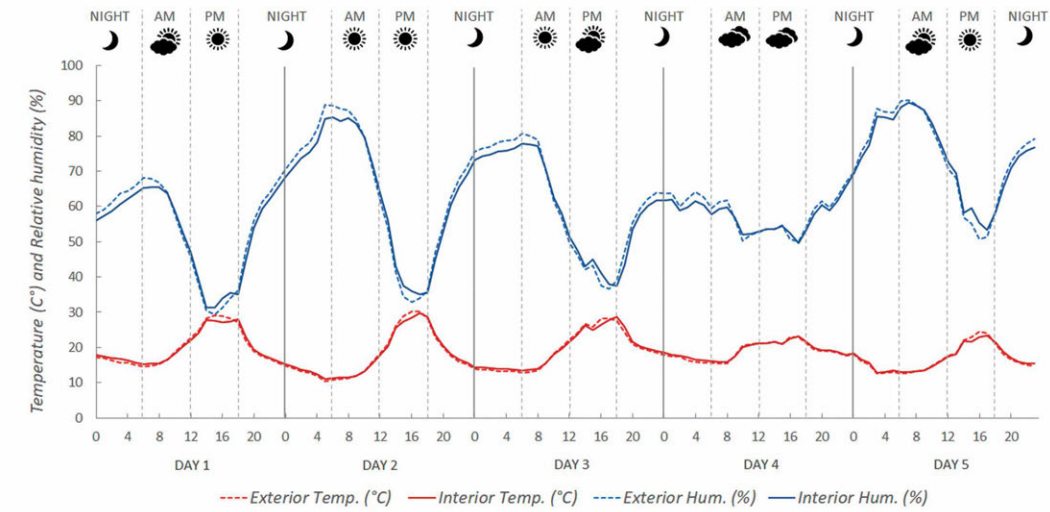

FIG. 11 Daily interior/exterior cavity temperature and relative humidity recorded for Case 3

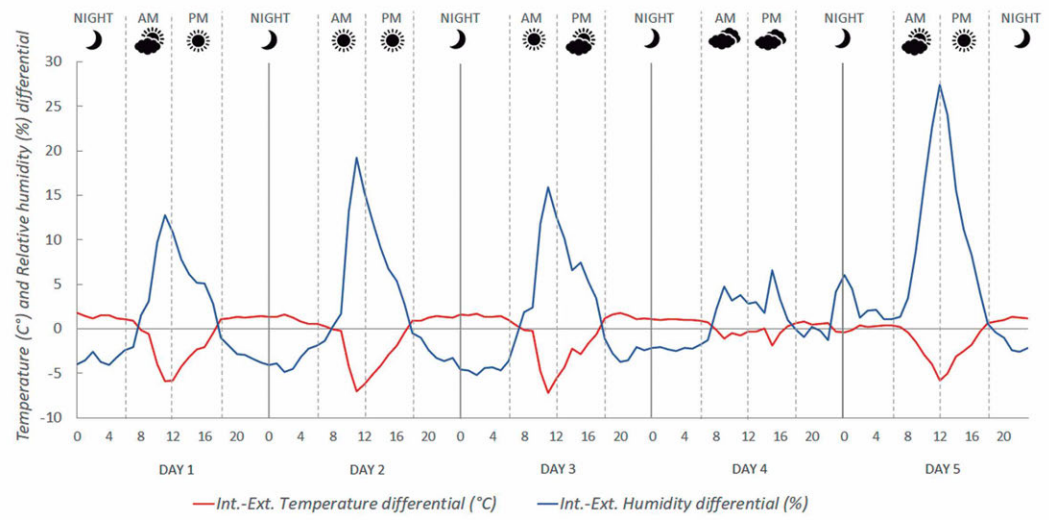

FIG. 12 Daily interior/exterior cavity temperature and relative humidity differential recorded in Case 1

Fig. 12 shows that, within the cavity, the same phenomenon of thermal hygrothermal inversion occurred between day and evening, at 9:00 and 18:00 respectively. In this case, the general operation was less efficient than the previous ones, with few differences in temperature and humidity on sunny days and was practically non-functioning on cloudy days. This can be associated to the low sun exposure received due to its south-west orientation and its foliage, which was of medium density at the time of taking the measurements.

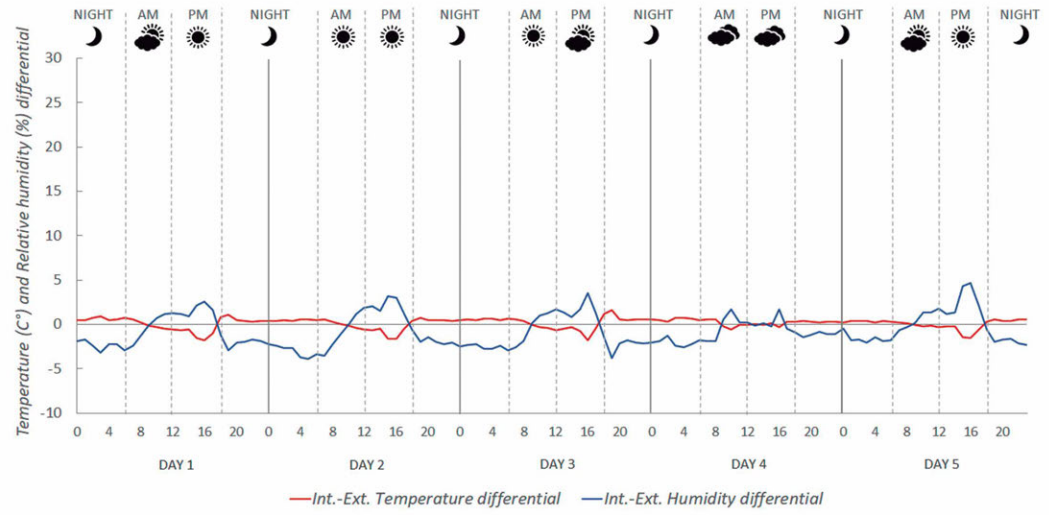

FIG. 13 Daily interior/exterior cavity temperature and relative humidity differential recorded in Case 3

3.4 CASE 4

Fig. 13 shows that the passive cooling effect due to evapotranspiration occurred between approximately 9:00 a.m. and 7:00 p.m. During this period, there was an average reduction of 0.9°C, with a maximum of 4.3°C and an increase in average relative humidity of 1.6% with a maximum

of 6.9%. The standard deviations of temperature and relative humidity were of 0.8°C and 1.4%, respectively, which shows persistent passive cooling and very low overall intensity. The performance of this GSF reached its peak between 12:00 and 16:00 on sunny days.

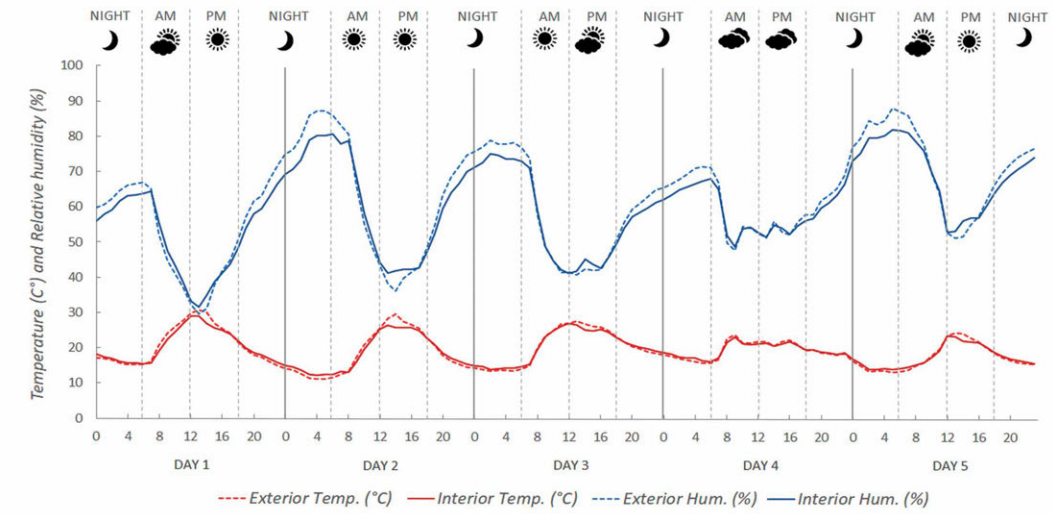

FIG. 14 Daily interior/exterior cavity temperature and relative humidity recorded for Case 4

Fig. 14 shows that, inside the cavity, the hygrothermal inversion occurred regularly at 9:00 and 19:00, and passive cooling was similar on cloudy and sunny days, with a greater decrease in relative humidity on cloudy days. Despite being well exposed to the sun due to its northeast orientation, the low density of the foliage did not allow the potential of this GSF to be reached.

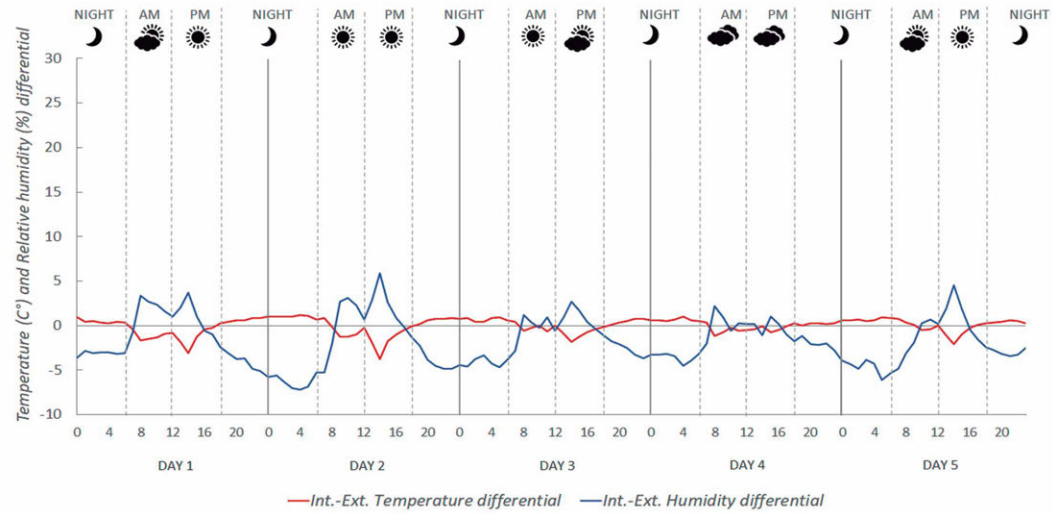

FIG. 15 Daily interior/exterior cavity temperature and relative humidity differential recorded in Case 4

4 DISCUSSION

Fig. 15 shows the temperature differential measured in the complete sample. Regularly, the temperature drops during the day and rises in the late evening, with minimal differences in the times when the hygrothermal inversion occurs inside the cavity. Case 1 is the one that reaches the best thermal performances, which is associated with the highest density of its foliage; it is followed by Case 2, where foliage follows in density. The differences in the temperature peaks show that the hours of highest cooling are different in each case, a matter that may be associated with their different orientations. Cases 1 and 2, which have a northern component, tend to reach their peaks around noon, whereas the rest, which have a western component, tend to do it in the afternoon.

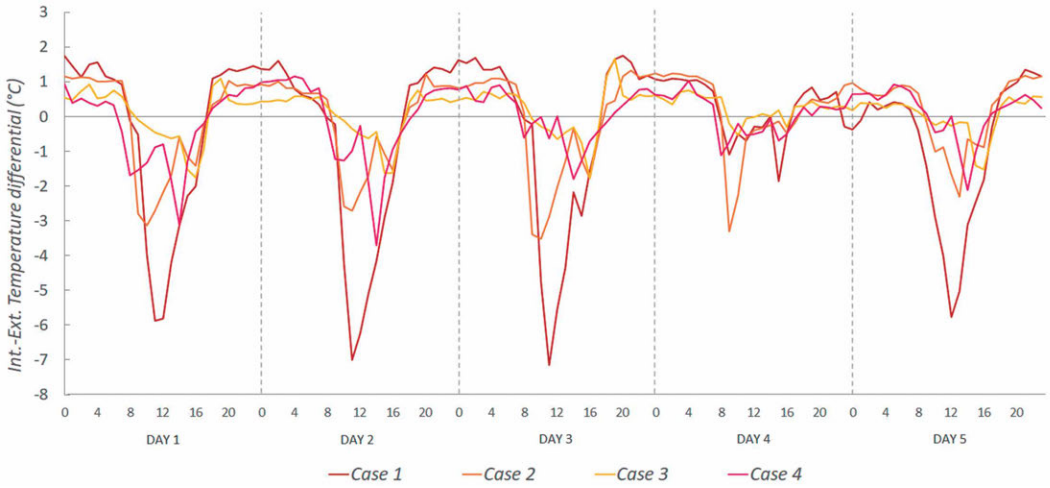

FIG. 16 Daily interior/exterior cavity temperature differential recorded in Case Studies 1 to 4

Fig. 16 shows the humidity differential in the cavities and accounts for phenomena similar to the previous one. Cases 1 and 2, which have denser foliage and a north-facing component in their orientation, are more effective in lowering the relative humidity of the cavity. The effect produced by the decrease in radiation is evident, since on day 4, which was cloudy, the time logic is lost in all cases.

From the above, it can be deduced that passive cooling is effective; however, it is dependent on two main factors: the foliage of the vegetation, which determines the intensity of the passive cooling by evapotranspiration, and the orientation, which is responsible for the hours in which it occurs by action of sun radiation.

The graphs in Fig. 17 synthetically show the differences in temperature and humidity observed in the sample. Case 1 is the one that has the best performance of the four, reaching an 8°C temperature reduction and a 30% increase in relative humidity, which represents an ideal of GSF, since it can become an effective support for cooling systems of the building. Case 2 follows in their overall performance and both have the highest foliage densities, a parameter that appears as a condition for the effectiveness of a GSF. The greater leaf thickness generates a greater evaporation surface, which results in higher passive cooling within the cavity.

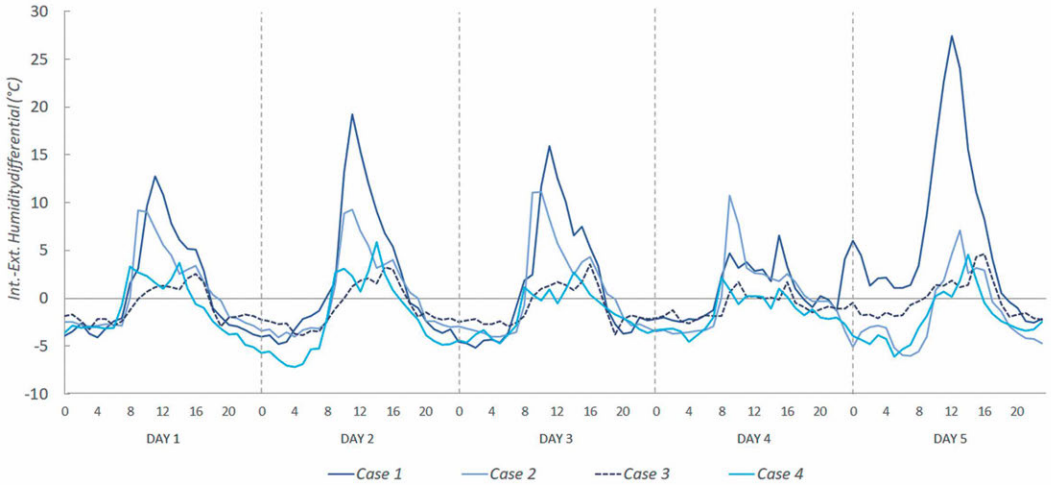

FIG. 17 Daily interior/exterior cavity relative humidity differential recorded in Case Studies 1 to 4

Cases 3 and 4 are those with the lowest foliage density and worst performances; however, Case 3, with a south-west orientation and average density foliage, reaches lower temperature and relative humidity differentials in the cavity than Case 4, whose orientation is north-east and is provided with a lower amount of foliage. Between them, the best result is determined by the sun exposure they are subjected to, which highly depends on the orientation of the GSF. The comparison of these cases shows that the density of the foliage is not a sufficient parameter if the façade does not have an orientation that allows adequate sun exposure.

Fig. 18 shows the orientation of the different case studies, allowing the possibility to observe that the peak performance time in all four cases occurs at times when the angles of solar incidence are not perpendicular to the façade, but lateral, according to the predominant orientation. This suggests that orientation plays a fundamental role in the application of double vegetable skins and that their hygrothermal behaviour is associated with the radiation conditions to which they are exposed. On the other hand, passive cooling persists over many hours, therefore, its correct application would allow its contribution to the overall energy balance of buildings to be incorporated.

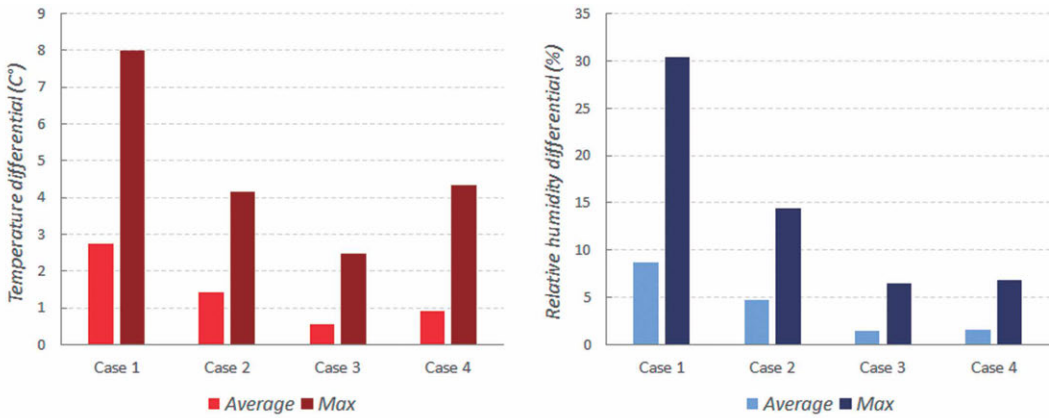

FIG. 18 Interior/exterior cavity temperature (°C) and relative humidity (%) differentials

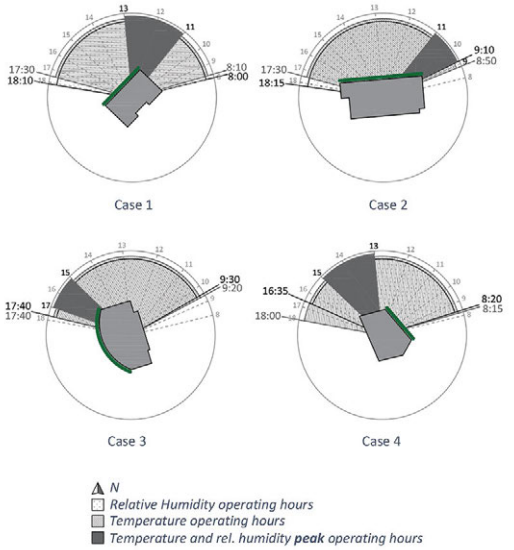

FIG. 19 GSF operating hours for Case Studies 1 to 4

The graphs in Fig. 19 show the correlation between the temperature and relative humidity differentials for each case and their R^2 values, which, in all cases, are greater than 0.8. It can also be observed that hygrothermal behaviour occurs inside the cavities. The points found in the first quadrant correspond to the moments when passive cooling takes place inside the cavities and the opposite situation appears in the fourth quadrant, that is, when heating occurs within the cavity.

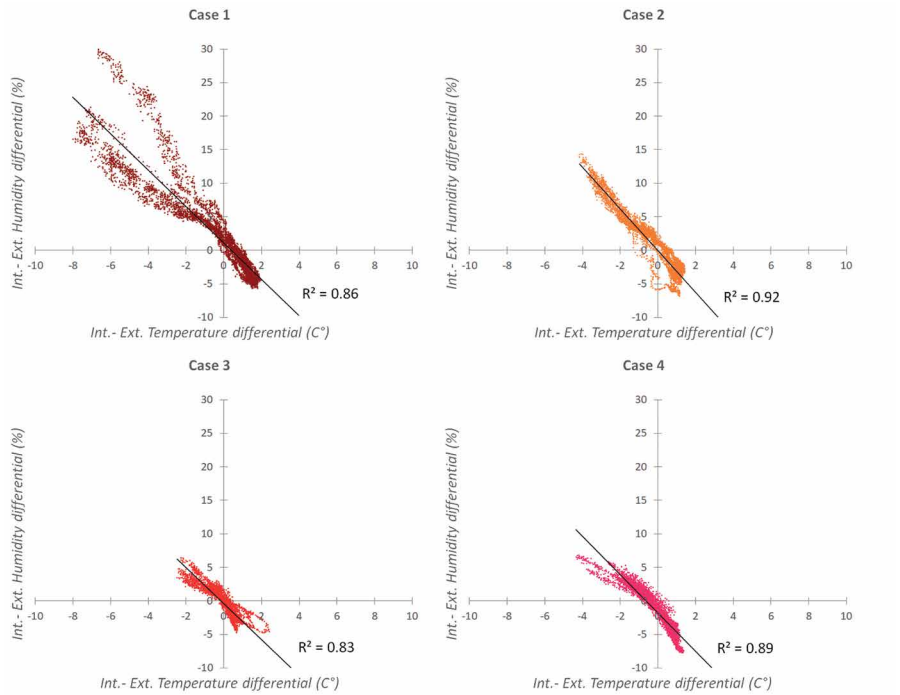

FIG. 20 Correlation between temperature and relative humidity differentials for each case and their R2 values

Cases 1 and 2 are the ones that show a greater development in the first quadrant and cases 3 and 4 tend to develop symmetrically in the first and fourth.

Case 1 shows its high efficiency in obtaining passive cooling, showing two different series in the first quadrant: one where the slope is greater, representing the passive cooling peak moments; and another with a lower slope, that represents the regular operation during the day. On the other hand, the fourth quadrant shows little development, which accounts for the fact that warming is marginal compared to cooling.

Case 2 shows a regular slope in the first quadrant, although it reaches lower values of temperature and relative humidity compared to the previous case. In the fourth quadrant, its trend is similar to the previous one, raising the temperature by almost 2°C and lowering the humidity by around 7%.

Case 3 shows a symmetrical development in quadrants 1 and 4, exceeding 2°C at times when the cavity warms up. The cooling observed in quadrant 1 is scarce compared to the previous cases.

Case 4 shows a performance similar to the previous; however, cooling is more efficient, reaching up to a difference of 4°C and similar humidity differentials. Its performance in the fourth quadrant is the one that achieves the highest relative humidity losses of all cases.

This comparison confirms the aforementioned: cases 1 and 2, which are those with greater foliage and better orientation, perform better, proving the relevance of their foliage; and with respect to cases 3 and 4, which have less foliage, worse orientation, and performance, orientation prevails as the most relevant aspect, since despite the fact of having less foliage and better orientation, Case 3 gives a better performance.

5 CONCLUSIONS

By contrasting the results of these four case studies, we can conclude that the decisive parameters in the performance of a GSF in a temperate-warm climate, such as that of Santiago de Chile, are the orientation of the façade and the density of foliage of the selected plant species.

Regarding orientation, we found that sun exposure is directly proportional to the behaviour of a GSF. When the angle of solar incidence is between 0° and 50° with respect to the façade, the performance peaks are reached. On the other hand, the intensity of solar radiation determines the hygrothermal variations inside the cavity, promoting evapotranspiration that produces passive cooling.

The second determining factor is the foliage density of the selected plant species. The more plant tissue the double plant skin develops, the greater the moisture retention and release capacity in the inner cavity, thus increasing its passive cooling properties during the day.

In this way, we can claim that GSF are a solution that has great potential to be developed in the city of Santiago. However, it is necessary to carry out further research to find the ideal species and the application conditions that allow their operation as a passive cooling system that collaborates with the building's own cooling devices to be optimised.

This study shows the need to carry out experimental studies in order to establish the parameters for a correct design of the double vegetable skins in Santiago de Chile, so that they become part of the building's cooling system and are not only considered as ornamental solutions.

References

Allan, S., & Kim, H. (2016). A study of workflow for simulations of vertical greenery systems. *Architecture Research*(6), 142-153. doi:10.5923/j.arch.20160606.02

Cameron, R., Taylor, J., & Emmet, M. (2014). What's 'cool' in the world of green façades? How plant choice influences the cooling properties of green walls. *Building and Environment*(73), 198-207. doi:10.1016/j.buildenv.2013.12.005

Carpenter, C., & Sikander, E. (2015). Green building envelopes - Moisture safety in ventilated light- weight building envelopes. 6th International Building Physics Conference , IBPC 2015. *Energy Procedia*(78), 458-464. doi: 10.1016/j.egypro.2015.11.179

Chen, Q., Li, B., & Lui, X. (2013). An experimental evaluation of the living wall system in hot and humid climate. *Energy Build*(63), 298-307. doi:10.1016/j.enbuild.2013.02.030

Cheng, C., Cheung, K., & Chu, L. (2010). Thermal performance of a vegetated cladding system on face walls. *Build Environment*(45), 1779-1789. doi:10.1016/j.buildenv.2010.02.005

Cifuentes, L., & Mesa, F. (2008). *Cambio Climático: consecuencias y desafíos para Chile.* Santiago: Universidad Católica.

Dahanayake, K., Chow, C., & Hou, G. (2017). Selection of suitable plant species for energy efficient Vertical Greenery Systems (VGS). *Energy Procedia*(142), 2473-2478. doi:doi:10.1016/j.enbuild.2017.03.066

Den Dubbelden, K., & Oosterbeek, B. (1995). The availability of external support affects allocation patterns and morphology of herbaceous climbing plants. *Functional Ecology*(9), 628-634. doi:10.2307/2390154

Djedjig, R., Bozonnet, E., & Belarbi, R. (2015). Analysis of thermal effects of vegetated envelopes: Integration of a validated model in building energy simulation program. *Energy and Building*(86), 93-103. doi:10.1016/j.enbuild.2014.09.057

Hoelscher, M., Nehls, T., Jänicke, B., & Wessolek, G. (2016). Quantifying cooling effects of facades greening: shading, transpiration and isulation. *Energy and Buildings*(114), 283-290. doi:10.1016/j.enbuild.2015.06.047

Hunter, A., Williams, R., Rayner, J., Aye, L., Hes, D., & Livesley, S. (2014). Quantifying the termal performance of Green façades: a critical review. *Ecological Engineering*(67), 103-113. doi:10.1016/j.ecoleng.2013.12.021

Manso, M., & Castro-Gómez, J. (2016). Thermal analysis of a new modular system for green walls. *Journal of Building Engineering*(7), 53-62. doi:10.1016/j.jobe.2016.03.006

Mohamed, S., & Magdy, N. (2012). Green Facades as a New Sustainable Approach Towards Climate Change. *Energy Procedia*(18), 507-520. doi:10.1016/j.egypro.2012.05.062

Pan, L., & Chu, L. (2016). Energy saving potentical and life cycle environmental impacts of a vertical greenery system in Hong Kong: A case study. *Building and Environment*(96), 293-300. doi:10.1016/j.buildenv.2015.06.033

Pan, L., Wei, S., & Chu, L. (2018). Orientation effect on thermal and energy performance of vertical greenery systems. *Energy and Buildings*(175), 102-112. doi:10.1016/j.enbuild.2018.07.024

Pan, L., Wei, S., Lai, P., & Chu, L. (2020). Effect of plant traits and substrate moisture on the thermal performance of different plant species in vertical greenery systems. *Building and Environment*(175). doi:10.1016/j.buildenv.2020.106815

Peel, M., Finlayson, B., & McMahon, T. (2007). Updated world map of the Köppen-Geiger climate classification. *Hydrology and Earth System Sciences Discussions, 11*, 1633-1644. doi:10.5194/hess-11-1633-2007

Pérez, G., Coma, J., Sol, S., & Cabeza, L. (2017). Green facade for energy savings in buildings: The influence of leaf area index and facade orientation on the shadow effect. *Applied Energy*(187), 424-437. doi:10.1016/j.apenergy.2016.11.055

Pérez, G., Rincón, L., Vila, A., González, J., & Cabeza, L. (2011). Behaviour of green façades in Mediterranean Continental Climate. *Energy Conversion and Management*(52), 1861-1867. doi:10.1016/j.enconman.2010.11.008

Romero, H., Irarrázaval, F., Opazo, D., Salgado, M., & Smith, P. (2010). Climas Urbanos y Contaminación atmosférica en Santiago de Chile. *EURE*(36), 35-62. doi:10.4067/S0250-71612010000300002

Safikhani, T., Megat, A., Remaz, D., & Baharvand, M. (2014). A review of energy characteristic of vertical greenery systems. *Renewable and Sustainable Energy Reviews*(40), 450-462. doi:10.1016/j.rser.2014.07.166

Schettini, E., Blanco, I., Campiotti, C., Bebbiani, C., Fantozzi, F., & Vox, G. (2016). Green control of microclimate in building. *Agriculture and agricultural science procedia*(8), 576-582. doi:10.1016/j.aaspro.2016.02.078

Šuklje, T., Medved, S., & Arkar, C. (2016). On detailed thermal response modeling of vertical greenery systems as cooling measure for buildings and cities in summer conditions. *Energy*(115), 1055-1068. doi:10.1016/j.energy.2016.08.095

Susorova, I., Angulo, M., Bahrami, P., & Stephens, B. (2013). A model of vegetated exterior facades for evaluation of wall thermal performance. *Building and Environment*(67), 1-13. doi:10.1016/j.buildenv.2013.04.027

Yang, F., Yuan, F., Zhuang, Z., & Yao, J. (2018). Summertime thermal and energy performance of a double-skin green facade: A case study in Shanghai. *Sustainable Cities and Society*(39), 43-51. doi:0.1016/j.scs.2018.01.049

Development of an Offsite Prefabricated Rainscreen Façade System for Building Energy Retrofitting

Stefano Avesani[1*], Annalisa Andaloro[1], Silvia Ilardi[2], Matteo Orlandi[2], Stefano Terletti[3], Roberto Fedrizzi[1]

* Corresponding author
1 Institute for Renewable Energy, Eurac Research, Bolzano, Italy, stefano.avesani@eurac.edu
2 Arup Italia, Milano, Italy
3 Halfen Italia, Bergamo, Italy

Abstract

As the European building stock is in evident need of deep energy retrofitting to meet current European decarbonisation targets, the construction market calls for industrialised systems to boost massive renovations and activate economies of scale. The article outlines the development of an offsite fabricated system for building energy refurbishment through rainscreen façade elements. A focus is placed on such elements as they offer excellent system integration possibilities and the opportunity to boost the level of offsite fabrication, compared to other already industrialised façade systems, such as unitised façades. This research was carried out within the framework of BuildHEAT research project, funded by the European Union Horizon 2020 framework programme. The system concept is based on a systemic approach that combines energy efficiency, multifunctionality, integration of renewable energies, and ease of installation as design drivers. System development has rolled out through different phases, with an increased level of detail. During the schematic design phase, a set of different prefabricated façade panel dimensions were analysed. Afterwards, the component and system integration were assessed according to their impacts in terms of energy performance and fulfilment of mandatory technical requirements. As a last step, the most promising technical combinations underwent detailed design to verify construction feasibility and eliminate any bottlenecks during the fabrication phase. Results show that the proposed prefabricated solutions allowed: (i) simplified active system integration (photovoltaics, solar thermal, and building services), (ii) ease of installation on site, minimising the impact of renovation actions on occupants without compromising on final quality and reducing installation costs. Current limitations to extensive market diffusion of the system are related to two main aspects: (i) the need for on-site adjustments; and (ii) increased manufacturing costs compared to traditional external insulation interventions (e.g. ETICS). The current cost of the system (2020) is in the range of 3 - 1.5x the cost of, respectively, an ETICS or a vented rainscreen façade. However, as a next step, including the life-cycle perspective in the calculation, as well as accounting for economies of scale, the system will be evaluated, expecting a cost figure comparable to the rainscreen façade.

Keywords

Renewable energy integration, re-cladding, prefabricated construction, system integration

DOI 10.7480/jfde.2020.2.4830

1 INTRODUCTION

When tackling deep energy retrofitting interventions of buildings, higher complexities and costs are incurred with respect to lower impact energy retrofitting solutions, due to the number of components to be considered, as well as their interconnection. Moreover, building to meet high energy performance standards have to include the RES generation, in particular PhotoVoltaic (PV) and Solar Thermal (ST) systems that are widely used. Such solutions incur extra costs needed to adapt the design onto traditional building components and to ensure a reliable installation. For this reason, a better economic case for deep renovation has to be found adopting a more systemic approach to renovation. As such, the retrofit action works has the chance to improve energy efficiency, as well as occupants´ comfort and safety, together with increasing the overall building value. Such solutions tend to endow the envelope with multiple functions that complement thermal insulation, it being the primary objective of the intervention. Specifically, it is possible to include building services – both energy generation and distribution systems – in the package, as well as punctual system terminals or shading systems. On the other hand, the inclusion of system components in the envelope is deemed to make renovation works more complex and impactful on building occupants. This is mainly due to need to access the building from the inside in order to complete ducts and cabling connections.

Currently used technologies for opaque façade retrofits rely on the use of External Thermal Insulation Composite Systems (ETICS), which do not offer any dedicated technical solutions to integrate PV panels and ST collectors and building services components (electric cabling, water piping and air ducting). In addition to the above, ETICS also require the use of fixed scaffolding infrastructure during the installation phase and strongly rely on the workmanship handcrafting experience to guarantee results that match expected performance and aesthetics.

Ad hoc products and systems for PV and ST building integration - BIPV-BIST state technologies are available (EPFL, 2016), having been developed for many years, but are still mainly a niche market. The SWOT matrix reported in Bonato, Fedrizzi, D'Antoni, and Meir (2019) as well as the barriers highlighted in Maurer et al. (2018) show how the limits of implementation of innovative solar façade systems can be found in many interdisciplinary aspects, from the economic to the social fields.

Besides these developments, which focus only on solar integration, research and innovation has been recently developing envelope solution sets, which may be installed with minimal impact and disruption to occupants, despite the inclusion of active systems for energy production and distribution, as described, for example, in Andaloro, Avesani, Belleri, Machado, and Lovati (2018) and Ochs, Siegele, Dermentzis, and Feist, 2015). A list of further research projects developing multifunctional envelope solutions for the retrofit of buildings is reported in D'Oca et al., (2018). In fact, the impact of renovation works on building occupants can be significantly reduced when taking advantage of offsite fabrication techniques, which allow the construction site phase to be speeded up and minimise construction works on the indoor space (Colinart, Bendouma, and Glouannec (2019). This is possibly thanks to the anticipated design and engineering effort that has to take place before the component production phase (Arashpour, Abbasi, Arashpour, Reza Hosseini, & Yang, 2017; Lu, Chen, Xue, & Pan, 2018). Pre-assembled components can be then installed on-site in a shorter time and with less need for supporting structures and works. It must not be neglected that the adoption of such systems requires an accurate energy and geometrical audit, as it is not possible to perform component modifications on site (Lattke & Cronhjort, 2014; Silva, Almeida, Bragança, & Mesquita, 2013). It is easily inferred that the offsite fabricated solutions allow for a shorter construction site duration and support the achievement of higher quality results, due to the

elimination of several potential installation errors that can possibly occur in traditional construction sites (Gasparri & Aitchison, 2019; Ochs et al., 2015; Op't Veld, 2015). Finally, offsite production has a potential 20% cost saving for owners, as estimated in Bertram et al. (2019).

The Offsite prefabricated Rainscreen Façade (ORF) concept presented in this paper takes the need for systemic façade retrofit solutions - specifically to ease the integration of PV and ST components to decrease the building non-renewable final energy consumption, and the benefits offered by the adoption of an offsite fabrication approach, as development drivers. The ORF aim is to bridge the technological gap between the traditional ETICS-based passive façade and the aforementioned R&D experiences of the multifunctional prefabricated façade, through the development of a systemic façade solution based on components mainly available on the market. Hence, the use of a customisable standardised frame system has been addressed as a core aspect of the façade concept development. In this sense, the choice of starting the development from a rainscreen façade is justified by the presence of a substructure, meeting the need to host several kinds of cladding elements (passive and active) and offering the potential for offsite production and plug-and-play installation.

The objectives of the paper are to give an overview of the development process, to present the façade's main features as well as to discuss the achieved façade technological solution. The paper is structured in different sections, zooming into details of the design and development process. A complete overview of the development process is provided as follows: (i) first, design drivers on which the façade system is developed are presented, together with the schematic design method applied to preliminary technology development; (ii) then, both mandatory and non-mandatory technical requirements for the new façade system are introduced. Once the methodology is thoroughly illustrated, façade development results and its main features are showcased: detailed designs are presented, together with the testing of technical requirements and the achievement of performance targets. A deep dive into main components is also made, focusing on the façade interface with existing wall, active systems, anchoring and fixing systems, and cladding. The paper closes with a list of current application possibilities and limitations, as well as providing preliminary insights into cost issues arising during the development phase. Cost issues are presented at an aggregated level of detail and will be further investigated at a later stage. However, authors identify the life-cycle approach as an option to overcome current cost limitations.

2 MATERIALS AND METHODS

2.1 FAÇADE DEVELOPMENT DRIVERS AND DESIGN PROCESS

The Offsite prefabricated Rainscreen Façade (ORF) system has been developed based on the ventilated façade concept, exploiting compatibility with market-available construction materials and components, but proposes a project specific panel concept, which has to satisfy the technical requirements of the European building product regulations and the following peculiar development drivers, derived from the research project framework under which this system was developed. The new façade must (i) ease the installation of passive and solar active cladding, in order to assure the implementation of systemic deep energy retrofit, reducing the building's heating demand while preventing overheating and assuring indoor comfort; (ii) lower the installation effort and the impact on inhabitants for a deep retrofit action, simplifying and standardising the installation of active elements, piping, and ductwork on the outside of the existing façade, with consideration also given to the maintenance operations. This means that both active and passive cladding, as well as the building services components, have to be accessible and replaceable. The façade system developed within the framework of this research must respond to the technical requirements set by the European Commission within the H2020 framework programme call topic, under which this work has been developed. The above requirements determine that the novel façade system has to be: (iii) cost-effective, being able to compete on the market; (iv) replicable, able to be easily adapted to a broad portfolio of residential building typologies; (v) flexible, compatible with the commercial passive and active cladding systems (such as PhotoVoltaic panel – PV, and Solar Thermal collector - ST) needed by the energy concept of the renovation.

Consequently, the ORF has been developed through a multi-stage design process, grounded on existing literature review from past research projects on prefabricated façade systems for energy retrofit. Research projects in the review include, but are not limited to, the following: H2020 More Connect, 4RinEu, Drive0, Energy Matching. The adopted approach was "research by design", refining the technical solution according to design drivers set by the H2020 programme and specific project requirements until a shared solution among research partners was found. This complex design process spanned from the preliminary system concept to the definition of the final solution to be applied on-site for two demo case buildings, using an increasing level of detail. Based on the above-mentioned background and guided by the design drivers reported here above, the design process started with a schematic design phase. Its objective was to identify possible façade technological concepts, with technical features able to fulfil the product, and to address the expected impacts. The three pre-assembled façade concepts are: (i) micro-panels, (ii) sandwich panels, (iii) macro-panel.

2.2 ORF SYSTEM COMPONENTS

The main components that constitute the façade system are described in Table 1, including their main functional requirements.

TABLE 1 List of OPVF system main components and related function details

COMPONENT	FUNCTION DESCRIPTION
SUB-STRUCTURE	The system sub-structure is the façade main frame that hosts the functional components (passive and active claddings), connecting the new façade to the existing external wall, as well as retaining the external cladding. Main sub-structure requirements are mechanical resistance, to bear dead and wind loads, ease of installation, construction tolerances absorption, accessibility, and removability of the outer layer for maintenance and flexibility purposes.
THERMAL INSULATION	The thermal insulation is needed to increase overall façade thermal resistance and should also have appropriate fire reaction, in order to minimize risk of fire spread along the façade plan. Its hygrothermal behaviour is very relevant to avoid condensation risks and therefore to increase durability.
PASSIVE CLADDING	The façade finishing determines the aesthetic appearance of the building and its durability. The façade system is conceived to host different façade market-available passive claddings using the same type of substructure.
ACTIVE CLADDING	Façade integration of ST and PV modules is more and more an option to increase the solar energy self-consumption towards a net Zero Energy Building. A number of products and documentation can be found in literature. Nevertheless, active cladding integration increases the degree of complexity of the whole facade and requires dedicated engineering effort to optimize system connection to the inside of the building, as well as the integration of distribution systems within the façade. This is one of the main barriers that prevents their diffusion on the market and that the ORF want to tackle through the development of a pre-assembled and flexible façade sub-structure.
ENERGY AND SERVICE DISTRIBUTIONS	Façade integrated piping, ducting, and cabling distributions can provide each flat the needed thermal energy, fresh air and electric power minimizing the indoor construction works and therefore the impact on inhabitants. The advantage of such kind of integration might be counterweighted by a more complex façade installation phase, as well as requiring accessibility for maintenance.
WINDOWS	The window node solution is a critical step to achieve overall indoor comfort, energy demand reduction as well as durability of the components. Two different approaches for the window integration in the prefab façade has been studied, addressing a fully integrated and a non-integrated window. In the first case, the window is hosted in an insulated frame, loaded on the façade prefabricated substructure. In the second, the new window is not integrated in the prefab façade, which is hence a macro-panel, wider than the base one – constituted of cladding elements, insulation layer and substructure shaped around the window hole
HEAT RECOVERY MECHANICAL VENTILATION	The use of a mechanical ventilation system is considered as necessary when pursuing a deep energy retrofit action, to reduce heat losses and increase indoor air quality. Decentralized mechanical ventilation unit can also be considered, as they allow easier integration within the façade system, avoiding space and cost consuming indoor ducting installations.

2.3 FAÇADE TECHNICAL REQUIREMENTS

After the finalisation of the façade concept, a further list of requirements was defined based on the essential requirements established in the 305/2011 EU directive for construction products (European Parliament, 2011) and complemented with the technical standard ETAG034 for ventilated façades (EOTA, 2012b). The regulatory assessment skipped the air-tightness requirement verification due to the assumption that the façade as retrofit kit is a second layer on an already existing façade, for this reason such a requirement has less priority than in the case of new construction. This is not true in the case of window integration, which has not been considered in this paper.

The macro-panel structure was developed by adopting an integrated design logic, focused on both construction process optimisation and performance achievement. In fact, on the one hand, it was designed in detail, providing information on materials to be used, macro-panel dimension ranges, anchoring to the existing structure and customisation opportunities in terms of cladding options, as well as active component integration. On the other hand, the designed solution has then been verified in terms of technical performance requirements, such as: mechanical, thermal, hygro-thermal and condensation risk, water tightness, impact and wind resistance, and fire reaction. As the ORF is still

a non-standard market product, all of the above have been assessed based on calculations and tests undertaken on a series of 1:1 scale mock-ups. The summary of the performance requirements and their related assessment method within the project is provided in Table 2.

TABLE 2 List of OPVF system technical requirements and related assessment method used in the project

REQUIREMENT	ASSESSMENT METHOD
MECHANICAL RESISTANCE	The mechanical resistance of the ORF system is measured on the main frame (see "substructure" in TAB. 1). The maximum expected deformation has been assessed on the frame elements as representative of failure risks for the whole system. Calculation has been made according to the Italian decree D.M 14/01/2008 (Italian Government, 2008)- given that one of the demo-site buildings is in Italy, which is derived from the current European regulatory framework for mechanical resistance calculation in the construction sector. KPI: maximum deformation in operation [mm], calculated
THERMAL RESISTANCE	The thermal resistance calculations have been performed following the procedures defined in the EN ISO 10077:2017 (EN ISO, 2017). Linear thermal loss coefficient has been calculated based on a bi-dimensional parametric analysis, which has informed the final shaping of panel geometry, as seen in the results section. After that, the incidence of thermal bridges generated at panel edges has been evaluated. The ORF has been compared against a reference building standard energy renovation case. The façade has been considered as adjacent to the existing one, in contact through a 100 mm-thick continuous soft rockwool insulation layer. The incidence of thermal bridges has been evaluated as difference between the ORF façade and a traditional external insulation (reference). KPI: thermal resistance [m^2 K/W], thermal transmittance [$W/m^2/K$, thermal linear loss coefficient [W/m/K], calculated
HYGRO-THERMAL AND CONDENSATION RISK	The hygro-thermal behaviour of the solution has been assessed coupling a steady state Glaser diagram and a dynamic state calculation performed with Delphin software. The latter allows to consider the hygrothermal dynamic behaviour on a 2D domain, as needed for the presence of the substructure in the insulation panels. Calculations are based on some assumptions: short-wave solar radiation is not considered, as well as rainwater flow on the external side of the surface. The simulation time has been set to two full years, considering the first year as a stabilization phase. KPI: cumulated mass of condensation water [g/m^3], calculated
WATER TIGHTNESS	Water tightness does not need to be certified in the case of a ventilated façade kit, as stated in the ETAG034 (EOTA, 2012a). However, a test campaign has been performed, directing a continuous water jet against the surface for 10 minutes with no interruption. This phase has been followed by a visual inspection at all layers. KPI: presence of water drops, visual inspection
IMPACT AND WIND RESISTANCE	Impact resistance has been verified using a hard body impact procedure on the external cladding system, using three different bodies: 0,5 kg hard body plus 3 joules, 1 kg hard body plus 10 joules, 3 kg soft body plus 10 joules. The test has focused especially on the Polymer Concrete cladding panel, which has been developed as innovative material within the ORF project for the passive cladding. On the other hand, this test was not performed on PV and ST modules that can also be used as external cladding, being them commercial products equipped with own product declaration and performance certificates. Wind resistance has been assessed using a support test bench with a steel frame, where façade modules have been positioned and joints sealed to create an airtight chamber that allows to apply wind pressure or suction. Pressure levels up to 3000 Pa have been applied. Effects of wind pressure on façade system have been assessed through deformation meters located at fixed points and a visual inspection of components after test completion. KPI: presence of breaks, tested
FIRE REACTION	Fire reaction of the PC cladding panel has been assessed at façade system level based on single burning item test (SBI) according to EN 13823:2020 (EN, 2020). The SBI test is performed directing a flame source with determined firing power (30,7 ± 2,0 kW) generated through propane burning towards the sample to be tested from an interior corner point. The test lasts for 20 minutes, and the assessment process is based on the following set of parameters, aiming at determining the material fire reaction class. KPIs: Total Heat Release during the first 600 seconds (THR 600) [MJ], Fire Growth Rate Index (FIGRA) [kW/s], Lateral Flame Spread (LFS) [m], Smoke Growth Rate Index (SMOGRA) [m2/s2].

2.4 FAÇADE COST CALCULATION

Façade design, manufacturing, and installation costs have been calculated based on expenses incurred during the research project demonstration phase within which the solution was developed. The façade manufacturer noted in a bill of expenses all costs, allowing the system cost per m^2 installed to be calculated (Table 3).

It must be noted that transportation costs have been accounted for in the bill of expenses. However, in larger deployments of the same system, transportation costs should be less impactful, provided that the designers choose manufacturers located within a certain geographical range of operation.

TABLE 3 Cost analysis breakdown

	COMPONENT	DESCRIPTION
1	**Anchoring elements**	Commercial products (as per curtain wall) to anchor the macro panel frame to the building structure
2	**Soft insulation layer**	Insulation material (e.g. rockwool) and related fixings
3	**Macro panel frame**	Alu profiles needed for the macro panel assembling of the macro panel
		Assembling of the macro panel with all its components
4	**Rigid insulation layer**	Insulation material and related fixing
5	**Waterproof layer**	Gaskets to be applied between macro-panels
6	**External finishing layer**	Anchoring system that allows the single finishing panel dismantling
		External finishing material
7	**Packaging**	Wooden frame and plastic to allow the safe handling of the assembled macro-panels
8	**Transport**	Truck from the factory to the construction-site
9	**Site work**	Installation phase, as well required construction site equipment, additional materials, general expenses

3 RESULTS

The output of the development and design phases are presented in this section, in terms of façade macro-panel features and performance assessment results.

3.1 FAÇADE FINAL DESIGN

3.1.1 Overall façade system features

The schematic design phase resulted in three main concepts being investigated, as illustrated in Fig. 1. The micro-panel concept (Fig. 1 -1) is built on a metal frame structure carrying both the cladding and insulation layer, equipped with a connection element to favour easy anchoring to the substructure. Its functioning mimics a vented rainscreen façade, including the use of a mullion substructure to support the panels. The sandwich panel concept (Fig. 1 – 2) is based on a pre-assembled multi-layer element including cladding and insulation, directly screwed to the substructure, with no need for an additional frame, conversely to previous case. No air cavity is

present in this configuration. The macro-panel concept (Fig. 1 -3) mimics a unitised system and is equipped with a half frame on each edge of the panel. These halves are then coupled with their twins as two panels are positioned adjacent to one another, in both the horizontal and vertical direction. The frame is conceived with multiple slots to allow both flexibility in terms of cladding anchoring and to allocate further layers as per the rainwater protection. In this case, the existing-new façade fixing is realised exclusively through multi-directional brackets.

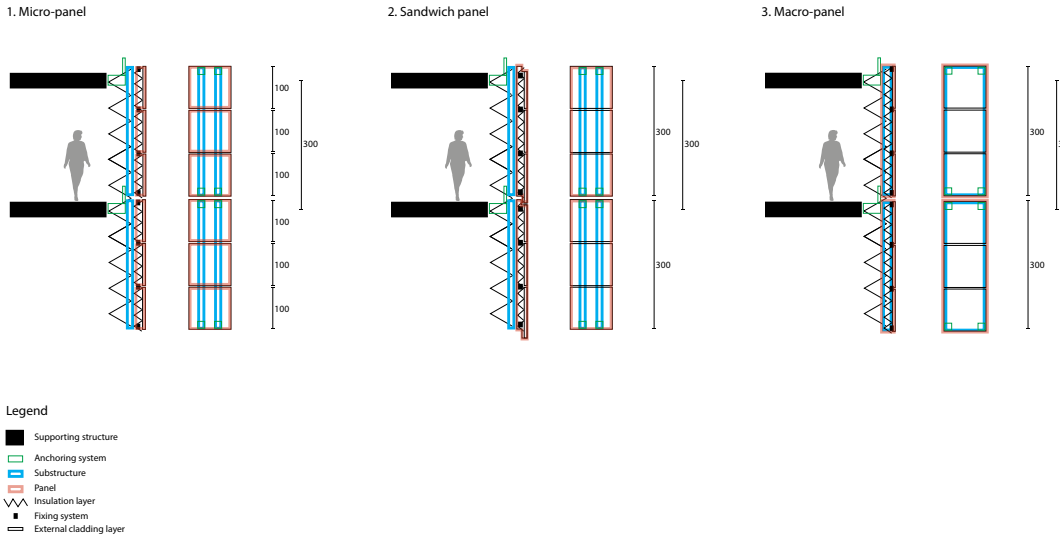

FIG. 1 First preliminary concepts of the offsite prefabricated façade. In red pre-assembled panel units, in blue substructures, in green anchoring system, zigzag line for insulation layer, filled black for building slab

With respect to the three façade concepts of Fig. 1, the refining phase in concept design led to the exclusion of the micro-panel approach, as the latter brought about similar advantages to the other two proposals, but with increased costs generated by the large number of fixing points and increased total length of the framing structure (needed to cover the same façade surface as in the macro-panel scenario). Further on, the sandwich panel was also discarded for two main reasons: it did not provide a suitable solution for the simple integration of active systems and it required a complex geometrical solution to panel joining, in order to avoid manual work being performed on site. The above are deemed to generate extra costs in case system integration is a mandatory project requirement and an extra degree of complexity to be managed during both the production and transportation phases. In fact, the rebated shape of the modules is easily subjected to breakage and needs to be handled with special care.

Hence, as the first result, the preliminary design identified the macro-panel approach as the most suitable to be developed in further detail. Specifically, the macro-panel choice was based on three main features: (i) full exploitation of the industrialisation potential, through the replacement of the traditional metal substructure applied in vented rainscreens with the more comprehensive macro-panel metal frame, (ii) flexibility both in cladding and active system integration, as well as in panel sizing, as the metal frame can be adapted to different structural needs, (iii) commercial availability of ORF system components, to improve replicability and to allow for a partially optimised value chain of the macro-panel, at present limited to the offsite fabrication phase.

In general, the ORF macro-panels are conceived to cover the inter-floor distance in height, to allow for pre-determined fixing points at slab level and so they can have variable widths based on the type of cladding element (both passive and active) to be applied and therefore on the desired façade appearance pattern (Fig. 2).

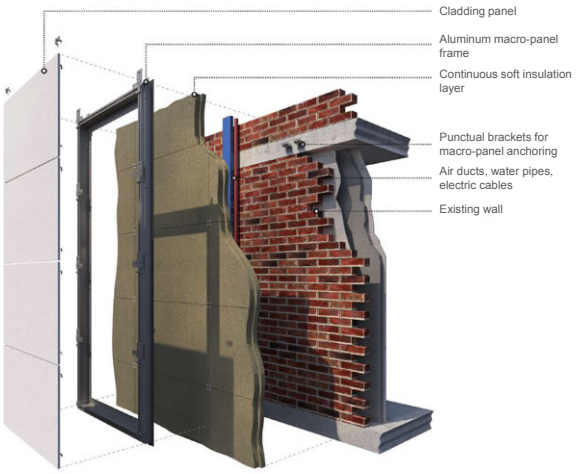

FIG. 2 Rendered image of the BuildHEAT façade final concept and its constituent layers

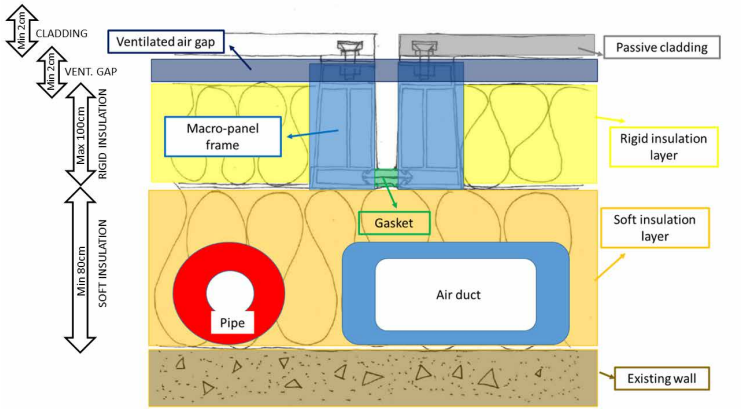

FIG. 3 Concept horizontal cross section of the different layers for the ORF system in the passive cladding configuration (moderately ventilated air cavity and cladding)

In terms of system thickness, the system requires a minimum of 200 mm front translation of the façade plan, considering at least 80 mm compressible soft insulation to absorb eventual construction tolerances, related to non-verticality or non-horizontality of the existing wall. This insulation layer sizing is also driven by the final façade thermal transmittance to be reached. From this perspective, the possibility to host a rigid second insulation layer in the macro-panel has to be considered. Consequently, this information on system thickness has been calibrated on a Mediterranean climate as the first demo installation and is subject to verification and variation in case more severe climate conditions apply. The final schematic design of the ORF horizontal or vertical section is illustrated in Fig.3.

The preassembled façade module is composed of an extruded aluminium frame, running all along the macro-panel edges, which is able to host a rigid second insulation in its thickness and allows for different type of cladding fixings thanks to its peculiar innovative shape. This frame shape (Fig. 4) allows for an easy adaptation to several cladding types, spanning from opaque passive to active systems, such as PV or ST, mimicking the vented rainscreen physical functioning. A set of horizontal and vertical gaskets can be additionally fixed to the frame dedicated groove, drastically reducing the risk of driven rainwater penetration to the soft insulation layer.

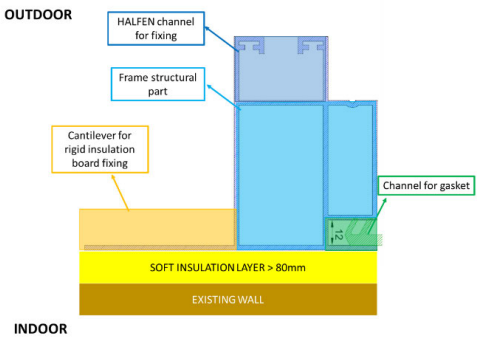

FIG. 4 Detail of the macro-panel aluminium frame in its main parts and functionalities (drawing not to scale)

3.1.2 Macro-panel anchoring and cladding fixing

Following the driver of flexibility in integration, a further key element of the new façade is the standardised cladding fixing to the sub-structure (Fig. 5), which allows for easy removability of passive cladding as well as the PV panel.

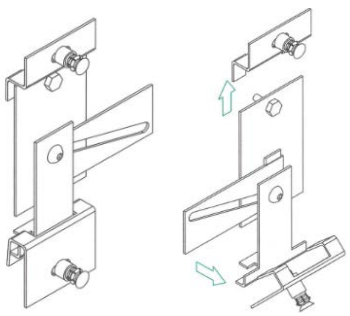

FIG. 5 Standardised fixing system for removable passive and active (PV) claddings

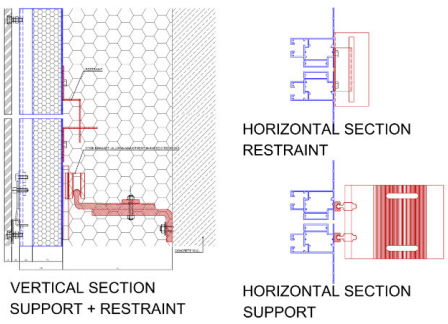

FIG. 6 Macro-panel frame anchoring system to the concrete slab, as for curtain wall

The ST fixing has been developed ad hoc using Z-shaped steel plates connecting the macro-panel frame to the ST. The collector dead-load is however carried by the macro-panel frame transom (or an additional suspended one). The macro-panel anchoring to the existing façade is realised at slab front level through metal brackets (Fig. 6), the same kind of commercially available system used for a curtain walling system.

3.1.3 Interface

Managing the interface between the existing façade and the retrofit module is crucial for a well-executed retrofit action. As said before, in the ORF concept, as has also emerged from literature, this is done by including a compressible insulation layer located between the new and the existing façade. This first insulation layer aims to guarantee continuity of insulation and provide eventual space for active system distribution components, such as cabling, ducting, or piping. At present, this layer is not engineered to be assembled offsite and its installation requires manual work to be performed on site. However, there is room for the industrialisation of this element.

3.1.4 PV and ST integration as active cladding

The integration of active components was investigated in depth during the concept definition phase, as a relevant parameter to develop a flexible and replicable façade solution for the systemic deep energy retrofitting of buildings. As mentioned, the integration of commercially available PV and ST systems were assessed through a technical market analysis. Based on these (PV and ST main relevant features such as sizes, fixing requirements, cabling and piping, wet connections) were the macro-panel substructure design, the fixing system selection (in order to allow the removability for maintenance purposes), in close contact with PV and ST manufacturers, and the use of a dressing cap (as for a curtain wall) to cover the exposed frame view and improve the overall macro-panel aesthetic. All system connections (electrical, wet connections) have been solved using commercial products for plug-in junctions available on the market. The final design of the macro-panel frames is reported in FIG. 7, Fig. 8 and Fig. 9.

FIG. 7 Base macro-panel frame front view. Top, mid, and bottom passive cladding fixings' types are indicated.

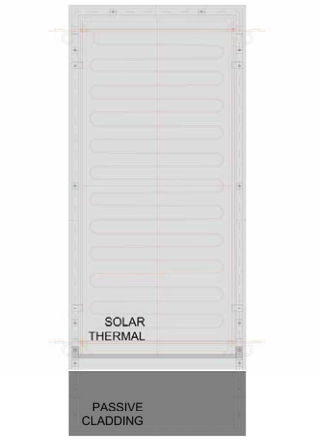

FIG. 8 Front view of the ST integration in a dedicated macro panel with bottom passive cladding. In this case, an additional removable transom is foreseen as well as dedicated fixing points for the ST collector retention against horizontal loads

FIG. 9 Front view of the PV macro-panel hosting a top passive cladding. The PV panel frame is mechanically fixed to the removable façade fixing system (as per the passive claddings) thanks to rivets.

3.1.5 Decentralised mechanical ventilation unit

On the other hand, the decentralised mechanical ventilation unit façade integration was investigated in more detail, with the aim of designing a brand-new ventilation machine unit, optimising both the machine performance and the impact on building occupants. The maintenance-related accessibility requirement is easily achieved using a vented rainscreen with removable cladding, which was already a core technical requirement related to the flexibility and cladding customisation of the system itself. Hence, four different options for decentralised ventilation unit integration have been qualitatively analysed according to machine positioning with respect to the façade and related window holes. They can be described as (in italics, the short name adopted in the table below): (i) in the existing façade, below the window unit - under window, (ii) in the existing façade, hanging from the upper ceiling – ceiling hung, (iii) in the existing façade, above the window unit and exploiting the shutter box space, when possible - shutter box, (iv) in the new façade, adjacent to the existing one and located below the window unit – new façade. The four scenarios have been compared in terms of technical requirements and functionalities related to both the façade system in general and the ventilation machine integration.

TABLE 4 Summary of comparative analysis among the four different scenarios identified for decentralized ventilation machine integration

	UNDER WINDOW	CEILING HANGED	SHUTTER BOX	NEW FACADE
impact	*	**	**	***
social acceptance	**	*	**	***
noise protection	*	*	*	***
replicability potential	*	**	**	***
façade thickness	***	***	***	*
machine thermal losses	***	***	***	*
ease of maintenance	***	***	***	**
construction cost	*	**	*	***
component cost	*	**	**	**
duct connection	***	**	*	***

** worst case / ** average case / *** preferred option*

Results are summarised in Table 4, ranked from worst to preferred according to configuration issues. As seen in the synthetic table, there is no optimal solution, each scenario carrying both advantages and disadvantages. As a consequence, within the frame of this project the integration of the decentralised ventilation unit as a stand-alone system has been discarded. The integration of a decentralised ventilation unit as a separate system still remains in the range of customisation opportunities to be further investigated in the future.

3.1.6 Window integration

As noted in Table 1, the prefabricated window macro-panel was conceived in two ways. In the first one, the new window is fully integrated into the window macro-panel thanks to the use of an insulating frame made of high density XPS, loaded on the macro panel aluminium substructure. The second scenario foresees that the new window installation is done separately from the façade insulation, cladding, and window jamb finishing, which are integrated in the prefabricated macro-panel. As a result, this latter approach was finally chosen because of the overall minor complexity of the prefabrication, transport, and installation phases of a prefab macro-panel without the presence of the window onboard. Moreover, the macro-panel development explained up to now has led to the design choice of a distance of at least 80 mm between the macro-panel substructure and the existing wall. As a result, it would have been too challenging for the macro-panel to bear the window weight with such a cantilever. Finally, a fully integrated window scenario would have added the requirement for airtightness on to the window macro panel. Such a feature would have needed a dedicated development that deviated from the original idea of a unique macro-panel sub-structure able to host different kind of components. The final design of a prefab macro-panel that matches the window opening is represented in Fig. 10.

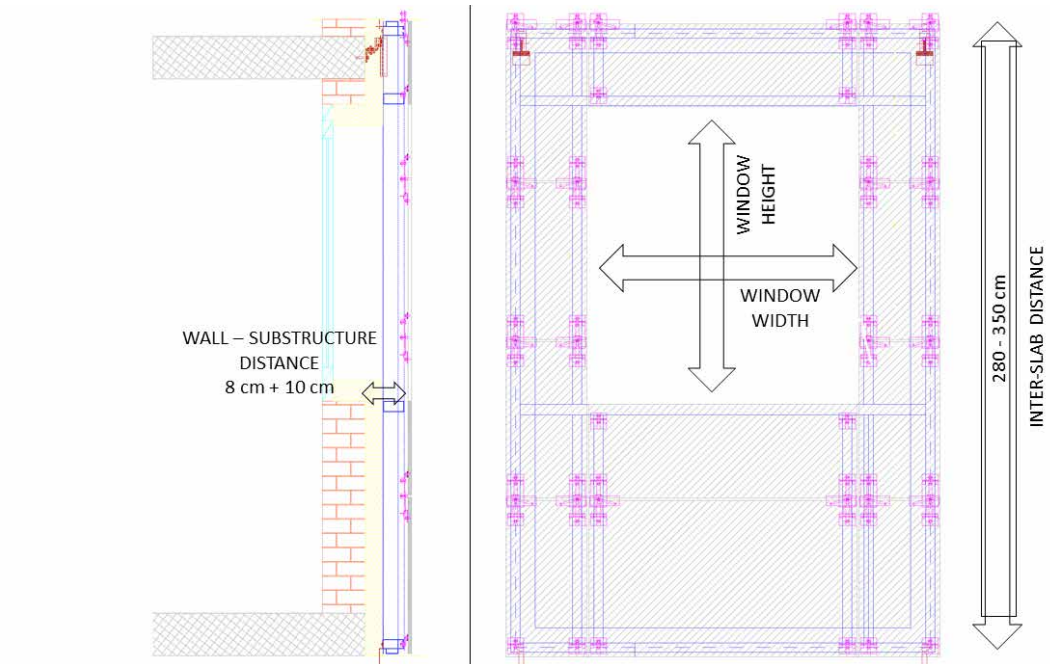

FIG. 10 Design of the window macro-panel without the integration of the window

3.2 TECHNICAL PERFORMANCE ASSESSMENT RESULTS

The ORF system performances have been assessed based on the requirements identified in the methodology section. The results are briefly summarised in Table. 5.

TABLE 5 Summary of technical performance assessment results

REQUIREMENT	ASSESSMENT RESULTS
Mechanical resistance	The extruded aluminium frame shape has been dimensioned in order to obtain a maximum 1/200 of frame length deflection at centre point. This resulted in a total frame length equal to 100 mm, which ensures a sufficiently rigid system to comply with the constraint of maximum deformation within 15 mm (calculated as 1/200 over the 3000 mm slab-to-slab distance).
Thermal resistance	Thermal resistance has been verified against a baseline retrofitted wall made of the following layers: internal plaster, 15 mm; hollow brick layer, 80 mm; air cavity, 80 mm; hollow brick layer, 120 mm. The reference building is retrofitted using 160 mm rockwool insulation, while the ORF is characterized by the same amount of insulation plus the external extruded aluminium frame. The calculated U value for the reference retrofit and ORF are respectively equal to 0.189 $W/m^2/K$ and 0.217 $W/m^2/K$. The psi-value (thermal linear loss coefficient) for the ORF is equal to 0.0167 W/m/K. Hence, the effect of thermal bridge and consequently reduced average U-value needs to be accounted for when designing the retrofit action. As a further development option, thermal break within the frame or a different framing material, such as timber, could be considered to mitigate the impact of the thermal discontinuity on the overall energy performance. Overall, a traditional ETICS system results more convenient in terms of cost/thermal performance ratio. However, the design driver was to push the industrialized approach towards a plug-and-play façade system. In this case, energy performance falls within regulatory limits but is not pushed to the maximum achievable performance levels.
Hygro-thermal and condensation risk	Based on both the steady-state and dynamic calculations, the eventual risk of surface condensation is not expected. However, when wall materials with very low or zero vapor resistance are used in the existing wall, a high moisture transfer towards the outside could occur. In this configuration, in a limited number of peak conditions over the two-year simulation timeframe, the 95 % threshold in relative humidity could be passed at the contact between insulation and the metal frame. However, the spatial integral calculated shows that the surface condensation phase is rapidly followed by a drying phase, with no accumulation foreseen in the insulation material. As a result, the risk of interstitial condensation is also is unlikely to happen in the case of existing buildings. In addition, this risk is analogous to what can take place in the case of a vented rainscreen at the fixing locations, wall to substructure interface.
Water tightness	The visual inspection performed after the water jetting test presented in the methodology section has shown water drops have entered the air cavity behind the external cladding in a significant quantity, entering both vertical and horizontal joints of the system. In addition, the test highlighted inappropriate positioning of the anchoring hook of the panel, which was causing water infiltration from the air cavity towards the back of the panel through the frame. This issue has been however easily solved fixing it on the main-frame back without any break of the watertight layer. The test proved that the system composed by the extruded aluminium frame and inserted gaskets was overall working properly in terms of water tightness.
Impact and wind resistance	Impact resistance of the system integrating a peculiar innovative polymer concrete cladding has been assessed and determined as CLASS III, meaning that the ORF façade can be installed in building, but not at ground level in areas with public access. Impact tests have been performed on three different sized passive cladding panels, namely 813 x 402 mm, 813 x 410 mm, 1210 x 443 mm, and breaks have been registered for the combination of 1 kg + 10 joules on a 1210 x 443 mm panel. Wind resistance has been tested up to 3000 Pa pressure/suction for all the three cladding options: passive, PV and ST. No breaks have been registered.
Fire reaction	Fire reaction has been tested on a façade corner specimen, equipped with PC passive cladding, with two façade elements, respectively 1000 x 1500 mm, and 500 x 1500 mm sized. According to test procedure, two joints need to be placed in the larger module (1000 x 1500 mm). One of the prototypes was coated with a cool surface reflective paint, while the other was left uncoated. The coated prototype performed better than the other in terms of both heat release and smoke production. In terms of lateral flame spread, the distance was below module width. The materials did not produce any hot melted drops within the first 600 seconds. As the system was not intended for certification, the procedure was executed on a single occurrence, instead of the three-time repetition prescribed by the regulation for certification purposes. Test results were in the range to obtain a B,s1,d0 classification, over the minimum threshold of B,s3,d0 that is required to operate in both the Italian and Spanish construction markets, which were involved in the project through demo case building.

3.3 FAÇADE COST

At the end of the development and after the first demonstration in a real building, the costs of system design, manufacturing, and installation are in the range of 1.5 to 3 times the cost for a traditional façade retrofit solution. More specifically, the authors calculated the ORF system costs at around 3 times the cost of a baseline ETICS insulation and 1.5 times the cost of a vented rainscreen insulated system. A detailed cost breakdown of this system is not shown for confidentiality reasons. However, more details on potential optimisation margins are provided in section 4.2.1.

4 ORF SYSTEM STRENGTHS AND LIMITATIONS

4.1 OVERVIEW

The presented façade system in its final configuration results in a flexible façade retrofit kit for the energy deep renovation of buildings.

The chosen final solution, based on the macro-panel concept, allows for the integration of different cladding solutions, from passive to active (as per mock-up Fig.11 and demo building Fig. 12 installations).

FIG. 11 Performance mock-up of the façade integration, passive (left), PV (centre), and ST (right) claddings

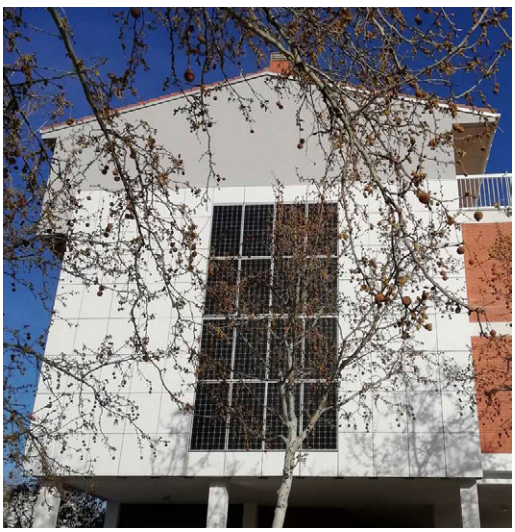

FIG. 12 First demo building installation in Zaragoza (Spain), 2019

The system ensures adequate performance, verified in terms of mechanical resistance, thermal resistance, hygrothermal behaviour, water tightness, impact and wind resistance, and fire reaction. Easy access to all components across the system section is guaranteed, thanks to the offsite assembly design approach and to the use of a removable cladding fixing system.

The current sizing of the first and second insulation layer, and the frame features, determines a reduction of the whole façade's thermal resistance compared to traditional ETICS, which might be not fully appreciated in cold climates. Nevertheless, the macro-panel frame has to be considered under a custom-made vision, for which the use of thermal breaks, grooves, and wooden parts can reduce the thermal performance gap with a continuous insulation system, satisfying the customer specifications. The anticipated engineering effort spent during the project phase also allows for a reduction in construction time, as the substructure and the anchoring systems are both working as plug-and-play. The installation on site is performed without scaffoldings, using just cranes and/or moving platforms. This solution is flexible enough to accommodate intervention on façades up to 30 m in height (i.e. buildings of approximately 10 storey). The first figure relating to timing performance of on-site installation is about 160 m^2/day. A reduction in the installation time is therefore one of the most readily quantifiable notable advantages, saving installation costs in terms of manpower, equipment, and construction-site related expenses (e.g. public land occupancy). However, a more detailed analysis based on a series of complete experiences is needed.

4.2 DISCUSSION

4.2.1 Costs and business models

Based on the cost categories in Table 3, as applied to the demonstration building mentioned above, average façade-specific costs have been calculated to be in the range of 1.5 – 3 times the cost of a traditional façade external retrofit intervention. This is certainly a current limitation to broad market penetration, and the challenges of cost optimisation and value engineering are already being addressed within the frame of the project. In more detail, the ORF system cost is in the range of 3 times the cost of an ETICS system with no external cladding, and 1.5 times the cost of a vented rainscreen with insulated air gap. If the ORF system could be deployed to a larger extent in the construction market, economies of scale can be triggered, lowering down the components' prices. However, comparing the ORF, and multifunctional façade systems in general, to ETICS should be avoided in the future, given the substantial difference in physical behaviour and the number of functionalities that can be integrated exclusively in the ORF system, and not in the passive ETICS system.

To sum up, the main justifications to extra costs incurred in implementing the ORF are found in the following: (i) the ORF system has been implemented within the frame of a research project and only one demo-case building, with a few square meters of façade, implying that economies of scale have not yet been activated; (ii) the ORF value chain is still at an early stage of development, currently initiated but still limited to the offsite fabrication phase, resulting in scattered design and assembly process with very low cost optimisation; (iii) added value to the solution, deemed to lower down costs over the life-cycle lie in novel business models based on the circularity principles. Such models have been already analysed in Orlandi, Ilardi, Catgiu, and Carra (2019). Moreover, experiences of "façade leasing", like the one discussed in Prieto, Klein, Knaack, and Auer (2017), are setting the basis for a paradigm shift in façade from product to service. In this light, ease of dismantling and re-installing is a key feature. In this framework, the ORF could be a mature technology to be exploited thanks to its features of being easy to dismantle and to re-install.

For the above, a reduction in cost can be reasonably foreseen once the production line is stabilised, in terms of physical location component supply network, experienced manpower for manufacturing and installation, increased manufactured quantities.

A more comprehensive value engineering analysis, currently under development, can also demonstrate that the difference in cost at time of intervention is consistently reduced when considering the entire façade lifecycle. The delta can be further mitigated by the inclusion of the commercial value parameter in this analysis. In fact, the offsite fabricated system allows for technical risk reduction, as it minimises construction works to be performed on-site. This impacts the final quality of the result and can be accounted for in the life-cycle analysis when using the multiple-benefit approach. At present, there is no standardised methodology for a coherent cost comparison between the façade energy renovation standard technologies and the offsite fabricated approach. Nevertheless, the inclusion of all relevant technical and commercial parameters in the cost comparison analysis is needed and can support the ORF system business case. Further effort will be dedicated to this specific task in the future.

4.2.2 Technical review

Diving deeper into the technological limitations of the system, which also bear an impact on the total cost of ownership for the system, the authors have identified the use of multiple framing systems according to cladding type as another issue to be tackled in the next developments. The frame section itself is also a main cost consideration, as the profiles have been purposely extruded to couple and create multiple decompression chambers, to allow for the use of a gasket system in a unitised façade fashion. Finally, the use of metal in the ORF frame could be coupled with a timber-based frame and be used exclusively to provide increased stiffness to a timber-based system. Eventually, it could also be totally discarded and just be applied in the system fixing (link to existing wall and panel substructure). However, these options will be investigated as a potential outlook for the medium-term future, also relying on a number of successful renovation actions developed on a timber-based system.

In addition, the integration of a decentralised ventilation unit within the macro-panel (conversely to the level of detail reached in the case of both PV and ST modules) has only been developed at a preliminary stage. It would be worth further investigation in the future to check whether the added functionality can support the ORF system value determination and decrease the cost difference between the non-prefabricated and the prefabricated solution.

4.2.3 Processes

In terms of the construction process, the ORF presents margins for optimisation, as the system at the current level of development still requires a quota of the assembly work to be performed on site prior to macro-panel installation, namely: anchoring of building services distributions, of the brackets at the concrete slabs and of the first insulation layer.

In addition, a construction process issue arises from the presence of the on-site installed insulation at the interface between the existing wall and the new façade system, as it generates manual work that can reduce the impact of benefits brought about by macro-panel offsite assembly. Although the soft insulation layer has to be manually placed over the existing façade, movable auxiliary equipment can be used for this task (no need of fix scaffolds).

5 CONCLUSIONS

This article has presented findings from the research and development activities focused on the development of an offsite fabricated system for ventilated façade energy refurbishment that can provide the construction market with a systemic approach to renovation, combining energy efficiency, multifunctionality, integration of renewable energies and ease of installation as design drivers.

Building heating demand is reduced thanks to a traditional continuous insulation layer and the additional prefab panel, while overheating is prevented thanks to the natural micro-ventilation behind the cladding.

The ORF system development drivers has allowed the following strength points to be achieved. The designed ORF macro-panel frame (i) allows for the installation of many kinds of different passive and active (PV and ST) cladding elements, (ii) the ORF system showed lowered installation efforts thanks to the high degree of prefabrication of the solution, based on a design-for-assembly and maintenance approach, as well as simplified integration of extra technical equipment besides insulation, such as wires, ducts, and other distribution elements. In addition, the system is also compatible with a variety of cladding types, spanning from passive opaque materials, traditionally applied in vented rainscreens, to active systems for the renewable energy sources exploitation, such as PV or ST modules.

The proposed façade system solution can be broken down into three main functional layers (from inside to outside): (i) adaptation layer between the existing wall and the new façade system, composed of soft compressible insulation where eventual piping, ducting, and cabling can be hosted in case an energy system renovation is addressed; (ii) offsite fabricated extruded aluminium macro-panel frame, anchored to the existing wall through brackets and adaptable with both passive or active cladding. This layer also includes an additional insulation element to complement thermal resistance provided by the compressible insulation layer; (iii) external cladding, installed offsite with a removable plug-and-play anchoring system based on a combined gravity and mechanical retention system.

The functioning principle of the ORF is based on the plug-and-play installation approach, so to allow quick and reliable installation as well as permitting easy access to components during building service life. In the current state, this is achieved through the combination of a metal mullion substructure and a metal frame running all-around the panel edges. This is deemed to increase costs and the system could be further optimised in terms of frame typology to be applied according to panel dimension and weight. In addition, the frame structure at current state still requires minor manual operations to be performed on site.

The cost analysis carried out within the project proved that current cost ratio of a traditional façade retrofit solution versus the ORF is in the range of 1:2 – 1:3. However, the attempt to quantify specific costs at a coherent level between ORF façade and a traditional approach showed that there is no current methodology available to compare costs. This is due to the difference in system intrinsic value, as well as the current difficulty encountered in determining added value generated by the increased quality output the pre-assembled solution can guarantee, together with the ease of assigning multiple functions to the façade. However, a substantial improvement in the economic case for adopting prefabricated systems in façade energy retrofitting could be supported by analysing cost variations when adopting different load bearing structure, insulation, and external cladding system, as well as adopting a life-cycle costing perspective and including the added-value of system integration in the analysis.

In terms of future research development, the authors are investigating cost optimisation opportunities in the system. The current manufacturing cost is deemed excessive to allow a broad market penetration of the system. Specifically, cost optimisation is being pursued evaluating both alternative configurations of the same concept (frame dimension variations and number of fixings), as well as the use of alternative framing technologies (e.g. combining a timber frame with a metal mechanical fixing).

Acknowledgements

The authors kindly acknowledge Ignacio Gonzalez Perez and Cristina Criado Camargo (ACCIONA), for the deep involvement in the façade system development, especially focusing on the passive cladding and the verification of the technical requirements. This research was undertaken within the BuildHEAT project, which has received funding from the European Union's Horizon 2020 research and innovation programme under grant agreement No. 680658. The European Commission has no liability for any use that may be made of the information it contains.

References

Andaloro, A., Avesani, S., Belleri, A., Machado, M., & Lovati, M. (2018). Adaptive window block for residential use: Optimization of energy matching and user´s comfort. *Proceedings of the COST Action TU1403 Adaptive Façades Network Final Conference, 9*. Lucerne: TU Delft Open.

Arashpour, M., Abbasi, B., Arashpour, M., Reza Hosseini, M., & Yang, R. (2017). Integrated management of on-site, coordination and off-site uncertainty: Theorizing risk analysis within a hybrid project setting. *International Journal of Project Management*, 35(4), 647–655. https://doi.org/10.1016/j.ijproman.2017.02.016

Bertram, N., Fuchs, S., Mischke, J., Palter, R., Strube, G., & Woetzel, J. (2019). Modular construction: From projects to products (p. 34). McKinsey & Company.

Bonato, P., Fedrizzi, R., D'Antoni, M., & Meir, M. (2019). State-of-the-art and SWOT analysis of building integrated solar envelope systems. *IEA SHC Task 56*. https://doi.org/10.18777/ieashc-task56-2019-0001

Colinart, T., Bendouma, M., & Glouannec, P. (2019). Building renovation with prefabricated ventilated façade element: A case study. *Energy and Buildings,* 186, 221–229. https://doi.org/10.1016/j.enbuild.2019.01.033

D'Oca, S., Ferrante, A., Ferrer, C., Pernetti, R., Gralka, A., Sebastian, R., & op 't Veld, P. (2018). Technical, Financial, and Social Barriers and Challenges in Deep Building Renovation: Integration of Lessons Learned from the H2020 Cluster Projects. *Buildings,* 8(12), 174. https://doi.org/10.3390/buildings8120174

EN. (2020, May 20). EN 13823:2020 Reaction to fire tests for building products—Building products excluding floorings exposed to the thermal attack by a single burning item. EN.

EN ISO. (2017). EN ISO 10077 Thermal performance of windows, doors and shutters—Calculation of thermal transmittance—Part 2: Numerical method for frames. EN ISO.

EOTA. (2012a). ETAG 034-1: Guideline for European Technical Approval of Kits for External Wall Claddings—Part I: Ventilated Cladding Kits Comprising Cladding Components and Associated Fixings. (April).

EOTA. (2012b, April). ETAG 034, Guideline For European Technical Approval Of Kits For External Wall Claddings. EOTA. Retrieved from www.eota.eu/en-GB/content/etags/26/

EPFL. (2016). IEA SHC Task 41 Innovative solar products for building integration. Retrieved 3 August 2020, from https://leso2.epfl.ch/solar/index.php?page=home

European Parliament. (2011, September 3). Regulation (Eu) No 305/2011 Of The European Parliament And Of The Council. *Official Journal of the European Union*. Retrieved from https://eur-lex.europa.eu/eli/reg/2011/305/oj

Gasparri, E., & Aitchison, M. (2019). Unitised timber envelopes. A novel approach to the design of prefabricated mass timber envelopes for multi-storey buildings. *Journal of Building Engineering,* 26, 100898. https://doi.org/10.1016/j.jobe.2019.100898

Italian Government. (2008, April 2). DM 14 Gennaio 2008. Gazzetta Ufficiale della Repubblica Italiana [Official Journal of the Italian Republic]. Retrieved from https://www.gazzettaufficiale.it/eli/gu/2008/02/04/29/so/30/sg/pdf

Lattke, F., & Cronhjort, Y. (2014). smartTES: Introduction to a new retrofit method. München: Technische Universität München Fakultät für Architektur. Retrieved from http://www.holz.ar.tum.de/fileadmin/w00bne/www/04_Forschung/02_Abgeschlossen/BMBF033R057_978-3-941370-44-9_Introduction_smartTES.pdf

Lu, W., Chen, K., Xue, F., & Pan, W. (2018). Searching for an optimal level of prefabrication in construction: An analytical framework. *Journal of Cleaner Production,* 201, 236–245. https://doi.org/10.1016/j.jclepro.2018.07.319

Maurer, C., Hubschneider, C., Maurer, C., Taveres-Cachat, E., Hollick, J., Lemarchand, P., Aagesen, V. (2018). Report on Barriers for New Solar Envelope Systems. IEA SHC Task 56. https://doi.org/10.18777/ieashc-task56-2018-0001

Ochs, F., Siegele, D., Dermentzis, G., & Feist, W. (2015). Prefabricated Timber Frame Façade with Integrated Active Components for Minimal Invasive Renovations. *Energy Procedia*, 78, 61–66. https://doi.org/10.1016/j.egypro.2015.11.115

Op't Veld, P. (2015). MORE-CONNECT: Development and Advanced Prefabrication of Innovative, Multifunctional Building Envelope Elements for Modular Retrofitting and Smart Connections. *Energy Procedia*, 78, 1057–1062. https://doi.org/10.1016/j.egypro.2015.11.026

Orlandi, M., Ilardi, S., Catgiu, C., & Carra, G. (2019). Circular economy principles for active façade systems (Deliverable No. D3.10b). Retrieved from www.buildheat.eu/wp-content/uploads/2020/05/20200302_WP3_D3.10b_PP01_Report-on-active-face-kit_Circula-economy-addendum.pdf

Prieto, A., Klein, T., Knaack, U., & Auer, T. (2017). Main perceived barriers for the development of building service integrated façades: Results from an exploratory expert survey. *Journal of Building Engineering*, 13, 96–106. https://doi.org/10.1016/j.jobe.2017.07.008

Silva, P. C. P., Almeida, M., Bragança, L., & Mesquita, V. (2013). Development of prefabricated retrofit module towards nearly zero energy buildings. *Energy and Buildings,* 56, 115–125. https://doi.org/10.1016/j.enbuild.2012.09.034

From Architectural Requirements to Physical Creations An Algorithmic-based Approach for Façade Design

Inês Caetano[1*], António Leitão[1], Francisco Bastos[2]

* Corresponding author
1 INESC-ID/Instituto Superior Técnico, University of Lisbon, Portugal, ines.caetano@tecnico.ulisboa.pt
2 CiTUA, Centro de Inovação em Território, Urbanismo e Arquitetura, University of Lisbon, Portugal

Abstract

Computation-based approaches are increasingly important in architecture, namely Algorithmic Design (AD), which is based on the use of algorithms to generate designs. Besides enhancing design exploration, AD helps architects deal with recurrent design changes and with the pressure to quickly obtain results. Moreover, AD supports the search for better-performing solutions that satisfy environmental demands. Unfortunately, the complexity and specialized knowledge required by AD are still restraining architects due to the amount of effort and time needed to implement the necessary algorithms. To make AD and design optimization techniques more accessible, we propose a theoretical framework to help architects with the algorithmic generation, evaluation, and manufacturing of a large variety of designs, by following a continuous design workflow that merges the typically detached design stages.
In order to be useful, the framework needs to focus on a domain of application, and, in this paper, we target the development of buildings' façades due to their aesthetical and environmental relevance.
We evaluate the framework in the context of a real case study resulting from a collaboration between a team of architects specialized in AD and a traditional design studio.

Keywords

Algorithmic design, façade panels, geometric patterns, fabrication techniques

DOI 10.7480/jfde.2020.2.4543

1 INTRODUCTION

Nowadays, digital tools and computation-based design approaches play a relevant role in the conception, analysis, and production of architecture. Algorithmic Design (AD) is one such approach that uses algorithms to generate designs. AD promotes design exploration and the emergence of complex shapes and geometric patterns that would be difficult and costly to produce without it (Moneo, 2001). Additionally, AD enables design optimization, i.e., the search for better-performing design solutions, and fabrication (Gibson, Rosen, & Stucker, 2010).

Unfortunately, AD is not yet widespread, mainly due to its complexity and the specialized knowledge required. The challenge, then, is to make AD more accessible and more purposeful. To this end, we explore its application in building design, more specifically, in envelopes. In order to help architects with the algorithmic development of a large variety of façade designs, we propose a theoretical framework that implements, in a single and continuous workflow, the design exploration, analysis, optimization, and rationalization stages. Differently from other approaches, the one proposed here is based on a set of mathematical principles that underlie the computational description of façade designs, independently of the specific implementation of those principles. This allows the framework to be portable across different design tools.

2 BACKGROUND

2.1 ON THE IMPORTANCE OF THE FAÇADE

Considered the "public face of architecture" (Baper & Hassan, 2012), the architectural façade is regarded as the outer layer of a building, separating the indoor environment from the outside. This element plays an important role in building design, having many associated functions: environmental performance (Picco, Lollini, & Marengo, 2014), acting as a filter towards energy-reduction, daylighting, ventilation, and good indoor quality spaces (El Sheikh, 2011); structural function (Al-Kodmany & Ali, 2016), integrating the building's structural elements; cultural identity (Schittich, 2006; Schulz, 1971), marking the aesthetical evolution of the city and its architecture; and urban communication (Picco et al., 2014; Stojšić, 2017; Venturi, Brown, & Izenour, 1972).

With the increase of architectural design constraints, including environmental concerns, economic limitations, and tight deadlines, façade design grew in complexity. Moreover, designing intricate geometries/patterns that are low-cost and simultaneously have good performance is a hard and error-prone process. AD helps overcome these problems by allowing a more flexible and iterative design process that shortens the time needed to explore different design solutions. Still, designing façades using an AD approach requires the use of different programming techniques and algorithmic strategies, for which most architects are not yet well-trained. Consequently, its use often ends up limiting their creative and design exploration processes. We believe that solving this challenge entails the delivery of a flexible computational framework that tames the complexity of procedural modelling, analysis processes, and optimization strategies.

Previous research structured the intricacy of architectural façades (Moussavi & Kubo, 2006; Otani & Kishimoto, 2008; Pell, 2010). Inspired by works confirming that sets of algorithms can be generalized and reused in the exploration of new designs (Chien, Su, & Huang, 2015; Qian, 2009; Woodbury, Aish, & Kilian, 2007), Caetano, Santos, & Leitão (2015) developed an algorithmic-oriented framework for façade design that identifies sets of predefined algorithms and strategies addressing the modelling needs of different designs. Nevertheless, this framework is restricted to initial design stages and does not consider design analysis or manufacturing stages.

2.2 ON THE IMPORTANCE OF PERFORMANCE

The idea of an informed and conscientious design process has always been present in architecture, but it has evolved throughout the last decades. Currently, it persuades architects to focus more on the exploration of multiple solutions in order to find those with the best performance regarding different metrics. This trend is particularly relevant in the design of façades, which are increasingly approached as filters between the environment and interior spaces that aim at providing better indoor environmental quality (e.g., regarding natural light, ventilation, and thermal comfort), while reducing the buildings' energy costs (El Sheikh, 2011).

Improving buildings' performance clearly benefits from an AD approach, namely, in automating the generation of design variations and in analysing and optimizing their performance (Kolarevic, 2005). Moreover, this combination enables a continuous workflow where design exploration, analysis, and optimization are merged into a single design process.

Nevertheless, analysis and optimization processes are often time-consuming, lack real-time feedback (Choo & Janssen, 2015), and, generally, hardly evaluate all possible solutions, usually resulting in just a partial improvement (Nguyen, Reiter, & Rigo, 2014). Moreover, optimization processes are scarcely applied at early design stages (Lin & Gerber, 2013) and are typically postponed to later phases where the integration of design changes is much more toilsome, hindering the search for better performing solutions (Konis, Gamas, & Kensek, 2016). Finally, given the variety of available methods, the selection of the most suitable optimization algorithm for a given problem becomes a non-trivial task (Nguyen et al., 2014).

3 METHODS

The aim of this research is to support architects in obtaining better-performing design solutions in a shorter amount of time, while respecting their design intent. To that end, we propose a theoretical framework to help architects with the algorithmic generation, evaluation, and manufacturing of a large variety of designs, by following a continuous design workflow that covers design exploration, evaluation, and rationalization.

This investigation is part of a larger research project focusing on the design of algorithmic façades, which has already studied (1) the use of Computation-based Design approaches in architecture, (2) the current architectural design processes, especially those using AD, and their limitations, (3) the trends found for modelling different geometries and geometric patterns in architecture, and (4) the most used analysis, optimization, and rationalization processes in architecture. Based on the previous findings, we conducted this investigation in a three-stage process that includes:

— Developing a mathematical theory of the building façade (Section 4.1);
— Implementing the proposed theory in an algorithmic-based framework, containing a collection of predefined algorithms and known design strategies specifically targeting buildings' façades (sections 4.2 and 4.3);
— Evaluating the framework's suitability for architectural design (section 5).

The first stage involved the analysis of the current trends in façade design patterns and the structuring of a classification to organize them mathematically.

The second stage entailed two main tasks: implementing the previously developed mathematical-based perspective into an algorithmic framework specifically dedicated to façade designs and structuring the combination of the different types of algorithms implemented. The result is a framework tailored to support an architectural design process based on informed design decisions, which promises to:

— Facilitate the use of AD processes in the design, analysis, optimization, and rationalization of façade designs, providing algorithms that address a wide variety of geometries, evaluation techniques, and design scenarios;
— Solve the current problem of having to use multiple design tools and specialized digital environments, since the available algorithms are portable between the different specialized tools, being capable of automatically adapting the obtained model to the specific modelling requirements of each tool;
— Inform architects about the most suitable algorithms and design strategies for a specific design scenario.

Finally, in the last stage, we evaluated the framework in the development of several case studies of diversified design characteristics and distinct design scenarios, from an early design stage to preparation for manufacturing. In this paper we present one of such case studies, which resulted from our collaboration with a design studio without AD experience, and we discuss the advantages of using the framework throughout its development.

4 THEORY: ALGORITHMIC UBIQUITY IN FAÇADE DESIGN

Notwithstanding AD's advantages in the design, analysis, and optimization of buildings, its use requires architects to learn these new techniques. Considering this, we propose a theoretically supported algorithmic-based framework for façade design that encompasses the entire design process. For each scenario, it provides a set of algorithms and strategies according to the different design stages, helping the architect not only to select the most appropriate algorithms, but also to avoid extensive and potentially error-prone programming efforts. This results in AD models that are geometrically precise and informed about their performance. The next sections present the proposed theory and its implementation in an algorithmic framework specialized in façade design.

4.1 FRAMEWORK STRUCTURE

Architectural practice is highly dependent on the specific circumstances of the design brief and, thus, it is unlikely that the exact same approach can be used in different projects. This applies

to both non-AD and AD approaches. Since we are addressing the latter, we must deal with the variability that typically occurs in architectural design in a perspective that is simultaneously understood by a computer.

Computational tools operate by following a set of instructions described using Programming Languages (PLs). Despite the expressive power of modern PLs, they still follow a formal perspective increasingly inspired by the universally understood language of mathematics. Therefore, this research considered the formalism of mathematics in (1) structuring the overall AD theory, (2) defining the algorithmic strategies, and (3) implementing them in an algorithmic framework specialized in façade design.

A mathematical theory that supports AD tasks for the design exploration, analysis, optimization, and rationalization stages, should provide:

- Flexibility, to support architectural design variability;
- Diversity, to address a large range of design problems;
- Multiplicity of criteria, to accurately evaluate different scenarios;
- Coherency, to correctly link the diverse types of information to the different design stages in a single and continuous workflow.

To cover a wide range of design scenarios, we explored some existing modular programming and Design Pattern (DP) techniques (Qian, 2009; Woodbury et al., 2007), which reuse and adapt ideas from different projects. Having these techniques available at initial design stages allows architects to spend much less time and effort in the programming task, avoiding writing algorithms from scratch every time they start a new design. Accordingly, despite not considering all possible design scenarios, the proposed theory responds to the most common ones and can be adapted to more specific ones.

The theory is structured in a multi-dimensional classification that organizes the available algorithms by typology:

- Geometry: defines the building façade geometry;
- Pattern: explores the combination of geometric elements and transformations;
- Distribution: distributes the geometric elements;
- Optimization: adapts the design solution to a fitness goal;
- Rationalization: makes a balance between design intent and feasibility.

The next section explains the classified algorithms and how they are combined with each other.

4.2 FRAMEWORK APPLICATION

In general, our framework provides $\mathbb{R} \to \mathbb{R}$, $\mathbb{R} \to \mathbb{R}^2$, $\mathbb{R}^2 \to \mathbb{R}^2$, and $\mathbb{R}^2 \to \mathbb{R}^3$ algorithmic functions for each of the different typologies, which are then combined with one another through different function compositions. To better explain this process, we first introduce some notions regarding the framework's implementation and, then, we explain its application.

To simplify the mathematical presentation, all surface-related functions in the framework $S(u,v)$ range over the domain $0 \le u \le 1, 0 \le v \le 1$. Moreover, fundamental operators that can be arbitrarily combined are also available, namely the one-dimensional linear variation function $linear(a,b) = \lambda(t).a + (b-a)t$, wherein $\lambda(t)$ is the **λ**-calculus notation for an anonymous function with parameter t (Leitão, 2014), and the (paradoxical) constant "variation" function $constant(c) = \lambda(t\ldots).c$. Note that the latter returns an anonymous function that can be combined with functions of any number of arguments, adapting its number of arguments according to those of the combined function.

Given that the façade geometry domain is usually two-dimensional, it is necessary to extend the domain of the above one-dimensional variations into $\mathbb{R}^2$ and, to this end, we use higher-order functions (HOFs), i.e., functions that receive other functions as arguments and/or return other functions as results (Leitão, 2014). We define the two HOFs $\dim_u(f) = \lambda(u,v).f(u)$ and $\dim_v(f) = \lambda(u,v).f(v)$, which cause a function f to vary only in one dimension, i.e., in the u or v dimension accordingly. Finally, for function composition, we provide an operator to generalize this operation:

$$\circ(f, g_1, \cdots, g_n) = \lambda(x_1, \cdots, x_m).f(g_1(x_1, \cdots, x_m), \cdots, g_n(x_1, \cdots, x_m))$$

To obtain a simplified notation, we define $u \otimes lim = \dim_u(linear(0,lim))$ and $v \otimes lim = \dim_v(linear(0,lim))$, wherein lim is the domain's limit, we treat all numbers *n* in a function context as $constant(n)$, and we represent any first-order function f that receives functional arguments $g_1, \cdots, g_n$ as $\circ(f, g_1, \cdots, g_n)$. Based on this, $f \times g$ is the same as $\circ(\times, f, g)$.

By using HOFs, we can move from the numeric space, in which numbers are combined using numeric operators, into the functional space, where functions are combined using functional operators. In this space, a straight façade can be defined by the $straight$ algorithm $straight(w,h) = \lambda(u,v).XYZ(u \times w,\ 0,\ v \times h)$ of the Geometry category, which produces a matrix of vectors of points representing a $w \times h$ planar parametric surface, and whose equivalent representation is now $straight(w,h) = XYZ(u \otimes w,\ 0,\ v \otimes h)$. Then, to create a geometric pattern on that same surface, we select one or more algorithms from both the Pattern and Distribution categories: the first one creates the shape(s) to be applied, whereas the second one distributes the shapes on the surface domain.

Note that any function in the Distribution category receives as input not the surface itself but a matrix containing the surface points on which the distribution will be made; information provided by the functions of the Geometry category. As a result, they return another matrix with the same points but rearranged to generate different types of distributions. For example, the function $grid_{squares}$ receives a matrix of points describing a surface and returns a matrix of four points vectors describing squared areas on that same surface. This is visible in Fig. 1, which, from left to right, shows the distributions implemented by $grid_{squares}$, $grid_{triangles}$, $grid_{parallelograms}$, and $grid_{hexagons}$ when applied to a $straight$ surface.

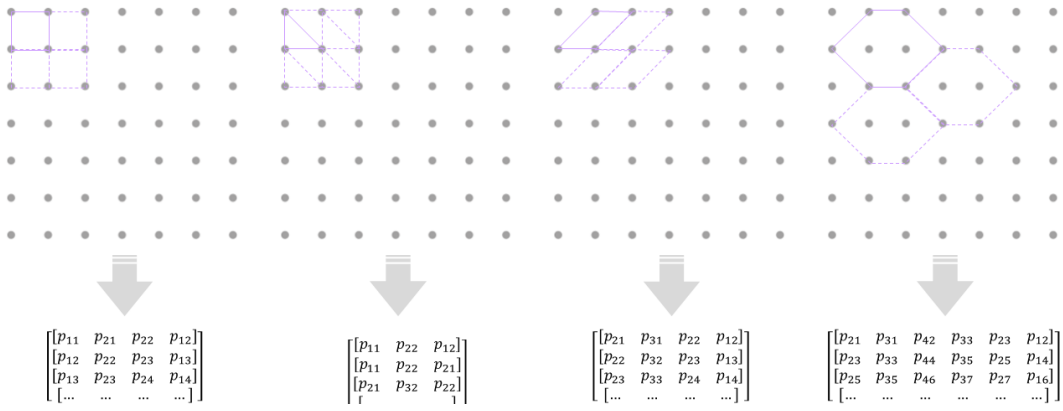

FIG. 1 Algorithms to iterate elements: a conceptual representation of how the surface points are organized in the framework.

Now, consider the Pattern function $shape_{polygon}$ that creates regular polygons. It receives as input the set of points where to centre each polygon (pts) (Fig. 2A-C), as well as the number of sides (n_{sides}) and radius size (r_{size}). To distribute regular-polygonal shaped elements on a straight façade following a matrix of points distributed in squares, we have to combine the three algorithms $straight$, $grid_{squares}$ and $shape_{polygon}$: the first informs the program about the points describing the surface, the second rearranges those points into a matrix of square vertices, and the last one creates a regular polygon fitting each square. Fig. 2D illustrates the result of this combination. The use of a functional representation therefore simplifies the composition of these functions: e.g., $\circ(grid_{squares}, straight)(w,h)$ can be simplified to $grid_{squares}(straight(w,h))$. To facilitate the mathematical representation of functions that deal with matrices containing vectors, e.g., the function $shape_{polygon}$, we introduce the notion of *broadcasting*. Broadcasting allows us to apply a function f to an array of elements, even if it has a different number of dimensions from the other arguments. Syntactically, broadcasting is represented by the *dot syntax* $f.(args...)$ and it can be applied in single or nested calls $f.(g.(args...))$. Based on this, $shape_{polygon}(\circ(grid_{squares}, straight)(w,h), constant(n_{sides}), constant(r_{size}))$ can be simplified to $shape_{polygon}.(grid_{squares}(straight(w,h)), n_{sides}, r_{size})$.

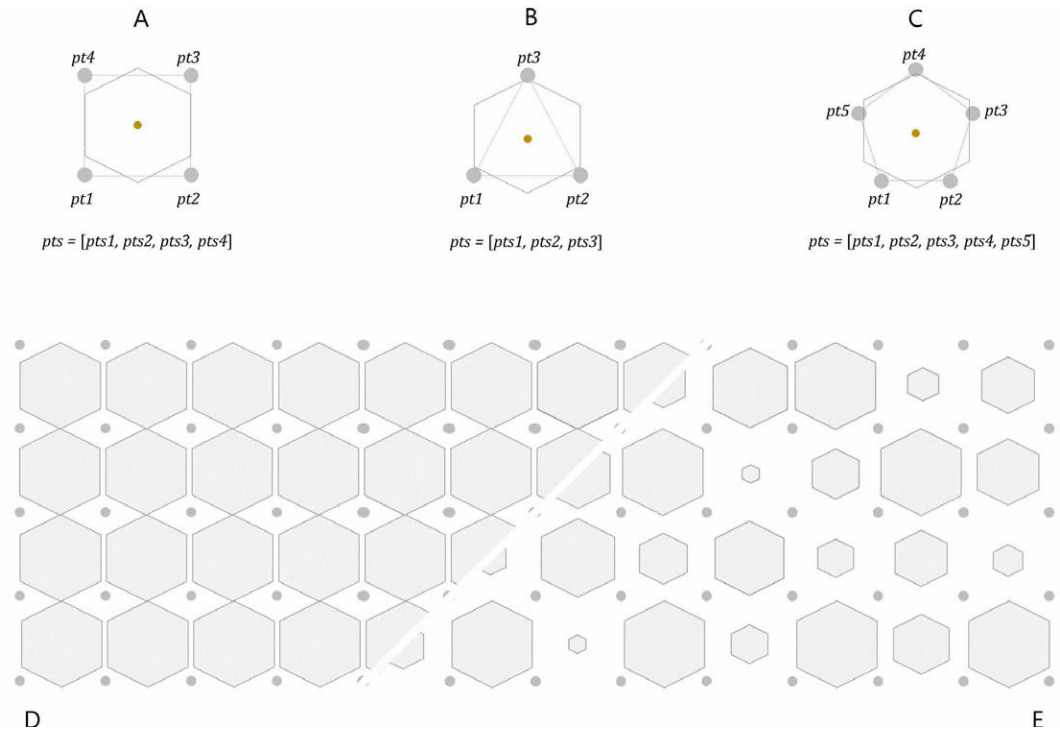

FIG. 2 Algorithms to create and transform geometrical elements: a conceptual representation of the algorithm $shape_{polygon}$: A to C illustrate how the algorithm adapts the polygonal shape to the set of points received (pts); D represents the result of the composition of functions $shape_{polygon}$ and $grid_{squares}$, and *E* the result of the previous composition plus the scale algorithm.

Equally important is the Transformation category, which provides algorithms to deal with different types of geometric transformations, including contracting/expanding (represented by the algorithm $scale$), reflection (algorithm $mirror$), rotation (algorithm $rotate$), among others. Combining these algorithms with those available in the Pattern category allows the generation of a wider variety of more dynamic geometric patterns.

As another example, consider a pattern based on hexagonal apertures, horizontally and vertically aligned, and whose size vary randomly (Fig. 2E). The algorithms selected are, therefore:

- $grid_{squares}$ to distribute the apertures in a squared grid;
- $shape_{polygon}$ to create the hexagonal apertures;
- $scale$ to control their size.

Note that the last algorithm returns, based on the surface position (pt) and a rule to control the transformation process (f_{scale}), the information about which scaling factors to use and where to use them.

We can combine these three algorithms through function composition and, given that the parameters pts and r_{size} of the algorithm $shape_{polygon}$ are informed by the output of the algorithms $grid_{squares}$ and $scale$, respectively, we have the following composition $shape_{polygon}.\left(grid_{squares}\left(ptss\right),\ n_{sides},\ r_{size}\times scale\left(pt,\ f_{scale}\right)\right)$. Note that $grid_{squares}$ receives as argument a matrix of points ($ptss$) representing a surface, whereas $scale$ receives a position on that surface (pt). Assuming the surface is flat, we use the algorithm $straight$ to obtain the surface points $ptss$ needed for both functions $grid_{squares}$ and $scale$. Although $ptss$ constitutes a direct input for the former, i.e., $grid_{squares}\left(straight\left(w,h\right)\right)$, in the

case of $scale$, each of its points has to be applied individually, suggesting the application of the broadcasting technique, i.e., $scale.\left(straight\left(w,h\right),\ f_{scale}\right)$. In the end, we obtain the composition $shape_{polygon}.\left(grid_{squares}\left(straight\left(w,h\right)\right),\ n_{sides},\ r_{size}\times scale.\left(straight\left(w,h\right),\ f_{scale}\right)\right)$, in which we apply the broadcasting technique in nested function calls.

To optimize or rationalize the developed solution, we use the algorithms available in the Optimization and Rationalization categories to either drive the geometric modifications made to the elements or control the number of different elements composing the final solution.

For example, to improve the natural ventilation of the previous design (Fig. 2D), we select an appropriate algorithm from the Optimization category, namely, $opt_{ventilation}$, which receives information about the design's desired performance, context, and geometric characteristics, returning a matrix containing the ideal aperture area for each façade opening. We use $opt_{ventilation}$ to iteratively inform the parameter f_{scale} of the $scale$ algorithm, i.e., $scale.\left(straight\left(w,h\right),\ opt_{ventilation}\left(args\ldots\right)\right)$, and, consequentially, the parameter r_{size} of the $shape_{polygon}$ algorithm, obtaining the following composition $shape_{polygon}.\left(grid_{squares}\left(straight\left(w,h\right)\right),\ n_{sides},\ r_{size}\times scale.\left(straight\left(w,h\right),\ opt_{ventilation}\left(args\ldots\right)\right)\right)$.

Finally, to minimize the manufacturing costs of a design solution, while addressing its construction viability, we have the algorithms of the Rationalization category, which includes both algorithms $discretize$ and $tallying$, among others. These are important for balancing the design intent and performance and the number of different façade elements, as well as for identifying and counting different typologies. Mathematically speaking, a discretization process aims at reducing the number of values accepted by a continuous variable, converting a continuous set of values into a finite range grouped into *n* intervals. Similarly, $discretize$ allows setting the maximum number n_{max} of intervals of the discretized range, which, in turn, corresponds to n_{max} different elements.

In practice, to reduce the manufacturing cost of the previous design, we select the $discretize$ algorithm to control the number of different opening sizes. This is important because the fewer window sizes are allowed, the less expensive the solution's manufacturing will be. When combined with the previous algorithms, $discretize$ affects the range of values received by the $scale$ algorithm, being that the fewer they are, the more viable the solution gets. Note that we now have two algorithms, $opt_{ventilation}$ and $discretize$, informing the parameter f_{scale} of the $scale$ algorithm, originating the following composition $scale.\left(straight\left(w,h\right),\ discretize\left(n_{max},\ opt_{ventilation}\left(args\ldots\right)\right)\right)$. In practice, it is the composition $discretize\left(n_{max}\right)\circ opt_{ventilation}\left(args\ldots\right)$ that balances the design's performance with the maximum allowed number of opening sizes: $opt_{ventilation}$ finds the best values for f_{scale}, which in turn can originate a very broad set of values, while $discretize$ reduces that same range. In the end, we are provided with a set of better-performing design solutions of minimized manufacturing costs and different geometric characteristics, from which we can select the one that best fits both the design's context and intent.

To proceed to the manufacturing stage, it is important to access information about the range of values used in the final design and where they are used. To this end, we can use the $tallying$ algorithm to force the $discretize$ algorithm to store this information. Regarding the previous example, this means we can know the exact positions of the different elements on the façade, allowing us to manage their placement on site.

4.3 WORKFLOW

In order to take advantage of the framework, we propose the use of the workflow in Fig. 3. It starts with the architect's design intent (arrow 1), which he then implements using the framework's algorithms (arrow 2). During this stage (Design Exploration), he tests several design variations and, when satisfied with the result (arrow 3), he moves to the following stage (Design Optimization) and focuses on improving the design regarding different criteria, such as natural lighting illumination, energy consumption, privacy levels, among others. To this end, he selects and combines one or more optimization algorithms from the framework, obtaining the design solution that best fits the requirements (arrow 4). The architect then evaluates this solution and if it does not meet his design intent, he goes back to testing further design variations and their subsequent optimization. Otherwise, the architect proceeds to the ensuing stage (Design Rationalization), which aims at assessing the solution's construction feasibility (arrow 5). For such, he applies the framework's algorithms to control the diversity of elements composing the design solution, thus reducing its manufacturing cost and material waste. The solutions that balance both design intent and feasibility become the set of acceptable design options (the Design Space in Fig. 3) from which the architect then chooses the one that most pleases him (arrow 6).

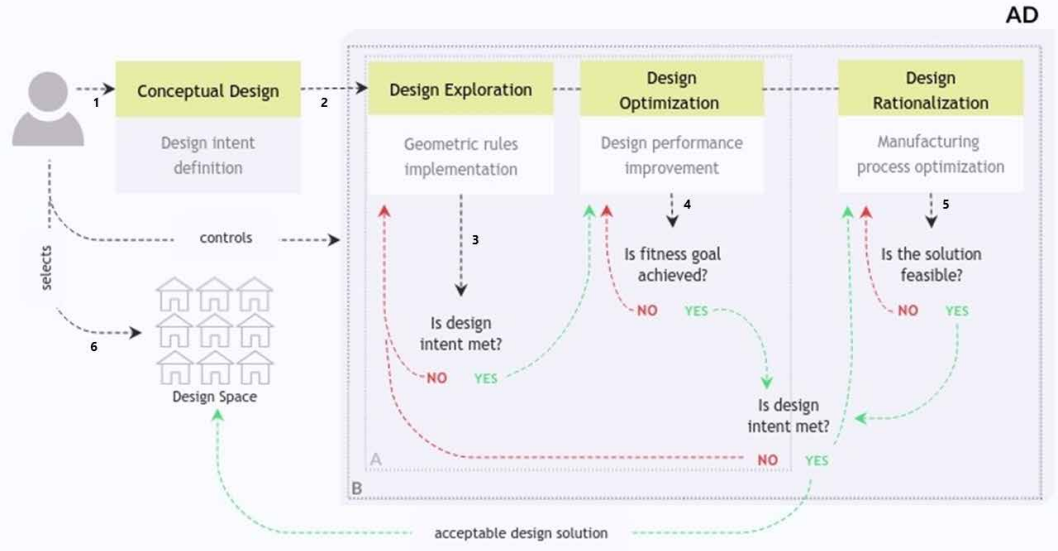

FIG. 3 Design workflow supported by the algorithmic framework: 1. definition of the architect's design intent; 2. algorithmic implementation of the design intent using the framework's algorithms; 3. geometric implementation and design exploration; 4. improvement of the design solution regarding a certain fitness criterion; 5. optimization of the solution's manufacturing costs and waste; 6. selection of the final design solution; A. the iterative process of adjusting the solution's geometric characteristics to meet the fitness goal set; B. the iterative process of balancing the solution's geometry, performance, and feasibility.

In the next section, we evaluate both the framework's suitability for architectural design and the proposed workflow in a real case study entirely based on the algorithms provided and embracing the previously mentioned design stages.

5 RESULTS AND DISCUSSION

We were recently involved in the design of a façade for a residential building. The original design concept for the façade was a composition of geometrically different *cobogó* bricks (Rytel, 2013). As architects specialized in AD, we collaborated with a traditional design studio and applied the framework not only to geometrically explore different options based on the initial design intent, but also to improve, rationalize, and fabricate the final solution. This collaboration demonstrated the framework's flexibility and adaptability to multiple design scenarios and processes, while highlighting the growing need to integrate teams of differently skilled architects.

5.1 CASE STUDY: *COBOGÓ* FAÇADE PANELS

Cobogó is a type of hollow brick used for air circulation and light penetration control in geographical areas with a hot and humid climate (Rytel, 2013), regulating the interior space comfort of buildings. In Portugal, these elements were widely used during the Modern architecture period.

The design studio aimed at integrating some of the local culture in this case study, whose location was Lisbon (Sousa & Batista-Bastos, 2015). Therefore, the architects decided to use *cobogó*-inspired elements in the design of the building's façade. Nevertheless, they wanted to avoid the use of standardized *cobogó* elements and take advantage of geometric variations to improve the building's natural lighting and ventilation performance. The result was an intricate façade pattern combining the influence of the local architecture with the search for an architectural identity.

The next sections explain the design process using the proposed framework.

5.2 DESIGN EXPLORATION

At this stage, together with the design studio, we established a simple geometric rule that, when varying its parameters, originated a set of different brick options. The algorithm implementing such rule receives as input a set of points defining the brick's corners (Fig. 4A) and, based on these points, it then outlines the brick's shape and calculates its centre (Fig. 4B). Thereafter, it allows the user to choose between two options: link the brick's central position either with its edges' midpoints or its vertices (Fig. 4C). Lastly, given the need to integrate different natural lighting and ventilation degrees on the façade, we combined an additional algorithm to create bricks with different opacity levels (Fig. 4D). Fig. 4E illustrates all possible brick options for a given set of four points (Fig. 4A).

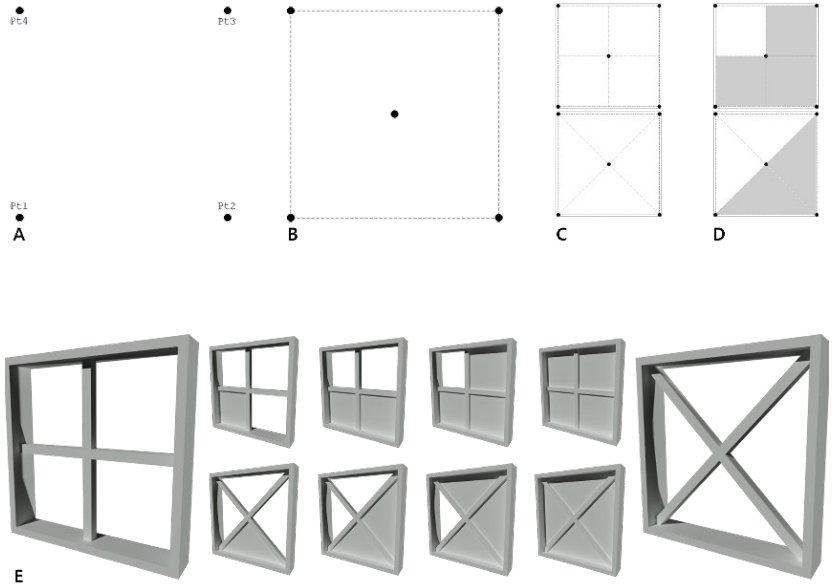

FIG. 4 The application of the cobogó geometric rule when receiving as input a set of four points: A. the received points defining the frame's shape; B. the creation of the frame; C. the selection between two possible rules – connect the frame's centre to the corners or to the edges' midpoints; D. the application of different opacity degrees; E. the range of possible solutions.

In a second stage, we developed different façade designs using these elements. We explored different combinations between the algorithms available in the Distribution category and the algorithm producing each brick. This ensured the bricks' shape was adapted to correctly fit the façade surface. Fig. 5 shows some of the stacking possibilities explored.

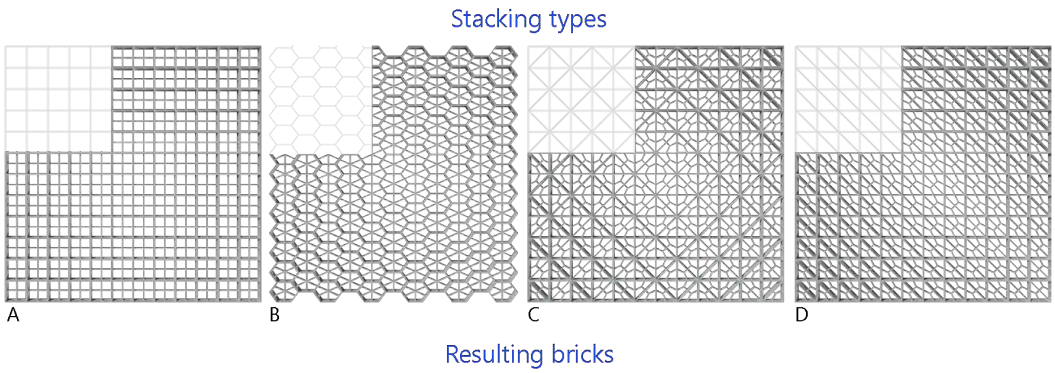

FIG. 5 The different stacking options selected: each scheme from A to D represents a different type of stacking, as well as the set of bricks resulting from its combination with the algorithm producing each brick (the brick's shape adapts to allow a perfect fit).

After deciding on the stacking option(s) to explore, we implemented gradual geometric variations to the façade design that responded to the initial design intent (Fig. 6):

- Apply both geometric rules (Fig. 4C);
- Explore different opacities (Fig. 4E);
- Combine two types of stacking (Fig. 5A and 5D).

One of the advantages of AD is the ability to generate a wide range of design solutions in a short time. However, this raises the problem of how to present a potentially large set of solutions to the architect. This was already addressed by others (Erhan, Wang, & Shireen, 2015), however no consensus on a practical solution currently exists. Therefore, we opted for gradually exploring the design space in a process guided by the architect himself: the decision-making process results from repeating the presentation of design solutions to the architect and using his feedback to guide the generation of additional solutions until the architect is satisfied. So, despite not presenting the entire design space to the architect, we allowed him to control the navigation through the set of potential solutions, among which he could choose the one that most pleased him.

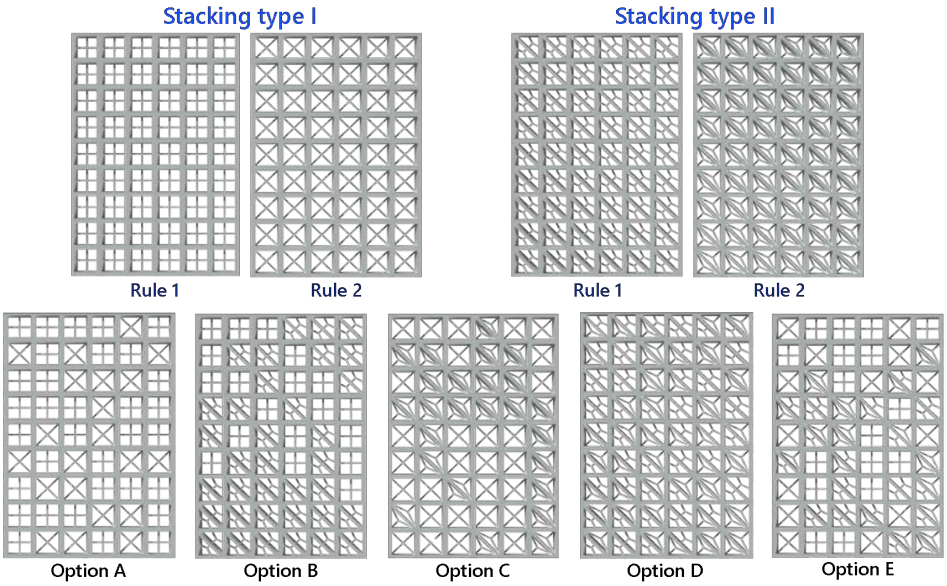

FIG. 6 The evolution of the façade's geometric pattern: option A combines both rules and the stacking type I; option B combines rule 1 and both stacking types; option C combines rule 2 and both stacking types; option D combines both rules and the stacking type II; and option E combines all rules and stacking types.

5.3 DESIGN IMPROVEMENT

This stage aimed at improving the façade design of our case study. Therefore, we considered more design requirements regarding (1) privacy levels, (2) natural lighting, and (3) natural ventilation, that were entirely based on the architect's own practical experience. To address these, we took advantage of another set of algorithms to control the geometric characteristics of each brick in order to respond to the following criteria:

- In private areas and circulation spaces, the fraction and size of the voids should be smaller, meaning that the use of triangular bricks should supplant those of squared ones in these areas;
- In living rooms, terraces, and courtyards, a larger number of squared, less opaque bricks were advisable to provide better views and greater amounts of natural daylight.
- In areas exposed to direct sunlight there should be a preference for more opaque bricks;
- To promote a general natural ventilation, the façade opacity levels should always be higher at its middle than at its top or base.

These requirements originated a set of values for each spatial functionality, each one matching the desired natural lighting, privacy, and natural ventilation levels (Fig. 7) as well as the ratio of squared-shaped to triangular-shaped elements (Fig. 8). Integrating this information with the framework's algorithms allowed the team to iteratively visualize several design options and then, based on their evaluation, produce new solutions exploring only the most favourable design characteristics. Similar to the previous design stage, this process enabled the team to gradually explore the design space in a controlled and conscientious way, quickly refining the façade design solution. Fig. 7 and 8 synthetize the values established for the final solution, after several design iterations.

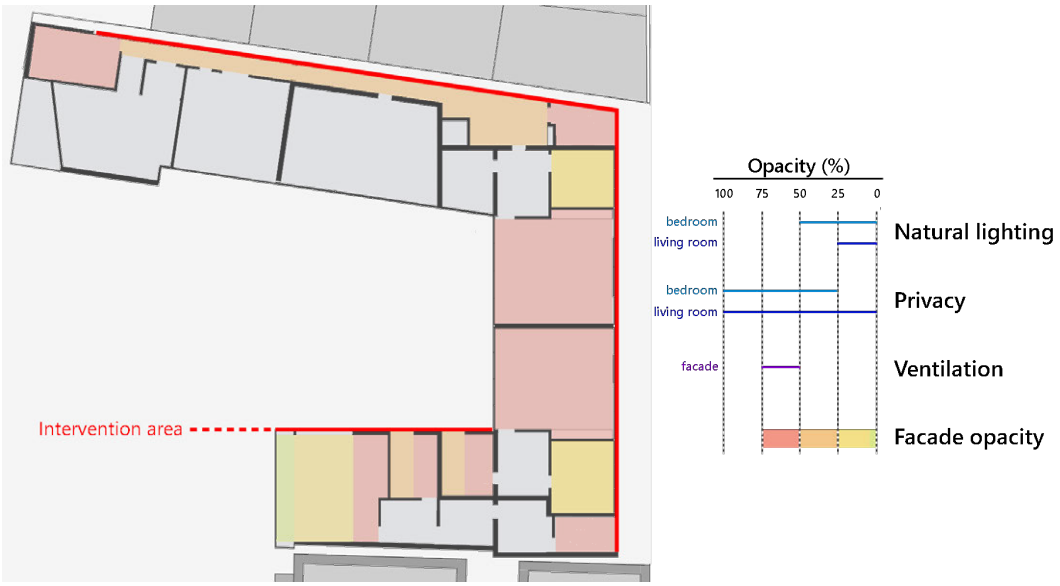

FIG. 7 Case study plan: the red lines represent the façade intervention areas and the coloured areas the different opacity levels explained in the right-side diagram.

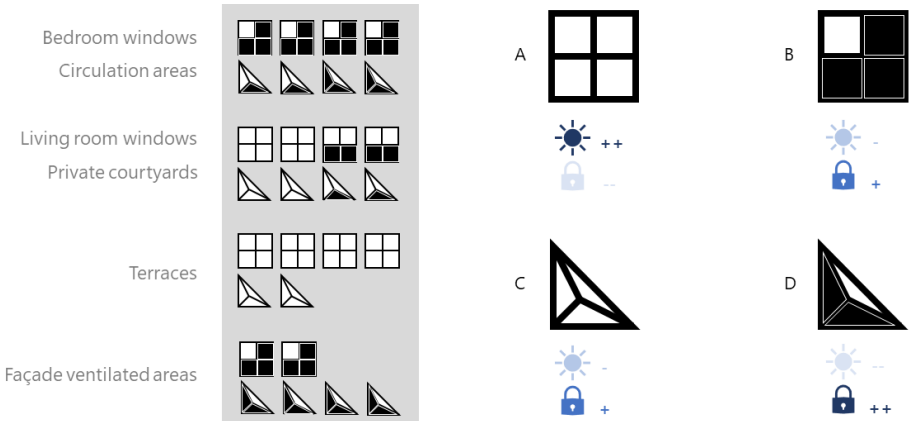

FIG. 8 Left: the ratios of squared-shape to triangular-shaped elements by indoor spatial functionality; right: privacy (the lock symbol) and natural light (the sun symbol) levels provided by each brick type, e.g., A has the highest natural light and the lowest privacy levels, whereas D has the opposite; B and C provide higher levels of privacy than of natural light.

In the end, the process was entirely controlled by the architects, who were responsible for the iterative design choices and derivations throughout the process. Therefore, the use of the framework gave them autonomy and consciousness about the impact their decisions had on the design's final performance. This feedback had a major role in achieving improved design solutions that performed according to the requirements set by the architects and that simultaneously satisfied the initial design intent.

5.4 DESIGN RATIONALIZATION

As AD allows for further design exploration and geometric complexity, it is important to ensure the feasibility of the obtained solutions. Therefore, the framework integrates algorithmic strategies that make their manufacturing viable. These strategies, mainly those of rationalization, become even more relevant in designs whose elements vary in shape, material, size, etc., and where it is, thus, important to control:

- the number of different elements;
- the positioning of elements;
- the manufacturing strategy to follow.

Given the case study's geometric characteristics, the team first considered a manufacturing strategy based on the traditional use of ceramic and moulds to produce each façade element. We used our framework to obtain each brick typology frequency, list of positions (Fig. 9), and 3D model of the mould. This information allowed us to proceed to the following stage, i.e., the bricks' fabrication and subsequent assembly.

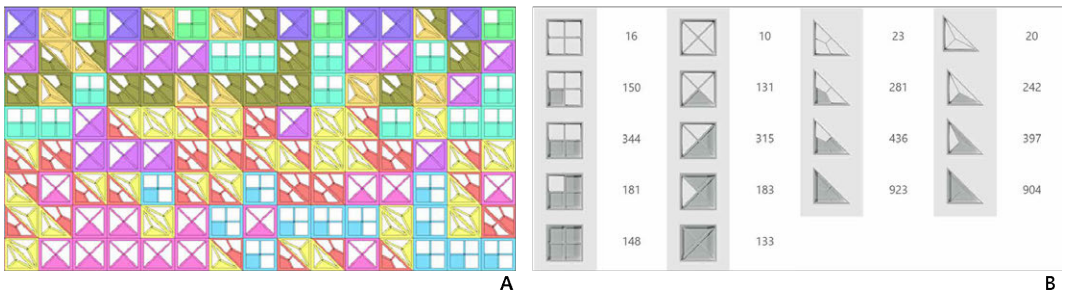

FIG. 9 The application of the framework's rationalization algorithms: A. a section of the façade's 3D model identifying each brick typology (each colour corresponds to a brick type); B. the frequency table of the typologies used.

During this stage, the architects evaluated the constraints resulting from the use of customized bricks. These included, on the one hand, the cost and production of the eighteen types of customized bricks used in the final design solution, whose manufacture required eighteen customized moulds, suggesting the use of the framework's rationalization algorithms to reduce the number of brick typologies. On the other hand, there were façade areas that should act as movable window shutters, which constituted a more serious constraint due to the massiveness and fragility of the *cobogó* bricks.

To deal with these problems, the team decided to follow a different fabrication strategy based on lightweight wood façade panels representing the composition of different *cobogó* elements, allowing to maintain the geometric diversity and plastic expression of the original solution while removing the need for mould production. To evaluate this strategy, we decided to manufacture the wood panels by layers that, when overlapped, originated the desired thicknesses and shapes (Fig. 10). This process again took advantage of the framework's algorithms to, first, generate the façade panels with different geometric compositions and levels of opacity and, then, automatically produce the information needed for their subsequent manufacturing. Fig. 11 illustrates some of the prototypes developed and Fig. 12 the final design solution.

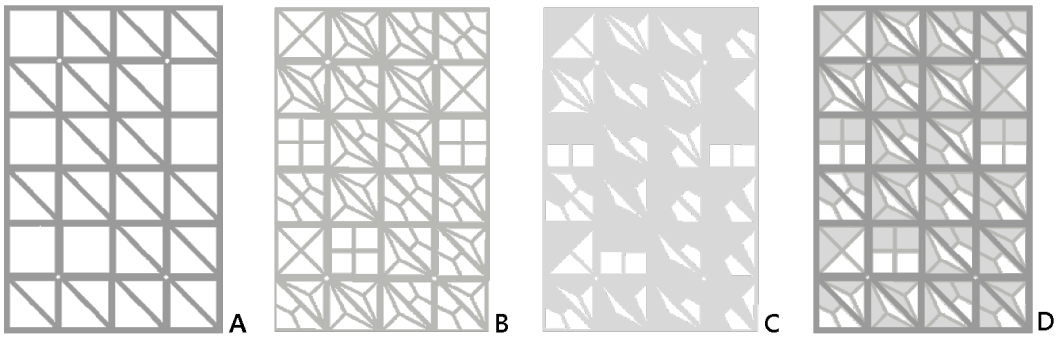

FIG. 10 The set of layers of a panel: A. the outer frame delineating the general shape of the cobogó elements; B. the middle frame outlining their interior elements; C. the inner layer delimiting the existing void and opaque areas; D. the wood panel after overlapping the different layers in the following order: A-B-C-B-A.

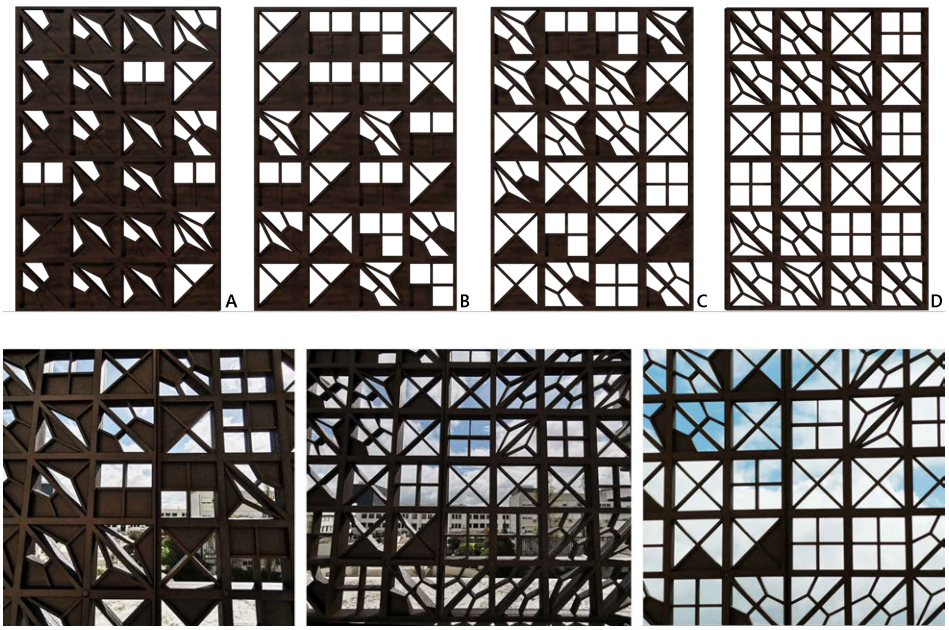

FIG. 11 Prototypes with different opacity levels and ratios of squared to triangular-shape elements. Top: four typologies whose opacity decreases from A to D; Bottom: some of the produced prototypes.

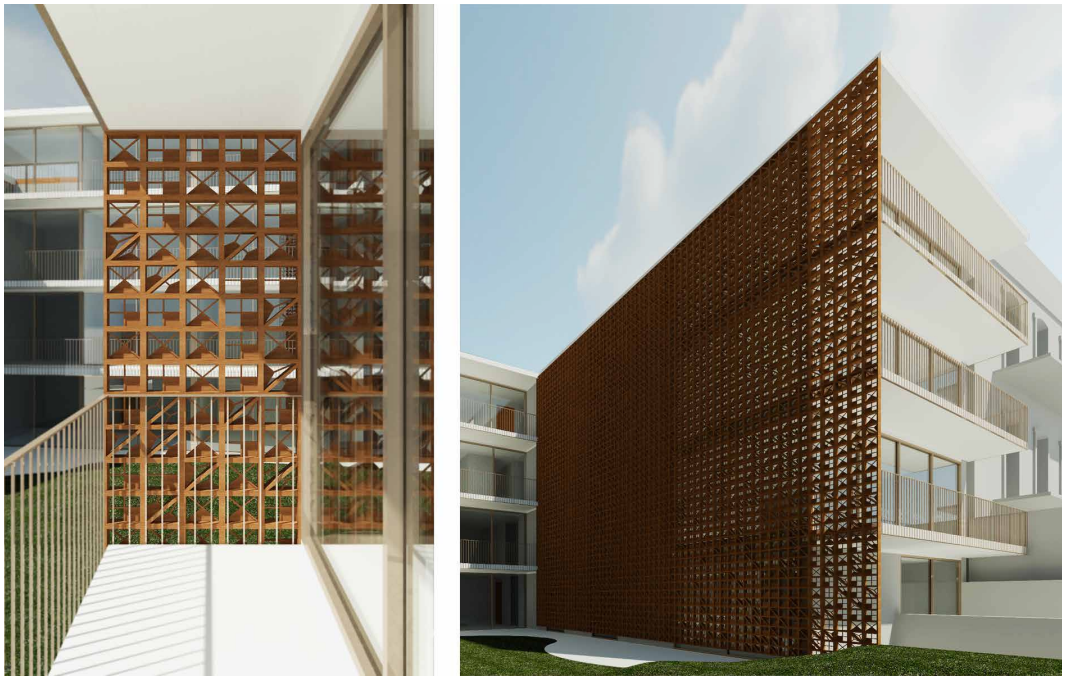

FIG. 12 Two perspective views of the final solution's 3D model in Revit.

5.5 EVALUATION/DISCUSSION

This case study was done in the context of a collaboration between a team of AD specialists and a traditional design studio with no AD experience. After understanding the architect's design intents and his difficulties to make several alternative drawings and model experiments, it was proposed to try an AD approach. We applied the AD framework from an initial design stage, to develop the underlying geometric rules of the façade's elements, until a final design stage, to manufacture the set of panels. The evaluation criteria for measuring the success of this process was the ability to:

- Elaborate a rational for dealing with the principles imposed by conceptual intents;
- Create different geometric patterns following the same principles;
- Balance the most visually interesting patterns with the initial programmatic intents.

By comparing this design workflow with a non-AD one, we can highlight their main differences and the advantages resulting from the use of an AD approach and, more specifically, of the proposed framework.

Regarding the Design Exploration stage (Fig. 3), the generation of different *cobogó* elements would have been more limited if we had used a non-AD design approach: not only would it have taken more time to explore each of the suggested ideas, but it would have also hindered the application of small-to-large design changes during the entire process. The process would probably result in a different set of façade elements from those obtained; it would either not present as many options or not respond as well to the architect's design intentions. In contrast, the use of the framework in an AD approach proved to facilitate not only the exploration of different element geometries, by implementing the set of geometric rules resulting from the initial design intent, but also the application of continuous and iterative design changes, by automatically adapting the solutions being

explored according to the team's feedback (Fig. 3, arrow 3), which in turn is an asset for the ensuing design phases, as we will show.

Considering the Design Improvement stage, where the focus was to improve the solution obtained (Fig. 3, arrow 4), the framework played an active role in enhancing the design options regarding their natural ventilation performance and privacy levels. In practice, it supported a continuous, two-way design process between this stage and the previous one, allowing us to iteratively adjust the geometric characteristics of the façade's elements in order to achieve the fitness goals set by the architects. The rectangular area A in Fig. 3 illustrates this process. The result was a balance between the façade's desired geometric characteristics and overall performance.

Furthermore, the different inputs provided to the algorithm that shaped each *cobogó* brick produced geometric variations that were totally controlled by the team: depending on the values received, the algorithm could generate, at each position, either a squared brick or two triangular ones whose geometric subdivision followed either rule 1 or rule 2 and had a smaller or larger opaque area. As previously mentioned, the allowed options and the ratio between them were both set by the team, meaning that most of the variations obtained were within the design space established by the initial design intent.

Moreover, given the limited time provided for this iterative process, the team could explore more design options, as well as increasingly improve their corresponding performance. If we were to use a non-AD design process instead, it would require manually changing the design after each evaluation process so as to include the modifications needed for the following iteration, which would mean more time spent at each iteration and, therefore, less time available to explore other design variations. Hence, as the range of options analysed would be smaller, the final façade design would probably have a poorer performance compared to those produced with the framework.

Regarding the Design Rationalization stage, whose main concern was the design's feasibility (Fig. 3, arrow 5), using the framework proved to facilitate the search for a constructively viable solution that simultaneously met both performance and aesthetic requirements. The rectangular area B in Fig. 3 represents this process. During this process, we controlled the maximum number of brick typologies allowed, forcing the algorithm to automatically adapt to the design's constraints. Furthermore, the algorithm also produced the information regarding the different typologies used in the final design (including the number of bricks of each typology and their exact positions on the façade), providing the team with the necessary data for the ensuing manufacturing stage. In the end, the team received a set of solutions fitting the design requirements (Fig. 3's design space), from which we could choose the final design (Fig. 3, arrow 6).

Table 1 compares a non-AD design approach with an algorithmic one, evidencing both their advantages and shortcomings. Although AD has a higher initial investment and steeper learning curve for most architects, its long-term application is advantageous to the architectural design practice, as it:

- Improves the creative process – it is flexible, automates repetitive tasks, facilitates design changes, and supports higher levels of design complexity.
- Promotes design improvement – it automates the *generation-evaluation-regeneration* process that improves the design in a viable time.
- Facilitates design rationalization – it supports the generation of designs with controlled variations between elements.

— Supports a continuous workflow – it enables the design changes made at one design stage to have a direct impact on the others.

TABLE 1 Comparison between a non-AD and an AD approach on each design stage

	DESIGN STAGE ACTIVITIES	NON-AD APPROACH	AD APPROACH
Design Exploration	Design concept definition	Intuitive	Reasoned
	Design instantiation	Hard	Easy
	Design space explored	Small	Large
	Implementation of small changes	Easy	Easy
	Implementation of large changes	Difficult (sometimes unfeasible)	Easy
	Propagation of changes	Tedious and error-prone	Automatic and accurate
	Application of iterative changes	Time-consuming and hardworking	Fast and mechanized
	Feedback on the impact of changes	Reduced	Increased
	Model flexibility	Small	Large
	Traceability	Obvious	Non-obvious
	Ability to support complexity	Low	High
Design Improvement	Integration of evaluation results	Manual	Automatic
	Execution of iterative evaluations	Time-consuming and error-prone	Automatic
	Design space explored	Limited	Extensive
Design Rationalization	Ability to support rationalization	Reduced	Increased
	Integration of rationalization rules	Manual	Automatic
	Generation of rationalized models	Manual	Automatic
	Design space explored	Limited	Extensive
	Production of analytical models	Manual	Automatic
	Production of construction information	Dependent on the design tool	Automatic

Typically, any design exploration process starts with the architect using a non-AD approach: he thinks and materializes his design ideas through sketches and handmade schemes to help him establish the design intent. When already delineated, the architect can explore his design idea by following the same approach throughout the entire design process or he can instead opt to transition to an AD approach and benefit from its advantages, for example, in the geometric exploration, in the automation of repetitive design tasks, in the application of rationalization processes, among others. Despite its multiple advantages, the decision to use AD should take into account the initial investment required. When the project being developed is geometrically simple and does not require design variations, the use of AD is not justified, as the initial investment needed to algorithmically implement the design is not paid off later. In most other cases, however, the adoption of an AD approach becomes advantageous, as shown in Table 1.

According to Table 1, the geometric exploration stage generally benefits from the use of an AD approach. Although a non-AD approach is more intuitive, resorting to freehand sketching and physical modelling, when the process is deepened, more time is spent on design exploration, as it relies on repetitive manual design changes. Therefore, within the same time period, it produces fewer complex design options whose corresponding models are also less flexible. Moreover, the ability of AD to automatically and coherently integrate small-to-large design changes in the model not only provides visual feedback on the impact of changes, but also enables the iterative application of changes to meet aesthetic requirements. Nevertheless, identifying the parts of the

code that correspond to the parts of the model that we want to change is not always straightforward or obvious in an AD approach. Contrarily, although the same design changes in a non-AD scenario are more easily tracked because they are directly made to the model, they require manually modifying the model or even redoing the model from scratch. This repetitive and time-consuming process therefore hinders the iterative application of design changes, thus resulting in only slightly improved design solutions.

Table 1 also evidences the differences between both approaches in terms of improving designs. In the non-AD approach, improving a solution requires the manual production of different designs to then evaluate them. Additionally, before proceeding to the next iteration, the evaluation results must be incorporated through manual changes to the design model. As this cycle has to be repeated multiple times until better solutions are found, it becomes extremely time-consuming, tedious, and error prone. Differently from the non-AD approach, AD automates the production of design variations, allowing us to evaluate a greater number of solutions when compared to a non-AD approach.

Table 1 also highlights the potential of AD for rationalization processes. AD allows controlling the variety of elements composing a design solution by iteratively producing variations of it with a decreasing number of different elements. This process results in a set of rationalized solutions from which we can choose the one that best balances design intention and feasibility. In contrast, the same scenario in a non-AD design approach would suffer from the same limitations regarding design improvement processes. Moreover, while an AD approach can automatically produce all the constructive information needed for the construction stage, a non-AD approach depends on the capabilities of the modelling tool being used.

Important lessons can be learned from this experiment. Firstly, when the design can be geometrically parameterized, the design exploration benefits from AD because it makes it possible to explore a wider range of solutions. Conversely, when the project is geometrically simple and has few potential design variations, there is no need to adopt an AD approach, as the required effort might not pay off. Secondly, when the design includes both aesthetical and performance requirements, switching to AD is advantageous, as the initial investment required to algorithmically implement the design is recovered in the iterative evaluation and balancing of the different requirements. Finally, when the project is geometrically complex and/or its manufacture is likely to benefit from rationalization processes, it is advantageous to use AD, as it allows the design feasibility to be increased while maintaining its design identity.

6 CONCLUSION AND FUTURE WORK

The relevance of Algorithmic Design (AD) in architecture is a reality. It not only provides design flexibility and the ability to explore larger design spaces, but also supports the search for better performing design solutions and their subsequent fabrication. Still, in many countries, AD is not yet widespread due to its complexity and the specialized knowledge required. To make AD and design optimization techniques more accessible to architects, we focused on their application, particularly in the design of building envelopes.

In this paper, we proposed a theoretical framework to support architects with the generation, evaluation, and manufacturing of several façade designs by following a single and continuous design workflow. Firstly, we explained the framework's mathematical structure and how to apply and

combine the provided algorithms. Then, we evaluated the framework in a real case study: a façade design composed of different elements inspired by traditional *cobogó* bricks. The final solution resulted entirely from the application of the framework's algorithms to (1) explore the geometric characteristics of the façade's design; (2) improve the design according to a set of requirements; (3) rationalize the design to make its manufacturing process viable; and (4) produce the necessary information for the fabrication of the façade elements.

The case study demonstrated the framework's ability to help the development of a façade design from its conceptual design phase to its actual fabrication, reducing the effort and time needed. Moreover, it proved the framework's capacity to inform the architect throughout the entire design process, providing him with a more conscious and autonomous view on the solutions' performance regarding different requirements and their constructive viability. Finally, its application in a traditional design context, i.e., within a design studio without AD experience, proved the framework's flexibility and adaptability to multiple design scenarios and processes, while evidencing the current need to integrate architects with AD skills within architectural design studios.

As future work, we plan to continue developing geometric rules inspired by traditional *cobogó* bricks and evaluate different fabrication strategies that are more appropriate for other materials (e.g., 3D printing with polymers and customized moulds with concrete). We also intend to continue refining the framework by applying it to other façade designs and extending it with additional analysis tools and optimization techniques.

Acknowledgments

This work was supported by national funds through *Fundação para a Ciência e a Tecnologia* (FCT) with references UIDB/50021/2020 and PTDC/ARTDAQ/31061/2017, and by the PhD grant under contract of FCT with reference SFRH/BD/128628/2017. We also thank *Atelier dos Remédios* for participating in this research.

References

Al-Kodmany, K., & Ali, M. M. (2016). An Overview of Structural and Aesthetic Developments in Tall Buildings Using Exterior Bracing and Diagrid Systems. International Journal of High-Rise Buildings, 5(4), 271–291.

Baper, S. Y., & Hassan, A. S. (2012). Factors Affecting the Continuity of Architectural Identity. American Transactions on Engineering & Applied Sciences, 1(3), 227–236.

Caetano, I., Santos, L., & Leitão, A. (2015). From Idea to Shape, From Algorithm to Design: A Framework for the Generation of Contemporary Façades. In The next city - New technologies and the future of the built environment [16th International Conference CAAD Futures 2015 (p. 483). São Paulo, Brazil.

Chien, S., Su, H., & Huang, Y. (2015). PARADE: A pattern-based knowledge repository for parametric designs. In Emerging Experience in Past, Present and Future of Digital Architecture, Proceedings of the 20th International Conference of the Association for Computer-Aided Architectural Design Research in Asia.

Choo, T.-S., & Janssen, P. (2015). Performance-based parametric design. In Emerging Experience in Past, Present and Future of Digital Architecture, Proceedings of the 20th International Conference of the Association for Computer-Aided Architectural Design Research in Asia (Vol. 1, pp. 1–10).

El Sheikh, M. M. (2011). Intelligent building skins: Parametric-based algorithm for kinetic façades design and daylighting performance integration. Ph.D Thesis. University of Soutern California. https://doi.org/10.1017/CBO9781107415324.004

Erhan, H., Wang, I. Y., & Shireen, N. (2015). Harnessing design space: A similarity-based exploration method for generative design. International Journal of Architectural Computing, 12(4), 217–236. https://doi.org/10.1260/1478-0771.13.2.217

Gibson, I., Rosen, D., & Stucker, B. (2010). Development of Additive Manufacturing Technology. In Additive Manufacturing Technologies: 3D Printing, Rapid Prototyping, and Direct Digital Manufacturing (pp. 19–43). Springer.

Kolarevic, B. (2005). Towards the performative in Architecture. In B. Kolarevic & A. M. Malkawi (Eds.), Performative Architecture: Beyond Instrumentality (pp. 203–214). London, United Kingdom: Spon Press.

Konis, K., Gamas, A., & Kensek, K. (2016). Passive performance and building form: An optimization framework for early-stage design support. Solar Energy, 125(February), 161–179. https://doi.org/10.1016/j.solener.2015.12.020

Leitão, A. (2014). Improving generative design by combining abstract geometry and higher-order programming. In Rethinking Comprehensive Design: Speculative Counterculture, Proceedings of the 19th International Conference on Computer- Aided Architectural Design Research in Asia CAADRIA 2014 (pp. 575–584).

Lin, S. E., & Gerber, D. J. (2013). Designing-in performance: evolutionary energy performance feedback for early stage design. In 13th Conference of International Building Performance Simulation Association (pp. 386–393).
Moneo, R. (2001). The Thing Called Architecture. In C. Davidson (Ed.), Anything (pp. 120–123). New York: Anyone Corporation.
Moussavi, F., & Kubo, M. (Eds.). (2006). The Function of Ornament. Actar.
Nguyen, A.-T., Reiter, S., & Rigo, P. (2014). A review on simulation-based optimization methods applied to building performance analysis. Applied Energy, 113, 1043–1058. https://doi.org/10.1016/j.apenergy.2013.08.061
Otani, M., & Kishimoto, T. (2008). Fluctuating Patterns of Architecture Façade and their Automatic Creation. In CAADRIA 2008 [Proceedings of the 13th International Conference on Computer Aided Architectural Design Research in Asia] (pp. 375–382).
Pell, B. (2010). The Articulate Surface: Ornament and Technology in Contemporary Architecture. Germany: Birkhäuser GmbH.
Picco, M., Lollini, R., & Marengo, M. (2014). Towards energy performance evaluation in early stage building design: A simplification methodology for commercial building models. Energy & Buildings, 76, 497–505. https://doi.org/10.1016/j.enbuild.2014.03.016
Qian, Z. C. (2009). Design Patterns: Augmenting Design Practice in Parametric CAD Systems. SIMON FRASER UNIVERSITY, Burnaby, Canada.
Rytel, G. (2013). The Influence of Climate on the Forms of Brazilian Modernist Archiecture in the Years 1925-1960. Kwartalnik Architektury I Urbanistyki, 4, 57–78.
Schittich, C. (Ed.). (2006). Building Skins. Birkhäuser. https://doi.org/10.11129/detail.9783034615082
Schulz, C. N. (1971). Existence, space & architecture. New York: Praeger. Stamps.
Sousa, S., & Batista-Bastos, M. (2015). O tempo e a Diferença: Análise e Readaptação num Edifício em Lisboa [Time and Difference: Analysis and Readaptation in a Building of Lisbon]. Cadernos de Arquitectura e Urbanismo, 22(33), 58.
Stojšić, M. (2017). (New) Media Façades: Architecture and/as a Medium in Urban Context. AM Journal, (12), 135–148. https://doi.org/10.25038/am.v0i12.173
Venturi, R., Brown, D. S., & Izenour, S. (1972). Learning from Las Vegas. MIT Press.
Woodbury, R., Aish, R., & Kilian, A. (2007). Some Patterns for Parametric Modeling. 27th Annual Conference of the Association for Computer Aided Design in Architecture, 222–229. Retrieved from http://moodle.ncku.edu.tw/file.php/2687/assignments/ParametricPatterns.pdf

A Detailed Look at Ceramic Façade Systems in Bogotá Searching Innovation Opportunities

Rafael Villazón*, Juan Manuel Medina, Nicolás Parra, Laura Daniela Murillo, Daniel Ramos

* Corresponding author
Department of Architecture, Universidad de los Andes, rvillazo@uniandes.edu.co

Abstract

The tradition of ceramic façades in Bogotá dates back to more than a century ago. However, this tradition has been characterised by keeping a conventional construction approach, without any considerable evolution. This paper focuses on significant turning points in Bogotá's tradition that have led to improvements in the construction environment, leading to possible paths for innovation with new proposals for ceramic façades. The central turning-point cases discussed are: Torres del Parque, the North Tower-Hilton International Hotel, brick façades for buildings that emerged after the Colombian Earthquake-resistant Building Standard (NSR-98), and the extension of the Santa Fe Foundation building. Through a detailed focus on these four cases in terms of their technological and morphological solutions, this paper aims to yield innovation opportunities for developing ceramic façade systems within an earthquake prone region.

Keywords

Ceramic façade systems, Bogotá, historical review

DOI 10.7480/jfde.2020.2.4210

1 INTRODUCTION

The use of ceramic in Bogotá is a history that has lasted more than a century, in which technological and morphological evolution has been minimal. This paper refers to technological evolution as the level of productivity that can be achieved in the façade's construction, in order to improve the efficiency of the overall construction process of the building. Morphological evolution places concern on those metrics which determine the relationship between the façade and the building's structure, as these comprise the interdependence between the two systems, along with the façade's slenderness and weight. The lack of development in technological and morphological matters is due to the use of this material as an element of the constructive tradition in which architects and builders have repeated their conventional solutions with very limited critical vision. This situation, added to the complexity of responding to the current demands of seismic behaviour of façades, has led to a limited level of innovation in ceramics. Manufacturers, along with some architects, have made efforts to search for new applications and alternative systems that are generally shown at local construction tradeshows, but the takeover by industry-leading architects and engineers has been minimal. Some of the conventional solutions have become the default answer for any project and have been standardised by manufacturing requirements, leading to constant repetition.

There are some cases that have left this repetitive path, introducing unconventional solutions for ceramic façades, which are labelled in this paper as "turning points". These examples are Torres del Parque, the North Tower-Hilton International Hotel, brick façades for buildings that emerged after the Colombian Earthquake-Resistant Building Standard (NSR-98), and the extension of the Santa Fe Foundation building. These projects make evident the need for creating a line of research that allows for proposals for new and better ways of using ceramic as a contemporary material. Furthermore, innovations must be coherent with a high seismic risk area where the displacement of heavy façades (built with brick and reinforced with concrete and steel reinforcing) by lightweight façades is becoming more and more common.

Taking into account the fact that there is a disconnect between the tradition of ceramic use in Bogotá and its technological and morphological evolution, this paper aims to provide a detailed description of the turning points, and then compare these with each other in order to determine which innovation lines of technological and morphological aspects presented by these cases can be taken into consideration to add value to ceramic façades in Bogotá. Chapter 2 explains the methodology applied to identify the turning points and to establish the comparison axes between them. In Chapter 3, a brief context of the tradition of ceramic façades in Bogotá between 1920 and 1980 is provided, given that the most significant transformations in the application of this material occurred within this time period. Chapter 4 deals with key parameters to determine when a project can be considered as a turning point within the tradition. Finally, Chapter 5 gives a detailed description of the turning points and makes a comparison between them. In the conclusion section, a hypothesis is put forward in terms of an innovation path that might overcome the disconnect between the tradition of ceramic use and its technological and morphological evolution.

2 METHODOLOGY

The article's methodological steps taken to identify turning points within Bogota's tradition of ceramic façades and compare them to each other are undertaken in the following order: Firstly, a description of the tradition is developed through a review of the state of the art of ceramic façades.

Secondly, understanding the tradition and its minimal evolution in technological and morphological aspects, a definition of these two qualities is made to use them as indicators for detecting turning points within the tradition. Thirdly, a baseline that represents the tradition is described in order to establish a starting point for the technological and morphological indicators. By this means, a façade that presents a different degree of technological or morphological development to the one presented in the baseline, is recognised as a turning point. The chart below (Fig. 1) is used to make a detailed description of both the tradition baseline and the turning points. The chart's recorded description of each case is put together in a single table in order to make a comparison between the tradition baseline and the turning points. Finally, the information gathered through the turning point's description and comparison, is used as an input to outline innovation opportunities for developing ceramic façade systems within an earthquake prone region.

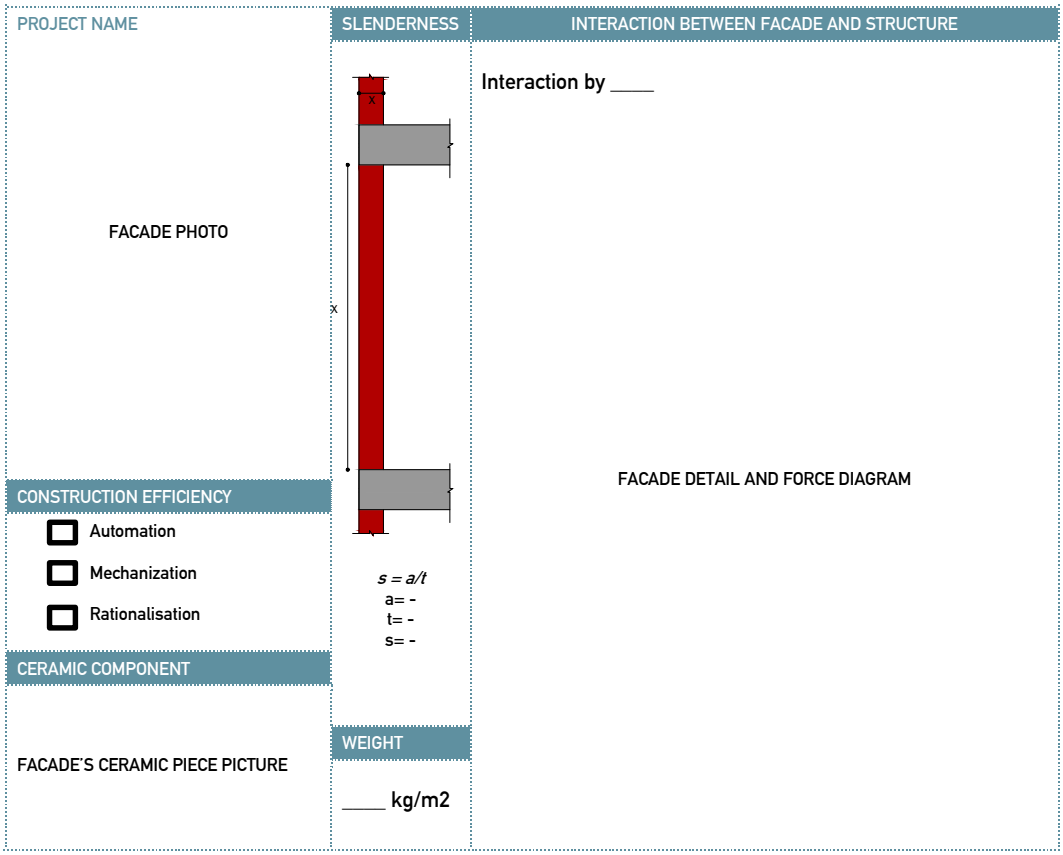

FIG. 1 Description template for the turning points.

3 BACKGROUND: STATE OF THE ART

The first brick production factories in Bogotá were established at the base of the Monserrate and Guadalupe hills because these are clay extraction areas and there is easy access to wood for furnace fuel (López & Gossens, 2018). The beginning of production came with the Calvo brick factory around 1859. However, the use of brick didn't increase until the end of the nineteenth century, when it became one of the most common materials for house façades.

After the opening of the Moore brick factory in 1906, the clay industry was consolidated in Bogotá. Saldarriaga and Fonseca (1986) describe the trajectory of brick and the implementation of the material in architectural façades, in their article *El Ladrillo y la Arquitectura Bogotana* (The Brick and the Architecture of Bogotá). They describe four periods: a period of transition between 1920 and 1940, a formative period between 1936 and 1948, a consolidation period between 1948 and 1960, and a period of diversification from 1960 to 1980. The most significant changes occurred in the first three periods, while in the fourth period, constructive solutions were established and have continued repeatedly up until today.

The transition period began in the 1920s when Bogotá's elite began to move to the north of the city and settle there. In this process, the *Teusaquillo*, *La Merced,* and *Quinta Camacho* neighbourhoods were founded, where the English style was adopted for the design of houses and brick began to be used as a gesture of social identity (Fig. 2). This strongly influenced the aesthetic and technical appreciation of this material, which, in the 1930s, motivated an exploration of different visual languages for the exposed brick façades. The respect for brick also became an urban issue as neighbourhoods began building with this material, creating a homogeneous visual landscape.

FIG. 2 Quinta Camacho neighbourhood façades, 1930. (Photograph by Faculty of Architecture & Design, Universidad de los Andes)

FIG. 3 San Carlos Hospital Building by Cuéllar Serrano Gómez architects, 1948. (Photograph by Faculty of Architecture & Design, Universidad de los Andes)

The formative period refers to a stage of brick experimentation between the traditional eclecticism of the time and the new modern international models that were being adopted in Bogotá. Examples of brick façades of this period reflect a mix between the new and the traditional, both in form and technique, as demonstrated in the San Carlos Hospital Building of Cuellar Serrano Gómez, constructed in 1948 (Fig. 3). It is said that influence of modern architecture on brick use is evident in some hints, since the culture, construction techniques, teaching and practice of architecture, was at that time in Bogotá traditional in relation to new models expected to be adopted.

Subsequently, during the period of consolidation, political, economic, and social factors led to an urban renewal at the end of the 1940s. As a product of this wave of modernism, marked by Le Corbusier's visit to Bogotá, materials such as concrete began to compete with brick as the favoured material for the façades of contemporary buildings. However, firms such as Cuellar Serrano Gómez, as well as other architects, kept exploring and using brick, thus boosting the brick industry (Fig. 4). The use of blocks and hollow pressed bricks began under this evolution.

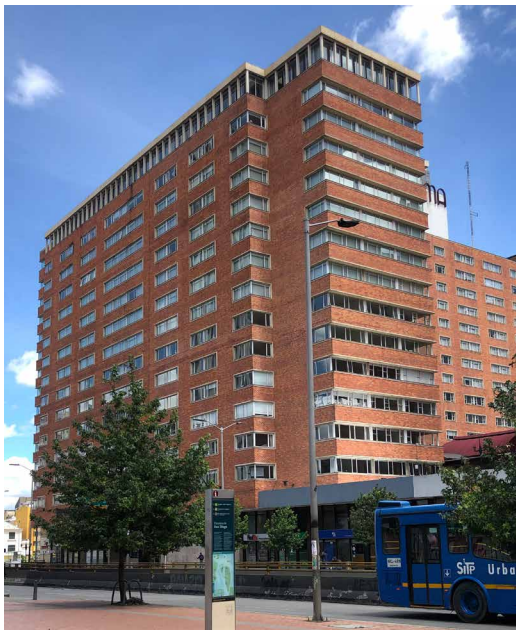

FIG. 4 North-east façade of the Tequendama Hotel by Holabird, Root, and Burgee office, and Cuéllar Serrano Gómez firm, 1951. (Photograph by Faculty of Architecture & Design, Universidad de los Andes)

FIG. 5 Building of the Colombian Society of Architects by Rogelio Salmona and Luis Torres, 1974. (Photograph by Faculty of Architecture & Design, Universidad de los Andes)

By 1960, a period of diversification had begun, in which architecture went through a stage of institutionalisation and commercialisation as architects began to practice in public and on commercial entities, leading to a diversification of the profession. Consequently, different kinds of buildings (especially of a greater height than those previously built) began to be produced, where the expressive potential of ceramic was demonstrated (Fig. 5). From 1970 to 1980, the 'brick school' began to consolidate as the application of the material spread throughout all levels of professional work. Saldarriaga and Fonseca (1986) referred to the years following 1980 as a period during which ceramic prevailed in the constructive tradition. The preference for using exposed brick is attributed to the influence of architects such as Fernando Martínez Sanabria - a trend that began to position itself as the universal language of Bogotá's identity and led ceramics to a higher level of appreciation. "What in previous decades had just been a search, from 1980 onwards was already a fad" (Saldarriaga & Fonseca, 1986, p.12).

This appreciation for using brick as a façade material in Bogotá is still maintained, however, there is no remarkable difference between those examples built 40 years ago and those that are being built nowadays, neither in technological aspects of construction nor in the morphology of the façade. The construction of ceramic façades in Bogotá continues to be carried out manually by one or more operators, and in the case of brick, pieces are assembled one by one. In morphological terms, ceramic façades continue to be typically associated with the use of brick and therefore, maintain a minimum thickness of 12 cm. In general terms, ceramics are part of the visual landscape of Bogotá but new needs have arisen and an alternative to the traditional façade has not yet been introduced to meet emerging demands.

4 KEY PARAMETERS TO DETECT TURNING POINTS WITHIN THE TRADITION

Since construction needs have evolved, while, on the contrary, ceramic façades have remained the same over the years, technological and morphological parameters are key aspects to determine the degree of a ceramic façade's evolution in Bogotá's architecture. This is due to the fact that integration of certain characteristics of these two parameters enables a solution to keep in force ceramic façades when facing current challenges such as practical construction methods for high-rise buildings, and optimal structural performance in case of earthquakes. These happen to be challenges the traditional ceramic façade in Bogotá has not yet solved, and therefore, a proposal which provides a way to overcome these issues through either a technological or morphological solution, can be considered as a turning point. To address the façade's technological aspect, a description will address the efficiency of the building's construction stages. Regarding the morphological aspect, the description will address its slenderness, weight, and level of interdependence with the structure.

4.1 CONSTRUCTION EFFICIENCY

Given that the current demands of the construction sector are mainly focused towards high-rise buildings, it is common to see construction techniques that save time and reduce costs on ceramic façade systems. Alfonso Del Águila (2006) defines some levels of construction efficiency that can be achieved through different techniques for saving time and reducing costs. In first place, there is the stage of rationalisation that refers to the set of strategies which seeks to improve production methods. At this level, basic tools are used, such as modular and dimensional coordination of materials in order to reduce improvisation. In second place, rationalisation may be taken into a higher level called mechanisation when people are freed from manual tasks through specialised tools that allow more production while investing less time and effort. At this level, we are no longer talking only about the manufacture of the façade components, but also about mechanising their operation and assembly. Finally, efficiency can be further improved by automation with advanced technologies, when using computerised systems or elements to control machinery and industrial processes that replace human operators. The scope is greater at this level than in mechanisation, given that even intellectual human activities are replaced by technology.

Taking this into account, for this particular case, construction efficiency will be measured, taking into account the following parameters: we refer to a level of rationalisation for traditional façades made of brick, which are built using a technique for which no specialised tools are needed. Bricks are manufactured with defined measurements in order to fit within a certain modulation of the building, however, this type of façade requires a construction methodology that implies a wet assembly whereby an operator must build piece by piece, and therefore, it is not a process that stands out for its efficiency. In order to step further into a level of mechanisation, we make reference to façade systems that consist of prefabricated panels manufactured on-site or off-site, at the same time as other construction processes are being carried out. These systems incorporate specialised tools to assist workers, involve a dry assembly, and also enable the overlap of the façade's construction with other on-site construction processes. Although the ideal scenario is to reach a higher level of construction efficiency through automation, there is not yet an example of a ceramic façade in Bogotá that serves as a reference for this methodology.

4.2 SLENDERNESS AND WEIGHT

The façade's slenderness and weight are linked concepts, which, depending on their value, influence the structural behaviour. A lightweight façade implies advantages for the building's earthquake resistance, by decreasing the overall weight of the construction system. However, ceramic façades in Bogotá made of bricks do not fit within this trend, because the traditional offer has been above 100 kg/m^2. This aspect can be attributed to the fact that the 6 x 12 x 24 cm brick has remained the most common component of ceramic façades in Bogotá, without presenting any evolution that marks a difference in the façade's morphology. Given that a variation in any of these two aspects can mean a disruption of tradition, the self-weight of the façade and its slenderness will be taken into account for the description and comparison phase.

$$s = a/t$$

s = Slenderness
a = Façade's vertical distance between supports
t = Façade thickness

4.3 INTERACTION BETWEEN THE FAÇADE AND THE STRUCTURE

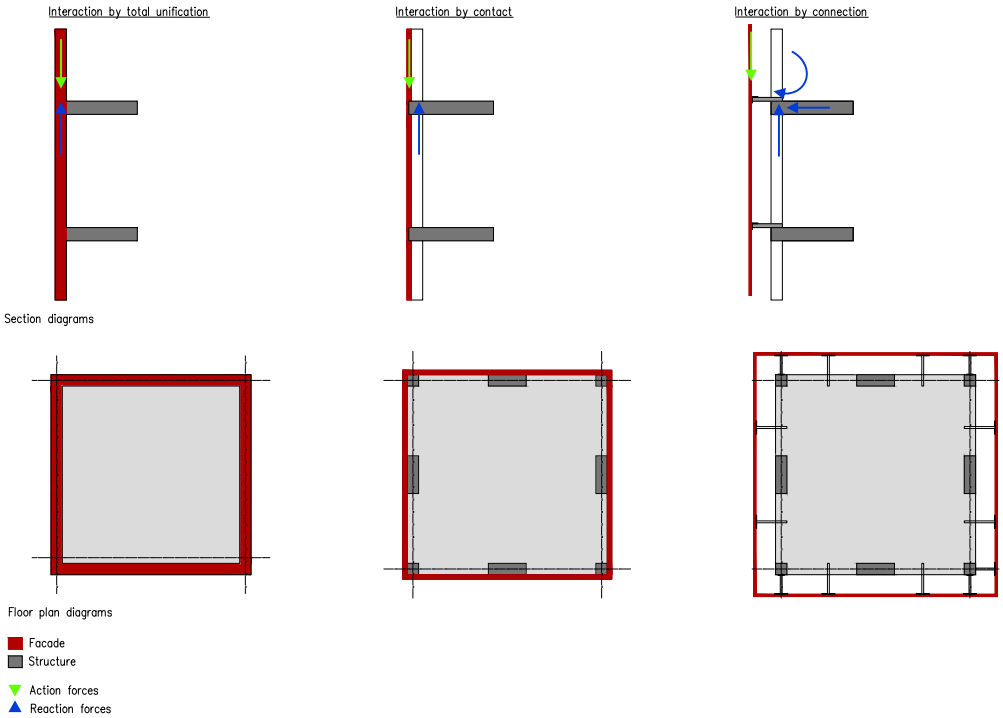

FIG. 6 Levels of interdependence between façade and structure.

The façade interaction with the building's structure is a fundamental factor in dictating the behaviour of the entire system in event of a seism. Based on the connection levels between the structure and the exterior envelope described by Richard Rush (1986), three levels of interdependence were considered in this methodology to describe the façade interaction with the structure (Fig. 6). Firstly, there is interaction by total unification, where a single element works as an enclosure and structural system. Secondly, there is interaction by contact, where the façade rests directly on the building's slabs, transmitting the vertical compression loads to the main structure. In this configuration, the performance against horizontal loads depends on the capacity of the anchors and the bending behaviour of the façade wall. And thirdly, there is interaction by connection, where the façade passes in front of the structure and transmits the loads through specific fixings. In this case, the performance against horizontal loads is defined by the flexural capacity, either through a metallic substructure of posts that supports the enclosure, or through the resistance of the panel itself.

5 THE TURNING POINTS: A DETAILED LOOK AT CERAMIC FAÇADES IN BOGOTÁ

As explained before, Bogotá's tradition has been repetitive and static in terms of a constructive evolution. However, at some stages in its history, there have been turning points demanded by contextual needs, which (when carefully reviewed) can yield interesting guidelines for this research and new lines of innovation. In this paper, we have selected four relevant examples of innovative contributions regarding façade construction systems, which are described and compared below, along with a representative case of the tradition.

5.1 DESCRIPTION

Baseline: Colinsa Building by Fernando Martinez

The Colinsa Building by Fernando Martinez happens to be a suitable representation of Bogota's tradition in ceramic façades and is used as a baseline for this methodology. This building, constructed in 1969, reveals an alternative that has still been applied until recently. The building is constructed wholly in-situ, where construction workers manually place the bricks with a running bond. This means that constructive efficiency only reaches the level of rationalisation. The outer face of the façade is composed of solid pressed brick (5.5 x 12 x 24.5 cm) with mortar joints and the inner face is made of another type of brick called "Bloque #4" (10 x 20 x 30 cm). In some sections, part of the façade rests on a bracket and other times, it continues straightforward without interruption (Fig. 7). There is no doubt that since 1960, Fernando Martínez's work represents a breakthrough in ceramic used for façades in Bogotá. However, Martínez's constructive solution for exposed brick façades has been reproduced repetitively throughout Bogotá's subsequent history, from the 1980s onwards without any consideration given to the emerging needs at the time.

FIG. 7 Colinsa Building west and south façade, 1969, Bogotá, Colombia. (Photograph by Faculty of Architecture & Design, Universidad de los Andes).

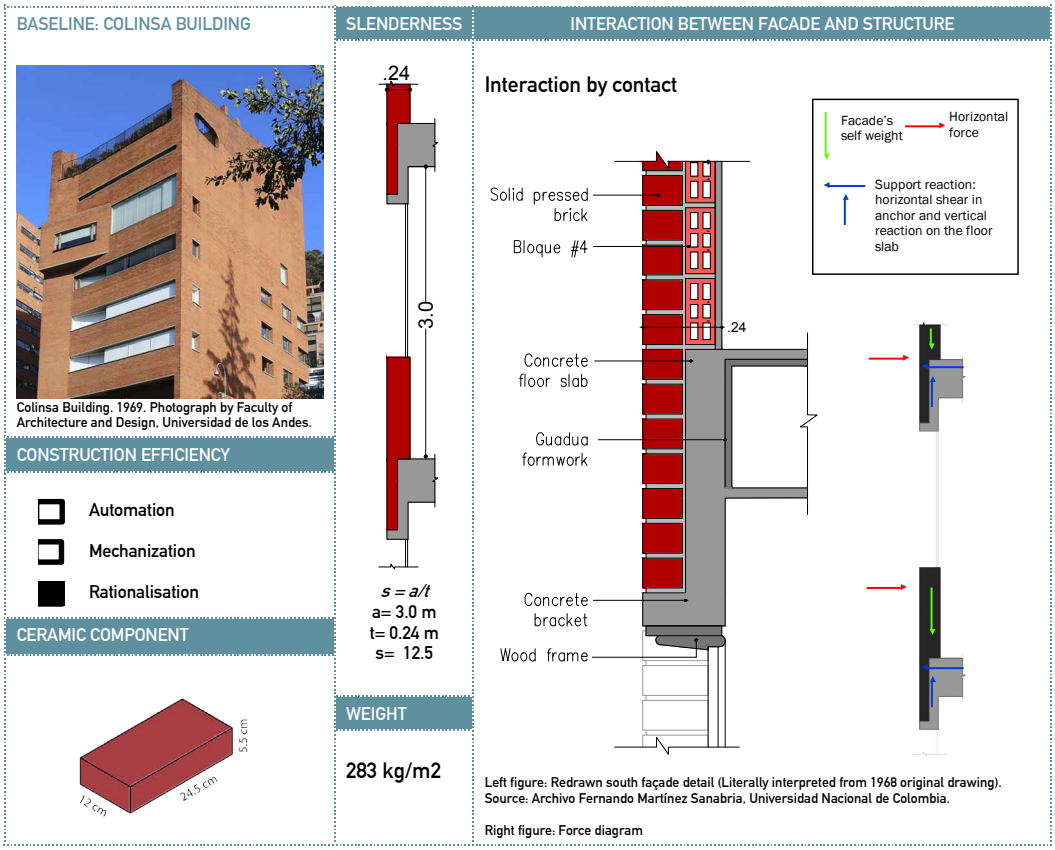

FIG. 8 Baseline description chart

Torres Del Parque

The 1950s was a period of increased production in architecture, implying that the housing unit scale increased to the neighbourhood scale (López & Gossens, 2018). Taller buildings began to be conceived in the city, with the Torres del Parque being one of the first examples of this trend. This residential project was designed by the architects Rogelio Salmona and Urbano Ripoll, and the engineer Doménico Parma. Its construction began in 1968 and ended in 1970.

Architects opted for a design that would keep in harmony with the context, using the exposed pressed brick as a façade material (Urrea, 2014). As Urban Ripoll points out, "A detailed study was devoted to the likelihood of the brick wrapping all structures. (...) Large horizontal windows were used to divide the 'brick belts' between one floor and the next; it was possible to make the brick enclosure work in conjunction with the structure in the event of an earthquake, preventing the non-structural elements from being subjected to stresses for which they are not designed." (Urrea, 2019). The façade's construction method is not different from the baseline since it was carried out in a traditional and rustic way, placing brick by brick manually, and using a wet assembly of pieces with mortar. Compared to the constructive detail of Fernando Martínez, the façade is made up of a single layer of ceramic, and thickness is reduced to 12 cm. The new lightweight façade was supported by a concrete bracket or corbel. In the corners, some walls functioned as buttresses to avoid the façade overturning (Fig. 9). In this way, the Torres del Parque project marks a turning point within Bogotá's tradition, as it addresses the challenges and demands of high-rise construction in an earthquake-prone region.

FIG. 9 Photograph of Torres del Parque light façade wall that works as a buttress, 1970. (Photograph by Faculty of Architecture & Design, Universidad de los Andes).

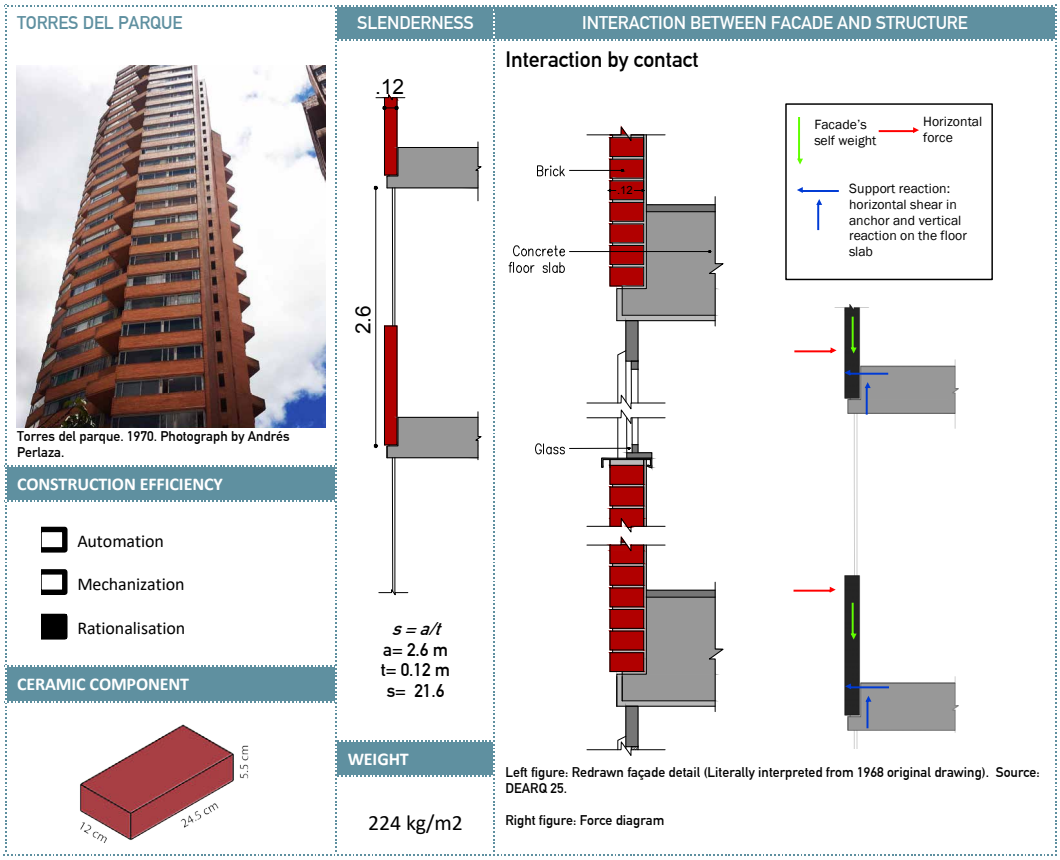

FIG. 10 Torres del Parque description chart.

North Tower - Hilton International Hotel

The North Tower of the Hilton International Hotel in Bogotá arose with the purpose of complementing the first tower of this hotel (South Tower), following an increase in tourism during the 1970s. The North Tower was born from an architectural contest in which Medardo Serna Vallejo and his collaborators, architects Jorge Moreno García, Jaime Moreno García, Holabird, & Root, and the engineer Doménico Parma were chosen as the winners on January 28th, 1980 (PROA, 1980). According to the project's documentation, in order to maintain a harmonious language with the surroundings, it was decided to use the same façade material as the hotel's South Tower (ESCALA, 1982).

For the North Tower, Doménico Parma presents a suspended façade solution composed of concrete prefabricated modules clad in ceramic tiles by *Ladrillos Moore*. This new façade proposal was intended to solve the problem of the detachment of ceramic tiles, which was a problem in the South Tower. In an interview with Jean-Guy Moggio (director of *Ladrillos Moore*), he reports that according to a study by Obregón and Valenzuela, the complications of the South Tower's façade (Fig. 11) were due to the insufficient expansion joints which failed to resist the substantial temperature changes (personal communication with Jean-Guy Moggio, November 27, 2018).

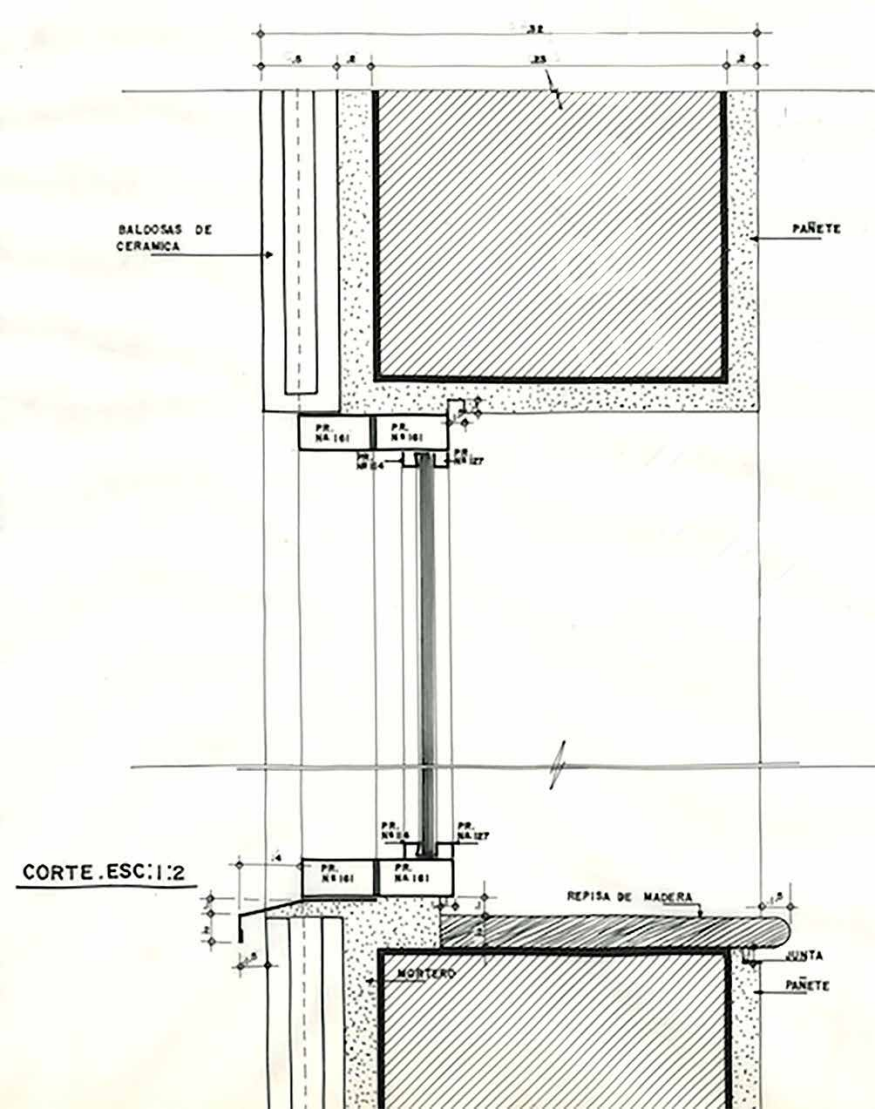

FIG. 11 Constructive detail of the South Tower's facade, 1963. (Source: Archivo Fernando Martínez Sanabria, Universidad Nacional.)

The relationship of the North Tower's façade to the floor slab turned out to be a novelty at the time since there were no precedents of suspended ceramic façades in Bogotá. As part of the anchoring system of the façade to the structure a metal profile is incorporated (Fig. 12), which also has the function of preventing the panel from bending. According to the construction records written by Parma (*Archivo Doménico Parma – Universidad de los Andes*, 1986), this element was considered essential to withstand the eccentricities of the façade, and at the same time, it could be used to place the central scaffolding elements. For this reason, *t* value in the slenderness calculation is taken as 18 cm thickness, because it has a 10 cm metallic profile for the panel's support. If this additional support did not exist, this facade's slenderness would be 34.7. This project represented an important innovation in Bogotá's construction at the time, taking on the challenges of incorporating ceramic façades to high-rise constructions. Doménico Parma introduced an industrialised ceramic façade solution, this being one of the main factors for considering this building as a turning point. Construction efficiency reached a level of mechanisation with a design of prefabricated ceramic and concrete panels that involved dry and practical installation through crane towers.

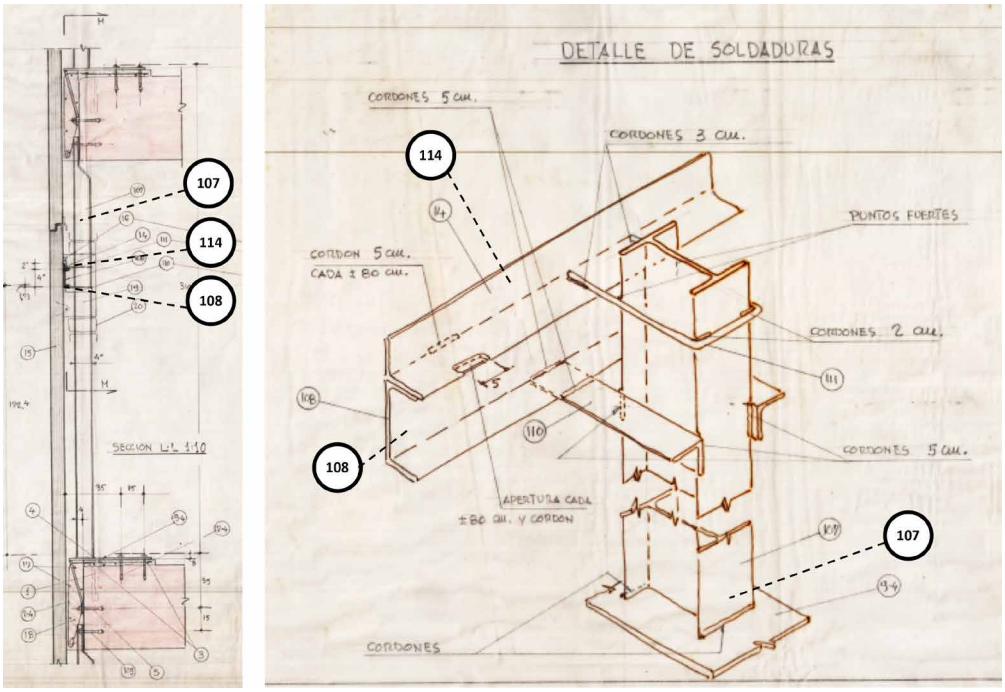

FIG. 12 Constructive detail of the North Tower's façade and welding detail of the supporting metal profile, 1986. (Source: Archivo Doménico Parma, Universidad de los Andes).

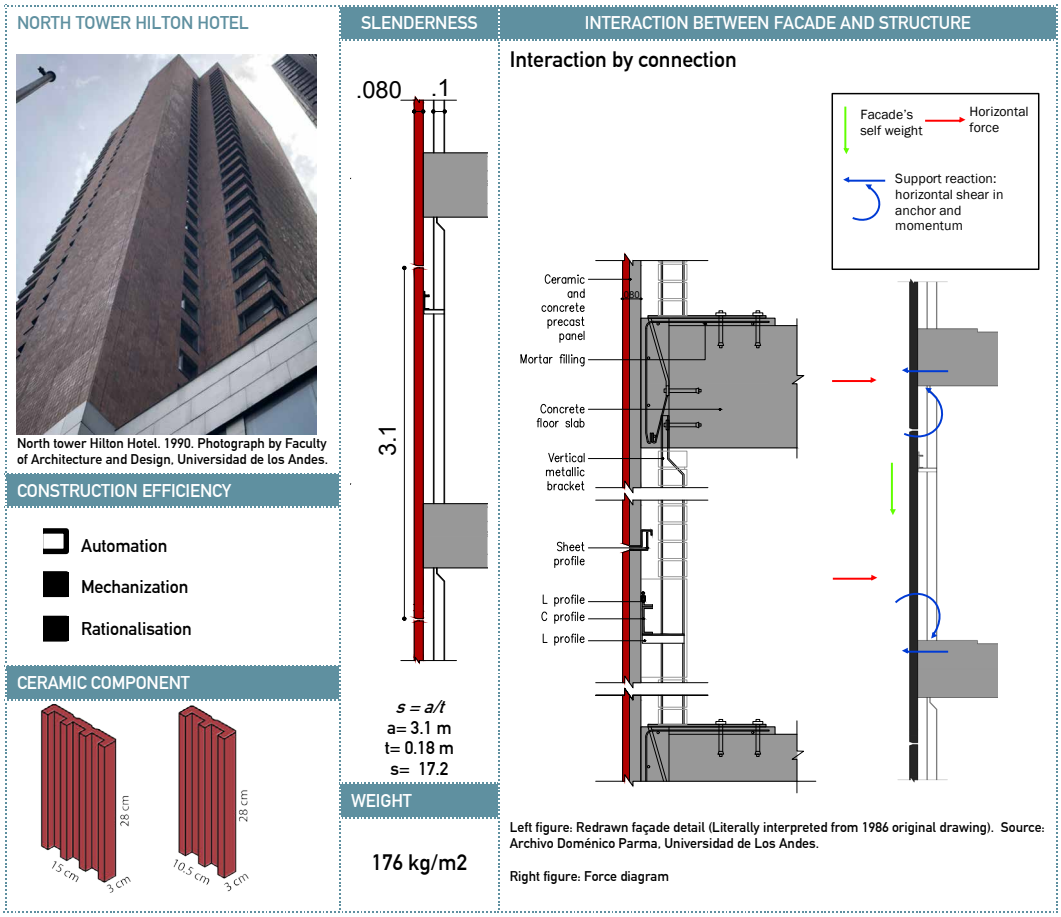

FIG. 13 North Tower Hilton Hotel description chart.

The first step in regulating earthquake-resistant constructions in Colombia took place in 1984 with the introduction of the Colombian Earthquake-resistant Building Code (Camacol, 2012). Prior to this point, architects had no responsibility for the behaviour of non-structural elements. In 1998, this code was reformed (NSR-98), and one of the main modifications established, Section A.9, refers to the regulation of structural calculation and liability of non-structural elements, where façades are included. Subsequently, a second update was made in 2010 (NSR-10) forming the document that is currently used. The NSR-98 set up a framework for brick façades among the requirements for earthquake resistance that had not previously been taken into account, and therefore, buildings with brick façades that addressed this regulation marked a turning point within the tradition.

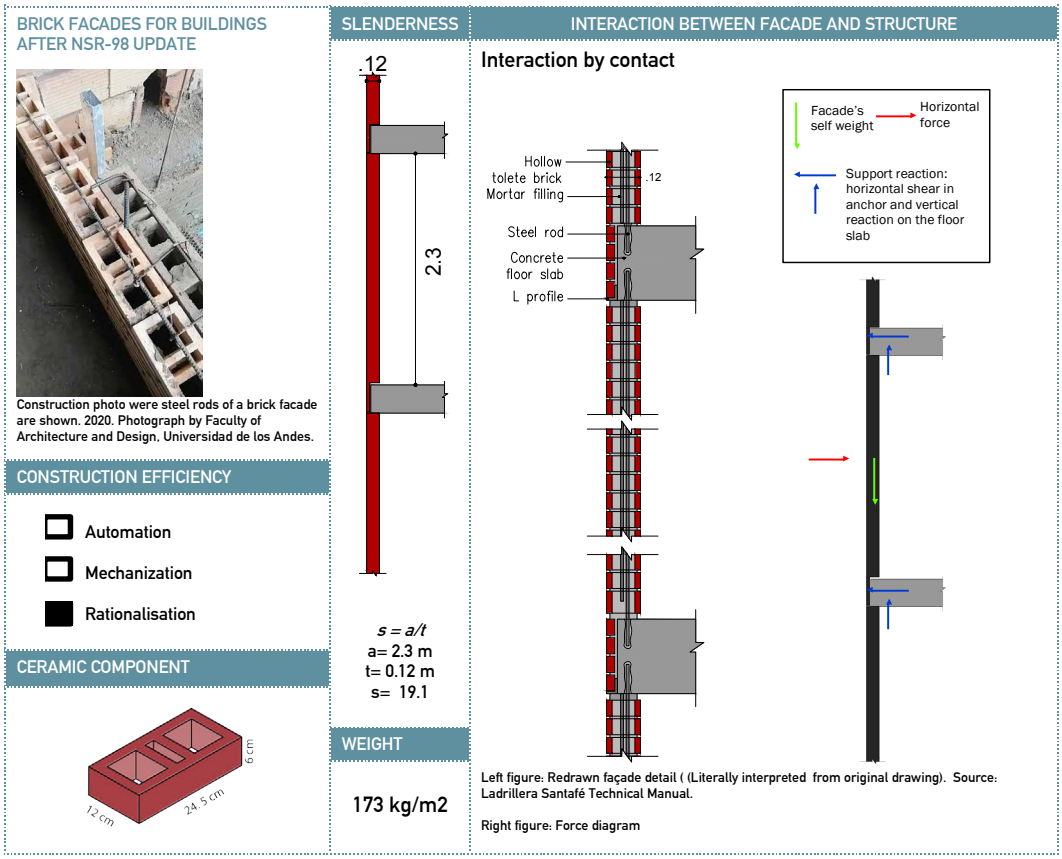

FIG. 14 Brick façades for buildings after the NSR-98 update description chart.

The outstanding factor that these cases represent is the incorporation of a perforated brick block through which steel reinforcements are introduced and, subsequently, these cavities are filled with mortar. The variation in the construction of this type of façade in contrast to the baseline or Torres del Parque examples, is the procedure that must be carried out to integrate the reinforcements of the façade. Brick-setting with a running bond, mortar application, along with the placement of steel bars, are undertaken by bricklayers in an artisanal and manual way. The façade's thickness remains around 12 cm, where bricks are supported on the floor slab and the edge of the slab is covered with ceramic cladding of smaller thickness. Reinforced brick façades established a "standard" alternative that most of the residential buildings adopted, and which is currently incorporated in catalogues of ceramic façades, as is the case in the Ladrillera Santafé technical manual.

Santa Fe Foundation is a private hospital in Bogotá, which extended its headquarters with a building for its university hospital. This extension began in 2012 with an architectural contest, of which a central requirement was to maintain the brick identity of the existing building. The contest was won by the Equipo Mazzanti, with a proposal using a brick façade that was unprecedented in Bogotá. The façade design was informed by Rolformados, the company that provided details of the system and managed its construction. On November of 2016, the twelve storey building for Santa Fe Foundation extension was launched, having as its façade a thin layer of ceramic pieces with different patterns, along with a special synergy between the interior and exterior of the building in terms of natural lighting and visuals.

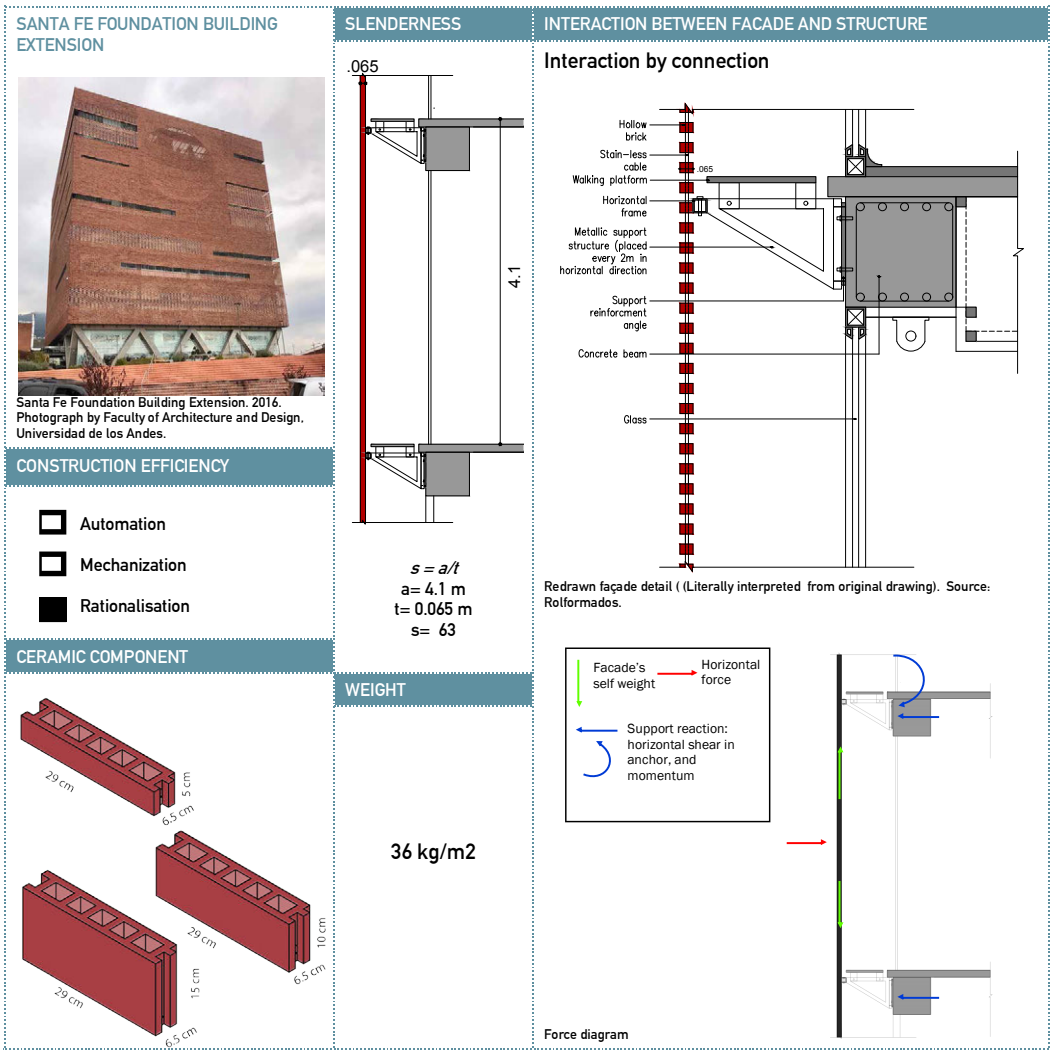

FIG. 15 Santa Fe Foundation Building extension description chart.

The façade system consists of 5 mm-diameter vertical stainless steel cables to which bricks are fastened by aluminium clips. These clips are supported on metallic bushings threaded in the cables, and their function is to keep the blocks in place horizontally, without supporting or transmitting any vertical loads. The cable structure has horizontal steel frames attached to metallic brackets that are anchored to the border concrete beams of the building, and horizontally spaced every 2.10 m. Certainly, this turning point presents significant modifications when compared with the baseline, considering that it uses a new language for brick when establishing a much more slender and lightweight façade. Furthermore, this façade suspended from the building structure achieves resistance to critical wind and seismic loading. It is not possible to speak of greater evolution regarding construction efficiency. Although this system involves a dry assembly of ceramic pieces, it was constructed on site and bricks were placed manually. Due to the fact that in contrast to the baseline the construction method used in this case does not present an increase in productivity, the degree of efficiency is also taken into account as a level of rationalisation.

5.2 COMPARISON BETWEEN THE BASELINE AND TURNING POINTS

	Baseline: Colinsa Building	Torres del Parque	North Tower Hilton Hotel	Brick facades for buildings after NSR-98 update	Extension of the Santa Fe Foundation
Construction efficiency	Rationalisation	Rationalisation	Mechanization	Rationalisation	Rationalisation
Slenderness	.24 3.1 s= 12.5	.12 2.6 s= 21.6	.080 .1 3.1 s= 17.2	.12 2.3 s= 19.1	.065 4.1 s= 63
Ceramic componet	12 cm 24.5 cm 5.5 cm	12 cm 24.5 cm 5.5 cm	13 cm 28 cm 5 cm	12 cm 24.5 cm 6 cm	29 cm 6.5 cm 5 cm
Weight	283 kg/m2	224 kg/m2	176 kg/m2	173 kg/m2	36 kg/m2
Interaction between the facade and the structure	By contact	By contact	By connection	By contact	By connection

FIG. 16 Comparison of the four turning points, together with the baseline case, according to their technological and morphological development.

The four cases mentioned above represent turning points within Bogotá's tradition because they suggest different innovations in the local context of ceramic façades. Torres del Parque project is one of the first precedents to use brick on high-rise building façades and provides a proposal for a more slender brick façade. The North Tower for the Hilton Hotel presents a particular alternative to industrialise the use of ceramics in façades. Although the constructive detail by *Ladrillera Santafé* has not evolved in its thickness or connection with the floor slab edge, it incorporates a fundamental criterion as it fulfils the earthquake-resistant requirement for the façade as a non-structural element. Finally, the extension of the Santa Fe Foundation building maintains a more significant slenderness and restores Bogotá's view of ceramic as a solid material by using it as a versatile and lightweight component in façades. Fig. 16 brings together the technological and morphological aspects of the turning points along with the baseline, in order to make easier the comparison between them and resemble the innovation paths these cases propose.

Taking the baseline as a point of comparison, the construction process of ceramic façade systems in Bogotá does not involve a developed level of efficiency since the standard and most used procedure is carried out manually on site, without using specialised machinery to increase productivity. In terms of performance, Santa Fe Foundation has two advantages: 1) It does not need glue, so even when it is installed brick by brick there is no glue placement or setting time; 2) As it is lattice, it uses half of the pieces. However, it is curious that the only turning point that presents a remarkable construction performance is the North Tower Hilton International Hotel built 35 years ago, with a proposal of "industrialised ceramic" by means of a mechanisation process for a suspended façade composed of prefabricated concrete panels with ceramic tiles. This case clearly exposes the need to incorporate a practical construction alternative for using ceramics in high-rise buildings. None of the turning points reached a level of automation, and just one works at a mechanisation level. The reason why the North Tower Hilton Hotel solution was not further developed in Bogotá is unknown. However, nowadays it could still be considered as an attractive proposal for the use of ceramics, due to the level of productivity that can be added to the construction stages.

Regarding the morphological matter, on the one hand, there has been a tendency among the turning points to increase the slenderness and reduce the façade's self-weight. In the exposed cases, the traditional solutions of façades supported on the structural slabs (Colinsa, Torres del Parque, and brick façades for buildings after NSR-98) produce heavier alternatives. This may be due to the fact that a greater thickness is generated to develop resistance to bending, and also because of the requirement to incorporate reinforcements within the masonry. Interdependence by means of a connection between the façade and the structure allows the appearance of prefabricated panels with a supporting metal substructure (such as the Hilton tower), or the tensioned façade of the Santa Fe Foundation. In both cases, horizontal forces are transmitted through the fixings, thanks to the flexural work of the support posts in the Hilton tower, or to the reaction of the cables that support the ceramic elements in the Santa Fe building. As a result, this allows for elements of lesser thickness and lower self-weight.

6 CONCLUSIONS

A detailed study of the turning points led to the identification of two trends: improvement of the construction techniques and lightweight thin façades that are resistant to bending. Both trends can be enhanced nowadays and become an innovation path for ceramic façades in Bogotá. On the one hand, the lack of productivity in manufacturing and assembly processes sets an opportunity to develop techniques that potentially improve construction efficiency in all of its stages. An advance of this technological matter is a key factor to maintain ceramics as a material which marks the identity of the city's façades and besides, exposes a competitive role in the construction field. On the other hand, the cases presented in this paper demonstrate a tendency towards more slender envelopes. However, the commitment to slender panels involved solutions with metal substructures in order to avoid the façade's bending. Therefore, an approach to a lightweight ceramic system with enough bending strength to withstand horizontal forces from wind and earthquakes is also an innovation path given that it may present a structural benefit by reducing the overall weight of the building. Besides, this will surely encourage an exploration of new morphological designs of the ceramic piece, as well as composite sections of the façade.

Acknowledgements

This paper is one of the outputs of the research project entitled "Ceramic façade systems study for earthquake-prone regions: Configuration and mass reduction strategies", which stemmed from a 2017 call for proposals, funded by Universidad de los Andes Vice Chancellor of Research and Faculty of Architecture and Design.

References

Archivo Doménico Parma, Universidad de los Andes. Hilton International Hotel Expansion Folder. Deformation of Hilton samples until Sept. 10/85. Jairo Varela F. Bogotá, September 10, 1985.

Archivo de Doménico Parma, Universidad de los Andes. Hilton International Hotel Expansion Folder. Building document August 15, 1986.

Archivo de Doménico Parma, Universidad de los Andes. Hilton International Hotel Expansion Folder. Tower II Façades - Contract No. 027 - Crane Tower Installation - Façade Assembly. CONSTRUCTORA COBSA LTDA. Bogotá, July 8, 1985.

Camacol (2012). Evolución de las normas técnicas y la inclusión de nuevos sistemas constructivos: Evolución de la norma técnica de construcción (Evolution of technical standards and the inclusion of new construction systems: Evolution of technical construction standards). *Informe Económico* (44). Retrieved from https://camacol.co/sites/default/files/secciones_internas/Informe%20Económico%20-%20Dic2012-%20No%2044.pdf

CEAM ltda., Saldarriaga, A., Fonseca, L. (1986). El ladrillo y la arquitectura bogotana (Brick and Bogota's architecture). *PROA,* 353: 11-13.

Del Águila, A. (2006). Industrializacion de la Edificacion de Viviendas, tomo 1: Sistemas (Industrialisation of Housing Building, volume 1: Systems). pp.17. Mairena Libros.

Deplazes, A. (2010). Construir la arquitectura: Del material en bruto al edificio: Un manual (Constructing Architecture: Materials, Processes, Structures: a Handbook). Pp.195. Barcelona: Gustavo Gili.

ESCALA (1982). Concurso para la ampliación del Bogotá Hilton Hilton (Architectural contest for the expansion of the Bogotá Hilton). *ESCALA* (103).

López, A., & Gossens, M. (2018). El ladrillo: Un principio inherente de la arquitectura moderna en Bogotá (Brick: An inherent principle of modern architecture in Bogotá) (Master's dissertation), pp.18. Bogotá: Universidad de Los Andes.

Monjo, J. (1986). Propuesta de evaluación de sistemas constructivos (Construction systems evaluation proposal). *Informes de la construcción, 38(385)*. https://doi.org/10.3989/ic.1986.v38.i385.1691

PROA (1980). Acta del jurado calificador de los proyectos arquitectónicos presentados al concurso para la construcción de la ampliación del Hotel Hilton de Bogotá (Minutes of the qualifying jury of the architectural projects submitted to the competition for the construction of the expansion of the Hilton Hotel in Bogotá). *PROA* (292). Pp.18-19.

Reyes, J., Correal, J., Gonzalez, A., Echeverry, J., Gómez, I., Sandoval, J., Ángel, C. (2020). Experimental evaluation of permeable cable-supported façades subjected to wind and earthquake loads. *Engineering Structures* (214). DOI: https://doi.org/10.1016/j.engstruct.2020.110679

Rodriguez, C., Coronado, M., D'Alessandro, M., & Medina, J. (2019). The importance of standardised data-collection methods in the improvement of thermal comfort assessment models for developing countries in the tropics. *Sustainability* (Switzerland), 11(15). https://doi.org/10.3390/su11154180

Rush, R., & American Institute of Architects. (1986). The building systems integration handbook. New York: Wiley.

Urrea, T. (2014). De la Calle a la Alfombra. Un espacio abierto en Bogotá (From the Street to the Carpet. An open space in Bogotá) (Doctoral dissertation). pp.364. Barcelona: Universitat Politècnica de Catalunya.

Urrea, T. (2019). Mayo del 68, se levantan las Torres del Parque en Bogotá. Conversación sobre las entrañas del proyecto de Rogelio Salmona (May 68, the Torres del Parque rise in Bogotá. Conversation about Rogelio Salmona's project). *De-arq*, (25), pp.86-97. https://doi.org/10.18389/dearq25.2019.08

Zalamea Costa, A., and Biblioteca Luis Angel Arango. (1993). Fernando Martínez Sanabria: Vida y obra (Fernando Martínez Sanabria: Life and work), pp. 34-37. Bogotá: Galería Deimos.

Development and Application of a Prefabricated Façade Panel Containing Recycled Construction and Demolition Waste

Ivana Banjad Pečur, Marina Bagarić* and Bojan Milovanović

* Corresponding author
University of Zagreb, Faculty of Civil Engineering, Department of Materials, Croatia marina.bagaric@grad.unizg.hr

Abstract

The construction sector, identified as one of the largest producers of construction and demolition waste (CDW) and one of the largest energy consumers, demands effective measures and applicable solutions to address sustainability challenges. The closed-loop recycling of CDW, integrated with the large-scale deployment of high energy performing buildings, represents a challenge for the whole construction sector, where the lack of waste efficient and energy efficient envelope systems is identified as one of the main barriers. The aim of this paper is to provide one possible solution to tackle the aforementioned issues – a highly insulated prefabricated ventilated façade panel with concrete layers produced using recycled CDW. The results of extensive research confirm that it is possible to replace a high percentage (50%) of natural coarse aggregate with recycled CDW and produce concrete with good mechanical, durability, and hygrothermal properties. Upscaling from initial research and optimisation at material level to an element level, i.e. development and testing of a ventilated façade panel, demonstrated that it is possible to produce a modular envelope system from recycled CDW that meets all performance requirements for certain construction product type (Declaration of performance and CE-marking). Moreover, the results of hygrothermal and energy consumption field monitoring at the whole building level suggest that the developed panel is suitable for use as a high-performing building envelope in real environmental conditions.

Keywords

Construction and demolition waste, recycling, high energy performing buildings, prefabricated ventilated façade panel, hygrothermal performance

DOI 10.7480/jfde.2020.2.4788

1 INTRODUCTION

The construction industry is one of the largest economic sectors in the world, while in Europe alone it employs 18 million people and generates approx. 9% of the European GDP (CECE, 2020). The impact of the intensive activities of the construction sector on our natural environment is an issue that is no longer subject to debate, as global effects of climate change and resource depletion unfold. The fact that in Europe nowadays 30% of all traffic, 40% of energy consumption, and 50% of material resources taken from nature are construction related; moreover, that 30 - 50% of European national waste production comes from the construction sector (Vyncke & Vrijders, 2016) is well known. (Self)-sustainability, both energy and environmental, has become a strategic priority of political and industrial actions. Through its Energy Performance of Buildings Directive – EPBD (European parliament, 2002; 2010; 2018a), the Directive on the promotion of the use of energy from renewable sources (European Parliament, 2018b) and the initiative to decarbonise the building sector by 2050 (European Commission, 2018), the building sector is undergoing a significant paradigm shift. High energy performing buildings, such as nearly zero-energy buildings (NZEB) have become imperative. According to EPBD, from 31 December 2020 in Europe all new buildings must be NZEB, which by definition means that they need to have a very high energy performance. This nearly zero, or very low, amount of energy required should be covered to a very significant extent by energy from renewable sources, including energy from renewable sources produced onsite or nearby. The definition given by EPBD (European parliament, 2002; 2010; 2018a) is only theoretical, and each EU Member state is obliged to define its own NZEB requirements (annual primary energy, annual specific heating energy demand, etc.) in relation to national context, i.e. climate, building tradition, cost-optimal analysis, etc. Achieving high energy performing buildings requires a change in established principles in design and construction. This is only possible if the building is considered as a dynamic system that is in constant interaction with the external environment, and whose main aim is to provide a high level of comfort and a healthy indoor climate for building users. Additionally, changing established principles requires thinking about the environmental impact of a building and its operating costs throughout its life cycle, with particular emphasis on the durability of building materials, building envelope elements, thermo-technical systems, and the building itself (Banjad Pečur, Bagarić & Bomberg, 2020). The interaction of the building with the outdoor environment and the interior of the building takes place via the building envelope which, as an active participant in the processes of heat, air, and moisture transfer – HAM (hygrothermal performance), is directly exposed to environmental loads and thus must be both robust and resilient. When looking at the building envelope, 75 - 90% of all construction damage is caused by moisture (Milovanović & Mikulić, 2011), which further indicates the need to predict and ensure the optimal dynamic hygrothermal performance of the envelope in a timely manner, especially in the case of new envelope systems and materials.

By encouraging the reduction of the use of non-renewable natural energy sources, Europe strongly supports the reduction of waste generation, and its reuse and recycling, in a closed-loop system, which is one of the cornerstones of the circular economy (European Commission, 2015a). Reuse of waste usually implies using the same material or product more than once for the same or for some other function. If waste cannot be reused, recycling should be taken into consideration. In a closed-loop recycling system, recycled material can substitute for the original material and be used in identical types of products as before, thus reducing waste to a minimum. With regard to construction and demolition waste (CDW), the Waste Framework Directive (European Parliament & Council, 2008) set the target for preparation of 70% of waste for reuse, recycling, and other recovery by EU Member States.

By recycling construction waste and using it to produce a new construction product, waste becomes a resource, thus gaining new added value and remaining in the life cycle, i.e. kept in a closed cycle, and thus its landfilling can be avoided.

Concrete is the most widely used man-made product in the world. Approximately 4.7 tons of concrete is produced each year per capita (some 33 billion tons per year) (ISO, 2016) and this number is growing each year (Statista, 2020). Despite its advantages from a construction point of view, it has an enormous negative impact on our environment, resulting from cement production and resource excavation.

Aggregate accounts for 60 - 80% of the volume and 70 - 85% of the weight of concrete, and thus it is clear that there is tremendous potential for incorporating CDW into concrete. Concrete produced with aggregate from recycled CDW is called recycled aggregate concrete (RAC). In that sense, buildings built with RAC can be considered as material banks, which reduces the extent of excavation of natural resources and offers closed-loop solutions for CDW with added value. However, one must be aware that recycled aggregate can dramatically change the properties of concrete compared to the same composition concrete made with virgin aggregates. RAC has generally inferior mechanical and durability properties compared to conventional concrete (Bagarić, Banjad Pečur & Milovanović, 2020), and thus balancing between material properties and environmental benefits is crucial to obtain construction products of required quality. Even though RAC is considered to be a sustainable alternative to conventional concrete, and its mechanical and durability properties were the main objective of many extensive research activities (Behera, Bhattacharyya, Minocha, Deoliya, & Maiti, 2014; Marco, 2014; Pickel, 2014; Fraile-Garcia, Ferreiro-Cabello, López-Ochoa, & López-González, 2017; Banjad Pečur, Štirmer & Milovanović, 2015), its inferior properties and the lack of a proper specification, especially those that would enable performance based design, inhibits extensive use in concrete (Behera et al., 2014). For example, standard HRN EN 206:2016 (HZN, 2016) gives a recommendation for using only coarse aggregate (fractions with aggregate size larger than 4 mm) divided into two categories (A and B) depending on the classification of coarse aggregate components. For both coarse aggregate categories, the maximum allowable percentage for replacement of natural coarse aggregate is defined in relation to environmental exposure class. For category A, the allowable replacement percentage ranges from 50 % (X0) to 30% (XC1, XC2, XC3, XC4, XF1, XA1, XD1), while for category B from 50% (X0) to 20% (XC1, XC2), respectively. For all other environmental exposure classes, replacing natural coarse aggregate with recycled aggregate is not allowable.

One of the main obstacles for the massive use of recycled aggregate is also its variable quality, since the uniformity of the aggregate origin cannot always be guaranteed (Banjad Pečur & Štirmer, 2012). It is necessary to provide adequate plant for storage, processing, and quality control of the material that will be recycled. In fact, natural aggregate can be completely replaced with recycled, however, this kind of concrete would require a high amount of cement to achieve adequate mechanical and durability properties, which is not economically and environmentally feasible. Therefore, the optimal replacement percentage should be defined in a way that balances economical aspects, mechanical and durability aspects of RAC, as well as its environmental impact. While mechanical and durability properties of RAC have been extensively researched, to the best of the authors' knowledge, there are only fragmented research findings about RAC's hygrothermal properties at material level (Fenollera, Míguez, Goicoechea, & Lorenzo, 2015; Zhu, Dai, Bai, & Zhang, 2015; Bagarić et al., 2020).

Although the assessment of the hygrothermal performance of the whole system is crucial for overall performance, and for constructing high energy performing, durable, as well as moisture-safe buildings, there is a lack of such analyses for RAC envelopes at a large scale that are exposed to real environment conditions.

The presented study was driven by the research question that emerged from identified knowledge gaps – how does a building envelope containing RAC perform under real environment conditions from a hygrothermal point of view? In addition, is the building envelope system under consideration applicable to high energy performing buildings, such as NZEBs or some other low energy standard?

The goal of this paper is to broaden the current knowledge of possibilities and limitations of using RAC for a high energy performing, sustainable, durable, and moisture-safe building envelope. In the context of this research, the sustainability of the building envelope is reflected through the significantly reduced use of natural resources (natural aggregate), utilisation of recycled CDW that reduces waste disposal, and provides added value to CDW. Moreover, after the end-of-use, concrete layers of the panel can be crushed and used as a recycled aggregate for production of new panels.

The paper consists of 6 sections. After the first section (Introduction), the research methodology is presented in Section 2. Section 3, with its sub-sections, outlines all activities conducted within the frame of this research and their results, including the RAC mix optimisation and testing at material level, panel development and testing at an element level, elaboration of construction details, as well as investigation of thermal mass. Section 4 presents the whole building level, i.e. the first implementation of the panel followed by the field monitoring of the panels' hygrothermal performance and numerical HAM simulations. For the building under consideration, annual energy consumption was also monitored and analysed (Section 5). The last section offers conclusions and presents plans for future work.

2 METHODOLOGY

To confront the challenges imposed on buildings to reduce energy consumption and on the entire construction sector to achieve a high level of recycling of CDW, the research methodology, as presented in Fig. 1, has been proposed.

The conducted research consists of five main phases. The first phase (State-of-the-art review) sets out the motivation and the research problem that derived from the knowledge niche identified by overlapping two specific research areas: i) heat, air, and moisture transfer with a focus on ventilated façades; ii) recycled aggregate concrete with a focus on its use as a heavyweight building envelope system. In the second phase (RAC laboratory testing at material level), the optimisation process was conducted to identify the most favourable replacement ratio of recycled aggregate in concrete. The most favourable replacement ratio implied the balance between mechanical, durability, and hygrothermal properties. During the third phase, the innovative prefabricated façade panel was developed at element level. After setting up the pilot production in a precast factory, all testing required for issuing the Declaration of Performance and CE-marking were performed. To evaluate the environmental impact of the developed panel, the life cycle analysis was also performed. As part of the third phase, two applications at the whole building level were realised: 3-storey family house and kindergarten. Both were designed as high energy performing buildings. A 3-storey family house,

as the first application of the developed innovative panel, was selected for further research activities (Phase 4). A field monitoring was carried out in order to evaluate the hygrothermal performance of the panel in real operating conditions, as well as whole building energy performance. Numerical HAM simulations are also a part of this phase, and they were validated with results of the monitoring. The fifth phase summed up the results from all research levels, which provides a wider perspective on RAC and performance of the specific envelope system. Directions for future research are also formulated in this last phase.

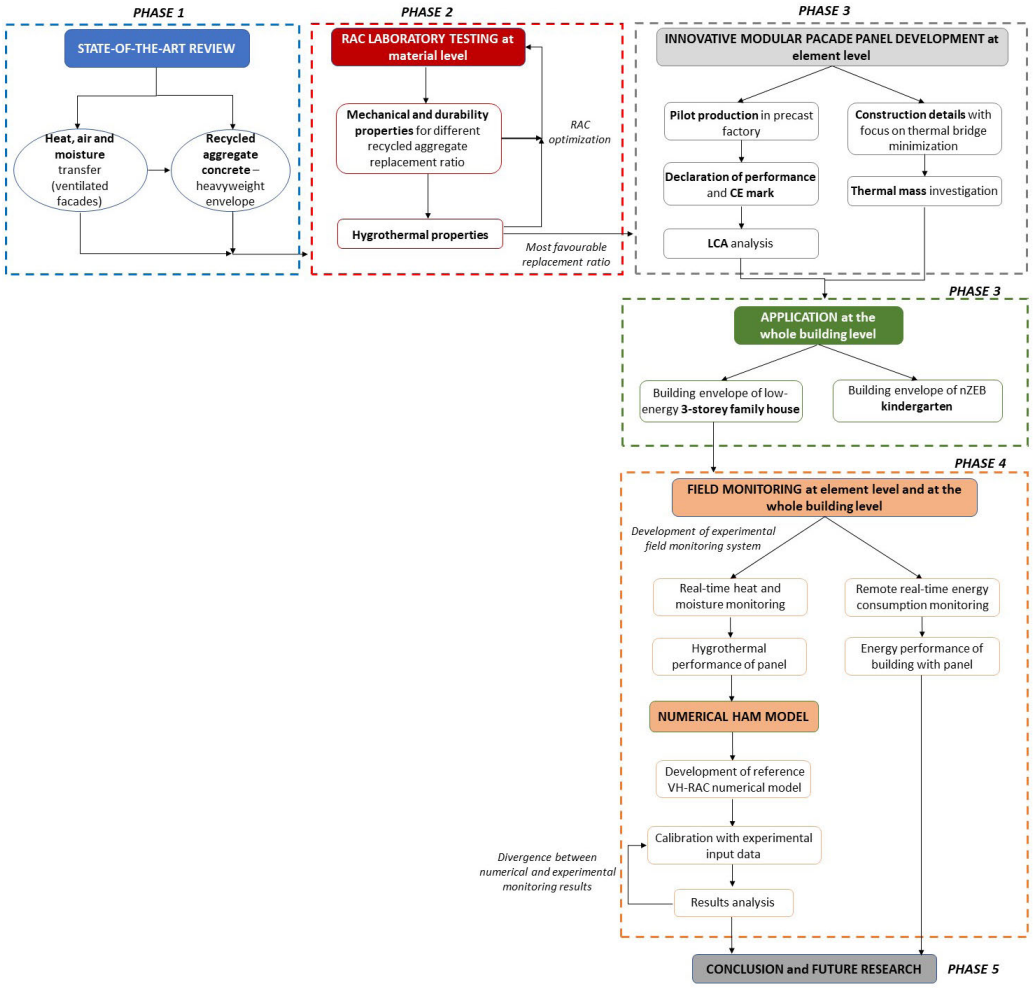

FIG. 1 Graphical representation of the research methodology

3 DEVELOPMENT OF PREFABRICATED FAÇADE PANEL

A highly thermally insulated façade system from a prefabricated ventilated sandwich panel comprising concrete from recycled CDW was developed at the Faculty of Civil Engineering, University of Zagreb (ECO-SANDWICH®, 2012).

3.1 CONCRETE OPTIMISATION AND TESTING – MATERIAL LEVEL

Two different types of RAC were investigated – one with recycled aggregate from old demolished concrete structures (RAC-Concrete) and the other with recycled brick from brick manufacturing waste (RAC-Brick) (Fig. 2).

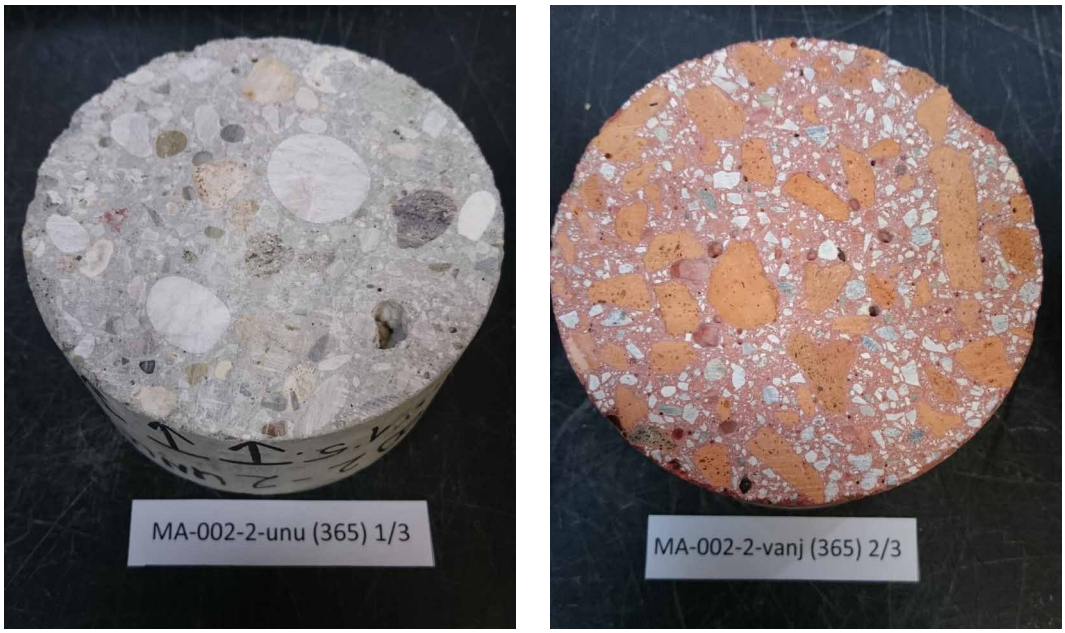

a *b*

FIG. 2 Recycled aggregate concrete: a) old crushed concrete as recycled aggregate; b) crushed brick as recycled aggregate

Optimisation of concrete mixtures was performed by varying the replacement ratio of natural with recycled aggregate (40%, 50%, 60%). From a mechanical and durability perspective, the replacement ratio of 50% was deemed to be the most favourable for both types of RAC, as shown in Banjad Pečur, Štirmer, & Milovanović (2015). Table 1 shows some of the main mechanical, durability, and hygrothermal properties of tested RAC types. Based on experimental results, both RAC-Concrete and RAC-Brick can be classified in compressive strength class C 30/37. Generally, RAC-Brick exhibited lower compressive strength compared to RAC-Concrete. Both concretes satisfy requirements for XF4 (56 cycles of freezing and thawing with de-icing salts) environmental exposure class. In comparison to conventional concrete made with natural aggregates (density of approximately 2400 kg/m^3), recycled aggregate concretes are lighter, but they have maintained good mechanical and durability properties. If there are no specific requirements and no significantly high loads are expected, then compressive strength class C 30/37 is suitable for most construction applications. Regarding thermal properties, RAC-Concrete and RAC-Brick have 13 - 27% and 29 - 40% lower thermal conductivity than the reported literature values for the dry concrete with approximately the same density. The water vapour diffusion coefficient for these concretes is 38 to 70% lower than the literature values for similar wet concrete (Banjad Pečur et al., 2015). These results indicate that recycled aggregate has a positive influence on the hygrothermal properties of concrete by improving thermal performance and contributing to more vapour-open performance.

TABLE 1 Main mechanical, durability, and hygrothermal properties of tested RACs for different replacement ratio

RAC-CONCRETE			
	40%	50%	60%
Dry density [kg/m^3]	2064.60	2105.00	2243.33
Compressive strength at 1 day [MPa]	15.76	23.43	18.51
Compressive strength at 28 days [MPa]	44.33	51.20	42.82
Tensile strength by bending at 28 days [MPa]	5.77	6,36	5.41
Elasticity modulus at 28 days [GPa]	27.38	33.80	27.99
Dry thermal conductivity at +10°C [W/(mK)]	0.867	0.858	/*
Water vapour diffusion resistance [-]	26	37	/*
Freeze/thaw class with de-icing salts	XF4	XF4	XF4
Capillary absorption [kg/(m^{2}h$^{0.5}$)]	1.29	1.0	0.80
RAC-BRICK			
	40%	50%	60%
Dry density [kg/m^3]	1912.70	1971.00	2099.67
Compressive strength [MPa] at 1 day	10.76	16.85	5.87
Compressive strength [MPa] at 28 days	44.33	39.74	40.66
Tensile strength by bending at 28 days [MPa]	5.83	5.94	5.19
Elasticity modulus at 28 days [GPa]	21.30	18.16	15.55
Dry thermal conductivity at +10°C [W/(mK)]	0.703	0.746	/*
Water vapour diffusion resistance [-]	18	29	/*
Freeze/thaw class with de-icing salts	XF4	XF4	XF4
Capillary absorption [kg/(m^{2}h$^{0.5}$)]	1.26	0.9	0.60

[*Not tested.]

3.2 PANEL DEVELOPMENT AND TESTING – ELEMENT LEVEL

Even though quite satisfactory mechanical, durability, and hygrothermal properties of RAC have been achieved by replacing a high amount (50%) of coarse natural aggregate with recycled CDW, the idea was to develop a robust and resilient façade system whose overall performance will not be compromised by material properties of RACs. Therefore, choosing a self-load-bearing façade system, i.e., a system that doesn't function as an active structural building element, combined with prefabrication, i.e., production in a precast factory, was confirmed as a promising solution. Prefabrication is a well-known construction technology in which construction elements are produced in controlled conditions that enhance their quality. After production, construction elements are transported to the construction site and fixed to a load-bearing structure. This speeds up the construction process, minimises labour at the construction site, and reduces the overall construction costs. Despite its obvious advantages, prefabricated façade elements experienced stagnation in comparison to other façade systems and components, such as windows, thermal insulation materials, thermally enhanced bricks, etc. A paradigm shift in the construction industry is characterised by its re-orientation towards sustainability, resources, and energy efficiency.
A ventilated prefabricated façade panel from RAC, originally conceived in 2012, tackled sustainability by incorporating 50% recycled aggregate from CDW in concrete production and formaldehyde-free mineral wool thermal insulation, as well as introducing a naturally ventilated air layer which is not characteristic of conventional concrete sandwich façade panels. The latest development in prefabricated concrete panels are carbon concrete façade elements with aerogel-based insulating

materials, presented in 2019 (C3 project, 2020). Their innovation lies in utilising carbon-reinforced concrete and aerogel-based insulating panels, which results in a smaller thickness of concrete and insulation layers, and thus a lower overall panel weight, as well as less material use, which supports sustainability. The first implementation has not yet been realised, and thus, their influence on the dynamic energy performance of buildings, as well as overall dynamic hygrothermal performance at a large scale remains unknown. Therefore, it can be concluded that the utilisation of recycled CDW for production of concrete layers, as well as a naturally ventilated cavity, remain as specific characteristics of the ventilated prefabricated RAC façade panel that is the subject of this paper.

a b c d

FIG. 3 Prefabricated RAC façade panel: a) model; b)-d) production phases in precast factory

A self-load-bearing prefabricated façade panel produced in a precast factory (Fig. 3) consists of four characteristic layers interconnected with stainless steel girders and steel truss connectors: i) inner concrete layer (12 cm), ii) thermal insulation layer (20 cm), iii) air cavity (4 cm), iv) outer concrete cladding (6 cm). The inner concrete layer has the role of bearing the outer concrete cladding, and thus its thickness is derived from structural analysis calculations. The thickness of thermal insulation was defined to provide a thermal transmittance of a minimum 0.2 W/(m^{2}K), while the air cavity thickness was assumed according to the current rules of practice. The outer concrete cladding thickness was limited by environmental exposure class requirements, reinforcement arrangement, and the panel's production technology (ensuring an air cavity).

The specificity of the panel lies in utilising recycled CDW as aggregate for the production of concrete layers, naturally ventilated cavity, and formaldehyde-free thermal insulation. The inner concrete layer is produced from RAC-Concrete, while RAC-Brick is used for the outer concrete cladding. The naturally ventilated air cavity is foreseen to prevent the possibility of water vapour condensation, as well as to reduce heat gains in the summer period thanks to the passive cooling mechanism of the ventilated façade. Formaldehyde-free thermal insulation comprises glass wool with a weather-resistant protective barrier. At the end of the building's life cycle, a panel can be removed from the load-bearing structure and its characteristic layers can be separated. Concrete layers can be crushed and used as recycled aggregate for new concrete (de Brito, Gonçalves & Ramos dos Santos, 2006). Reinforcement and stainless-steel girders can also be recycled and used for steel production. Glass wool that is used as thermal insulation is also recyclable, and thus, for the panel under investigation the loop is closed with minimum waste generation.

After the truss connector was optimised from the structural point of view and the first prototypes were produced, testing at element level proceeded. The declared airborne sound insulation R_w of the whole panel is 53 dB, and the tested fire resistance is equal to class EI90, while the calculated thermal transmittance (U-value) is approx. 0.16 W/m^{2}K. Based on the material properties of individual layers shown in Table 1 and the main requirements of panel itself, the Declaration of Performance and CE mark were issued by the panel manufacturer (BETON-LUČKO Ltd., 2015). According to Bjegović et al. (2014), the developed façade panel is a non-load-bearing wall panel without structural purpose (standard EN 14992 *Precast concrete products – Wall elements)*, and thus the performance of its essential characteristics must be declared according to AVCP 4 system (AVCP – assessment and verification of constancy of performance) (European Commission, 2015b). AVCP 4 system states that the manufacturer is responsible for factory production control and assessment of performance. By declaring all essential characteristics and issuing the CE mark, the newly developed prefabricated panel was placed on the construction market, which made possible the first full scale implementation.

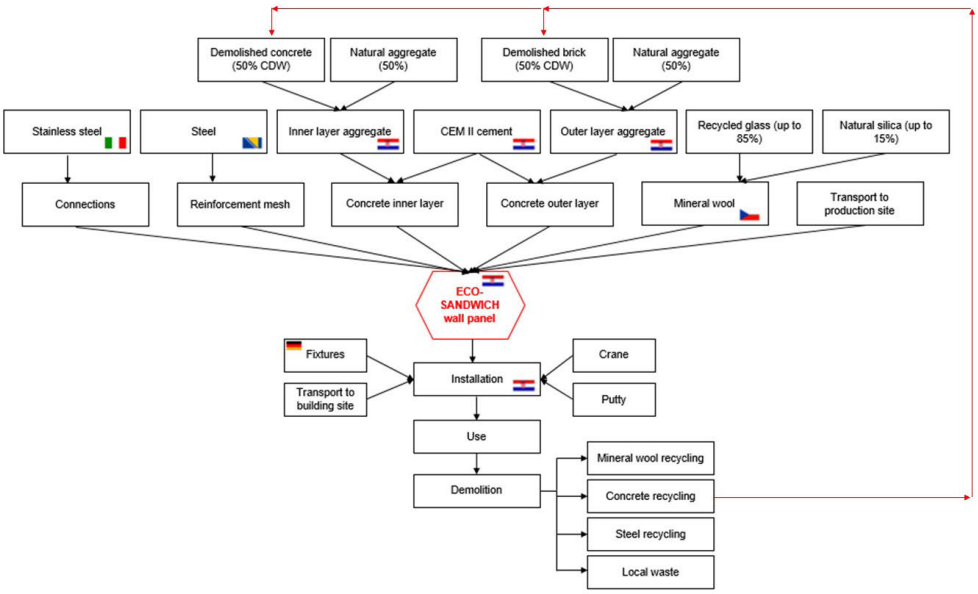

FIG. 4 Simplified flow chart of the life cycle of developed panel

Additionally, the environmental impact of the developed prefabricated façade panel from RAC was determined according to EN 15804 standard (EN 15804, 2013) and the environmental hotspots in its life cycle were identified. All activities throughout the life cycle of the panel were included in the assessment, from raw material extraction through to manufacturing, distribution, use of the panels and maintenance, replacements, demolition, waste processing for re-use, recovery, recycling, and the end-of-life disposal. A simplified flow chart of the panel's life cycle is shown in Fig. 4.

TABLE 2 Different recycling scenarios

RECYCLING SCENARIO	RECYCLING RATE [%]			LANDFILL	REFERENCES
	Mineral wool	Concrete	Steel		
SCENARIO 1: Current waste recycling rate [%] in Croatia	51	46	100	100 % of waste that is not recycled	EUROSTAT 2015; Calvo, Varela-Candamio & Novo-Corti, 2014; Monier et al., 2011
SCENARIO 2: Current waste recycling rate [%], average EU-27	79	46	100	100 % of waste that is not recycled	
SCENARIO 3: Future waste recycling rate [%] – Best case scenario	100	100	100	100 % of waste that is not recycled	Assumption

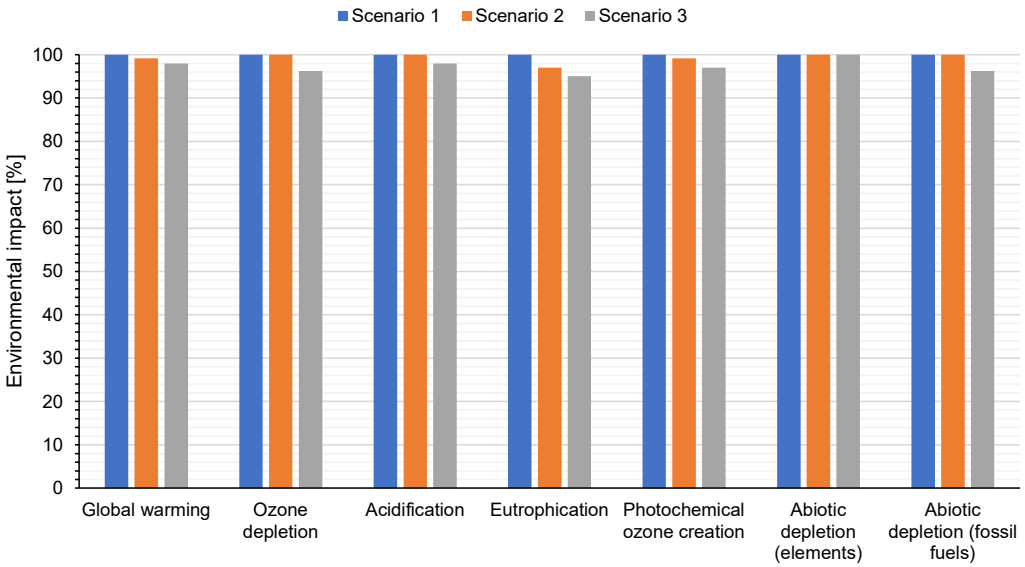

FIG. 5 The influence of different recycling scenarios on environmental impact

A detailed list of all inputs and outputs of the system can be found in Štirmer, Banjad Pečur & Milovanović (2015). The product life cycles were modelled using LCA software SimaPro, developed by PRéConsultants. The environmental impact of the panel is predominantly determined by the product itself. The total contribution of life stages such as raw materials, transport, production, and assembly ranges from 48% for the impact category Abiotic depletion (elements) to 84% for Global warming. Regarding the total contribution of transport to building site and installing of the wall panel, the lowest contribution is found for Global warming (13%) and the highest for Abiotic depletion (elements) (51%). The contribution of the waste treatment in the end of life ranges from 0% for Abiotic depletion (elements) to 7% for Eutrophication. The life cycle stages use and operation do

not contribute to the environmental impact, since no processes and/or emissions occur (Štirmer et al., 2015). Different recycling scenarios provided in Table 2 show that higher recycling percentages for mineral wool, concrete, and steel can have a positive effect on the results, especially where Eutrophication is concerned (Fig. 5).

3.3 CONSTRUCTION DETAILS

Some of the most common construction details have been built on the principles of minimising thermal bridges, achieving high airtightness of the building envelope, and ensuring adequate air flow in the cavity by designing cavity inlets and outlets (Fig. 6).

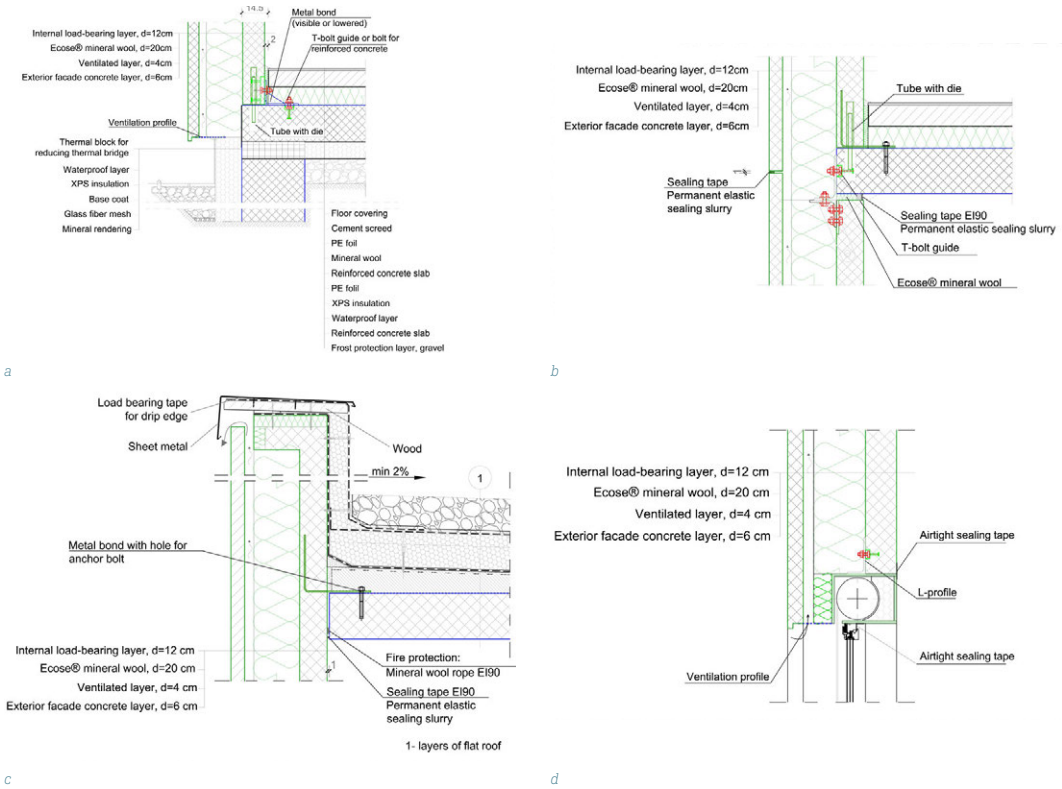

FIG. 6 Construction details: a) Vertical section of slab foundation; b) Vertical section of intermediate floor slab; c) Vertical section of flat roof; d) Vertical section of connection with upper part of the window (detail with the roller blind box)

The developed envelope system is modular and based on prefabrication, which allows a certain degree of architectural flexibility (Ku & Cardenas, 2008; Correia, 2017; Scuderi, 2019). The maximum panel dimensions of 8 × 4 m are limited by transportation possibilities. After mounting the panels to a load-bearing structure, panels need to be properly sealed from the interior side (joints between the inner concrete layer and load-bearing structure) in order to ensure continuity of the thermal envelope, adequate airtightness, and fire resistance of panels. Joints are sealed using mineral wool, autoclaved aerated concrete, and fire-resistant permanently elastic putty (Fig. 7).

FIG. 7 Sealing joints of panel and load-bearing structure

3.3.1 Point Thermal Bridges

The stainless steel girders (Ø=8 mm) connecting all characteristic layers of the panel act as point thermal bridges which can increase heat losses (Fig. 8). Since the exact type of stainless steel is not known, as well as its thermal conductivity, numerical analyses have been performed for two different values λ = 15 W/mK and λ = 50 W/mK and different boundary conditions. For the metal girders with λ = 50 W/mK and set of boundary conditions (interior surface of RAC-Concrete 20,58°C, outer surface of RAC-Brick 3,99°C). Fig. 8a shows the presence of point thermal bridges with a temperature difference of 2.54°C between the metal girder and the thermal insulation. This temperature difference increases with harsher boundary conditions, i.e. the influence of point thermal bridges becomes more pronounced.

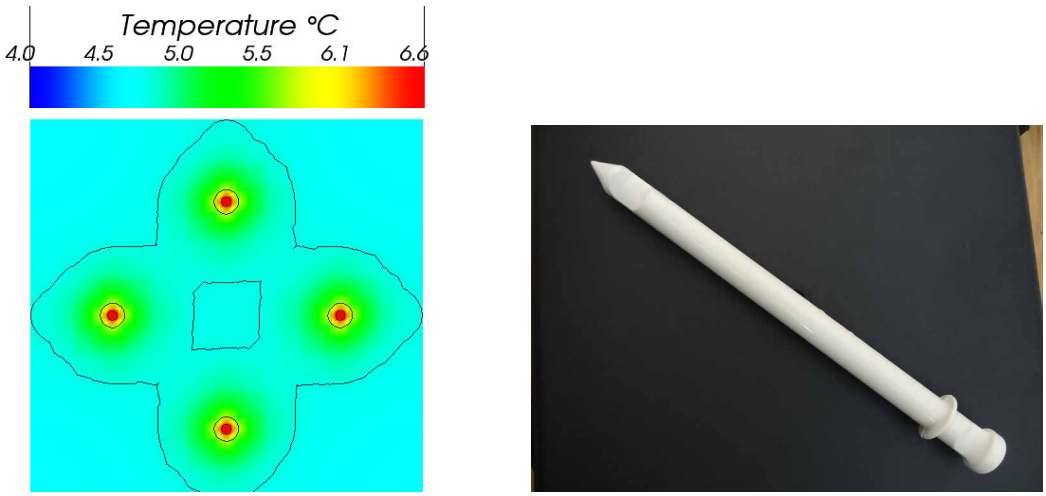

a b

FIG. 8 Girders: a) point thermal bridges caused by metal girders; b) polymer girder

One of the main design principles of NZEB, and generally all high energy performing buildings, is the minimisation of thermal bridges. Therefore, the possibility of replacing metal girders with polymer girders (Fig. 8b) was investigated. Numerical analysis has confirmed that it is possible to reduce point thermal bridges if metal girders (assumed λ = 16 W/mK) are replaced by polymer girders with low thermal conductivity (λ = 0.35 W/mK). The achieved reduction is approximately 91% for

assumed boundary conditions of 20°C and -10°C (Martinić, Pogačić & Marić, 2019). Moreover, this investigation has revealed that when using polymer girders, an optimisation of the arrangement of girders is necessary to ensure the panel's stiffness. The reorganisation of the arrangement of girders that results in minimal vertical and horizontal translations, compared to the original arrangement, is proposed (Martinić, Pogačić & Marić, 2019). In addition, polymers can be recycled, which supports their use from the sustainability perspective.

3.4 THERMAL MASS

The main difference between dynamic (transient) and steady-state performance of building elements and a building as a whole is energy storage. The ability to absorb, store thermal energy, and later release it to the environment, depending on the temperature difference of the immediate surroundings, is called thermal mass. Showed quite simplified in Eq. (1), heat energy storage can be described as a difference between the energy that enters building elements and the energy that "exits" from building elements.

$$\frac{dE_{storage}}{dt} = \frac{dE_g}{dt} + \frac{dE_{in}}{dt} - \frac{dE_{out}}{dt} \neq 0 \qquad [1]$$

Where ($dE_{storage}/dt$) states the rate of change of total energy, (dE_g/dt) is the rate of energy generated (e.g. internal gains), (dE_{in}/dt) is the rate of heat transfer in (e.g. solar gains) and (dE_{out}/dt) stands for the rate of heat transfer out (e.g. transmission and ventilation losses). From the Eq. (1) it is evident that the dynamic behaviour is a time-based problem.

A building envelope with a high thermal mass will respond to external changes, e.g. a sudden increase or decrease of outdoor temperature, with certain time delays and amplitude attenuation. This pattern of dynamic behaviour is defined as the thermal inertia of a building. A conventional approach in building design supports high thermal mass as beneficial for reducing energy consumption and maintaining indoor thermal comfort in both summer and winter periods. One should take into account that thermal mass is largely influenced by the arrangement of layers in a multi-layered construction element (Evangelisti, Battista, Guattari, Basilicata & de Lieto Vollaro, 2014), as well as insulation thickness. For example, an element that has a high thermal mass but is thermally insulated from interior will dynamically behave more like a lightweight element. A building envelope with high thermal mass acts like a "heat sink", i.e. it must first be "filled" with heat, so it can further release it to the indoor environment. Elements with high thermal mass and an excessive thickness of the thermal insulation layer, despite being very effective from the steady-state point of view (reducing heating energy need in winter), can cause overheating and thermal discomfort in summer.

Two concrete layers have contributed the most to the high thermal mass of the prefabricated panel. The panel has a surface mass of 458 kg/m^2 which classifies a building built with this envelope system as a heavyweight. The impact of the panel's high thermal mass on building energy need for two different Croatian climates (littoral and continental) and three different system operating modes (one continuous and two intermittent) was analysed according to EN ISO 52016-1 Standard (EN ISO 52016-1, 2017). Simulations of an exemplary building (Bagarić et al., 2020) covered only opaque

façade elements with high thermal mass (dynamic calculations) and without any capacity to store heat (static calculations). The hourly calculation procedure according to new Standard EN ISO 52016-1 showed that the thermal mass of the envelope system has a significant influence on the building's dynamic energy performance, whereas it cannot be analysed independently of the system operating mode and climate conditions. In the case of intermittent occupancy, a heavyweight building will require more heating energy but less cooling energy in comparison to the static scenario without heat storage capacity. When prolonging working hours of systems (continuous mode), high thermal mass will be beneficial from both heating and cooling energy demand aspects.

Even though the new Standard EN ISO 52016-1 has officially replaced EN ISO 13790 (EN ISO 13790, 2008), most European countries are still using procedures from EN ISO 13790 to calculate the energy performance of their buildings during this transition period. The comparison of the heavyweight exemplary building with other massiveness categories (very lightweight, lightweight, medium weight, very heavyweight) using the calculation procedure from EN ISO 13790 revealed that, for the continuous mode, a heavyweight building will consume somewhat less heating and cooling energy. This applies for both Croatian climates (littoral and continental). Contrary to that, for the intermittent mode, a heavyweight building can consume up to 6% more heating energy compared to a very lightweight building, but it will still require less cooling energy (up to 21%), respectively. Those results are valid for the exemplary building without transparent openings and all assumption made by authors (Bagarić, Banjad Pečur, Milovanović & Hozmec, 2019). Nevertheless, one must be aware that windows can have a dominant role in the energy balance of the whole building. Therefore, when designing a building with a prefabricated façade panel from RAC, in order to take advantages of its thermal mass, special attention should be given to defining the size and arrangement of windows.

4 APPLICATION OF PREFABRICATED PANELS

The first full scale application of a prefabricated RAC panel was a family house built in the city of Koprivnica, Croatia. Since the application of the panel was realised within the European research project ECO-SANDWICH (ECO-SANDWICH®, 2012) within which it was conceived and developed, the house was named "First ECO-SANDWICH® house" (Fig. 9a). The second application was NZEB kindergarten "Ribica" near the city of Osijek, Croatia (Fig. 9b).

a *b*

FIG. 9 First implementation of prefabricated modular façade panel from RAC: a) family house "First ECO-SANDWICH® house"; b) kindergarten "Ribica" (Cist racun, 2017)

4.1 "FIRST ECO-SANDWICH® HOUSE"

"First ECO-SANDWICH® house" is a 3-storey family house built within a socially supported housing programme of the city of Koprivnica, Croatia. Since the house was designed in 2015, when there were no regulations or requirements related to NZEB, its design principles followed passive house standards. These principles indicate large transparent openings to the south (Fig. 10a) and minimal transparent openings on the north façade, as well as mechanical ventilation with a heat recovery system. Thermal breaks from the neoprene pads (Fig. 10b) were installed to prevent thermal bridges due to anchoring systems. To ensure airtightness and fire resistance of panels, joints were properly sealed using autoclaved aerated concrete, mineral wool, and permanent elastic sealing slurry (Fig. 7). The main geometric characteristics of the house are shown in Table 3. As a first full-scale implementation of the prefabricated RAC panel in real environmental conditions and occupied by tenants, "First ECO-SANDWICH® house" was selected as a case study for investigating the panel's dynamic hygrothermal performance and energy consumption of the whole building.

a b

FIG. 10 "First ECO-SANDWICH® house": a) south façade; b) thermal break for anchoring systems

TABLE 3 Main characteristics of the "First ECO-SANDWICH® house"

	GROUND FLOOR APARTMENT	1ST FLOOR APARTMENT	2ND FLOOR APARTMENT	UNHEATED STAIRWELL
Useful heated floor area [m2]	95.69	101.44	67.47	/
	Total 264.60			
Net volume of heated air [m3]	258.36	273.89	182.17	/
	Total 714.42			
Shape ratio [-]	0.77			
Useful unheated floor area [m2]	/	/	/	41.52
Net volume of unheated air [m3]	/	/	/	144.50
Number of occupants	2 adults with 2 children (< 5 y.o.)	2 adults with 2 children (< 15 y.o.)	2 adults with one child (< 3 y.o.)	/

5 MONITORING OF FIELD PERFORMANCE – ELEMENT AND WHOLE BUILDING LEVEL

Extensive research activities have been conducted at a material level (Banjad Pečur et al., 2015) (Banjad Pečur & Štirmer, 2012) (Milovanović, Bagarić, Banjad Pečur & Štirmer, 2018) (Bagarić et al., 2019) and essential characteristics of the panel have been tested at element level (Bjegović et al., 2014) (BETON-LUČKO Ltd., 2015) (Štirmer et al., 2015) (PRéConsultants bv, 2015). However, despite the importance of understanding the dynamic hygrothermal performance of the developed RAC panel under variable climate conditions and occupants' behaviour on a large scale, it remains an under-researched area. To the best knowledge of the authors, there is still a gap between research and large scale practical applications of RAC (de Brito, Poon, Zhan, 2019), and thus a strong need to evaluate RAC's suitability for constructing building envelopes that are robust and resilient in a holistic manner: energy performance, moisture behaviour, durability, and sustainability.

5.1 HYGROTHERMAL PERFORMANCE AT THE ELEMENT LEVEL

Field monitoring of hygrothermal performance of the "First ECO-SANDWICH® house" envelope was commissioned on March 9th, 2017. In a ground floor apartment, three panels were selected for monitoring, as shown in Fig. 11. Those panels differ by orientation and indoor conditions (south-oriented M1 adjacent to conditioned living room, east-oriented M2 adjacent to conditioned bedroom and north-oriented M3 adjacent to unconditioned stairwell). In each characteristic layer (Fig. 3a) of selected panels, temperature and relative humidity (RH) sensors were installed to monitor heat and moisture transfer on an hourly basis. For the sake of brevity, results are shown only for south and north panels.

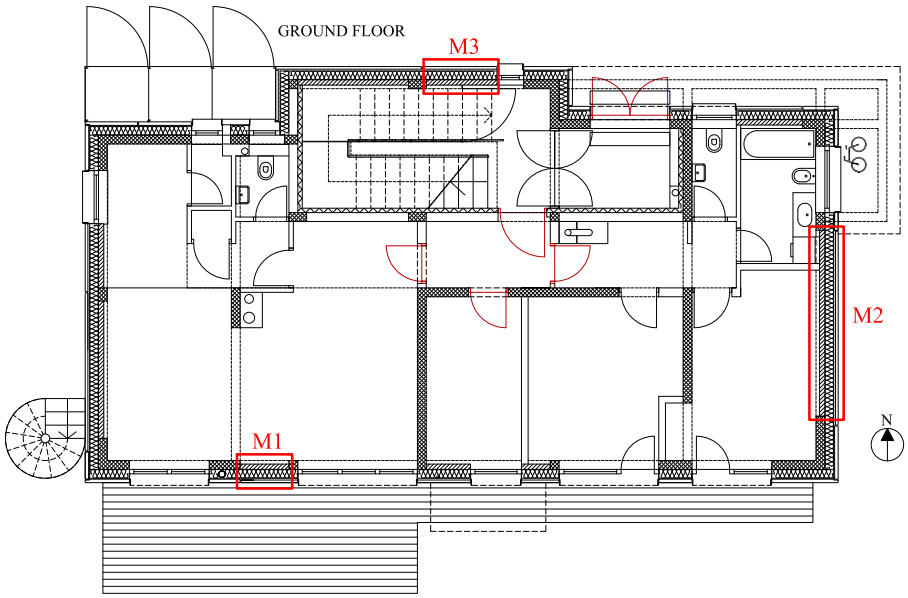

FIG. 11 Location of panels selected for hygrothermal monitoring

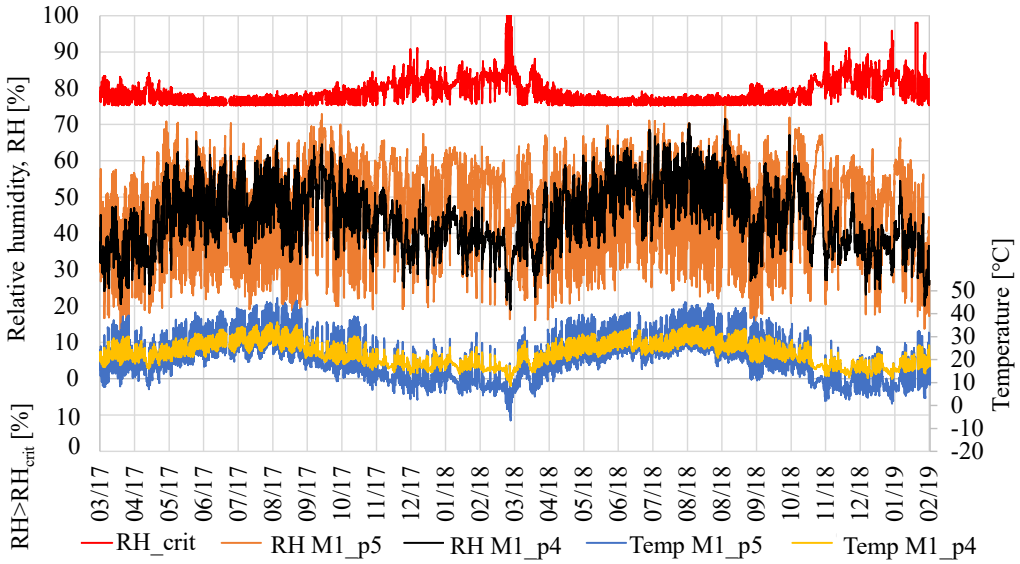

FIG. 12 Comparison of monitored RH at positions p5 and p4 in thermal insulation layer with RHcrit for south-oriented panel M1

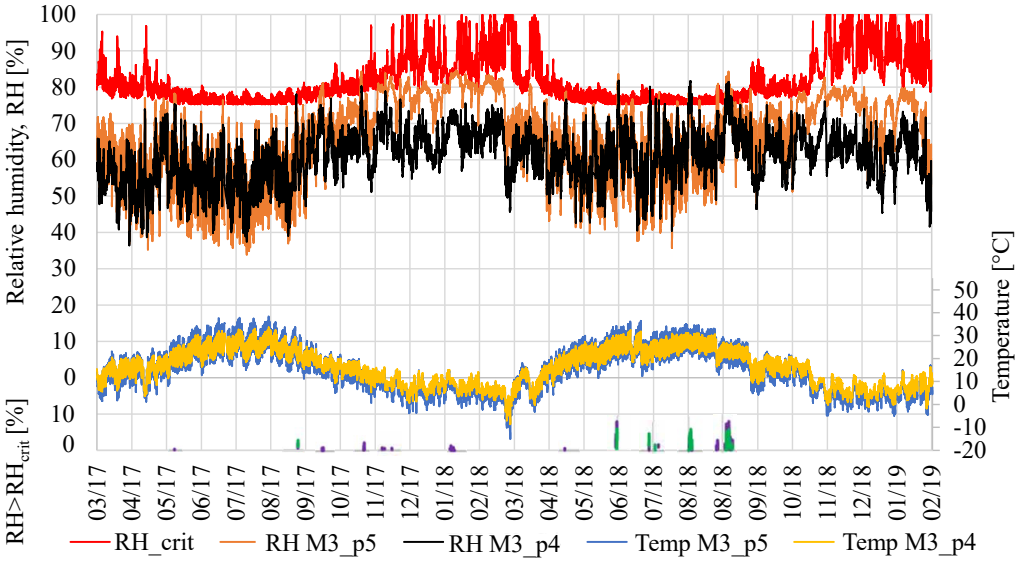

FIG. 13 Comparison of monitored RH at positions p5 and p4 in thermal insulation layer with RHcrit for north-oriented panel M3

Monitored RH values are displayed using Folos 2D visual mould chart (Mundt-Petersen, 2015), (Figs. 12 – 13) which shows developed temperatures and RH, calculated $RH_{crit,}$ and calculated $RH>RH_{crit}$ difference. Conditions at any specific time are visible, whereas of particular interest are the periods during which the RH exceeds RH_{crit} and their duration. Critical conditions depend on the prevailing RH and temperature, where a low temperature gives a higher RH_{crit}. More about Folos 2D chart and calculation of RH_{crit} can be found in the reference, Mundt-Petersen (2015). As can be seen from Fig. 12, during the two-year monitoring period, RH in the thermal insulation layer of south-oriented panel M1 never exceeded critical values. For the complete opposite orientation (north-oriented panel M3 presented in Fig. 13), occasional $RH > RH_{crit}$ occurs at positions p5 and p4 in the thermal insulation layer. This can be attributed to the lower solar radiation intensity on the north façade and thus lower

drying capacity. However, if time distribution of RH>RH_{crit} events is analysed (Table 4), it suggests that there is no longer continuity of critical conditions and no mould can occur (Sedlbauer, 2001). Therefore, it can be concluded that north-oriented is also moisture-safe.

TABLE 4 Time distribution of RH > RHcrit within thermal insulation layer of north-oriented panel M3

	POSITION P5	POSITION P4
05/2017	2	/
08/2017	3	5
09/2017	17	/
10/2017	18	/
11/2017	10	/
01/2018	25	/
04/2018	3	/
06/2018	32	17
07/2018	2	4
08/2018	73	36
09/2018	106	45
TOTAL [h]	**291**	**107**

5.2 NUMERICAL SIMULATIONS OF HYGROTHERMAL PERFORMANCE

To investigate if natural ventilation influences the thermal performance of the prefabricated façade RAC panel, the numerical model was developed using WUFI® Pro 5.2. WUFI® Pro is a tool capable of predicting one-dimensional transient heat, air, and moisture transfer through building elements. The numerical model was calibrated by monitoring results (Bagarić et al., 2020) and used to compare the prefabricated ventilated façade panel with the non-ventilated façade panel and ETICS system. The non-ventilated panel was modelled with the same geometry and material characteristics as the ventilated one, except for the cavity ventilation, which was omitted from the calculations. ETICS system was modelled with mineral wool insulation applied to the inner RAC-Concrete layer of same thickness, as in case of the ventilated and non-ventilated façade panel. The thermal transmittance of all three façade systems is comparable. In the case of the ventilated façade panel, cavity ventilation was modelled as a varying air change rate using a simplified Nore's model (Hägerstedt & Harderup, 2011).

When the south orientation is observed, the lowest heat gains during summer are present in the case of the ventilated façade RAC panel, and when compared to other systems the differences are in range from 29.07% (non-ventilated façade panel) up to 50.65% (ETICS system). In the winter period, heat losses through the ventilated panel are practically the same as for non-ventilated, but they are still slightly lower than for ETICS system (8.72%). For the completely opposite orientation, i.e. north, results suggest that during the winter period, the ventilated and non-ventilated façade RAC panels exhibited more favourable thermal behaviour than ETICS. In summer, for the north oriented envelope systems under consideration, the highest heat losses are attributed to the ventilated façade RAC panel. It needs to be highlighted that those summer thermal losses are very low for

all analysed façade systems. By comparing heat losses through north and south oriented façade systems in winter, it can be seen that they are less pronounced on the north side. Most probably this can be explained by the unconditioned stairwell subjected to façade systems facing north, and hence a lower temperature difference governing the heat exchange between stairwell and outdoor environment. Results from Table 5 confirm a generally more favourable thermal performance of the ventilated façade RAC panel compared to the non-ventilated and ETICS systems, especially for the south orientation, which makes this façade system suitable for hot climates. It can be concluded that naturally ventilated air in the cavity passively cools down the external surface of thermal insulation, and thus reduces heat gains.

TABLE 5 Total heat flow through analysed façade systems (flow from the outside to the inside of building is considered positive)

SOUTH ORIENTATION	August 2017 (summer period)		February 2018 (winter period)	
	Monthly [Wh/m2]	Average daily [Wh/m2]	Monthly [Wh/m2]	Average daily [Wh/m2]
Ventilated façade panel	331.72	10.70	-2122.17	-75.79
Non-ventilated façade panel	427.86	13.81	-2088.68	-74.60
ETICS system	499.84	16.12	-2307.11	-82.40
NORTH ORIENTATION	August 2017 (summer period)		February 2018 (winter period)	
	Monthly [Wh/m2]	Average daily [Wh/m2]	Monthly [Wh/m2]	Average daily [Wh/m2]
Ventilated façade panel	-27.60	-0.89	-1158.09	-41.36
Non-ventilated façade panel	-18.28	-0.59	-1150.80	-41.10
ETICS system	-12.06	-0.39	-1348.08	-48.15

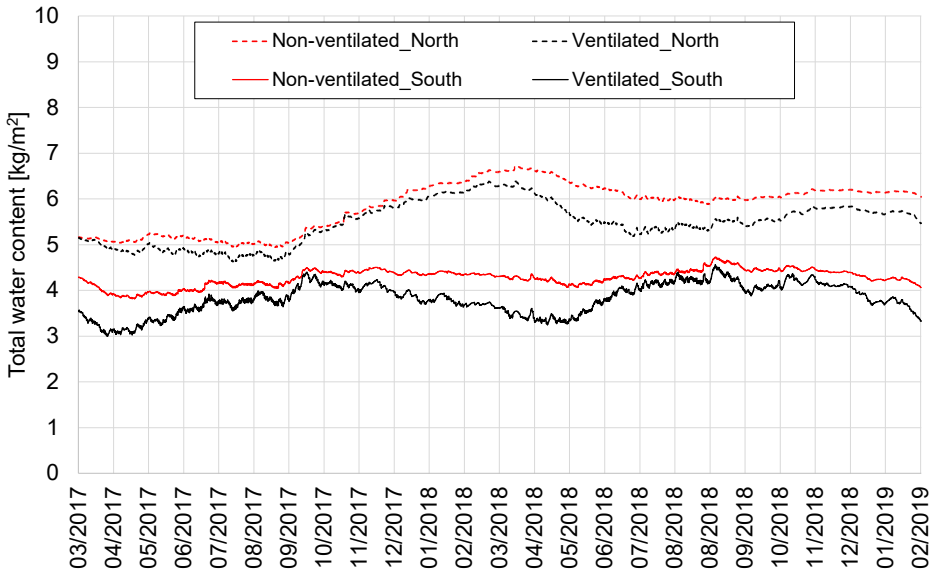

FIG. 14 Total water content in ventilated and non-ventilated panels for unexpected leakages scenario

The influence of naturally ventilated air in the cavity on the hygric performance was also investigated in case of unexpected leakages. Unexpected leakages may occur as a result of poor workmanship or poor design (e.g. wind-driven rain penetrating through cladding joints, joints between window and panels, etc.). The same numerical models of ventilated and non-ventilated panels, as presented above, were used for this investigation. For the purpose of simulating unexpected leakages, the penetration through the façade was assumed to be 1% of the amount of wind-driven rain and this amount was added as a moisture source in the middle of the thermal insulation layer. For both analysed orientations, south and north, the non-ventilated panel contains more water content than the ventilated panel (Fig. 14). Results suggest that naturally ventilated air in the cavity helped to dry out excessive moisture caused by leakages. Fig. 15 indicates that this drying efficiency (reduction of total water content in comparison to the non-ventilated panel of the same orientation) is more pronounced for the south-oriented ventilated panel (10.75%) than for north-oriented ventilated panel (6.33%).

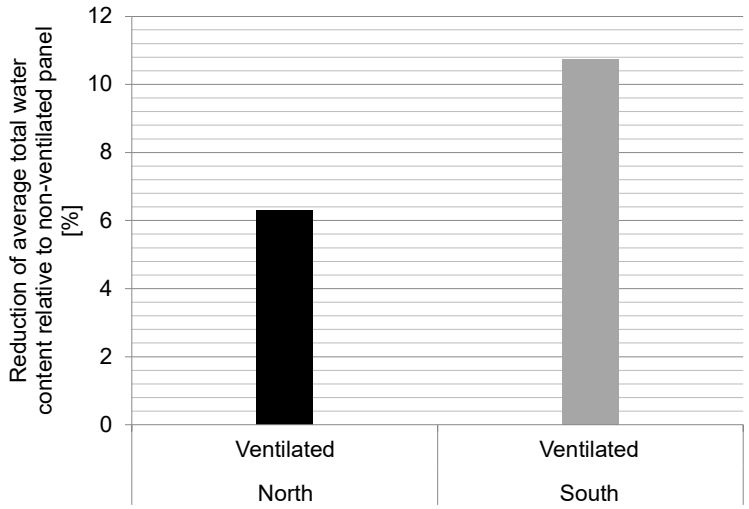

FIG. 15 Efficiency of ventilated panels in terms of reducing total water content when exposed to unexpected leakages, compared to non-ventilated panels

5.3 BUILDING'S ENERGY CONSUMPTION

The "First ECO-SANDWICH® house" was designed in 2015 as a very low-energy house with an annual specific energy demand for heating $Q_{H,nd}$" = 14.95 kWh/m^2 and cooling $Q_{C,nd}$" = 10.86 kWh/m^2, respectively. At the time of project design, Croatian legislation and methodology for calculating energy performance of buildings required only specific energy needs, and thus, for the building under investigation no design values of delivered and/or primary energy are available. For each apartment, energy consumption (electrical energy and natural gas) is being monitored, as well as electrical energy in the common area (unheated stairwell). All data can be accessed and analysed through a computer system for real-time remote energy supervision called ESCO Monitor® (HEP ESCO, 2018). Table 6 shows the energy consumed by the occupants for a one-year period (01.01.2019 – 01.01.2020). For different energy resources, Republic of Croatia had defined different values of primary energy factors f_{prim} (MGIPU, 2014) for conversion of delivered energy E_{del} into primary E_{prim}. Using those values (f_{prim} = 1.614 for electrical energy and f_{prim} = 1.6095 for natural gas), annual primary energy of "First ECO-SANDWICH® house" was calculated (Table 7).

TABLE 6 Measured delivered energy E_{del}

DELIVERED ENERGY E_{DEL}	Electrical energy [kWh]	Natural gas [kWh]
Ground floor apartment	3113.03	10896.50
1st floor apartment	1668.95	4750.00
2nd floor apartment	1146.57	8236.50
TOTAL HEATED	**5928.55**	**23883.00**
Unheated stairwell	584.92	/
TOTAL HEATED + UNHEATED	**6513.47**	**23883.00**

TABLE 7 Annual primary energy E_{prim} calculated based on measured delivered energy E_{del}

PRIMARY ENERGY E_{DEL}	[kWh]	[kWh/m^2]
Heated part of building (apartments, useful floor area 264.60 m^2)	35720.56	134.99
Common area (unheated stairwell, useful floor area 41.52 m^2)	944.06	22.74
TOTAL	**36664.62**	**119.77**

According to the Croatian legislation (MGIPU, 2018), the annual primary energy for a new residential building (family house) in a continental climate needs to be less than 115 kWh/m^2, while for a NZEB family house it needs to be less than 45 kWh/m^2. However, it must be noted that according to the current Croatian legislation, the primary energy for a family house covers only the energy needed for heating, domestic hot water, and mechanical ventilation (if installed). For the building under consideration, monitoring of overall energy consumption was conducted, which also implies energy for lighting, cooking, home devices, cooling, etc. without the contribution of renewable energy sources. Moreover, methodology for energy calculations assumes certain indoor temperature conditions and working hours of technical systems, which in reality, completely depends on occupants' habits and comfort perception. Based on the monitoring results, it can be concluded that it is possible to construct a family house with ventilated prefabricated RAC façade panels that will consume less than 120 kWh/m^2 of the total primary energy annually, covering all energy sources used by occupants. It can be assumed that with other thermo-technical systems and with integration of renewable energy systems, the total primary energy consumption could be additionally reduced.

6 CONCLUSION

This paper discusses the development and application of an innovative ventilated façade system from recycled construction and demolition waste (CDW). A comprehensive methodological approach consisted of upscaling the research from material level (initial research activities focused on material properties) to the element level (optimisation and production of prototype panel) and finally to the whole building level (application of panel in real environmental conditions and performance monitoring).

The extensive research activities at the material level confirmed the possibility of using crushed brick and recycled concrete from CDW as a partial replacement of natural aggregates in concrete production. The high replacement ratio of coarse natural aggregate (50%) with recycled aggregate from CDW resulted in two types of recycled aggregate concrete (RAC). Their mechanical, durability,

and hygrothermal properties showed to be satisfactory and acceptable for producing a prefabricated self-load bearing façade panel. Both RAC-Concrete and RAC-Brick can be classified in compressive strength class C 30/37, and they satisfy requirements for XF4 (56 cycled of freezing and thawing with de-icing salts) environmental exposure class. A high percentage of recycled aggregate resulted in up to 13 - 27 % (RAC-Concrete) and 29 - 40 % (RAC-brick) lower thermal conductivity than the reported literature values for the dry concrete with approximately the same density. The water vapour diffusion coefficient for these concretes is 38 - 70% lower than the literature values for similar wet concrete.

Besides incorporating a high amount of CDW, the main specificity of the developed prefabricated façade system is a cavity with naturally ventilated air, which is not common for conventional concrete sandwich wall panels. Prefabrication ensured the production of the panel in controlled conditions, which increases product quality and reduces construction time. The Declaration of Performance and CE mark were issued by manufacturer after testing all essential characteristics at material and element level (AVCP 4 system). This enabled the panel to be put on the market and confirmed that it is possible to produce a high quality envelope system by incorporating high amount of recycled CDW.

The first application of the developed panel in real environmental conditions served as a case study to evaluate panel's suitability for constructing high energy performing, durable, and moisture-safe building envelope. For the 3-storey family house in the city of Koprivnica (Croatia), results from two years of monitoring confirmed that the naturally ventilated air layer helps to maintain acceptable humidity conditions in the thermal insulation layer, whereas the south orientation is completely moisture safe. For the north oriented panel there are certain periods in which relative humidity exceeds critical values (in total 291 hours at the surface of thermal insulation adjacent to the air cavity and 107 hours in the middle of thermal insulation). However, these periods are quite short (a few hours per day) and thus, not long enough for mycelia germination and degradation of thermal insulation.

Furthermore, numerical simulation results indicate the presence of a passive cooling mechanism for the ventilated façade panel, and thus its positive impact on reducing heat gains. Summer heat gains through the ventilated façade panel were up to 29.07% lower than the non-ventilated façade panel and up to 50.65% lower than the ETICS system, respectively. This confirms the suitability of the developed panel for hot climates. A ventilated air cavity was also shown to be beneficial when drying of extensive moisture from the unexpected leakages is observed. This drying efficiency (reduction of total water content in comparison to the non-ventilated panel of the same orientation) is more pronounced for the south-oriented ventilated panel (10.75%) than for the north-oriented ventilated panel (6.33%).

The panel's high thermal mass, depending on the climate and system operating mode, can have a positive impact on a building's heating and cooling energy needs. However, the size and location of transparent openings need to be carefully considered during the design phase. For the family house under consideration, the total annual primary energy consumption was less than 120 kWh/m^2, but it encompasses the total energy consumed by occupants and no contribution from renewable energy sources.

It can be concluded that the developed prefabricated ventilated façade panel is a robust and resilient façade system, which offers a closed-loop solution for CDW with lower environmental impact and contributes to reducing energy needs in the building sector. Therefore, it can certainly

foster the breakthrough of RAC in high energy performing and healthy buildings, as well as their large-scale deployment.

Further research will include the specific design of air cavity openings and its influence on cavity ventilation. A climate-dependent analysis will be performed to evaluate the applicability of the developed panel for different conditions in practice. Different cladding materials and the possibility of integrating photovoltaics will be analysed, whereby building envelope and mechanical service would be integrated, and thus, the applicability for NZEB buildings increased. Moreover, the long-term monitoring of indoor comfort parameters in "First ECO-SANDWICH® house" will be performed.

Acknowledgements

The presented research was performed within two scientific and research projects: "ECO-SANDWICH", funded in the frame of CIP ECO Innovation programme (ECO/11/304438/SI2.626301) and "Monitoring and analyses of energy consumption and comfort parameters in ECO-SANDWICH house in Koprivnica using computer system ESCO Monitor" in collaboration with Croatian energy service-providing company, HEP ESCO.

References

Bagarić, M., Banjad Pečur, I., Milovanović, B., & Hozmec, S. (2019). Ventilated sandwich wall panel from recycled aggregate concrete: Hygrothermal characterization, *Proceedings of International Conference on Sustainable Materials, Systems and Structures - Energy Efficient Building Design and Legislation*, RILEM Publications S.A.R.L., Rovinj, Croatia, 102–110.

Bagarić, M., Banjad Pečur, I., & Milovanović, B. (2020). Hygrothermal performance of ventilated prefabricated sandwich wall panel from recycled construction and demolition waste – A case study, *Energy and Buildings 206*. doi:10.1016/j.enbuild.2019.109573.

Banjad Pečur, I., Štirmer, N., & Milovanović, B. (2015). Recycled aggregate concrete for nearly zero-energy buildings, *Magazine of Concrete Research 67, 575–584*. doi:10.1680/macr.14.00220.

Banjad Pečur, I., Bagarić, M., & Bomberg, M. (2020). GUEST EDITORS' PREFACE: Special issue "A Paradigm Shift in Integrated Building Design - Towards Dynamically Operated Buildings," *Advances in Building Energy Research*. doi:10.1080/17512549.2020.1731710. – *Accepted for publishing*

Banjad Pečur, I. & Štirmer, N. (2012). Application of recycling aggregate in concrete - Experiences in Croatia, *Proceedings of 19. Slovenski Kolokvij o Betonih: Doseganje Posebnih Betonov z Uporabo Odpadlih Materialov [Slovenian Colloquium on Concrete: Achieving Special Concretes with the Use of Waste Materials],* IRMA Inštitut za raziskavo materialov in aplikacije, Ljubljana, Slovenija, pp. 51–62.

Behera, M., Bhattacharyya, S.K., Minocha, A.K., Deoliya, R., & Maiti, S. (2014). Recycled aggregate from C&D waste & its use in concrete - A breakthrough towards sustainability in construction sector: A review, *Construction and Building Materials (68),* 501–516. doi:10.1016/j.conbuildmat.2014.07.003.

BETON-LUČKO Ltd. (2015). Declaration of performance ECO-SANDWICH wall panel, http://www.eco-sandwich.hr/repository/declaration-of-performance/.

Bjegović, D., Banjad Pečur, I., Štirmer, N., Milovanovic, B., Carević, I., & Alagušić, M. (2014). Ventilated precast wall panel ECO-SANDWICH®, *Proceedings of International Symposium on researching and application of contemporary achievements in civil engineering in the field of materials and structures*, Vrnjačka Banja, Srbija, 533–544.

Calvo, N., Varela-Candamio L., & Novo-Corti I. A. (2014). Dynamic Model for Construction and Demolition (C&D) Waste Management in Spain: Driving Policies Based on Economic Incentives and Tax Penalties, *Sustainability 6*, 416-435. doi:10.3390/su6010416

CECE (2020). Construction and Infrastructure Sector. https://www.cece.eu/industry-and-market/construction-and-infrastructure-sector

Cist racun (2017). Kindergarten Ribica Sarvaš. https://cistracun.net/tag/djecji-vrtic-ribica-sarvas/

Correia, A. L. (2017). *Fabricating architecture: From Modern to Global Space*, PhD thesis, University of Coimbra, Portugal

C3 project (2020). Carbon Concrete Composite. http://www.bauen-neu-denken.de/

de Brito, J., Gonçalves, A. P., & Ramos dos Santos, R. (2006). Recycled concrete production: Multiple recycling of concrete coarse aggregates, *Revista Ingenieria de Construccion [Journal of Construction Engineering] 21 (1)*, 33-40

de Brito, J., Poon, C. S., & Zhan, B. (2019). New Trends in Recycled Aggregate Concrete – Special issue of *Applied Sciences*. https://www.mdpi.com/journal/applsci/special_issues/Recycled_Aggregate_Concrete?view=compact&listby=date#published

ECO-SANDWICH® (2012). *Energy efficient, recycled concrete sandwich façade panel* – EU funded project, https://www.eco-sandwich.hr/

EN ISO 13790 (2008). Energy performance of buildings – Calculation of energy use for space heating and cooling

EN 15804 (2013). Sustainability of construction works – Environmental product declarations – Core rules for the product category of construction products

EN ISO 52016-1 (2017). Energy performance of buildings – Energy needs for heating and cooling; internal temperatures and sensible and latent heat loads – Part 1: Calculation procedures

European Commission (2015a). Closing the loop - An EU action plan for the Circular Economy, COM(2015) 614 final

European Commission (2015b). CE marking of construction products step by step. https://ec.europa.eu/growth/content/ce-marking-construction-products-step-step-guide-now-available-all-eu-languages-0_en

European Commission (2018). A Clean Planet for all, A European strategic long-term vision for a prosperous, modern, competitive and climate neutral economy, COM(2018) 773 final, Brussels

European Parliament (2002). Directive 2002/91/EC of the European Parliament and of the Council of 16 December 2002 on the energy performance of buildings, *Official Journal of the European Communities. L 1/65*

European Parliament and Council (2008), Directive 2008/98/EC of the European Parliament and of the Council of 19 November 2008 on waste and repealing certain directives, *Official Journal of the European Union. L312/3*. doi:2008/98/EC.; 32008L0098.

European Parliament (2010). Directive 2010/31/EU of the European Parliament and of the Council of 19 May 2010 on the energy performance of buildings (recast), *Official Journal of the European Union. L 153/13*

European Parliament (2018a). Directive (EU) 2018/844 of the European Parliament and of the Council of 30 May 2018 amending Directive 2010/31/EU on the energy performance of buildings and Directive 2012/27/EU on energy efficiency, *Official Journal of the European Union. L156/75*

European Parliament (2018b). Directive (EU) 2018/2001 of the European Parliament and of the Council of 11 December 2018 on the promotion of the use of energy from renewable sources (recast), *Official Journal of the European Union. L 328/82*

EUROSTAT 2015, http://appsso.eurostat.ec.europa.eu/nui/setupModifyTableLayout.do?state=new&currentDime nsion=DS-052688WASTE (accessed April 30 2015)

Evangelisti, L., Battista, G., Guattari, C., Basilicata, C., & de Lieto Vollaro, R. (2014). Influence of the thermal inertia in the European simplified procedures for the assessment of buildings' energy performance, *Sustainability 6 (7)*, 4514–4524. doi:10.3390/su6074514.

Fenollera, M., Míguez, J., Goicoechea, I., & Lorenzo, J. (2015) Experimental Study on Thermal Conductivity of Self-Compacting Concrete with Recycled Aggregate, *Materials (8).* 4457–4478. doi:10.3390/ma8074457.

Fraile-Garcia, E., Ferreiro-Cabello, J., López-Ochoa, L.M., & López-González, L.M. (2017). Study of the technical feasibility of increasing the amount of recycled concrete waste used in ready-mix concrete production, *Materials (10).* doi:10.3390/ma10070817.

Hägerstedt, S. O. & Harderup, L.-E. (2011). Comparison of measured and calculated temperature and relative humidity with varied and constant air flow in the façade air gap, *Proceedings of 9th Nordic Symposium on Building Phys*ics, Tampere, Finland. 147–154.

HEP ESCO (2018). ESCO Monitor®. http://www.hep.hr/esco/energy-services/esco-monitor-1766/1766

HZN (Croatian Standards Institute) (2016). HRN EN 206: Concrete – Specification, performance, production and conformity (EN 206:2013+A:2016)

ISO (2016). Strategic business plan ISO/TC 071. https://isotc.iso.org/livelink/livelink/fetch/2000/2122/687806/ISO_TC_071__Concrete__reinforced_concrete_and_pre-stressed_concrete_.pdf?nodeid=1162199&vernum=0

Ku, K. & Cardenas, C. (2008). Flexibility in prefabrication approaches: Lessons from two US homebuilders, *2008 ACSA Northeast Fall Conference Proceedings*, USA

Marco, P. (2014). *A conceptual model to design recycled aggregate concrete for structural applications*. Springer Theses, Springer. doi:10.1007/978-3-319-26473-8 ISSN.

Martinić, L., Pogačić, V., & Marić, K. (2019). *The impact of ties on point thermal bridges and optimisation of their arrangement for increasing the stiffness of precast wall panels*, University of Zagreb, Faculty of Civil Engineering, Zagreb. (Student work awarded by Rector, on Croatian)

MGIPU (Ministry of Construction and Physical Planning, Republic of Croatia) (2014). Primary energy and CO2 emission factors. http://www.mgipu.hr/doc/EnergetskaUcinkovitost/FAKTORI_primarne_energije.pdf.

MGIPU (2018). Technical regulation on energy economy and heat retention in buildings, *Official Gazette 128/15, 70/18, 73/18, 86/18.*

Milovanović, B., Bagarić, M., Banjad Pečur, I., & Štirmer, N. (2018). Use of recycled aggregate concrete for energy efficient buildings, *Proceedings of 3rd R.N. Raikar Memorial International Conference and Gettu-Kodur International Symposium on Advances in Science and Technology of Concrete*, Mumbai, India

Milovanović, B. & Mikulić, D. (2011). Assessment Method for Combined Heat, Air and Moisture Transfer in Building Components, *Proceedings of International Conference on Energy Management in Cultural Heritage*, Dubrovnik, Croatia

Monier, V., Hestin, M., Trarieux, M., Mimid, S., Domröse, L., Van Acoleyen, M., Hjerp, P., & Mudgal, S. (2011). Study on the management of Construction and demolition waste in the EU. Contract 07.0307/2009/540863/SER/G2, Final report for the European Commission (DG Environment)

Mundt-Petersen, S. O. (2015). *Moisture safety in wood frame buildings - Blind evaluation of the hygrothermal calculation tool WUFI using field measurements and determination of factors affecting the moisture safety* (Doctoral dissertation), Lund University.

Pickel, D. (2014). *Recycled Concrete Aggregate: Influence of Aggregate Pre-Saturation and Curing Conditions on the Hardened Properties of Concrete.* (Master's Thesis), University of Waterloo, Waterloo, Ontario, Canada

PRéConsultants bv (2015). LCA of ECO-SANDWICH® wall panels – Assessing the sustainability of a wall panel made of recycled and innovative materials in residential and commercial buildings. https://www.construction21.org/data/sources/users/24897/150902peer-reviewed-lca-of-eco-sandwich-wall-panelsv22final-signed.pdf (accessed August 21, 2020)

Scuderi, G. (2019). Designing Flexibility and Adaptability: The Answer to Integrated Residential Building Retrofit, *Designs 3, 3*. doi:10.3390/designs3010003

Sedlbauer, K. (2001). *Prediction of mould fungus formation on the surface of and inside building components*, Doctoral thesis, Universität Stuttgart, 2001. http://www.ibp.fraunhofer.de/content/dam/ibp/en/documents/ks_dissertation_etcm1021-30729.pdf.

Statista (2020). Major countries in worldwide cement production 2015-2019. https://www.statista.com/statistics/267364/world-cement-production-by-country/

Štirmer, N., Banjad Pečur, I., & Milovanović, B. (2015). Life Cycle Assessment of Energy Efficient, Recycled Concrete Sandwich Façade Panel, Proceedings of International UKIERI Concrete Congress, Jalandhar, Punjab, India, 717–726.

Vyncke, J. & Vrijders, J. (2016). Recycling of Construction and Demolition Waste - An Overview of RILEM Achievements and State of the Art in the EU, *Proceedings of the Second International Conference on Concrete Sustainability* – ICCS16, Madrid, Spain

Zhu, L., Dai, J., Bai, G., & Zhang, F. (2015). Study on thermal properties of recycled aggregate concrete and recycled concrete blocks, *Construction and Building Materials (94)*. 620–628. doi:10.1016/j.conbuildmat.2015.07.058.

Construction Aspects of Hybrid Water-Filled Building Envelopes

Matyas Gutai[1*], Shwu-Ting Lee[2], Bumpei Magori[3], Yu Morishita[3], Abolfazl Ganji Kheybari[4] and Joshua Spencer[1]

* Corresponding author
1 School of Architecture, Building and Civil Engineering, Loughborough University, Loughborough, United Kingdom, M.Gutai@lboro.ac.uk
2 School of Architecture, Feng Chia University, Taichung, Taiwan
3 Institute of Industrial Science, The University of Tokyo, Tokyo, Japan
4 Faculty of Civil Engineering, TU Kaiserslautern, Kaiserslautern, Germany

Abstract

Water-filled building envelopes are hybrid constructions with a solid and a fluid component, typically a glass or steel shell filled with water. The paper introduces the challenges of developing a water-filled façade structure and evaluates the possibility to utilise it as a viable construction system on a building scale. Water-filled glass (WFG) has been researched in the past and it was presented as an independent window element of a conventional building, where energy savings are achieved by using the absorption of the water layer for energy management of the building envelope. The results suggest that WFG's efficiency could be improved further if the system is assembled as a united building envelope in which the fluid can flow between panels and building parts. The paper presents two experimental 'water house' buildings with these design parameters, designed and constructed by the author. The importance of these buildings is that a connected water-filled envelope is built for the first time. The discussion presents two construction methods for water-filled façades, evaluates their viability for different climates, introduces the design-construction aspects of the technology, and offers a comparison with existing construction methods.

A fluid-solid building envelope provides significant savings for both operational and embodied energy, by lowering cooling load, reusing absorbed heat, balancing thermal differences between parts of the envelope and the rest of the building, while making additional construction elements (e.g. external shadings) obsolete.

Keywords

Glass buildings, solar control, water house, water-flow building envelope, water-filled glass, fluid-solid hybrid construction, advanced glazing, building sustainability, energy-efficiency, energy-efficient building envelope

DOI 10.7480/jfde.2020.2.4784

1 INTRODUCTION

Structural materials have a significant impact on the ecological footprint of the built environment. This applies specifically to building envelopes that play a main role in energy efficiency and thermal comfort in a building. In particular, building envelopes with high window-to-wall ratios (WWR) are a good example, as glass façades utilise energy intensive materials (Adalberth, 1997) and increase operational energy demand (Gasparella, Pernigotto, Cappelletti, Romagnoni, & Baggio, 2011). Innovations in glass envelopes have great potential for positive change in the environmental impact of buildings, especially if they are able to lower both embodied and operational energy. This is especially the case where higher life-cycle assessment (LCA) is reported for zero energy buildings compared to low energy constructions (Ramesh, Prakash, & Shukla, 2010), which is mainly due to the increased embodied energy component (i.e. added PV or solar panels) of the former when compared to the latter. This implies that there is a need for innovations that can improve energy performance without an increase in embodied energy.

In terms of the energy management of building envelopes, the current state of research on optically clear windows can be divided into four groups. The first category addresses solar gain (SHGC) with coating, dynamic or active glazing. Solutions for this include Low-E coating (Cui & Mizutani, 2016), electrochromic glazing or EC (DeForest et al., 2015), suspended particle device glazing or SPD (Ghosh, Norton, & Duffy, 2016) and polymer dispersed liquid crystal or PDLC (Hemaida, Ghosh, Sundaram, & Mallick, 2020). The second category is to improve the thermal resistance (U-value) of the building envelope, like multi-layered glazing (Arici, Karabay, & Kan, 2015). The third approach is to reduce cooling demand with shading (Tao, Jiang, Li, & Zheng, 2020). Finally, the last solution is to utilise a fluid medium, i.e. ventilated air stream in the glazing, which can, for example, cool the glass itself using outside air or be used to preheat the air before it enters the interior space (Ismail, Salinas, & Henriquez, 2009). An alternative to circulating air is utilising a "circulating water chamber", which has the benefit of capturing solar energy and turning that potential energy load into a renewable energy source (Chow, Li, & Lin, 2010).

Since the fluid-glass system has been introduced (Gutai, 2010) and was patented by the author (P 11 00 156, 2011; 6250530, 2012; EP2689192A2, 2012), the technology has been researched by different research groups. Among these, an important development was to establish a correlation between the intensity of pumped water flow in the cavity and the characteristics of the window (U-value and SHGC), which also showed that these values can be tailored to external conditions (Sierra & Hernández, 2017). In terms of energy consumption, a comparison of standard window with WFG in Hong Kong was presented (Chow, Li, & Lin, 2011a). A different approach was shown for a Madrid case, where WFG had a stable water temperature to lower energy demand for heating and cooling (Gil-Lopez & Gimenez-Molina, 2013). Additional research included energy simulation for annual energy demand in humid climates (Li & Chow, 2011), analysis on impact of solar angle (Chow, Li, & Lin, 2011b), evaluation of headers (Chow & Lyu, 2017), and performance in different climates in China (Lyu, Chow, & Wang, 2018).

These research projects present the technology as one window placed in a conventional building envelope. In addition to these, the author designed and built experimental buildings titled Water House 1.0 or WH01 (Gutai, 2015) and Water House 2.0 or WH02 (("Experimental - Future Projects - 2017 | World Architecture Festival," 2017), which explore the potential of connected building envelopes in which the water infill is allowed to flow between panels and building parts. The importance of this approach is the enhanced thermal, energy, and structural performance that resulted from water flow, as introduced in book Trans-structures (Gutai, 2015). The hybrid structure of WFG lowers energy consumption without increasing embodied energy as the water infill itself has low environmental impact when compared to other building materials. The two buildings also present two different construction methods: Structure Insulated Panel (SIP) and frame+infill system. The results of these structural developments are the key focus of this paper as they are essential for the development of an integrated WFG construction system that goes beyond the limitations of a single window.

2 METHODOLOGY

The paper presents an experimental research approach to the problem of developing continuous hybrid water-filled building envelopes through design and construction. These buildings are introduced in Chapter 3. The structural challenges specific to this technology are evaluated through tests introduced in Chapter 4 and 5.

TABLE 1 Current state of Water-glass research – structural development

PUBLICATION	Water in the structure		Proposed structural layout			Water flow		Experiment		
	Water on glass (open water)	Water in glass (enclosed water)	Single window units	Connected window units	Connected building envelope	Enhanced water flow (pump)	Hybrid behaviour (automated + pump)	Numerical simulation	Prototype test (window or model)	Experimental building
(Qahtan, Rao, & Keumala, 2014)	0		0			0			0	
(Sierra & Hernández, 2017)		0	0			0		0		
(Chow et al., 2011b)		0	0			0		0		
(Gil-Lopez & Gimenez-Molina, 2013)		0	0			0			0	
(Chow & Lyu, 2017)		0	0			0			0	
(Lyu et al., 2018)		0	0			0			0	
Water House 1.0 (presented in this article)		0		0			0			0
Water House 2.0 (presented in this article)		0			0		0			0

The importance of this exploration is twofold. Firstly, developing the technology from a window to a continuous envelope improves its performance: lower energy consumption (54 – 72% savings compared to double glazing and 34 - 61% compared to triple glazing) (Gutai & Kheybari, 2020), reduced energy demand due to smaller temperature differences within the building (water flow would disseminate energy gains within the building), (Gutai & Kheybari, 2021) and improved thermal comfort (water inside WFG can be heated/cooled for better Mean Radiant Temperature /MRT/). Secondly, the tests and analysis of the system are important because this particular kind of envelope was built for the first time, which had an impact on material use, manufacturing, assembly, and the integration of various functions (i.e. heating, cooling, solar absorption, etc.) into one construction system. The novelty of WH01 and WH02 is shown in Table 1 and Table 2, which present the structural and energy development of water-filled envelope projects.

TABLE 2 Current state of Water-glass research – energy performance and mechanical system development

PUBLICATION	Impact on thermal comfort		Mechanical system			Energy management					Climate			
	Window surface temperature	All surfaces (wall, floor, ceiling, etc.)	Pump only (water from mains)	Pump + Storage tank	Hybrid (storage tank + heating/cooling)	Cooling by absorption	Stable water temp. (external source)	Absorbed energy use (heating + DHW)	Absorbed energy use (cooling + heating + DHW)	Energy savings through dissemination of energy (lowering peak loads)	Tropics	Arid	Temperate	Every climate
(Qahtan et al., 2014)	0		0			0					0			
(Sierra & Hernández, 2017)	0		0			0							0	
(Chow et al., 2011b)	0		0					0			0			
(Gil-Lopez & Gimenez-Molina, 2013)	0		0				0						0	
(Chow & Lyu, 2017)	0			0			0				0	0	0	
(Lyu et al., 2018)	0			0		0					0	0	0	
Water House 1.0 (presented in this article)	0				0				0	0				0
Water House 2.0 (presented in this article)		0			0				0	0				0

The two prototype houses served as experimental buildings to identify, resolve, and test the critical aspects for viability of WFG technology. The research identified six critical areas, which were explored over the course of five years research. Table 3 shows these areas and the methodologies involved.

TABLE 3 Six critical areas of WFG viability and their research method implemented for test and validation

CRITICAL AREAS OF WFG	HYPOTHESIS	METHODOLOGY USED	RESULTS
Reaction between water and glass	The utilised fluid infill can be effectively used in WFG without corrosion or reaction between fluid and glass/ frame	Short term prototype tests Long term tests on buildings	Fluid performed stably
Water pollution	The utilised fluid infill can be effectively used in WFG without pollution and contamination	Short term prototype tests Long term tests on buildings	Fluid performed stably
Water leakage	The utilised frame can perform effectively as a sealant for both glass and steel panels	Short term prototype tests Long term tests on buildings	Sealing performed stably
Water pressure	The utilised framework and glass are sufficient for water pressure and pump operation	Short term prototype tests Simulation Long term tests on buildings	Structure performed stably
Construction	The designed WFG technology can be assembled effectively	Designing construction options Test on two buildings	Identified options proved to be appropriate for construction
Insulation, climate, energy	WFG technology performs effectively as an energy-effi-cient building envelope	Prototype tests Energy simulation Building monitoring	WFG performed as an energy-efficient building envelope and with significant energy savings (published in Gutai and Kheybari (2020))

3 WATER HOUSE CONSTRUCTION

WFG can be built as individual window unit or as a connected building envelope. The first type is basically a heat absorbing heating/cooling unit, which benefits from the absorption of water as shown in Fig. 2. This solution is described as "fluid-glass" or "water-glass" and operates with a pump and stable flow. The second type is titled water house construction, which is built as a set of panels that are connected to each other, as shown in Fig. 1 and Fig. 3. The panels are connected in a closed loop, which is typically formed by two opposite wall surfaces and floor + ceiling/roof panel in-between (as shown in Fig. 3).

Both options absorb heat which can be transported to a thermal storage unit, as shown in Fig. 3. A pump requires less energy than cooling or heating the space, which leads to direct energy savings. In addition, water house construction can distribute energy within the envelope, which increases energy savings further by exchanging energy between overheated and cold areas of a building (e.g., north-south façade, lower-upper building parts).

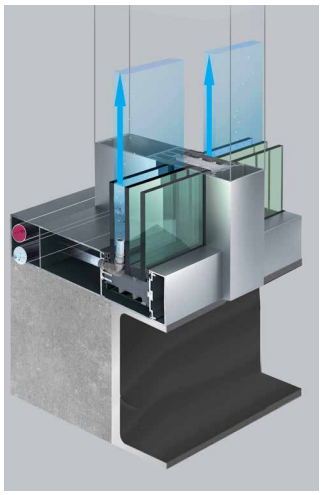

FIG. 1 Typical layout of Water House building envelope

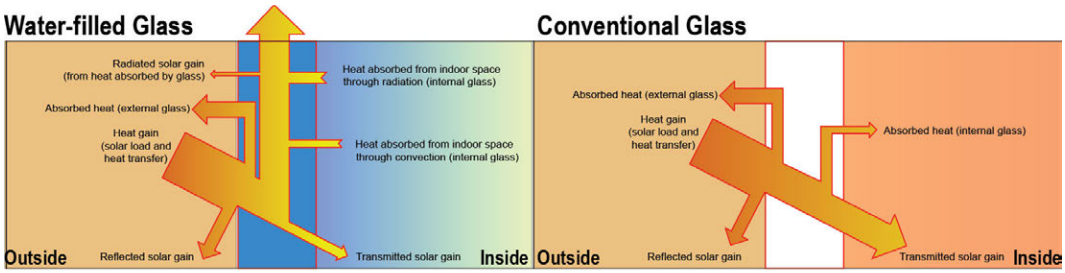

FIG. 2 Diagram showing the solar gain performance of WFG (left) and conventional glass (right). The most important difference is the absorption of the water layer that lowers cooling demand indoors and also transfers the captured energy to other parts of the building or to a thermal storage unit for later use

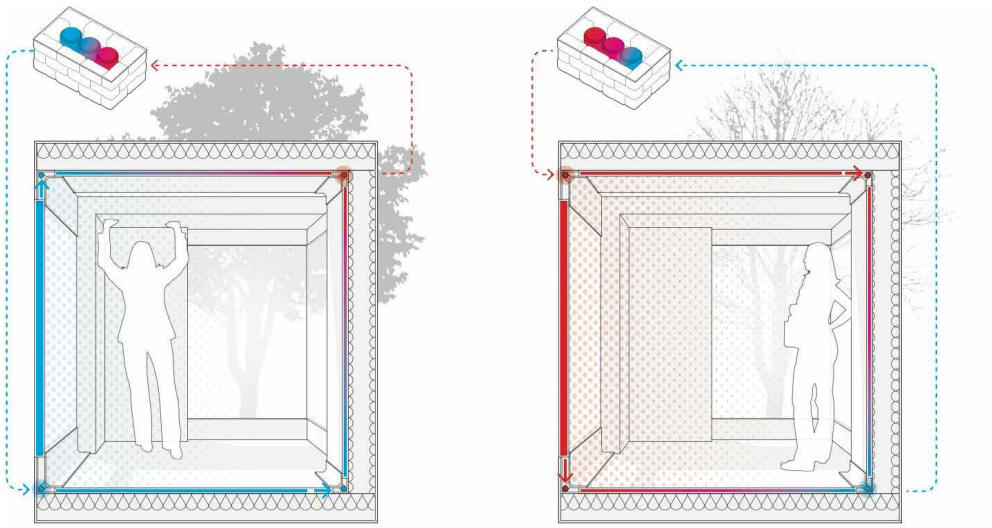

FIG. 3 Water House 1.0 – Energy balance in summer (left) and winter (right)

3.1 WATER HOUSE 1.0 PAVILION

The first Water House construction was built in Kecskemet, Hungary. The pavilion consisted of 4 water-filled glass (WFG) and 13 water-filled steel (WFS) panels, shown in Fig. 4. The WFS panel had 20 cm insulation and the WFG had an external argon layer. Pipework and cables were placed in maintenance gaps between wall panels and the floor (shown in Fig. 20), to protect them from impact of the cold climate (Köppen-Geiger D - heating dominated). Solar absorption of water was used to lower energy consumption for cooling and heating. This approach was validated in our previous publication (Gutai & Kheybari, 2020) with 61% savings compared to double glazing. This preference opted for the use of Low-E coatings that would maximise the amount of captured energy. The options were to have it only on #2 or #3 layer or both (#1, #4, #5, and #6 were not viable). Placing them on #2 maximised the absorption for both external and internal gains, which presented a best-case scenario.

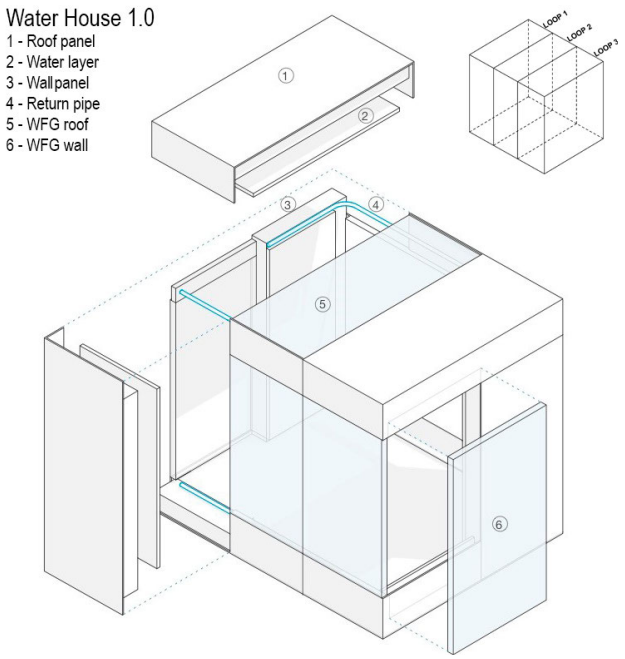

FIG. 4 Water House 1.0 – exploded diagram of the SIP structure. The south-facing panels (left) are connected to the opposite north-facing panels through a roof and a floor panel in between, forming a closed loop.

The absorbed energy was pumped to a seasonal thermal storage unit. The absorption occurred in the WFG panels and in the floor. Absorption saved energy and avoided overheating, which was likely because of high WWR (40%), south orientation, and Low-E coating. These conditions should be normally avoided, but for water house they became an asset because it increased the amount of captured energy. This showed the potential and viability of the Water House system for glazed buildings.

The seasonal storage for the building was a water tank. The tank was sized considering the thermal load of a one-week period in summer and was placed partially underground to minimise heat loss. The absorbed heat was stored for later use during heating season.

As Fig. 4 shows, the water flow was designed in three water loops of connected panels. Panels in different loops were not connected. Each loop consisted of a roof, floor, and two wall panels (one north and one south). The east and west façades included the door (without water) and WFG/WFS panels that were cooled/heated individually with direct supply and return pipes. The water flow was enhanced by a pump located in the pavilion that moved the fluid in the loops, and between storage unit and building when the indoor temperature was outside the comfort zone. A reversible heat pump was operated for heating and cooling in case of peak loads. The device was placed in the building and was installed with the pump (the cooling unit was placed outside).

WFS panels were insulated from the outside, which limited their solar absorption. These surfaces were important for MRT regulation (thermal comfort). WFS units also completed loops and increased the area of thermally active surfaces (Moe, 2010), which made heating/cooling more effective.

Fig. 5 shows the building completed and under construction. The WFS panels were designed as a Structure Insulated Panel (SIP) system utilising an external layer (load-bearing core and thermal insulation) and a water layer facing inwards. This was necessary because the connection of water panels required pipes that needed to remain accessible after construction. Placing these pipe connections inwards granted access to their 'maintenance gap' and avoided them penetrating the load-bearing structure. The building had no shading installed to ensure that there would be no interference with the results in energy performance. (The research assumed that real applications would use some kind of internal shading to avoid glare, which would improve absorption in the water layer further).

FIG. 5 Water House 1.0 completed (left) and during construction assembly (right)

3.2 WATER HOUSE 2.0 PAVILION

The second water house was built in Taichung, Taiwan, for a humid tropical climate. Since heating demand is minimal, the WFG panels are built with double glazing and a water layer. The WFS panels are without external insulation to maximise solar absorption. This was a major difference compared to WH01, because the whole building envelope could be used for the absorption of external heat load. Additionally, an absorption-based energy model was also more effective for the climate as the major load on cooling was a result of radiation since the temperature difference between indoor and ambient temperature is relatively low (Qahtan et al., 2014).

Fig. 6 shows the construction system for the building, which was a steel frame + infill panels. Similarly to WH01, the panels were connected in loops. Depending on the solar load and ambient temperature, the water flow was either automatic or enhanced with a pump. Fig. 7 shows the arrangement of the loops. The loops consisted of two walls (north and south) and floor + roof panels between.

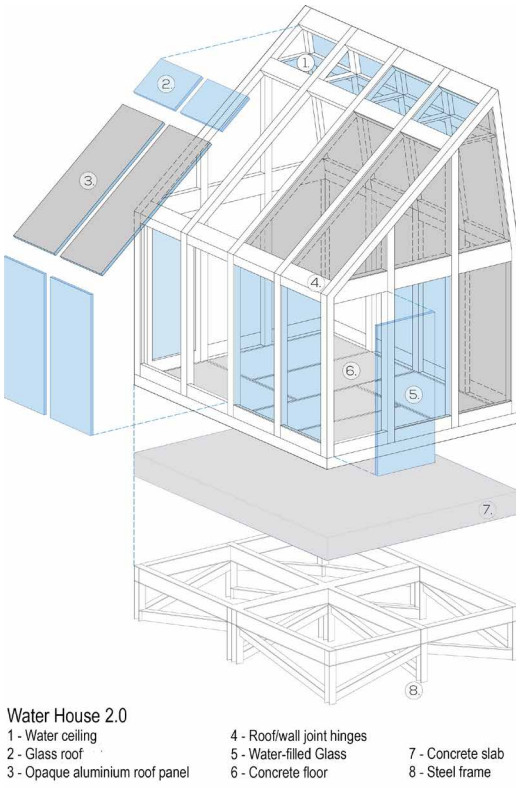

FIG. 6 Water House 2.0 – exploded view of the structure (steel frame + panels). The panels were connected in a closed loop for this case as well, connecting south-facing panels (left side) with opposite north façade panels through roof panels and floor.

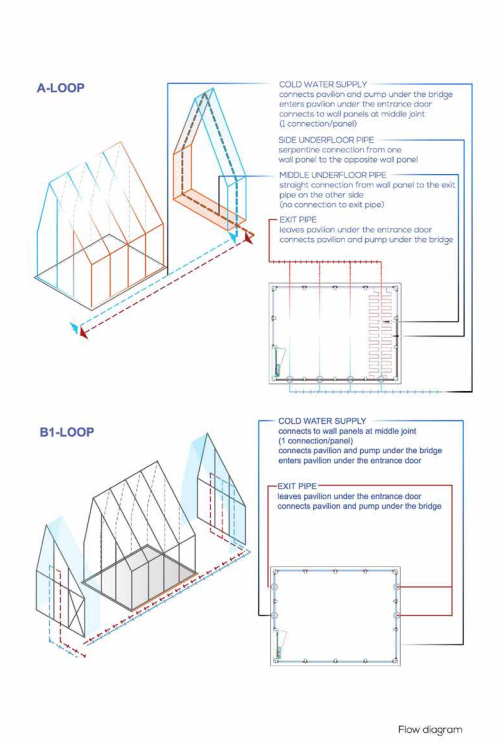

FIG. 7 Water House 2.0 – Diagram of water flow, arranged in loops

This absorption-based cooling was further enhanced by design; the north roof has no direct solar gain due to its angle and the orientation of the pavilion. Since insolation in Taichung is relatively high in any season, this geometry supported automated/pumped water flow between the two sides and provided a cooling effect as the north wall/roof radiated heat towards the outside. The south side was designed with glass panels towards the lake without shading (as shown in Fig. 8), which is not conventional for this climate. Indoor temperature was monitored, and the pump enhanced the water flow when cooling was required. The mechanical system balanced the flow with an expansion buffer in the thermal storage.

The structure of the pavilion used a curtain wall system, which consisted of structural 'frame and infill' WFG/WFS panels. The structural steel frame was prefabricated and assembled on site. The infill panels were installed after the frame was completed. The glass façade was fixed, and natural ventilation was through ventilation openings under the glass panels and at the top (through the ceiling).

FIG. 8 Photograph of Water House 2.0

As Fig. 9 shows, the curtain wall construction method was advantageous for assembly as it was easier to establish a gap between the panels. This was a challenge for the SIP method because the WFG panels in WH01 had to be placed on steel channels, which resulted in thermal bridging because the thickness of insulation was limited within the gap. In the case of the curtain wall system, the panels were directly attached to a structural steel frame and could be positioned more freely. This solution also proved to be more ideal in terms of loads because the structural and water layers overlapped and the panels could be supported from top and bottom as shown in Fig. 9.

FIG. 9 Water House 2.0 during construction, showing the steel frame (left), positioning the panels (middle), and establishing the maintenance zone between floor and panel (right)

4 STRUCTURAL CHALLENGES AND DESIGN ASPECTS OF CONNECTED WATER-PANEL BUILDING ENVELOPES

4.1 STRUCTURAL CHALLENGES

4.1.1 Reaction Between Water and Glass

Maintaining transparency is essential for glass because of its aesthetic and thermal characteristics. Glass corrosion and pollution can occur on both external and internal surfaces of WFG, particularly because the internal cavity is not sealed but connected to a water system.

The first liability is the possible pollution build-up on the glass surface. This could be caused internally (through polluted water) or externally (on the surface of the envelope). The former is a more important concern because the panel cannot be cleaned from the inside. Additionally, any pollution would also have an effect on the water flow, as the spacer and the valves are a potential target for contamination. This applies especially to the lower joints and spacer area where the pollution tends to gravitate during periods without water flow, which would normally occur during periods without solar gain and comfortable ambient temperature. Water infill has to be isolated and conditioned against physical or biological contamination.

Another possible issue is glass corrosion, which can be enhanced within the closed environment of the panel. Static aqueous corrosion occurs typically during fluid infill (i.e. construction) or fluid removal (i.e. repairs, partial replacements, system fallouts) because of the increased humidity within the panel. Internal glass surfaces are continuously exposed to dynamic aqueous corrosion because the glass is in constant contact with water. Alkali extraction and forming of Si-O bonds requires pH

levels higher than 9.0, therefore controlling the pH level is essential.(Douglas & El-Shamy, 1967; El-Shamy, Morsi, Taki-Eldin, & Ahmed, 1975)

4.1.2 Water Pollution

Water pollution is an important aspect of the structure because of visibility and sustainability. Since 'water house' buildings contain a large proportion of water, it is important to consider a method of purification that can avoid water pollution and operates in a material and energy-efficient manner because low embodied energy and recyclability are essential advantages of the technology.

The most important pollutants are disease causing agents (i.e. viruses, worms, and bacteria), oxygen demanding wastes, water soluble pollutants and nutrients (that generate growth of algae and plants). Additional heat storage and piping constitute difficulties in water maintenance.

4.1.3 Water Leakage

Water leakage is a significant liability considering the hydrostatic pressure of the system, the detailing of the header with joint-valves, and the air release valves.

The static pressure of the panels results from the weight and pressure of the water infill, which is proportional to the height and width of the panels. Additional pressure comes from operation (water pump) and dynamic external loads (i.e. wind pressure). The pressure in the panels plays an important role in waterproofing because the materials for water containment cannot accommodate large expansion. Leakage therefore can be caused by the deformation of the glass.

The second important factor is the detailing of the header and the joint between the glass layers. The material of the header needs to be able to withstand the water pressure, must resist corrosion and chemical effects, provide a continuous structural surface for waterproofing, and must incorporate the valves of the panel without compromising the integrity of the enclosure. The valves of the system are an important detail for two reasons. The first issue is manufacturing because the existing glass production techniques are developed for linear and continuous panel edges. The second issue is the connection of the valves. Mullions and transoms are kept at minimum size for curtain walls and the gap between glass panes is usually between 10-40 mm. This limited space is a significant challenge for panel assembly, especially considering waterproofing and joints.

The third difficulty for water containment is the position and operation of the air release valves, because these units need to be placed at the top of the panel. This poses a challenge because the air release valves need to be operational during construction, since water infill is the last step of the assembly. Another difficulty could be the geometry of the glass planes because of the need of air removal. The main difficulty for these valves is, however, is their accessibility and small size, which would suggest a mechanical closing system instead of an automatic one.

4.1.4 Water Pressure

Estimating water pressure for fluid-glass structures is critical for safe operation and transparency. The actual pressure in the glass panel is a sum of static and dynamic loads. The former comes from the hydrostatic pressure and the latter from either external loads (i.e. wind) or internal ones (i.e. pump). Water pressure changes the load of the glass plane because it works against wind pressure and increases wind suction. Another important aspect is the weight of water. Considering the balance of heat absorption capacity and hydrostatic pressure, the ideal thickness for the water layer is between 15-20 mm (Chow & Lyu, 2017) This is about 15-20kg/sqm, which is 25 - 33% or 18 - 25% increase for double or triple glazing, respectively. This increase plays an important role in the stability of the glass, since it is advantageous against lateral forces at the cost of increasing vertical loads.

Hydrostatic pressure is also significant in terms of visibility. The maximum bending of the glass should be kept below 0.3% to avoid an impact on transparency. Considering the typical height of curtain wall applications, this is a major caveat. WFG design should reflect this limitation by either determining an ideal width-height proportion for the panels or propose geometries that have lower widths in critical areas for the same height.

4.1.5 Construction

Although WFG windows and curtain walls are similar to other glass construction methods, there are some important differences, in particular the problem of the embedded water network and the assembly process including the fluid infill.

The problem of heat bridges results from the inserted joint valves for water circulation. There are three options for positioning the valves (shown in Fig. 10):

- On the header (spacer) of the water layer
- On the internal vertical surface of glass
- On the external vertical surface of glass

Considering potential heat bridges, the following aspects had to be considered:

- high conductivity of the joints
- limitations for proper thermal insulation
- temperature difference between indoors, outdoors, and water intake
- limitations of construction, operation and maintenance
- risk of freezing (blackout periods)
- aesthetic impact
- condensation
- water flow

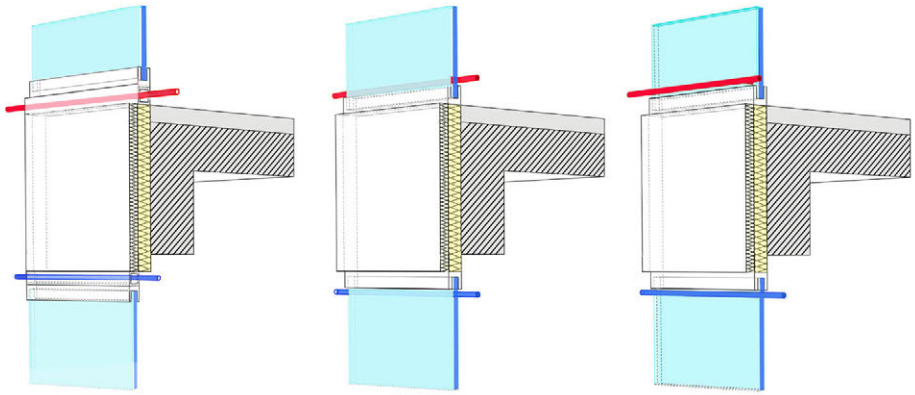

FIG. 10 Diagram showing the three options for positioning the valves: on the header (left), inside pane (middle), and outside pane (right)

Based on these criteria, the first is the most desirable option. The most important risk factor is freezing, which can most likely occur when the water network is outside. The second concern is the energy loss of the piping network, which again makes the first option preferable. The first option also has a better aesthetic impact. Finally, it is also better for water flow as the fluid enters the glass vertically. However, this solution comes at the cost of a higher U-value, because the joints penetrate the frame.

The second factor is the size of the embedded water network. The pipes themselves can be integrated into the structure (e.g., in transoms to reach the joint valves). The difficulty is the available space for joining, which is limited to the size of the structural members, typically 40 - 80 mm.

The final challenge is the construction and maintenance, especially considering the embedded joint valves and solving the infill process (including sufficient air release during the process).

4.1.6 Insulation, Climate, Energy, and Viability

The insulation capacity of WFG and the number of glass layers depends on the climate, similar to other glass structures: WH01 and WH02 utilise triple or double layers of glass for continental and hot-humid climates. This is a logical approach considering that WFG has as wide a range of U-values compared to standard glass as shown in Table 4 and Table 5. However, WFG is also utilised as cooling-heating device and its efficiency is compromised without external insulation, which makes the triple layered WFG ideal because external insulation can keep heating/cooling performance indoors. The internal water layer is also preferable to an external one for absorption (Sierra & Hernández, 2017).Finally, a third glass layer can improve the U-value for further energy savings. Our calculations on the economic value on energy savings have shown that the system has significant energy savings that could be as high as US$3-13/m2a, which offers a competitive return-on-investment (ROI) even for the triple glazed option, especially for large buildings (Gutai & Kheybari, 2020). The third layer is also ideal because of thermal stress on glass panes, which can occur with heat absorption.

In addition to insulation, coatings, in particular Low-E coatings, play a major role in the performance of WFG. Just like in the case of insulation, climate is an important factor in considering the

position and number of Low-E coatings. As presented above for WH01, climates with heating demand benefit from Low-E either on the #2 or #3 surface, which would maximise absorption for both summer and winter.

Finally, the preference for absorption or insulation should be considered for each climate scenario. WFG has a wide range for U-value (U = 2.9 – 6.34). The most important options are indicated below in Table 4. This gives the possibility to design insulation-based or absorption-based WFG panels. WFG can be tailored for specific climates, which is relevant because in tropical climates absorption has a stronger impact on energy consumption than insulation (Bui et al., 2017).

TABLE 4 WFG layout options and characteristics (calculated with LBNL Window)

WFG OPTIONS	UG-VALUE [W/M2K]	SHGC [%]	TSOL [%]	TVIS [%]
WFG double layer, clear (two panes of clear glass, 15 mm water infill)	6.34	58%	37%	55%
WFG triple layer, clear (three panes of clear glass, 15 mm water infill /internal gap/ 16 mm argon layer /external gap/)	2.9	57%	31%	47%
WFG triple layer, Low-E (three panes of clear glass, Low-e coating 15 mm water infill /internal gap/ 16 mm argon layer /external gap/)	1.75	51%	29%	46%

4.2 POSSIBLE SOLUTIONS AND CONSTRUCTION METHODS FOR WATER-PANEL BUILDING ENVELOPES

4.2.1 Glass Coating and Water Conditioning

The prototype tests and the buildings have shown that the risk of pollution and corrosion can be addressed effectively by controlling the chemical state of the water. Water had to be kept in a closed loop in order to maintain a stable water state. The easiest way to achieve this was to establish a closed loop of connected panels with minimum water piping that is connected to the rest of the mechanical system through a heat exchanger. In addition to the heat exchanger, the closed loop requires a pump for induced flow and a filter to capture any potential pollution in the fluid. In the case of the water houses presented here, these were placed between the pump and the panels, ideally just before the water intake valve.

Glass corrosion and degradation is usually a slow process and although L. Robinet established that the decomposition process could happen relatively quickly through the influence of pollutants (decades), this is still a long timeframe to consider it as a cause for concern. The determined period is also greater than the lifespan of glass façades (Robinet, Coupry, Eremin, & Hall, 2006). However,

the formation of silica film is much faster, and it is a more important issue because of its impact on transparency. There are several ways to avoid or to slow the process. The use of Hydrolytic glass (Type I.) with high water resistance (e.g. borosilicate glass) can lower the risk of weathering. Coatings added to the glass surface could offer sufficient protection as well, like the sol-gel developed by K. Kamitani (Kamitani & Teranishi, 2003) or the water repellent glass coating by A. Matsuda (Matsuda, Matsuno, Katayama, & Tsuno, 1989)

Additionally, the physical and chemical properties of the water can affect water corrosion. R.B. Ellestad and I.I. Ostroushko established the relationship between temperature and glass corrosion (US 2 516 109, 1950; Ostroushko, Filipova, & Ignateva, 1962). R.W. Douglas assumed that the corrosion rate is independent of the pH from 1 to 9.8 (Douglas & El-Shamy, 1967) and El-Shamy pointed out that higher pH rate results increased SiO_2 release rate (El-Shamy et al., 1975). Sanders et al. presented a model profile for corrosion to compare different types of binary glasses and discussed the effects of corrosion temperature on surface gel build-up (Sanders & Hench, 1973). Finally, A. Tournié et al. challenged the "gel build-up" during corrosion and pointed out the effect of base and acid attacks with boiling NaOH characterised as dissolution without structural modifications (Tournié, Ricciardi, & Colomban, 2008). Based on the research conducted, it can be established that glass corrosion can be effectively avoided if the water is kept at an ideal (room) temperature and pH level (below 9.8) to minimise weathering and pollution. This strategy also worked effectively for WH01 and WH02.

4.2.2 Water Pollution

Water pollution is an important aspect due to its aesthetic impact and the potential clogging of the pipes. The thickness of the water layer in WFG is between 15 - 20 mm, which limits the joint valve and makes pollution a significant factor. Since the water is in a closed circuit, the main pollution factors are biological contamination and non-solvable pollutants. The latter can be effectively addressed by a filtering mechanism that is placed between the panel and the pump. Depending on heat load, WFG panels operate by utilising induced or automatic flow. The automatic flow is much slower and can be blocked by the filter itself, which means that the filter and the pump have to be installed parallel to the closed circuit as an alternative route that is only active when the pump is turned on, as shown in Fig. 11. Because of the need for filtering, the pump needs to be turned on regularly, even if the heat load would not require it.

The most effective solution for biological contamination is UV filtering because it presents no adverse effects on water piping, glass or waterproofing. UV is effective against all waterborne pathogens: viruses and bacteria, especially Legionella (Hijnen, Beerendonk, & Medema, 2006). Z. Liu highlighted the importance of the filter as well, which should be ideally located close to the immediate water source (Liu et al., 1995). This suggests a dispersed filter system instead of a central one (i.e. in a water tank), which was the case for Water House projects.

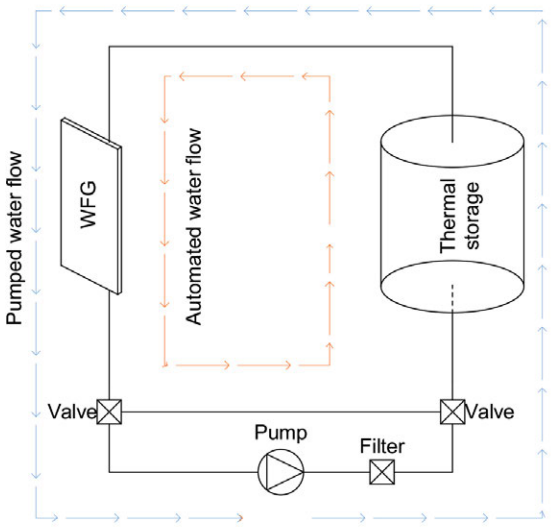

FIG. 11 Diagram showing the automated and pumped piping

4.2.3 Water-Proofing and Spacer

The constant water pressure in the panel would require a dual seal solution for the panel, which is predominant for insulated glass. The advantage of this solution is that it can adapt to current manufacturing techniques and it can deal with pressure more effectively because primary sealants have low expansion capacity. The utilised material and technique for the primary sealant also depends on the spacer.

Spacers for the water layer could be tubes or frames. The former has the advantage of being easy to bend, cut, or corner keyed, which is important for containing water where a continuous structural surface is essential. However, frames have the advantage of providing a stable and flat surface for waterproofing, which is more important for fluid-glass considering the water pressure involved. Spacers can be made of steel or aluminium. The case study projects presented here are made of the latter, as glass-aluminium joints are standard in the industry and the material has the additional advantage of resisting corrosion.

The secondary sealant is critical for the integrity of the glass ceiling. Its main function is to avoid moisture ingress in the structure. For fluid-glass panels, the secondary sealant also needs to have the capacity to support the primary sealant against deformation of the glass. This requires a larger thickness than usual, which means that both primary and secondary seals are exposed to sunlight. This has both aesthetic and structural impacts because the seals may become visible and exposed to UV radiation.

4.2.4 Glass Thickness

Determining constant and dynamic lateral loads on the glass envelope is essential in order to calculate the glass thickness of the structure. The research used two sets of tests to determine two variables: the impact of hydrostatic pressure (impact of height) and water thickness (impact of water volume).

Water pressure was simulated with a load model using water weight as a uniform load, assuming a uniform pressure in the panel. This model was simulated in Glastik software, using a specific wind load that was equal to the water pressure. The results are shown in Figs. 13 - 14. The simulation was validated with prototype tests shown in Fig. 12. Laminated glass, with thicknesses of 8, 10, and 12mm, were tested. The panels used for WH02 were 820 x 1800 mm. The deformation was about 6 mm as shown in Fig. 13. This was acceptable both in terms of structure and visibility (max 0.3%).

FIG. 12 Deformation of glass pane resulting from water pressure, experiment

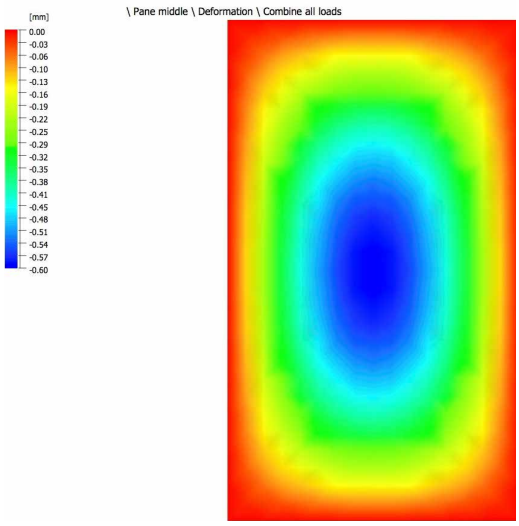

FIG. 13 Deformation of middle glass pane, simulation based on experimental results with Glastik

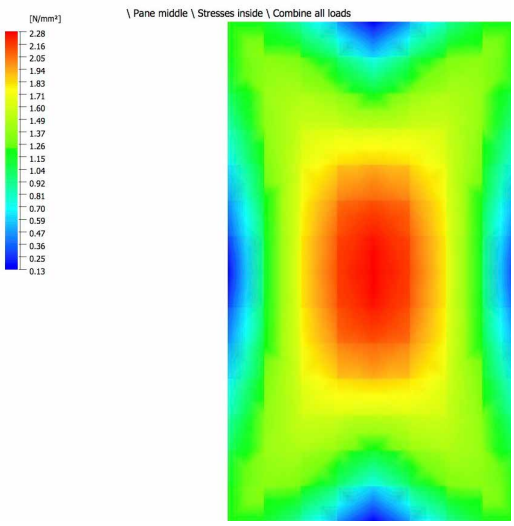

FIG. 14 Stresses of middle glass pane, simulation based on experimental results with Glastik

The second set of lab tests were conducted to determine the impact of water thickness. WFG was placed horizontally against vertical load in the middle of the glass plane as shown in Fig. 15. This installation had the advantage of eliminating the water pressure as a variable. Two prototypes were tested, with and without water. The panels had different water thickness as shown in Table 5. The results are shown in Fig. 15, which indicate lower deflection for the outside plane in a filled state, but higher deflection in the internal side of the panel. This suggests that the load is disseminated better in WFG by the fluid infill. Overall, the deflection rate did not show a significant increase in filled state, which suggested that neither water pressure nor infill thickness would compromise the viability of WFG critically. The load-deflection rate is much higher for BG due to its larger size and water thickness, which increases the section and strength of the spacer.

TABLE 5 WFG prototypes used in the structural test

GLASS OPTIONS	LENGTH [MM]	WIDTH [MM]	WATER THICKNESS [MM]	GLASS THICKNESS [MM]	TOTAL THICKNESS [MM]
WFG BG	700	450	31	4	39
WFG SM	700	300	16	4	24

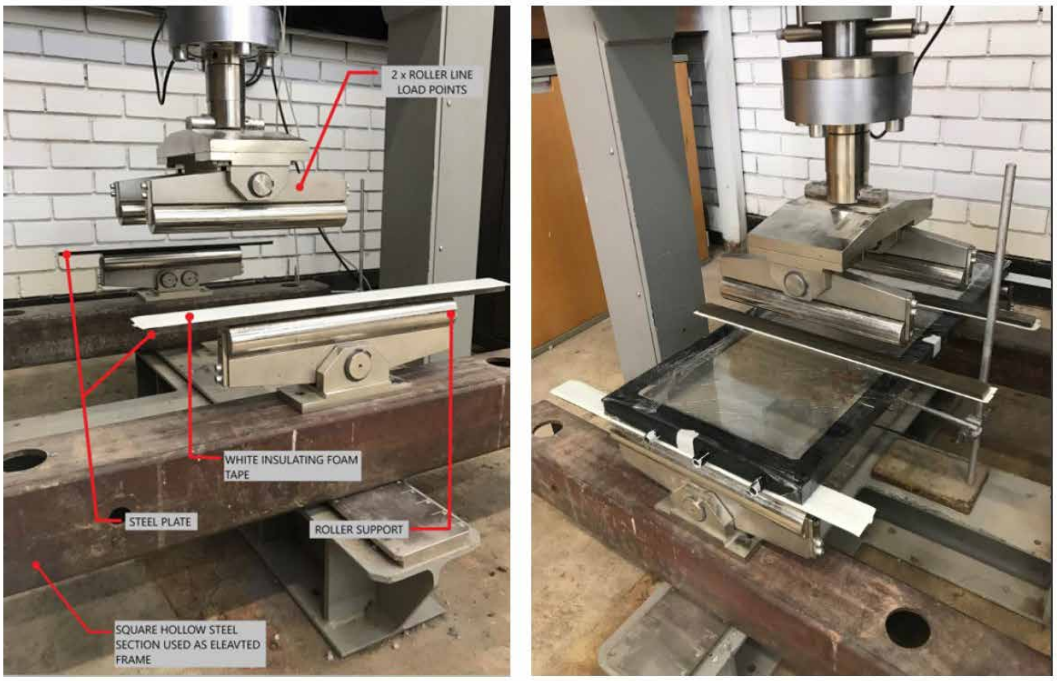

FIG. 15 WFG structural tests in the lab

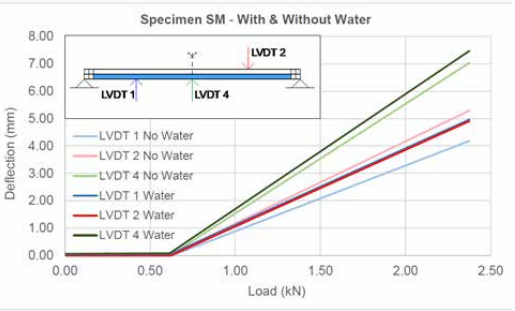

FIG. 16 Deflection of WFG (16 mm water layer) with and without water

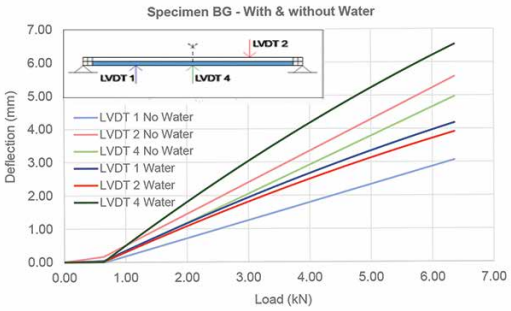

FIG. 17 Deflection of WFG (31 mm water layer) with and without water

4.2.5 Construction: Frame, Detailing, Infill, Air Release

The first challenge of construction is the detailing of fluid panels because water pipes and joint valves should be embedded within the structure of the curtain wall. There are two types of pipe network: one for automatic flow and another for the pump. The latter has supply and return pipes that connect to each loop separately. These pipes can be placed in mullions and transoms or simply below/above the panel in a gap as shown on Fig. 1 and Fig. 20. This approach was used for both water house projects for WFG panels. In the case of WFS, the detail was different in order to respond to the specific climates and insulation requirements of Hungary and Taiwan. For WH01, the panels were built as a SIP system and the water layer was attached to the structural core. In the case of WH02, the opaque panels needed no insulation, and the water-steel panels had a similar thickness to the glass units. The load-bearing structure was a steel frame, which was placed between the panel units as shown in Figs. 18 and 19.

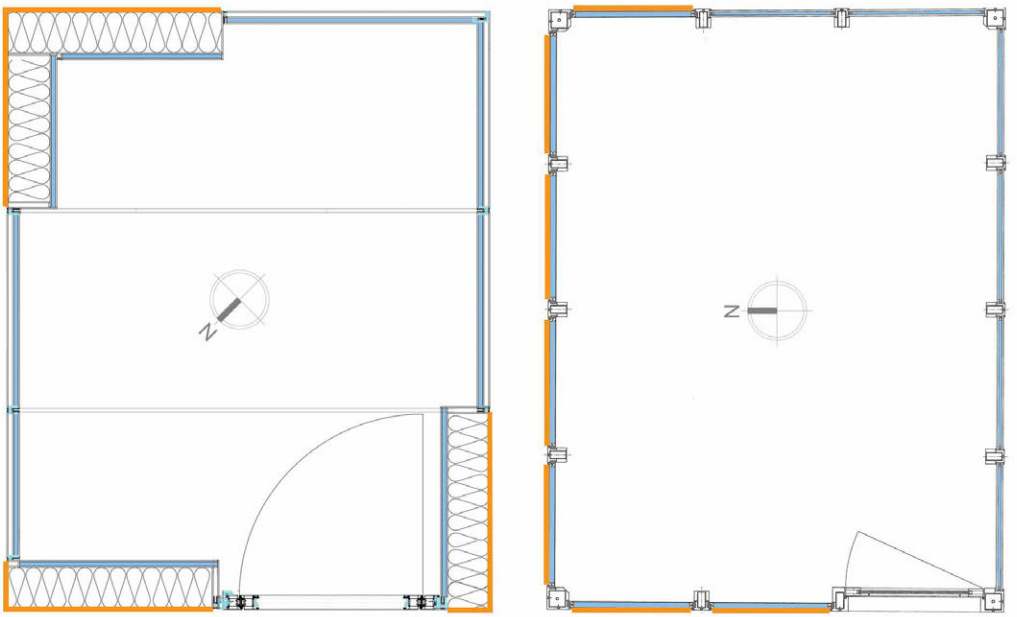

FIG. 18 Plans of Water House 1.0 (left) and Water House 2.0 (right) showing SIP and frame + infill structures, respectively. Steel panels (WFS) are highlighted with orange lines.

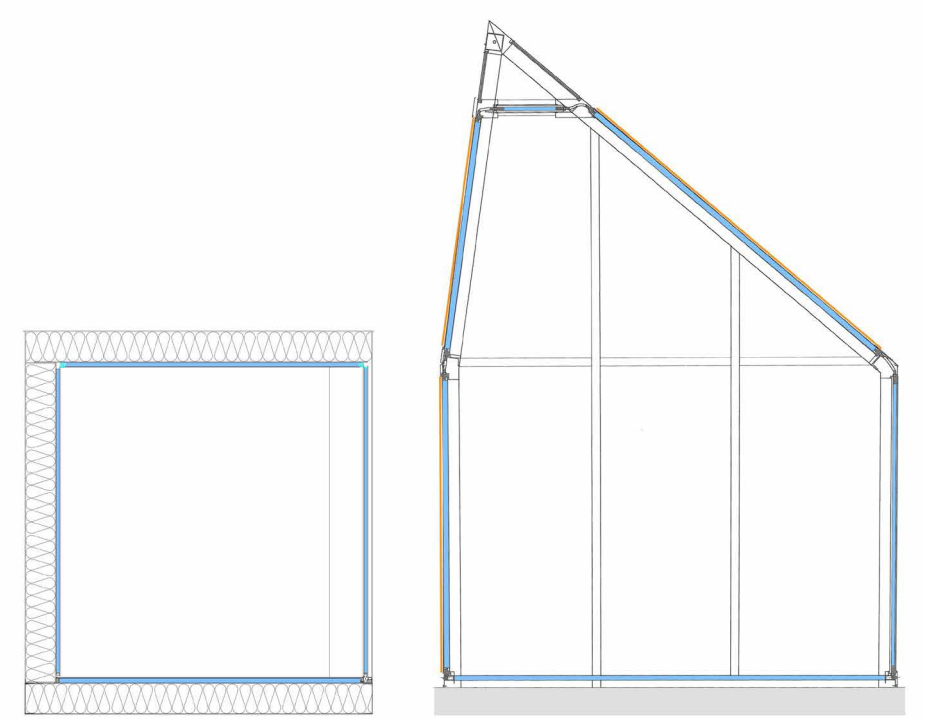

FIG. 19 Sections of Water House 1.0 (left) and Water House 2.0 (right) showing SIP and frame + infill structures, respectively. Opaque (steel) panels are highlighted with orange lines.

As shown on the sections (Fig. 19), from a structural perspective, the frame + infill solution is more ideal as the loads were kept along the central axis of the structural frame and the maintenance gaps between panels could be achieved easily. In the case of WH01, this was not possible because insulation was a priority and the water layer was attached on the inner side of the load bearing panels as an additional layer. This solution was not ideal from a structural perspective, but was necessary for proper insulation of the maintenance gap that provided access to the flexible joints between panels and distribution pipework that connects each loop with the main mechanical system. These gaps are visible between the panels on Fig. 1 (bottom) and Fig. 20 (top).

The sections on Fig. 19 and the detail on Fig. 1 also show that the SIP structural method has better thermal insulation because the steel spacer that establishes the gap between panels can be insulated from both the inside and outside, which makes the SIP options a more effective method of construction for WFG in heating dominated climates.

The second challenge of construction is the infill process and the air release from the panels. The solution for this again depends on the position of the supporting structure because fluid infill takes place when the structure is already assembled. In the case of a typical curtain wall construction, the transoms and mullions are placed behind the glass surface, which means that the air release valve can only be accessed from the outside. In the case of the SIP option, the valves can be oriented either towards the interior or exterior, as there is a gap between the glass and the roof/ ceiling. Ideally, the second option is preferable, as shown in Fig. 20.

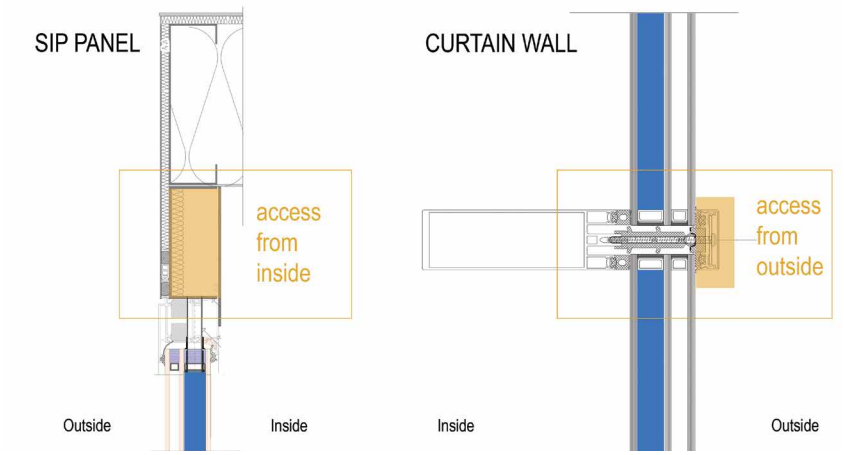

FIG. 20 Details showing the position of air release valves and their access for SIP and curtain wall construction

4.2.6 Energy and Climate

Determining the economic viability of a fluid-glass structure is essential, especially considering different climates. Based on the monitoring of WH01 and WH02 and prototype tests, a global simulation for WFG façades was conducted by the authors for 13 cities in all Köppen-Geiger climatic regions (Gutai & Kheybari, 2020). The research concluded that the system is viable in every climate region except polar climate. The research evaluated each climate, considering whether absorption or insulation should be prioritised, as this depends both on temperature and radiation. The research divided the cities into four climate groups depending on the utilised energy model: absorption-based, intermediate, hybrid, and insulation-based. The first case is when energy savings are based on absorption only (almost no heating demand). The second is when there is heating demand, and loss in U-value increases energy consumption for heating, but the improved absorption still yields more energy savings overall. The third is when the energy balance is only positive when the solar gain is stored and reused during the heating period. The fourth group is insulation-based regions that are heating dominated areas. The simulation presented two important results: 1) WFG is viable in both hot and cold conditions and; 2) energy performance of glass buildings can be increased just by improving absorption even if it happens at the cost of higher U-value. The energy savings were between 54 - 72% compared to double glazing and 34 - 61% compared to triple glazing, depending on climate, as shown in Fig. 22.

As a developed construction system, WH01 and WH02 informed the simulation model in terms of structural layout and tested the mechanical system. In case of WH01, the building utilised thermal storage and a reversible heat pump to heat or cool the water locally and keep the temperature of the water at comfort level. Fig. 21 shows WH02, which had the same system but was mainly used for cooling.

In relation to energy consumption and climate, it should be noted that the effect of external insulation (third glass pane and an argon layer) depends on whether the water is cooled/heated or only used for absorption. In the case of the latter, 2 layers of glass with water can be sufficient. This type of water-glass has been analysed by previous research projects and was utilised for WH02. The main reason behind this solution was that the building does not need heating for most of the year due to the climate of Taichung city.

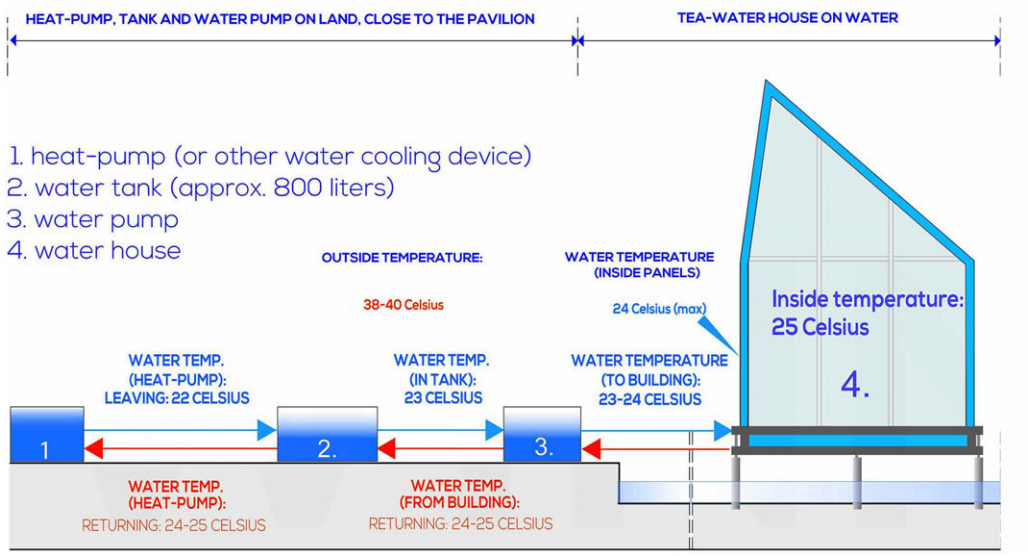

FIG. 21 Diagram of the functional concept of Water House 2.0

However, when heating is required, external insulation is ideal. This was the case for WH01. This improved the energy balance of the envelope and protected the water infill from freezing to a certain extent, by maintaining the indoor temperature at a higher level than the external one due to its insulation capacity.

A similar issue arose with the design of the glass coating. In the case of climates with predominant heating load, a Low-E layer can increase the absorption of the water layer. This was tested with WH01, and also justified the use of a second glass pane, which also acted as a protection for the external coating.

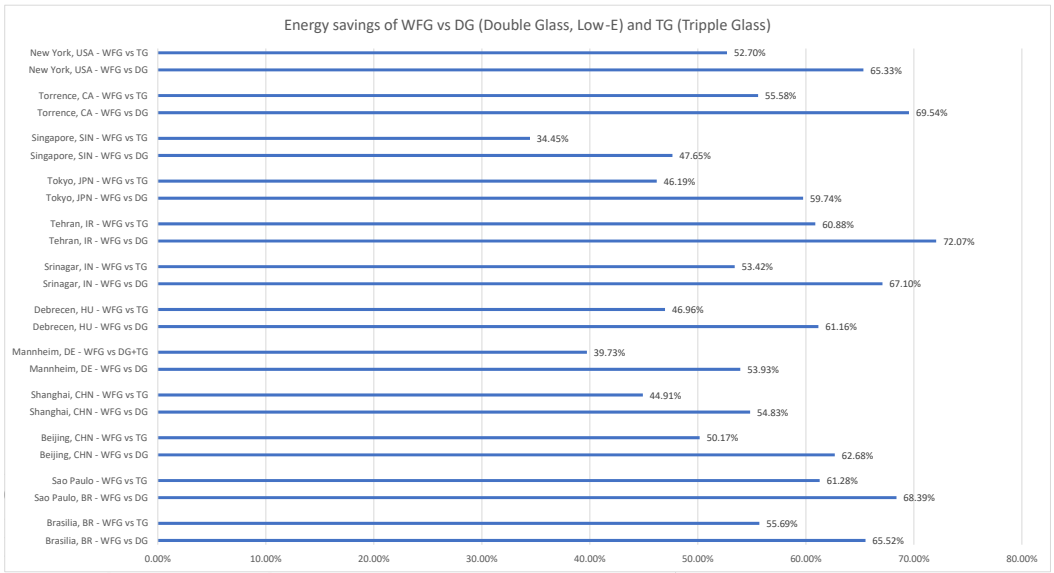

FIG. 22 Energy savings of WFG compared with conventional double glazing (DG) and triple glazing (TG)

The properties of the WFG and standard glass used as the base case in the simulation are shown in Table 5. Overall, the system showed significant energy savings in any inhabited climate region (every climate except polar), as shown in Fig. 22.

5 CONCLUSION

The experimental buildings presented that a 'water house' construction system is a viable solution and the potential issues of constructing WFG envelope can be effectively addressed by the following:

- Controlling the chemical state (pH) of the water is crucial to avoid glass corrosion
- The water should be kept in a closed loop to avoid pollution.

The two buildings explored different assembly options: WH01 utilised Structure Insulated Panel (SIP) and WH02 used a frame + infill panel method. After construction, their performance was analysed and the following conclusions can be drawn:

- The SIP system offers an effective solution for external insulation. This construction method could be more applicable for colder climates where external insulation is priority (transmissive heat losses outweigh gains of absorbed radiation) because the overall U-value of the envelope is higher with the same WWR
- Utilising frame + infill method is more ideal for assembly because the panels can be positioned freely. The necessary gaps between panels can be established easily and the structural load of the water remains a central load. The disadvantage of frame + infill method is the limited potential of external insulation, especially if the thickness of the building envelope is limited, which results in a lower U-value with the same WWR.

Both construction options have merits and could be implemented in any location, however, SIP has more advantages in colder climates and frame + infill for hot climates due to their advantages/disadvantages in insulation.

Impact of WFG in construction

WFG technology is presented here with two buildings that are the first examples of connected water building envelopes. The most important difference between such hybrid envelope and solid structures is that energy can be captured and distributed within the envelope between building parts with different exposures (i.e. north and south façades or lower and higher floors). This potential is a special characteristic of this assembly method (titled 'water house' construction), which distinguishes WH01 and WH02 from solid buildings or other water-glass research that focuses on a single window. The significance of water house construction is:

- Energy exchange within façade brings another layer of energy-savings for a building, which does not compromise existing passive solutions but complements their performance with additional savings
- The performance of WFG in energy savings and thermal comfort gives significant freedom for architects to design glass/transparent buildings as WFG makes glass an opportunity for comfort/energy instead of being a liability (WFG provides radiant heating/cooling and energy absorption with an optically clear surface)

— WFG lowers the life-cycle impact of a building in two ways: directly (with lower energy consumption) and indirectly (with lower embodied energy by making additional structures i.e. external shadings, unnecessary). WFG presents an opportunity to calculate the primary and secondary impact of life-cycle assessment (LCA). The secondary aspect is a novel approach, which is critical for future LCA of net zero buildings, where the embodied component is higher than average.
— Energy exchange of hybrid envelopes challenge the energy models that resolve energy demands independently for each space or building. In the case of WFG, a local energy surplus is an opportunity to be distributed somewhere else or to be stored for later use.
— Energy distribution of hybrid envelopes unlock the potential creating energy-exchange links between buildings, which transform our built environment into urban micro infrastructures that collect and distribute energy. The potentials of such an approach have a significant impact on the way we design and understand buildings and cities in the future.

Suggestions for future research:

There are several important research questions suggested by the current findings. The monitoring results of the closed water loop in water houses suggest that the autonomous water flow can play a more significant role in thermal comfort and energy savings of water-house projects. This was tested with WH02. This should be determined by future research efforts. There is a need for further investigation in different options for coatings and glass panes globally with energy simulation; especially in terms of scale, WWR, and climate would help to build up effective operation scenarios for water houses, depending on the function and location of the building.

Acknowledgements

This research project was a collaboration of Loughborough, Tokyo, and Feng Chia University and was supported by the Ministry of Science and Technology in Taiwan (MOST ID 106-2218-E-035-003). The authors are grateful for the continuous support of the enterprises involved in the construction process: Jüllich Glas in Hungary and Hesung Ltd in Taiwan for their generous and continuous support.

References

Adalberth, K. (1997). Energy use during the life cycle of buildings: A method. *Building and Environment*, *32*(4), 317–320. https://doi.org/10.1016/S0360-1323(96)00068-6

Arici, M., Karabay, H., & Kan, M. (2015). Flow and heat transfer in double, triple and quadruple pane windows. *Energy and Buildings*, *86*, 394–402. https://doi.org/10.1016/j.enbuild.2014.10.043

Bui, V. P., Liu, H. Z., Low, Y. Y., Tang, T., Zhu, Q., Shah, K. W., … Koh, W. S. (2017). Evaluation of building glass performance metrics for the tropical climate. *Energy and Buildings*, *157*, 195–203. https://doi.org/10.1016/j.enbuild.2017.01.009

Chow, T.-T., Li, C., & Lin, Z. (2011a). The function of solar absorbing window as water-heating device. *Building and Environment*, *46*(4), 955–960. https://doi.org/10.1016/j.buildenv.2010.10.027

Chow, T.-T., Li, C., & Lin, Z. (2011b). Thermal characteristics of water-flow double-pane window. *International Journal of Thermal Sciences*, *50*(2), 140–148. https://doi.org/10.1016/j.ijthermalsci.2010.10.006

Chow, T.-T., & Lyu, Y. (2017). Numerical analysis on the advantage of using PCM heat exchanger in liquid-flow window. *Applied Thermal Engineering*, *125*, 1218–1227. https://doi.org/10.1016/j.applthermaleng.2017.07.098

Chow, T. T., Li, C., & Lin, Z. (2010). Innovative solar windows for cooling-demand climate. *Solar Energy Materials and Solar Cells*, *94*(2), 212–220. https://doi.org/10.1016/j.solmat.2009.09.004

Chow, T. T., & Lyu, Y. (2017). Effect of design configurations on water flow window performance. *Solar Energy*, *155*, 354–362. https://doi.org/10.1016/j.solener.2017.06.050

Cui, Z., & Mizutani, A. (2016). Research on the reduction effect of transparent glass on cooling power energy consumption research on the reduction of cooling and heating loads by transparent solar heat absorbing glass panels (Part 2). *Journal of Asian Architecture and Building Engineering*, *15*(3), 651–658. https://doi.org/10.3130/jaabe.15.651

DeForest, N., Shehabi, A., O'Donnell, J., Garcia, G., Greenblatt, J., Lee, E. S., … Milliron, D. J. (2015). United States energy and CO<inf>2</inf> savings potential from deployment of near-infrared electrochromic window glazings. *Building and Environment*, *89*, 107–117. https://doi.org/10.1016/j.buildenv.2015.02.021

Douglas, R. W., & El-Shamy, T. M. M. (1967). Reactions of Glasses with Aqueous Solutions. *Journal of the American Society*, *50*, 1–8.

El-Shamy, T. M., Morsi, S. E., Taki-Eldin, H. D., & Ahmed, A. A. (1975). Chemical durability of Na<inf>2</inf>OCaOSiO<inf>2</inf> glasses in acid solutions. *Journal of Non-Crystalline Solids*, *19*(C), 241–250. https://doi.org/10.1016/0022-3093(75)90088-5

Ellestad, L. B., & Leute, K. M. (1950). *US 2 516 109*. United States.

Experimental - Future Projects - 2017 | World Architecture Festival. (2017). Retrieved September 2, 2019, from https://www.worldarchitecturefestival.com/experimental-future-projects-2017

Gasparella, A., Pernigotto, G., Cappelletti, F., Romagnoni, P., & Baggio, P. (2011). Analysis and modelling of window and glazing systems energy performance for a well insulated residential building. *Energy and Buildings*, *4*(43), 1030–1037.

Ghosh, A., Norton, B., & Duffy, A. (2016). Measured thermal performance of a combined suspended particle switchable device evacuated glazing. *Applied Energy*, *169*, 469–480. https://doi.org/10.1016/j.apenergy.2016.02.031

Gil-Lopez, T., & Gimenez-Molina, C. (2013). Influence of double glazing with a circulating water chamber on the thermal energy savings in buildings. *Energy and Buildings*, *56*, 56–65. https://doi.org/10.1016/j.enbuild.2012.10.008

Gutai, M. (2010). *Dissolution Method and Water House Model*. (Doctoral Dissertation, The University of Tokyo).

Gutai, M., & Kheybari, A. G. (2020). Energy consumption of water-filled glass (WFG) hybrid building envelope. *Energy and Buildings*, *218*. https://doi.org/10.1016/j.enbuild.2020.110050

Gutai, M., & Kheybari, A. G. (2021). Energy consumption of hybrid smart water-filled glass (SWFG) building envelope. *Energy and Buildings*, *230*. https://doi.org/10.1016/j.enbuild.2020.110508

Gutai, M. (2015). *Trans-structures*. New York: Actar Publishing.

Gutai, M. (2011). *P 11 00 156*. Hungary.

Gutai, M. (2012). *6250530*. Japan: Japan Patent Office.

Gutai, M. (2012). *EP2689192A2*. European Union.

Hemaida, A., Ghosh, A., Sundaram, S., & Mallick, T. K. (2020). Evaluation of thermal performance for a smart switchable adaptive polymer dispersed liquid crystal (PDLC) glazing. *Solar Energy*, *195*, 185–193. https://doi.org/10.1016/j.solener.2019.11.024

Hijnen, W. A. M., Beerendonk, E. F., & Medema, G. J. (2006). Inactivation credit of UV radiation for viruses, bacteria and protozoan (oo)cysts in water: A review. *Water Research*, *40*(1), 3–22. https://doi.org/10.1016/j.watres.2005.10.030

Ismail, K. A. R., Salinas, C. T., & Henriquez, J. R. (2009). A comparative study of naturally ventilated and gas filled windows for hot climates. *Energy Conversion and Management*, *50*(7), 1691–1703. https://doi.org/10.1016/j.enconman.2009.03.026

Kamitani, K., & Teranishi, T. (2003). Development of water-repellent glass improved water-sliding property and durability. *Journal of Sol-Gel Science and Technology*, *26*(1–3), 823–825. https://doi.org/10.1023/A:1020747632317

Li, C., & Chow, T.-T. (2011). Water-filled double reflective window and its year-round performance. In *Procedia Environmental Sciences* (Vol. 11, pp. 1039–1047). https://doi.org/10.1016/j.proenv.2011.12.158

Liu, Z., Stout, J. E., Tedesco, L., Boldin, M., Hwang, C., & Yu, V. L. (1995). Efficacy of ultraviolet light in preventing Legionella colonization of a hospital water distribution system. *Water Research*, *29*(10), 2275–2280. https://doi.org/10.1016/0043-1354(95)00048-P

Lyu, Y.-L., Chow, T.-T., & Wang, J.-L. (2018). Numerical prediction of thermal performance of liquid-flow window in different climates with anti-freeze. *Energy*, *157*, 412–423. https://doi.org/10.1016/j.energy.2018.05.140

Matsuda, A., Matsuno, Y., Katayama, S., & Tsuno, T. (1989). Weathering resistance of glass plated coated with sol-gel derived 9TiO2 91SiO2 films. *Journal of Materials Science Letters*, *8*, 902–904.

Moe, K. (2010). *Thermally Active Surfaces in Architecture*. New York: Princeton Architectural Press.

Ostroushko, Y. I., Filipova, K. ., & Ignateva, L. A. (1962). Reaction of spodumene with sulfuric acid. *Russ. Journal of Inorganic Chemistry*, *7*(2), 126–129.

Pal, S., Roy, B., & Neogi, S. (2009). Heat transfer modelling on windows and glazing under the exposure of solar radiation. *Energy and Buildings*, *41*(6), 654–661. https://doi.org/10.1016/j.enbuild.2009.01.003

Qahtan, A., Rao, S. P., & Keumala, N. (2014). The effectiveness of the sustainable flowing water film in improving the solar-optical properties of glazing in the tropics. *Energy and Buildings*, *77*, 247–255. https://doi.org/10.1016/j.enbuild.2014.03.051

Ramesh, T., Prakash, R., & Shukla, K. K. (2010). Life cycle energy analysis of buildings: An overview. *Energy and Buildings*, *42*(10), 1592–1600. https://doi.org/10.1016/j.enbuild.2010.05.007

Robinet, L., Coupry, C., Eremin, K., & Hall, C. (2006). The use of Raman spectrometry to predict the stability of historic glasses. *Journal of Raman Spectroscopy*, *37*(7), 789–797. https://doi.org/10.1002/jrs.1540

Sanders, D. M., & Hench, L. L. (1973). Mechanisms of Glass Corrosion. *Journal of the American Ceramics Society*, *56*(7), 373–377.

Sierra, P., & Hernández, J. A. (2017). Solar heat gain coefficient of water flow glazings. *Energy and Buildings*, *139*, 133–145. https://doi.org/10.1016/j.enbuild.2017.01.032

Tao, Q., Jiang, F., Li, Z., & Zheng, J. (2020). A model of heat gain calculation for buildings with shuttle louvers: Verification and a case study. *Journal of Building Engineering*, *29*. https://doi.org/10.1016/j.jobe.2019.101101

Tournié, A., Ricciardi, P., & Colomban, P. (2008). Glass corrosion mechanisms: A multiscale analysis. *Solid State Ionics*, *179*(38), 2142–2154. https://doi.org/10.1016/j.ssi.2008.07.019

JOURNAL OF FACADE DESIGN & ENGINEERING

VOLUME 8 / NUMBER 2 / 2020

TU DELFT OPEN
ISSN PRINT 2213-302X
ISSN ONLINE 2213-3038